
Synthesis of Sequence-Controlled Polymers by Combination of Post-Polymerization Modification and Chain Extension Reactions

Zur Erlangung des akademischen Grades eines

DOKTORS DER NATURWISSENSCHAFTEN

(Dr. rer. nat.)

von der KIT-Fakultät für Chemie und Biowissenschaften

des Karlsruher Instituts für Technologie (KIT)

genehmigte

DISSERTATION

von

M.Sc. Sven Schneider
aus Landau in der Pfalz

1. Referent: Prof. Dr. Patrick Théato

2. Referent: Prof. Dr. Pavel Levkin

Tag der mündlichen Prüfung: 17.07.2024

Für meine Eltern

Declaration of Authorship

Die vorliegende Arbeit wurde im Zeitraum von Februar 2021 bis Juni 2024 am Institut für Biologische Grenzflächen 3 (IBG-3) am Karlsruher Institut für Technologie (KIT) unter der wissenschaftlichen Betreuung von Prof. Dr. Patrick Théato angefertigt.

Hiermit erkläre ich, dass die vorliegende Arbeit im Rahmen der Betreuung durch Prof. Dr. Patrick Théato selbstständig verfasst und keine anderen als die angegebenen Quellen und Hilfsmittel verwendet wurden. Inhaltlich oder wörtlich übernommene Stellen wurden als solche gekennzeichnet, sowie wurde die Satzung des Karlsruher Instituts für Technologie (KIT) zur Sicherung guter wissenschaftlicher Praxis beachtet. Des Weiteren erkläre ich, dass ich mich derzeit in keinem laufenden Promotionsverfahren befinde, und auch keine vorausgegangenen Promotionsversuche unternommen habe. Die elektronische Version der Arbeit stimmt mit der schriftlichen Version überein und die Primärdaten sind gemäß Abs. A (6) der Regeln zur Sicherung guter wissenschaftlicher Praxis des KIT beim Institut abgegeben und archiviert.

Karlsruhe, den 19. Dezember 2024

Sven Schneider

Abstract

Polymers are an important substance class of materials, which have become an indispensable part of everyday life. From adhesives in automotive industry and electronic devices, via protective gear in sports through to dental technology, polymeric materials cover a broad field of applications with their countless properties. Among this class of material, sequence-controlled multiblock copolymers present a new and interesting special type of polymer, which convinces with its versatility and adaptability. Built from multiple different monomers, each building block contributes with their properties to the overall characteristics of the final structure, resulting in polymeric materials that combine the individual features or create new traits in one chain. A traditional way to obtain such sequence-controlled multiblock copolymers is by using polymerization techniques like Reversible Addition–Fragmentation Chain-Transfer (RAFT) polymerization, which allow for multiple polymerization steps in succession, as well as a high degree of control in terms of chain length and dispersity. However, depending on the number of desired building blocks and properties, a large variety of monomers is necessary, which can result in extensive monomer syntheses if not commercially available. Based on the complexity of each monomer molecule, these procedures can be laborious, time consuming and expensive. Additionally, depending on the reactivity of each monomer, complications during the chain extension (CE) process can occur, leading to side reactions or even failure of the synthesis.

In the present thesis, the topic of multiblock copolymers was addressed by developing and investigating a new technique, which only requires a single functional monomer instead of multiple different ones. Therefore, a system containing of CE reactions via Reversible-Deactivation Radical Polymerization (RDRP) as well as living ionic polymerizations and Post-Polymerization Modifications (PPMs) via thiol-ene is established, which resulted in the synthesis of multiblock copolymers with different functional pendant groups, derived from the same monomer.

The first major part of this work deals with the investigation of suitable polymerization techniques and the synthesis of different functional monomers. Thereby, first tests employing RDRP techniques like RAFT polymerization and Atom Transfer Radical Polymerization (ATRP) in combination with the functional active ester monomers pentafluorophenyl acrylate (PFPA) and pentafluorophenyl methacrylate (PFPMA) were conducted. After partially successful polymerizations and modification reactions,

these tests were aborted after unsuccessful CE reactions. Consequently, the focus was shifted away from radical polymerization techniques to ionic polymerizations, namely Cationic Ring-Opening Polymerization (CROP) and Anionic Ring-Opening Polymerization (AROP), of which the latter showed the most promising results. The alternating AROP of the functional epoxide allyl glycidyl ether (AGE) in combination with subsequent PPM reactions via thiol-ene reaction using different thiols, resulted in the successful synthesis of sequence-controlled multiblock copolymers based on a single monomer.

The second part of this thesis deals with the investigation of the limits of this newly established method. By reducing the average repeating unit of each added “block” to one, well-defined sequence-controlled macromolecules could be obtained, approaching the precision of sequence-defined polymers. Therefore, two different approaches were tested, one found on a kinetic approach due to the living character of the applied polymerization technique, the other based on a small feed excess of the monomer. While the first approach led to an inaccurate average repeating unit, the second approach was able to achieve the set goal of approximately one. In combination with subsequent thiol-ene reactions, precise macromolecules with different functional groups could be synthesized. Due to the anionic ring-opening character of the applied polymerization technique, as well as the addition of a single monomer, this method was called *Anionic Ring-Opening Monomer Addition*, short *AROMA*.

In summary, a new method to synthesize sequence-controlled multiblock copolymers with a single monomer could be successfully established by combining AROP with PPM reactions. In comparison to the more traditional way, in which multiple different monomers are necessary, this system only uses a single functional monomer. Thereby, possible tedious, time consuming and sometimes costly monomer syntheses can be reduced to a minimum, simplifying the synthesis of sequence-controlled multiblock copolymers. In addition, in an anionic ring-opening monomer addition (*AROMA*), this system is used to generate macromolecules with an average repeating unit of one, making them similar to sequence-defined polymers.

Zusammenfassung

Polymere sind eine wichtige Werkstoffklasse, welche für den Alltag unverzichtbar geworden ist. Von Klebstoffen in der Autoindustrie und elektronischen Geräten, über Schutzausrüstung im Bereich Sport, bis hin zur Zahntechnik, Kunststoffe decken mit ihren zahllosen Eigenschaften ein breites Anwendungsgebiet ab. Ein interessanter Spezialfall unter den Polymeren bilden die sequenzkontrollierten Multiblock-Copolymere, die durch ihre Vielseitigkeit und Anpassungsfähigkeit auffallen. Dabei ist jeder Blockteil des Polymers durch ein einziges Monomer aufgebaut, welches bestimmte charakteristischen Eigenschaften mit sich bringt und so die Gesamteigenschaft der Kette beeinflusst. Die Merkmale der Kette können dabei die Summe der Eigenschaften der einzelnen Blockteile, oder eine völlig neue sein. Eine mögliche Synthesemethode solcher sequenzkontrollierten Multiblock-Copolymere ist die Reversible Additions-Fragmentierungs Kettenübertragungspolymerisation (*engl.*: RAFT polymerization), welche eine fortlaufende Polymerisation ermöglicht, sowie Kontrolle über die Kettenlänge und Dispersität erlaubt. Abhängig von den gewünschten Eigenschaften und der Anzahl der Blöcke sind viele verschiedene Monomere notwendig. Dies kann, je nach Komplexität der Monomere, einen zeit- und kostenintensiven Syntheseaufwand bedeuten, falls die Monomere kommerziell nicht erhältlich sind. Neben diesen Punkten spielt die Reaktivität der Monomere bei der Kettenerweiterung ebenfalls eine wichtige Rolle, da Inkompatibilität zwischen Monomer und reaktivem Kettenende zu ungewollten Nebenreaktionen, bis hin zum Scheitern der Reaktion, führen kann.

Diese Dissertation widmet sich unter anderem diesen Themen. So wurde eine neue Technik entwickelt, bei der für die Synthese sequenz-kontrollierter Multiblock-Copolymere nicht wie üblich mehrere verschiedene, sondern nur ein einziges, funktionelles Monomer verwendet wird. Es wurden verschiedene Systeme untersucht, welche alle auf einer Kombination aus Kettenerweiterungsreaktionen via radikalischer Polymerisation mit reversibler Deaktivierung oder lebender ionischer Polymerisation mit Postpolymerisationsmodifikationen (PPM) Reaktionen basieren. Die dadurch gewonnenen Multiblock-Systeme sind alle durch das gleiche Monomer aufgebaut, besitzen jedoch unterschiedliche, funktionelle Seitengruppen.

Im ersten Teil der Arbeit geht es dabei um die Suche einer geeigneten Polymerisationstechnik und der Synthese verschiedener funktioneller Monomere. Die

ersten Tests fokussierten sich dabei auf radikalische Polymerisationen mit reversibler Deaktivierung wie der RAFT-Polymerisation und der radikalischen Atomtransferpolymerisation (*engl.*: ATRP) mit den Aktivstermonomeren Pentafluorophenylacrylat (PFPA) und Pentafluorophenylmethacrylat (PFPMA). Nach dem teilweisen Erfolg im Bereich der Polymerisationen und Modifikationen wurden die Tests nach fehlgeschlagenen Kettenerweiterungsreaktionen und unzureichenden Ergebnissen abgebrochen, weshalb der Fokus stattdessen auf ionischen Polymerisationstechniken, wie der kationischen und anionischen ringöffnenden Polymerisation (*engl.*: CROP und AROP) gelegt wurde. Dabei erzielte Letztere die vielversprechendsten Ergebnisse. Die abwechselnde Polymerisation des funktionellen Epoxids Allylglycidylether (AGE) in Kombination mit darauffolgender PPM durch Thiol-ene Reaktionen verschiedener Thiole, führte zur erfolgreichen Synthese sequenzkontrollierter Multiblock-Copolymeren, basierend auf einem einzelnen Monomer.

Der zweite Teil der Arbeit beschäftigt sich mit der Untersuchung der Grenzen des neuentwickelten Systems. Kann die durchschnittliche Wiederholeinheit eines „Blocks“ auf Eins reduziert werden, wäre die Synthese sequenzkontrollierter Makromoleküle möglich, welche der Präzision sequenzdefinierter nahek kommt. Um dies zu erreichen, wurden zwei verschiedene Ansätze untersucht, bei der ein Ansatz auf dem lebenden Charakter der Polymerisationstechnik basiert und der andere sich einem geringen Monomerüberschuss zunutze macht. Der erste Ansatz führte dabei zu unpräzisen Wiederholeinheiten. Durch die zweite Methode konnten Makromoleküle mit einer durchschnittlichen Wiederholeinheit von Eins erzielt werden. In Kombination mit darauffolgenden Thiol-ene Reaktionen war die Synthese präziser Polymere mit unterschiedlichen funktionellen Gruppen möglich. Aufgrund des anionisch ringöffnenden Charakters der angewendeten Polymerisationstechnik und der Addition einer einzigen Monomereinheit an die Kette, wurde die Technik anionische ringöffnende Monomeraddition, kurz AROMA, genannt.

Zusammenfassend lässt sich sagen, dass eine neue Methode zur Synthese sequenzkontrollierter Multiblock-Copolymere erfolgreich etabliert wurde, die auf der Kombination von AROP mit PPM basiert. Im Vergleich zu der eher herkömmlichen Methode, bei der mehrere unterschiedliche Monomere nötig sind, verwendet die hier gezeigte Methode nur ein einziges funktionelles Monomer, wodurch die Synthese

sequenzkontrollierter Multiblock-Copolymere vereinfacht und zeit- und kostenintensive Monomersynthesen auf ein Minimum reduziert werden kann. Zusätzlich kann das System dazu verwendet werden, um in einer anionischen ringöffnenden Monomeraddition (AROMA) Makromoleküle herzustellen, welche eine durchschnittliche Wiederholeinheit von Eins besitzen und somit sequenzdefinierten Polymeren ähneln.

Table of Contents

Abstract.....	I
Zusammenfassung.....	III
Table of Contents	VI
1. Introduction.....	1
2. Theoretical Background.....	4
2.1. Ionic Polymerization	4
2.1.1. Anionic Polymerization	4
2.1.2. Cationic Polymerization	8
2.2. Reversible-Deactivation Radical Polymerization	10
2.2.1. Atom Transfer Radical Polymerization	11
2.2.2. Reversible Addition-Fragmentation Chain-Transfer Polymerization	12
2.2.3. Nitroxide-Mediated Polymerization	14
2.3. Post-Polymerization Modification	15
2.4. Copolymers and their Types	17
2.5. Applications of Allyl Glycidyl Ether in Polymer Chemistry	20
3. Motivation and Goal	22
4. Results and Discussion	25
4.1. Synthesis of Multiblock Copolymers by Combining CE and PPM reactions...	25
4.1.1. General Prerequisites for the Choice of Monomer.....	25
4.1.2. Multiblock Copolymer Synthesis via RAFT Polymerization	27
4.1.3. Multiblock Copolymer Synthesis via ATRP	37
4.1.4. Multiblock Copolymer Synthesis via CROP	41
4.1.5. Multiblock Copolymer Synthesis via AROP	45
4.1.5.1. Synthesis of a Sequence-Controlled Network.....	62
4.2. AROMA - Anionic Ring-Opening Monomer Addition	66

4.2.1. Anionic Ring-opening Monomer Addition of AGE to Methoxy Polyethylene Glycol	67
4.2.2. Anionic Ring-Opening Monomer Addition via Kinetic Approach	70
4.2.3. Anionic Ring-Opening Monomer Addition via Monomer Excess Approach	75
5. Conclusion and Outlook	90
6. Experimental Part	93
6.1. Instruments	93
6.1.1. Nuclear Magnetic Resonance (NMR) Spectroscopy	93
6.1.2. Size Exclusion Chromatography (SEC)	93
6.1.3. Attenuated Total Reflection Fourier-Transform Infrared (ATR FT-IR) Spectroscopy.....	94
6.1.4. Differential Scanning Calorimetry (DSC)	94
6.2. Chemicals	95
6.3. Synthetic Procedures	96
6.3.1. Synthetic Procedures for “Multiblock Copolymer Synthesis via RAFT Polymerization”	96
6.3.1.1. Synthesis of Pentafluorophenyl Acrylate.....	96
6.3.1.2. Reversible Addition-Fragmentation Chain Transfer Polymerization of PFFPA with CDTPA.....	98
6.3.1.3. Post-Polymerization Modification of PFFPA with 2,2,2-Trifluoroethylamine	102
6.3.1.4. Chain Extension Reaction of Modified PFFPA with PFFPA.....	104
6.3.1.5. Base Stability Test of CDTPA with DMAP.....	106
6.3.1.6. Post-Polymerization Modification of PFFPA with 2,2,2-Trifluoroethanol	109
6.3.1.7. Chain Extension Reaction of Modified PFFPA with PFFPA.....	112
6.3.2. Synthetic Procedures for “Multiblock Copolymer Synthesis via ATRP” .	114
6.3.2.1. Synthesis of Pentafluorophenyl Methacrylate	114

6.3.2.2. Atom Transfer Radical Polymerization of PFPMA with EBiB and dNbp	116
6.3.2.3. Post-Polymerization Modification of PFPMA with 2,2,2-Trifluoroethylamine	119
6.3.2.4. Post-Polymerization Modification of PFPMA with 2,2,3,3,3-Pentafluoropropylamine	121
6.3.3. Synthetic Procedures for “Multiblock Copolymer Synthesis via CROP”	123
6.3.3.1. Cationic Ring-Opening Polymerization of CL	123
6.3.3.2. First Chain Extension Reaction of PCL with CL	125
6.3.3.3. Second Chain Extension Reaction of PCL with CL	127
6.3.3.4. Synthesis of α -Allyl-Caprolactone	129
6.3.3.5. Cationic Ring-Opening Polymerization of ACL	131
6.3.3.6. First Chain Extension Reaction of PACL with CL	133
6.3.4. Synthetic Procedures for “Multiblock Copolymer Synthesis via AROP”	135
6.3.4.1. Anionic Ring-Opening Polymerization of AGE using P ₄ -t-Bu	135
6.3.4.2. Post-Polymerization Modification of PAGE via Thiol-ene reaction using 1-Dodecanethiol	137
6.3.4.3. First Chain Extension of Modified PAGE with AGE and P ₄ -t-Bu	139
6.3.4.4. Post-Polymerization Modification of Once Chain Extended PAGE via Thiol-ene reaction using Benzyl Mercaptan	144
6.3.4.5. Second Chain Extension of Modified PAGE with AGE and P ₄ -t-Bu	146
6.3.4.6. Post-Polymerization Modification of Twice Chain Extended PAGE via Thiol-ene Reaction using Methyl-3-mercaptopropionate	148
6.3.4.7. Post-Polymerization Modification of Twice Chain Extended PAGE via Thiol-ene Reaction using Pentaerythritol tetrakis(3-mercaptopropionate)	151
6.3.4.8. Anionic Ring-Opening Polymerization of AGE using P ₄ -t-Bu without Initiator	154
6.3.5. Synthetic Procedure for “AROMA – Anionic Ring-Opening Monomer Addition”	156

6.3.5.1. Anionic Ring-Opening Polymerization of AGE using P ₄ -t-Bu with mPEG-1900 as Initiator.....	156
6.3.5.2. Kinetic Studies of the Polymerization of AGE using mPEG-1900 as Initiator	158
6.3.5.3. 1. Method: Chain Extension Reaction of mPEG-1900 with AGE using P ₄ -t-Bu based on the Kinetic Approach.....	160
6.3.5.4. 2. Method: Chain Extension Reaction of mPEG-1900 AGE using P ₄ -t-Bu based on Small Monomer Excess Approach (1. AROMA)	164
6.3.5.5. Post-Polymerization Modification of Once Chain Extended mPEG-1900 via Thiol-ene Reaction using 1-Dodecanethiol.....	168
6.3.5.6. Second Chain Extension Reaction of mPEG-1900 with AGE using P ₄ -t-Bu (2. AROMA).....	172
6.3.5.7. Post-Polymerization Modification of Twice Chain Extended mPEG-1900 via Thiol-ene Reaction using Benzyl Mercaptan	176
6.3.5.8. Third Chain Extension Reaction of mPEG-1900 with AGE using P ₄ -t-Bu (3. AROMA)	178
6.3.5.9. Post-Polymerization Modification of Thrice Chain Extended mPEG-1900 via Thiol-ene Reaction using Methyl-3-mercaptopropionate ...	180
7. Abbreviations.....	182
8. List of Figures	188
9. List of Schemes	198
10. List of Tables	202
11. Acknowledgments	203
12. Literature	205
13. Publications & Conference Contributions.....	225

1. Introduction

Polymers are a class of materials that are indispensable in today's society, finding application in a broad range of areas, reaching from everyday's tools like smartphones and drinking bottles to more specific uses in aerospace,^{1,2} dental technology^{3,4} and protective gear like bulletproof vests.⁵ The properties of a polymer and therefore its field of application are influenced by multiple factors, e.g., the choice of monomer, number of repeating units/chain length and the overall chain structure. Especially the macromolecule architecture is of high interest, because even though two macromolecules can be based on the same monomer, a difference in their chain structure results in different properties. One example for such a case are two constitutional isomers of polyethylene, low-density polyethylene (LDPE) and high-density polyethylene (HDPE). The former has a higher branched structure than the latter, leading to a lower crystallinity making it more flexible and softer.⁶ Therefore, LDPE is frequently used in dispensing and wash bottles, but also in plastic bags, while HDPE is used for pipe systems and outdoor furniture. Ultra-high-molecular-weight polyethylene (UHMWPE), a special kind of polyethylene (PE) with over 100,000 monomer units per molecule,⁷ is even used for total joint replacements^{8,9} and climbing equipment.¹⁰

Therefore, full control over the exact structure of a macromolecular chain is of high interest in the fields of polymer chemistry and materials science. A common synthetic way to achieve such control is by using living or controlled polymerization methods. The term living polymerization was firstly coined by Szwarc¹¹ in the 1950s, describing a polymerization with (i) absent termination or transfer reactions and (ii) a higher chain initiation rate than its propagation rate, leading to a constant number of active chains throughout the polymerization process. Two kinds of polymerization techniques fulfill those requirements, namely the anionic and cationic polymerization. Those methods can be used to obtain macromolecular systems with a defined number of repeating units, tailored molar mass and low dispersity ($\bar{D} = 1.01 - 1.11^{12}$). Controlled radical polymerization or Reversible-Deactivation Radical Polymerization (RDRP) are similar to living polymerizations, but do not fulfill all the requirements to be called living, because there are termination steps present. Hence, the International Union of Pure and Applied Chemistry (IUPAC) recommended the term RDRP instead of "living", but also allows the use of "controlled" polymerization as long as the type is defined at its

first occurrence.¹³ Three prominent examples for RDRP are Atom Transfer Radical Polymerization^{14,15} (ATRP), Nitroxide-Mediated Polymerization¹⁶ (NMP) and Reversible Addition–Fragmentation Chain-Transfer¹⁷ (RAFT) polymerization.

Beside the syntheses of homopolymers with tailored molar mass and chain length, living and controlled polymerization techniques can be used to synthesize multiblock copolymers by adding a new type of monomer to the reaction mixture, extending the active chain.¹⁸

If multiple monomers are added in a specific sequence, the preparation of *sequence-controlled polymers* is possible. Examples of such macromolecules can also be found in nature with deoxyribonucleic acid (DNA) being probably one of the most well-known examples. While synthetically prepared sequence-controlled polymers usually have a $\mathcal{D} > 1$, DNA has a unified chain length, leading to a \mathcal{D} of exactly one. These types of macromolecules/polymers are called *sequence-defined polymers* instead of sequence-controlled.

The control over the sequence is of high interest, because it allows for the preparation of polymeric material which find application in different fields, reaching from drug delivery^{19,20} over antimicrobial peptides^{21,22} to information storage.²³

Over the decades, efforts were made to close the gap in precision between artificial and natural polymers by improving synthetic processes, such as the utilization of solid-phase chemistry,^{24,25} though they are still vastly tedious.²⁶ Many man-made macromolecules, which are truly of controlled design, are mostly limited to biopolymers (e.g., proteins and nucleic acids), or of oligomeric nature such as peptidomimetics.²⁷

However, in comparison to biomolecules, non-natural based polymers could be seen as more beneficial, due to structural and chemical diversity, scalability and better environmental and biological stability,^{26,28} but their synthesis is still challenging.

In more recent years, new synthetic ways based on “classic” polymerization methods emerged, which utilize RDRP techniques for instance. Two promising examples are the RAFT approach by Moad and co-workers²⁹ as well as an ATRP variation by Tong et al.,³⁰ in which single monomer units are added together successively in sequence. Even with all the progress made, synthetic polymers made by “classic polymerization” techniques are typically based on radical approaches and still lack in terms of control in comparison to the natural counterparts, leaving room for new synthetic ways and further research.²⁶

With regards to the composition of a (sequence-controlled) multiblock copolymer, usually each block is constructed by one kind of monomer, making it necessary to have multiple different monomers available of which each has an influence on the macromolecule's properties. However, if the needed monomers are commercially not available, they need to be synthesized, which can be tedious and costly at times, making cheap and accessible molecules desirable. Additionally, the reactivity between the monomer and the propagating chain plays a significant role. If they differ too much, incomplete CEs and undesired side reactions could occur, leading to imperfections unsuitable for a multiblock copolymer synthesis. Due to the correspondence between the conjugated acid of the propagating chain end and the monomer, less reactive monomers lead to more reactive chain ends and contrariwise.³¹ A prominent example for this is the copolymerization of styrene and methyl methacrylate.³¹

A different way to influence properties of a polymer is by modifying pre-synthesized macromolecular chains after their synthesis. A prerequisite for such a PPM³² or polymer analogues modification, is the incorporation of functional monomers in the pre-polymer, which are available to subsequent reactions. Examples for such reactions are the aminolysis of poly(pentafluorophenyl methacrylate) (PPFPMA) with e.g., allylamine³³ or the thiol-ene reaction of poly(allyl ethylene glycol vinyl ether)s with different thiols³⁴.

To bypass the necessity of multiple different monomers, as stated above, the utilization of a single monomer in combination with PPM would be desirable. Therefore, this thesis will aim on implementing a new system, in which living/controlled polymerization techniques are combined with PPM reactions, resulting in a synthesis of sequence-controlled multiblock copolymers using a single monomer.

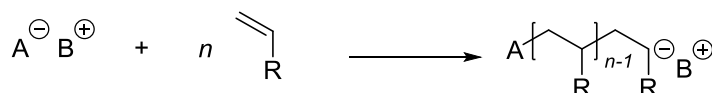
2. Theoretical Background

This chapter will give a short overview about the theoretical background of different ionic and radical based polymerization techniques, post-polymerization modification and multiple types of copolymers.

2.1. Ionic Polymerization

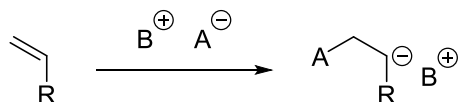
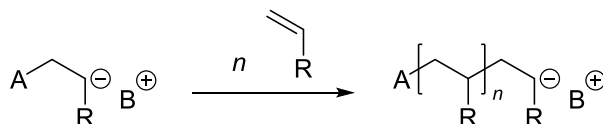
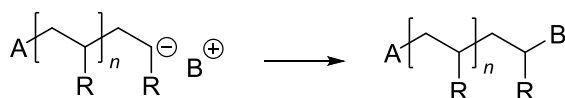
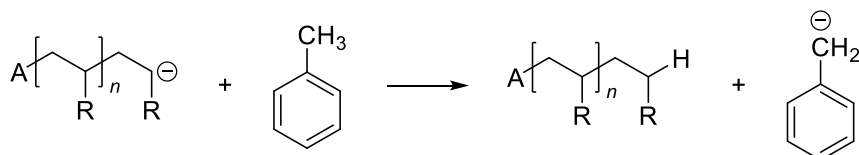
2.1.1. Anionic Polymerization

The anionic polymerization describes an ionic chain-growth polymerization in which the active chain end carries an anion.³⁵ In the beginning, an initiator reacts with a monomer, forming a transient species with an anionic functionality (refer to **Scheme 1**). This species can react with further monomers, extending the chain each time to create a macromolecule eventually. Common monomers are vinyl based and contain an electron withdrawing substitute, with styrene,^{36,37} 1,3-butadiene^{38,39} and acrylonitrile^{40–42} being typical monomers for anionic polymerization.⁴³ However, cyclic molecules like ethylene oxide^{44,45} (EO) and ϵ -caprolactone⁴⁶ (CL) can also be polymerized via an anionic ring-opening polymerization (AROP), which will be discussed in a later part of this chapter.



Scheme 1: Reaction of an anionic initiator with a monomer, forming an active macromolecule.

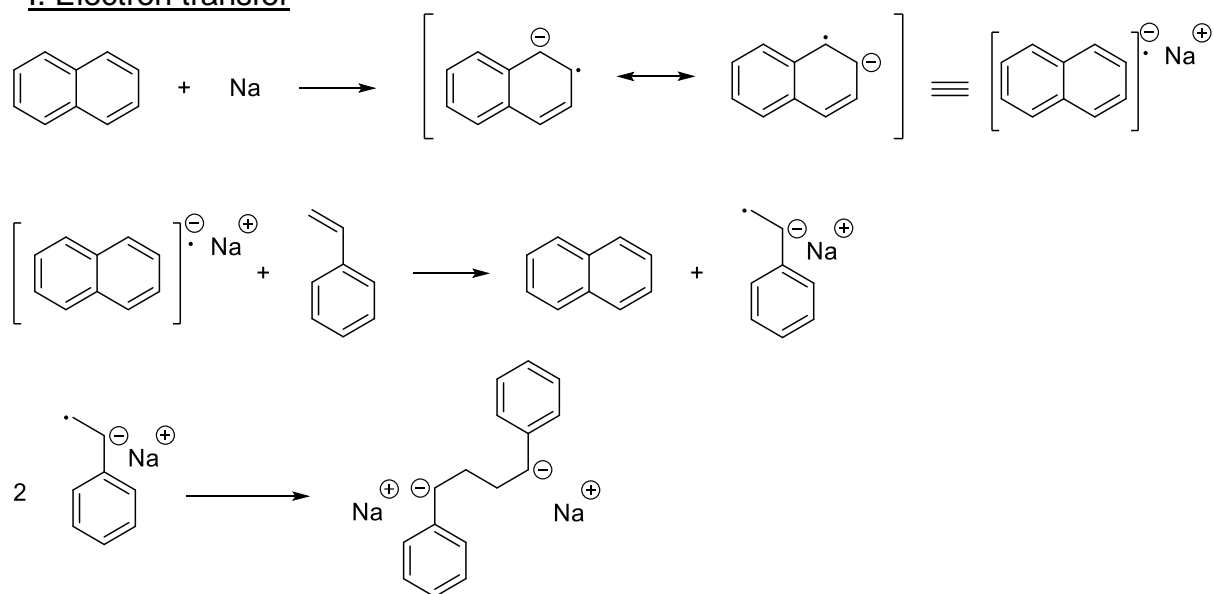
The general polymerization mechanism is similar to the one of a free radical polymerization and can be divided into four steps, namely (I) initiation, (II) propagation (III) termination and (IV) transfer (see **Scheme 2**).

I. InitiationII. PropagationIII. TerminationIV. Transfer

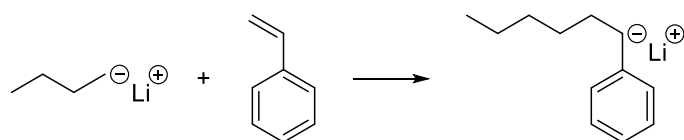
Scheme 2: Mechanism of the anionic polymerization divided into (i) initiation, (ii) propagation, (iii) termination and (iv) transfer. Redrawn after reference.⁴³

The initiation of an anionic polymerization mainly can take place in two ways: (i) initiation either by single electron transfer or (ii) nucleophilic addition. An example for the former is the initiation of styrene with sodium naphthalene, forming a difunctional propagating species by a radical coupling reaction (refer to **Scheme 3; I.**), while the initiation of styrene by *n*-butyllithium (*n*-BuLi) is an example for the latter (see **Scheme 3; II.**).⁴³ In case of *n*-Buli as initiator, the choice of solvent also plays an important role, since in hydrocarbon solvents, for example, the structure is hexameric instead of monomeric.⁴⁷

I. Electron transfer



II. Nucleophilic addition



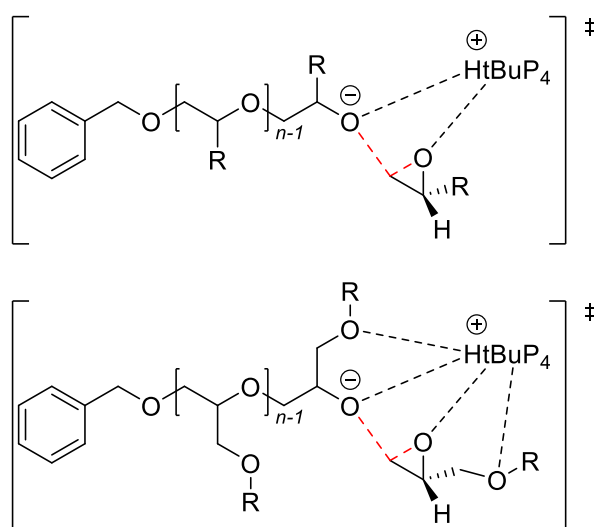
Scheme 3: (I) Initiation of styrene by single electron transfer using sodium naphthalene. Two possible resonance structures of the naphthalene radical anion are displayed. (II) Initiation of styrene by the nucleophilic addition using *n*-butyllithium. Redrawn after reference.⁴³

The termination and transfer processes that occur during an anionic polymerization differ significantly from those of a radical chain growth polymerization. Due to the repulsion of the equally charged anionic chain ends, a recombination of two chains is not possible,⁴⁸ while it is a well-known observation in radical polymerizations.⁴⁹ However, termination reactions still can occur in anionic polymerizations, primarily due to impurities (e.g., water) in the reaction mixture. Another possibility is the transfer reactions of the active chain end with solvent molecules such as toluene (**Scheme 2**).⁴³ Herein, the polymer chain is terminated but the kinetic chain growth continues.

As briefly mentioned above, cyclic monomers can also be polymerized via an anionic polymerization variation, which is known as AROP. In case of three-membered heterocycles, the high ring strain allows for their polymerization, while carbonyl group containing cyclic systems (e.g., lactones and lactams) are prone to nucleophilic attacks, whereas ring size influences the ring opening efficiency.⁴³

One example for such an AROP is the metal-free synthesis of homo- and diblock copolyethers at ambient temperature, using the epoxide allyl glycidyl ether (AGE) as monomer, which was presented by Ree's group in 2012.⁵⁰ In their work, the *Schwesinger base* 1-tert-Butyl-4,4,4-tris(dimethylamino)-2,2-bis[tris(dimethylamino)-phosphoranylideneamino]-2λ5,4λ5-catenadi(phosphazene) (P_4 -*t*-Bu), introduced by Reinhard Schwesinger,⁵¹ was applied as a promoter, allowing for the preparation of well-defined polymers with \bar{D} down to 1.08 under almost quantitative conversion. However, already in 1996, the utilization of strong phosphazene bases such as P_4 -*t*-Bu for the AROP of epoxides was investigated by Möller's group,⁵² setting the foundation for further research.

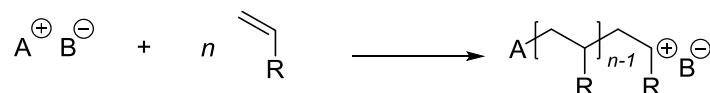
The suggested AROP mechanism proceeds via a tri-molecular transition state consisting of a monomer unit, the propagating center and the counter cation.⁵³ In the case of P_4 -*t*-Bu, the base acts as a Lewis acid, interacting with a monomer unit and the anionic propagating center (displayed in **Scheme 4**).⁵³



Scheme 4: Transition state of the monomer addition of an epoxide promoted by P_4 -*t*-Bu, depending on the substituents. Redrawn after reference.⁵³

2.1.2. Cationic Polymerization

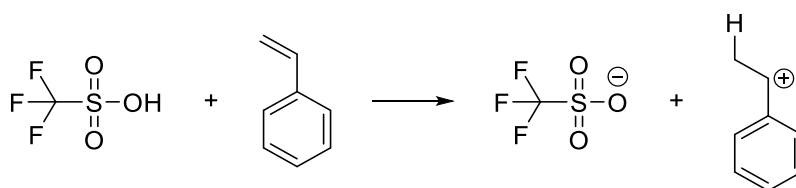
In addition to anionic polymerization, cationic polymerization is another ionic polymerization method. In contrast to the former, the reactive species of the latter is of cationic nature (see **Scheme 5**).



Scheme 5: Cationic initiation of a vinyl monomer, creating an active macromolecule in the end.

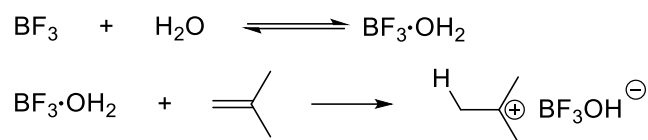
Opposite to the anionic polymerization, typical vinyl-based monomers for cationic polymerization inherent electron-donating substituents, e.g., alkoxy or aromatic⁵⁴ groups, to stabilize the active chain end by increasing the C=C double bond's electron density.³⁵ Prominent monomer examples are isobutylene,^{55–57} vinyl ethers such as cyclohexyl vinyl ether^{58–60} and styrene.^{61–63}

Like the anionic polymerization, the mechanism of the cationic polymerization is split into four steps: (I) initiation, (II) propagation, (III) termination and (IV) transfer. The two established ways to initiate the cationic polymerization are by protonic^{64,65} or Lewis acids.^{66–68} The former interacts with the C=C double bond of the monomer, resulting in a carbocation, which in turn can form a macromolecule by adding monomer units to the chain over time (refer to **Scheme 6**).



Scheme 6: Cationic polymerization of styrene using the protonic acid initiator trifluoromethanesulfonic acid.⁶⁹

The initiation via a Lewis acid requires beside the acid a co-initiator such as water,⁷⁰ acting as a proton source, or cationogens like alkyl halides.⁷¹ An exemplary system is the polymerization of isobutylene with water and boron trifluoride (displayed in **Scheme 7**³⁵), in which the initiator complex is also often depicted as $H^+(BF_3OH)^-$.



Scheme 7: Cationic polymerization of styrene using the Lewis acid boron trifluoride with water as co-initiator. Redrawn after reference.³⁵

Similar to anionic polymerization, termination and transfer reactions (e.g., impurities in the reaction mixture, covalent bonding with counter ion) occur to a small extent. Additionally, the unstable sp^2 -hybridized carbocation tends to β -proton elimination, turning the propagating chain end to an unsaturated inactive species.⁷² Meanwhile, the released proton can interact with monomer units to initiate propagation of a new macromolecule, continuing the kinetic chain.

Like the anionic polymerization, cationic polymerization also has a ring-opening variation, called cationic ring-opening polymerization (CROP) in which cyclic monomers can be polymerized. Similar to AROP, lactones,^{73–75} lactams^{76–79} and cyclic ethers are three of the possible monomer classes, with the polymerization of tetrahydrofuran⁸⁰ (THF) initiated by trimethylsilyl trifluoromethanesulfonate being a more specific example.

2.2. Reversible-Deactivation Radical Polymerization

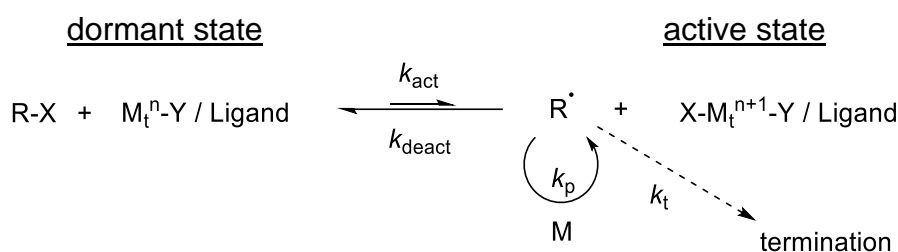
RDRP is like the ionic polymerization a way to obtain polymers with tailored molar masses, low \bar{D} and different architectures. However, in contrast to anionic and cationic polymerizations, the reactive species in RDRP is of radical nature rather than ionic. Furthermore, due to this radical nature and the subsequent unavoidable termination of two chains, IUPAC recommended the term RDRP instead of “living” radical polymerization.¹³

The most prominent examples of RDRP are ATRP, NMP and RAFT polymerization, which all use an equilibrium between an activated/active and deactivated/dormant species.⁸¹ In general, these methods can be described by two different mechanisms, reversible deactivation (NMP and ATRP) and degenerative transfer (RAFT).⁸² In case of the first mechanism, it is important that during the polymerization process the majority of chains are in the dormant state. This leads to a reduction of active radical chains in the reaction mixture and therefore minimizing the occurrence of termination reactions, ultimately resulting in a reaction in a living manner.⁸³

In the second case the overall number of radicals does not change during the activation-deactivation process, which is why an additional radical source is necessary.⁸² Additionally, another molecule is used, which acts as a chain transfer agent (CTA), enabling the equilibrium between the active and dormant species.⁸³

2.2.1. Atom Transfer Radical Polymerization

In 1995, the groups of Sawamoto¹⁴ and Matyjaszewski¹⁵ discovered ATRP independently of each other, which generally deploys alkyl halides (e.g., ethyl 2-bromoisobutyrate; EBiB^{84,85} and methyl 2-bromopropionate; MBP^{86,87}) as initiators and transition metal/ligand complexes as catalysts. As stated above, the mechanism is based on the equilibrium between an active and inactive state (see **Scheme 8**).



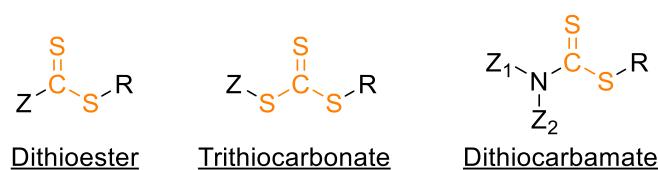
Scheme 8: General mechanism of ATRP showing the equilibrium between the dormant (left) and active (right) state. While the system is in the active state the propagation of the chain occurs. Redrawn after reference.⁸⁸

Via a one-electron oxidation and halogen abstraction of the metal complex (M_t^n-Y / Ligand) from the alkyl halide initiator ($R-X$), the equilibrium shifts from a previous dormant state to an active one with an activation rate k_{act} . In this state, monomer (M) units can add with a propagation rate k_p to the newly formed radical (R^\bullet) forming a macromolecular chain, before shifting back to the dormant state with the deactivation rate k_{deact} . Even though the concentration of active radical chains is reduced in the active state, termination reactions with a termination rate of k_t can occur.⁸⁸ A commonly used transition metal system is based on $\text{Cu(I)}/\text{Cu(II)}$,^{89–93} but other systems with metals like Fe ,^{94,95} Ru ^{96,97} and Os ⁹⁸ can also be found in literature. Important for the choice of metal is a one electron difference in the oxidation states, which also makes the ATRP sensitive towards oxygen.⁹⁹

While ATRP allows for the synthesis of polymers with special architectures such as star^{100–102} or bottlebrush^{103,104} polymers, the halogenide carrying chain end is one of the main advantages of the ATRP, because it grants access to further reactions (like the introduction of an allyl¹⁰⁵, propargyl¹⁰⁶ or azide¹⁰⁷ group), which can be used e.g., to generate α,ω -telechelic polymers¹⁰⁸ or introduce desired functionalities to the chain.

2.2.2. Reversible Addition-Fragmentation Chain-Transfer Polymerization

The RAFT polymerization was firstly discovered by the group of Rizzardo¹⁷ in 1998, describing a controlled polymerization in which CTAs, also known as RAFT agents, are utilized. Suitable agents are members of the class of dithioesters,^{109–111} trithiocarbonates^{112–114} and dithiocarbamates^{115,116} (displayed in **Scheme 9**).

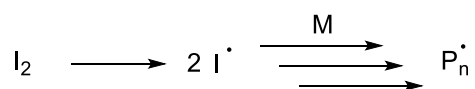
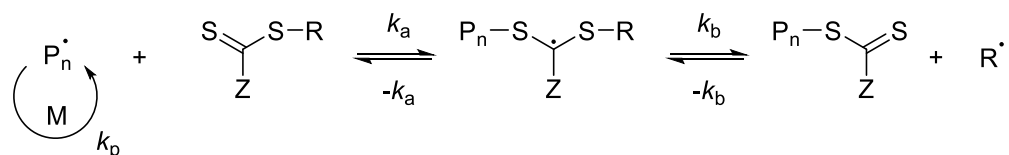
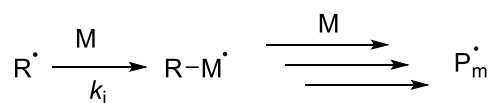
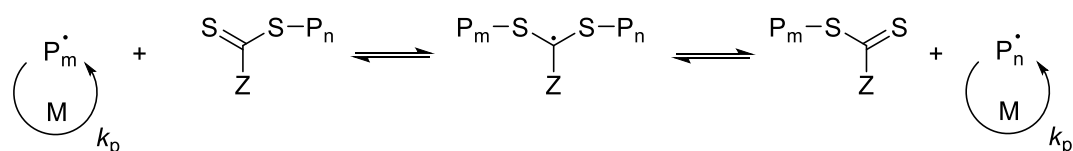
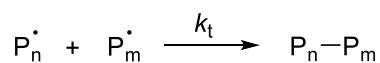


Scheme 9: Dithioester, trithiocarbonate and dithiocarbamate, three common classes of RAFT agents.

Hereby, R is a leaving group to (re)initiate the polymerization and Z a stabilizing group, influencing the reactivity of the C=S bond.¹¹⁷ The mechanism can be split into five parts: (I) Initiation, (II) reversible chain transfer, (III) reinitiation, (IV) chain equilibrium, (V) termination (refer to **Scheme 10**).

During the initiation step, a conventional initiator (I₂) such as 2,2'-Azobis(2-methylpropionitrile) (AIBN) breaks down into radicals, which subsequently react with monomer (M) units forming the reactive species P_n[•]. In the next step, this species reacts with the RAFT agent in a reversible chain transfer, which is also called pre-equilibrium,¹¹⁸ creating a stable radical intermediate, followed by the cleavage of a new radical species R[•]. In the third step, R[•] interacts with monomer (M) units to a reactive macromolecular chain P_m[•], similar to the initiation step. In the fourth step, the main-equilibrium¹¹⁸ between the cleavage of P_n[•] and P_m[•] from the RAFT agent is formed, in which the polymerization stays the rest of the time. Due to the radical character of the propagating chain, recombination of two active chains may occur, leading to their termination and a “dead” chain.¹¹⁹

The RAFT polymerization is ideal for building multiblock copolymers, which has been shown in an impressive way by Gody et al.¹²⁰ who synthesized an icosablock copolymer with a *Đ* of 1.36.

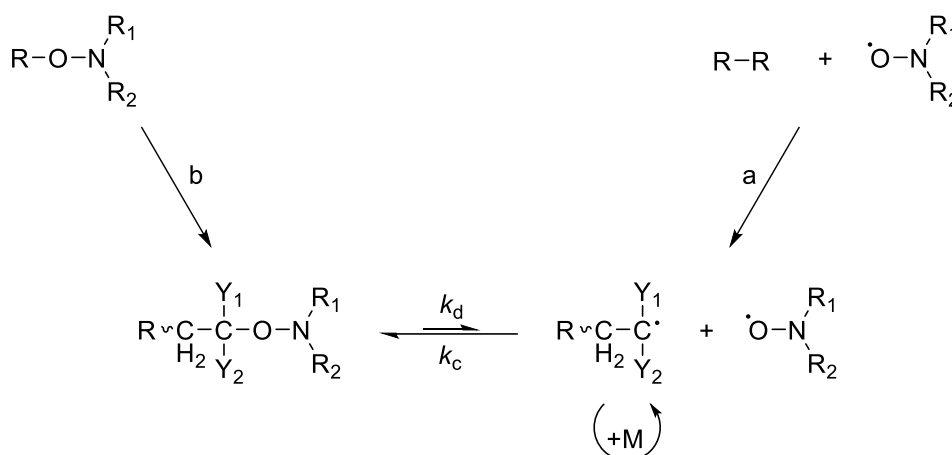
I. InitiationII. Reversible chain transfer (pre-equilibrium)III. ReinitiationIV. Chain equilibrium (main-equilibrium)V. Termination

Scheme 10: Schematic depiction of the general RAFT mechanism split into the respective parts: (I) Initiation, (II) reversible chain transfer, (III) reinitiation, (IV) chain equilibrium, (V) termination. Redrawn after reference.¹¹⁹

2.2.3. Nitroxide-Mediated Polymerization

NMP was firstly patented by Solomon and Rizzardo in 1986¹⁶ and is therefore the oldest RDRP method of the three described in this thesis. It uses alkoxyamines as initiators, which can be homolytically cleaved under specific conditions, forming a stable radical. The control is achieved by utilizing the persistent radical effect (PRE), preventing the nitroxides from initiating the polymerization by themselves.¹²¹

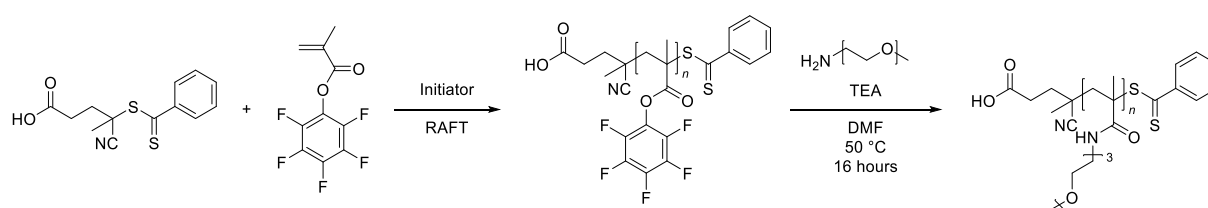
The general mechanism runs in two different ways, which are described in **Scheme 11**. In path a) a conventional radical initiator is paired with a free nitroxide creating a bicomponent initiating system (e.g., benzoyl peroxide (BPO) with (2,2,6,6-tetramethylpiperidin-1-yl)oxyl (TEMPO)),¹²² while path b) is a monocomponent system, in which only alkoxyamine^{123–125} is utilized. Due to the structure of the alkoxyamine, a 1:1 release ratio of radical to nitroxide during the dissociation process is achieved. This allows the monocomponent system to gain better control in comparison to the bimolecular system.¹²⁶



Scheme 11: General mechanism of NMP displaying two different approaches in which a) a conventional radical initiator or b) a monocomponent system is used. Redrawn after reference.¹²⁶

2.3. Post-Polymerization Modification

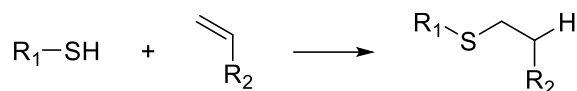
The properties of a polymeric material are influenced by a multitude of parameters, one of them is the choice of monomer. However, sometimes a desired monomer is unsuited for a given polymerization technique, due to possible side reactions between functional groups in the monomer and a reactive species such as the active chain end. One example would be the reaction of pendant alkene groups with the radical active species in RDRP techniques, which could lead to crosslinking. To avoid such unwanted reactions, the group responsible for the desired property is introduced into the polymer after the polymerization. In such a PPM,³² a reactive monomer is used to synthesize a precursor polymer, which subsequently is modified. An example for such a reaction is the RAFT polymerization of the functional active ester monomer PFPMA to PPFMA and the following aminolysis with monomethoxy triethyleneglycol amine, leading to a polymer with a pendant mPEG-group (displayed in **Scheme 12**).¹²⁷



Scheme 12: RAFT polymerization of PFPMA with subsequent PPM via aminolysis with monomethoxy triethyleneglycol amine to form a polymer with a pendant mPEG-group. Redrawn after reference.¹²⁷

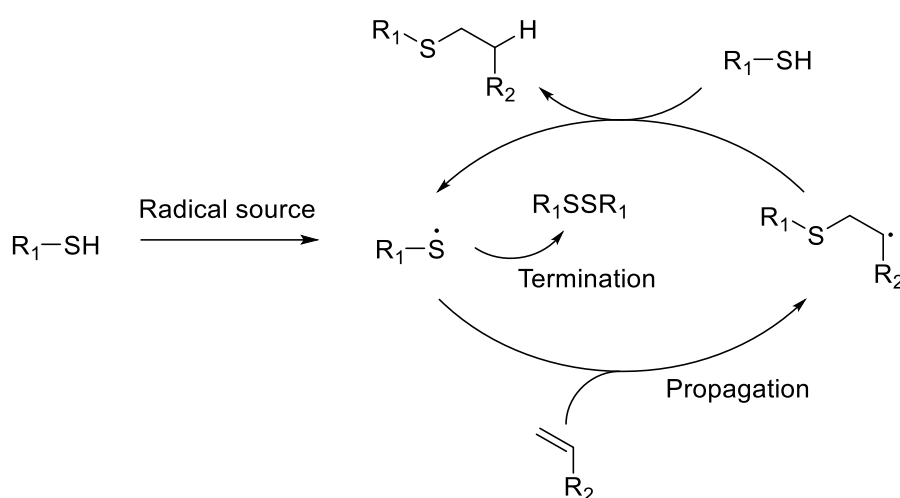
An especially interesting functional group are pendant C=C double bonds, due to their further use in other reactions such as “click”-reactions or inverse vulcanization (IV). The prior was firstly introduced by the group of Sharpless¹²⁸ in 2001, for which he received a Noble Prize in chemistry in 2022. A “click” reaction describes a reaction with simple reaction conditions, which is stereospecific, leads to inoffensive byproducts and has very high yields. Furthermore, starting components are commercially available and solvents should be excluded or at least easily removable.¹²⁸ Prominent examples for “click” or “click-like” reactions are the copper(I)-catalyzed alkyne-azide cycloaddition (CuAAC)^{129–131} and the thiol-ene reaction^{132–134}.

The latter of those two examples was already reported by Posner¹³⁵ in 1905 and describes a hydrothiolation of a C=C double bond via a radical or nucleophilic mechanism (see **Scheme 13**).



Scheme 13: General depiction of a thiol-ene reaction of a primary thiol with a double bond either by radical or the nucleophilic mechanism. Redrawn after reference.¹³⁶

The electron density of the C=C double bond dictates which mechanism is favored. While electron-deficient systems follow the catalyzed Michael addition, any C=C double bond can follow the radical addition,¹³⁷ initiated via a chemical initiator or UV radiation¹³⁸ (displayed in **Scheme 14**).



Scheme 14: Catalytic cycle of the thiol-ene reaction including the steps of thiyl radical formation by a radical source and the subsequent propagation. After a proton abstraction the desired product is formed. Redrawn after reference.¹³⁹

The mechanism of the radical addition includes the creation of a thiyl radical followed by its reaction with the C=C double bond in the propagation step. The newly formed alkyl radical abstracts the hydrogen of a thiol forming the new product in the anti-Markovnikov orientation, as well as a new thiyl radical, which continues the cycle until the termination with another radical.¹³⁹

2.4. Copolymers and their Types

If multiple monomers are used during a polymerization process, the resulting polymer is called copolymer. These polymers are highly interesting, because their properties are influenced by the used monomers, their ratio and how they are aligned along the chain.¹⁴⁰ There are five main groups of copolymers (I) statistical, (II) gradient, (III) alternating, (IV) block and (V) graft copolymer (refer to **Scheme 15**).

In a statistical copolymer the embedment of monomer units follows statistical laws, such as Markovian statistics of different orders. However, in literature statistical copolymers are often described as random copolymers, which is not perfectly correct. Due to the clustering of monomer units or other kinds of interactions between them, the statistical equation does not follow *a priori* principles and leads to a sequence distribution, which can be indicated by the numerical values of a function of reactivity ratios or related run numbers. A truly random copolymer is therefore only given if the probability of a given unit at any position is independent of its neighboring units.¹⁴¹ Statistical copolymers can be achieved by free radical homogeneous and heterogeneous polymerization of acrylonitrile and methyl acrylate, as shown by Bhanu et al..¹⁴²

The term gradient copolymer is used if the chain structure starts with monomer A and gradually changes to monomer B. Jouenne et al.¹⁴³ synthesized a styrene/butadiene gradient block copolymer via anionic polymerization.

In an alternating copolymer, units of monomer A and B are built into the backbone in alternating turns. An example is the copolymerization of styrene and maleic anhydride.¹⁴⁴

Diblock copolymers can be obtained via multiple ways. One option is to firstly polymerize monomer A until full conversion is achieved and then the subsequent addition and polymerization of monomer B. Alternatively, a precursor polymer derived of monomer A can be used as a macroinitiator for the polymerization of monomer B, also creating a diblock copolymer. Finally, two homopolymers, PA and PB, can be attached together e.g., with reactive groups at their chain ends and via a “click” reaction. An example for a multiblock copolymer consisting of multiple monomers is the icosablock copolymer presented by Gody et al..¹²⁰

In a graft polymer, the backbone of the chain is built by a single monomer with pendent chains of monomer B. A well-known example for graft copolymers is based on styrene and butadiene.¹⁴⁵

An effect which needs to be considered in copolymeric materials is the phase separation of block segments which are immiscible. Depending on the composition and ratio of the block segments, seven different morphologies can be self-assembled with four being (I) spherical, (II) cylindrical, (III) gyroidal and (IV) lamellar while the last three are the inverse of them.¹⁴⁶

I. Statistical



II. Gradient



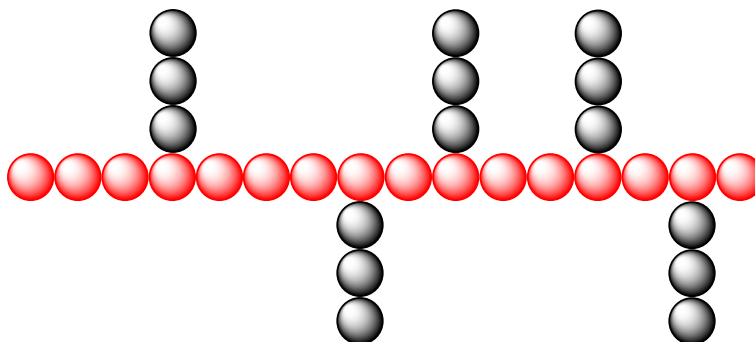
III. Alternating



IV. Block



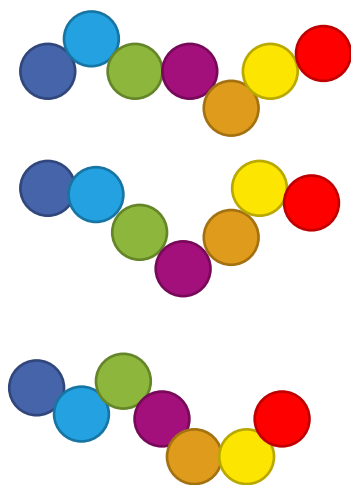
V. Graft



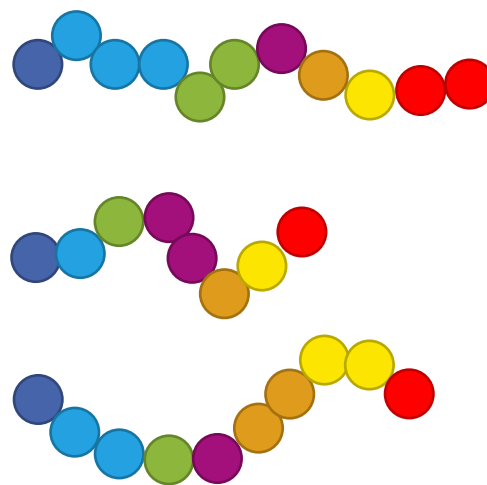
Scheme 15: Exemplary depiction of the five main groups of copolymers (I) statistical, (II) gradient, (III) alternating, (IV) block and (V) graft copolymer.

If the sequence of the added monomers takes place in a specific order, the obtained structures are called sequence-controlled or sequence-defined polymers. Even though both types of polymers have something in common, there is a specific difference. In both cases, sequence-defined and -controlled, the polymer chains are built in a specific order which is identical for each individual chain. That means, if three different monomers (A, B, C) are used in the synthesis of a multiblock copolymer, each chain first consists of a block of monomer A followed by a block of monomer B and finally a block of monomer C. However, while for the sequence-controlled polymer only the sequence of the blocks is relevant (see **Scheme 16**; right side) the exact number of repeating units in each block plays a significant role in sequence-defined polymer as well (depicted in **Scheme 16**; left side). This difference is also noticeable in the \bar{D} , while sequence-defined are monodisperse with a $\bar{D} = 1$, sequence-controlled polymers have a $\bar{D} > 1$.¹⁴⁷

Sequence-Defined ($\bar{D} = 1$)



Sequence-Controlled ($\bar{D} > 1$)



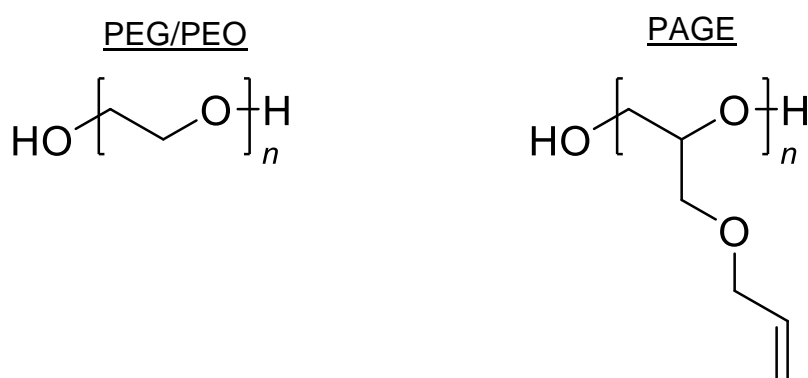
Scheme 16: Schematic depiction of the difference between sequence-defined and sequence-controlled polymers. While both are built from the same choices of monomer in the same order, only sequence-defined polymers have the same number of units per block and therefore an identical chain length. This is also noticeable in the \bar{D} because sequence-defined polymers have a $\bar{D} = 1$, while sequence-controlled polymers have a $\bar{D} > 1$.

2.5. Applications of Allyl Glycidyl Ether in Polymer Chemistry

Allyl glycidyl ether (AGE), a substituted ethylene oxide with a pendant C=C double bond, is a versatile monomer, which after polymerization can be used in a broad field of applications, reaching from polymer electrolytes for lithium-sulfur batteries,¹⁴⁸ via a basis for carbon dioxide separation¹⁴⁹ and possible antifouling coatings,¹⁵⁰ to hydrogel foundations for various biomedical applications.^{151,152}

While different initiator/promotor can be used to polymerize AGE, such as different alkali metal alkoxides systems (e.g., potassium benzoxide)^{153–155} or the previously mentioned *Schwesinger base*,^{50,53,156} they are usually conducted via AROP and result in controlled polymers with low \bar{D} (e.g., $\bar{D} = 1.08^{50}$). A crucial part for the success of the polymerization is a low Lewis acidity of the countercation, while having minimal interaction with the propagating chain end, which enables the oxyanion to function as an effective nucleophile.¹⁵⁷

The obtained polymeric structure of PAGE after the synthesis is similar to polyethylene glycol/polyethylene oxide (PEG/PEO), meaning the backbone of both polymers is based on -CH₂-CH₂-O- with one major difference, the pendant C=C double bond of PAGE, making it effectively a functional PEG (see **Scheme 17**).



Scheme 17: Comparison of the structures of PEG/PEO and PAGE. The structure is almost identical except for the pendant C=C double bond.

Due to their structural similarity, PAGE finds use in similar applications like PEG/PEO such as a foundation as polyelectrolyte in current research.^{158–160} Even though PEG/PEO has been the most frequently studied polyelectrolyte owning its ionic conductivity greater than 10⁻⁴ S cm⁻¹ above 70 °C, this value dramatic decrease at

temperatures below 65 °C due to occurring crystallization, making battery application at ambient temperatures challenging.¹⁶⁰ In contrast to PEG/PEO, the pendant allyl group in PAGE prevents the formation of crystalline regions and further helps in terms of ion conduction and solvation, making a copolymer of AGE and EO an interesting alternative with ionic conductivities near 10^{-4} S cm⁻¹ at room temperature.¹⁶⁰

The pendant C=C double bond of AGE is not only beneficial for polyelectrolyte application but can additionally participate in PPM reactions e.g., thiol-ene reactions,¹⁶¹ inverse-electron-demand Diels-Alder¹⁶² and inverse vulcanization,¹⁶³ enabling even further possibilities. While the first method can be exemplary used to generate polyampholytes with a possible application for the cryopreservation of living cells, as shown by Burkey et al.,¹⁶⁴ the latter results in high sulfur containing epoxy crosslinked polymers (70-50 wt% sulfur) with high tensile strength in the range of 10-60 MPa at break.¹⁶³

The versatility of AGE due to PPM reactions in combination with the possibility to obtain polymers of controlled structure via AROP, make this monomer a suitable and interesting candidate for the synthesis of sequence-controlled multiblock copolymers in this thesis.

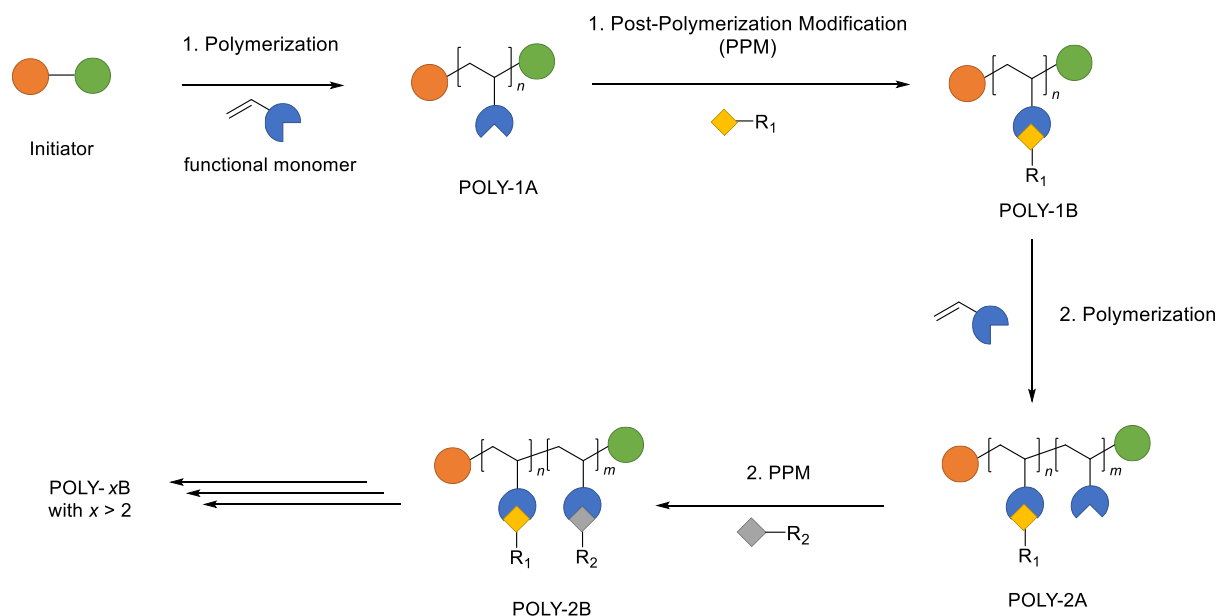
3. Motivation and Goal

As mentioned in the introduction, polymers are used in a multitude of different fields of application, which all have specific prerequisites for the properties of the used material. Two examples which influence those properties are (i) the choice of monomer and their functional groups, (ii) as well as the overall polymer chain structure, making control over both an important aspect in polymer chemistry. A special kind of polymer are multiblock copolymers, consisting of multiple, different monomers, in which each monomer influences the overall properties of the copolymer. Traditionally, those copolymers are done via polymerization techniques with living or living-like characteristics e.g., anionic or RAFT polymerization, resulting in chains with a specific block sequence, tailored molar mass and low \bar{D} . A large selection of monomers is commercially available, but more complex and special ones need to be synthesized, which can be costly, laborious and time-consuming at times.

Polymers with such a specific order of their monomers in the backbone are called sequence-controlled or sequence-defined, depending on whether the chains are monodisperse or not. Those polymers are of high interest, because they can be used in different fields of application e.g., as antimicrobial peptides, the foundation for drug delivery or information storage. Over the years, different methods emerged to obtain such polymers reaching from solid-phase synthesis to more “traditional” polymerization techniques such as variations of RAFT polymerization and ATRP. Even though progress were made, man-made macromolecules still lack precision over the exact sequence in comparison to sequence-defined polymers found in nature (e.g., DNA) making it an ongoing and interesting field of research.

Thus, the topic of this thesis was the establishment and investigation of new systems to synthesize sequence-controlled multiblock copolymers in an easy and fast-forward way, bypassing the disadvantage of laborious, time-consuming and costly monomer syntheses. The centerpiece of the system is the utilization of a single monomer instead of multiple, different ones, which is the traditional approach. By combining living polymerization techniques with PPM, functional groups responsible for the material properties will be introduced into the polymer after its synthesis, enabling the formation of polymers with desired characteristics. In addition, the use of a single monomer prevents possible CE problems, which can occur when using several monomers that differ in structure and reactivity. A classic example of this is the copolymerization of

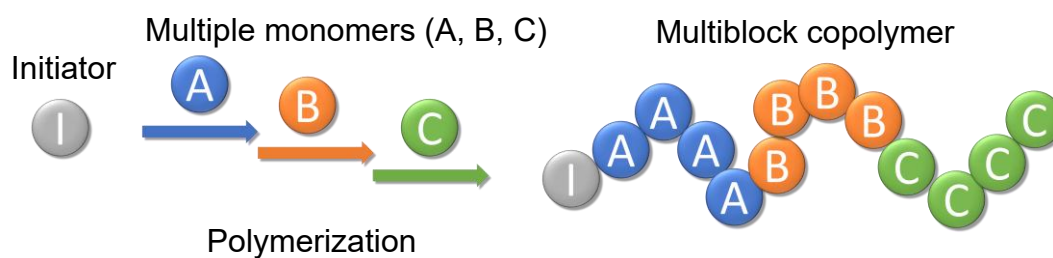
styrene and methyl methacrylate (MMA), where the sequence must be taken into account. The general concept to synthesize sequence-controlled multiblock copolymers consisting of a desired number of blocks x via a combination of CE and PPM is depicted below (**Scheme 18**).



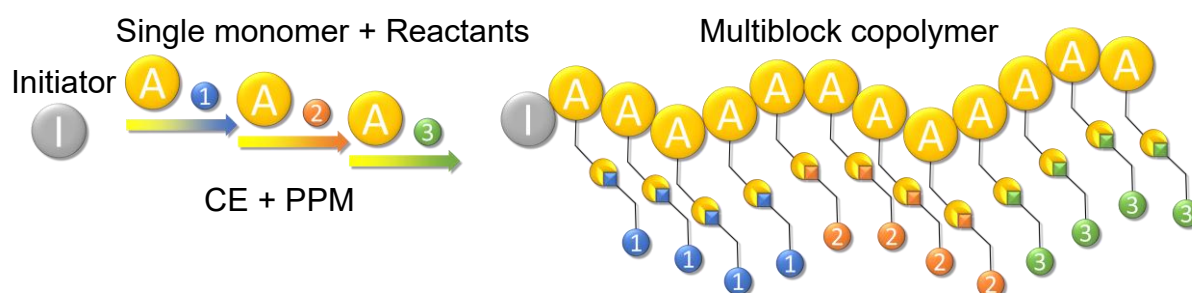
Scheme 18: General concept of the sequence-controlled multiblock copolymer synthesis by combining CE and PPM reactions. After the polymerization of a functional monomer resulting in POLY-1A, a follow-up modification reaction with a reactant containing the group R_1 is conducted. The obtained modified polymer (POLY-1B) functions as a macroinitiator in a subsequent polymerization with the identical monomer, resulting in POLY-2A, followed by a second PPM with a reactant containing the group R_2 . This procedure can be continued x times, resulting in a sequence-controlled multiblock copolymer with x blocks.

During this thesis, multiple functional monomers were polymerized using a variety of living/controlled polymerization techniques, namely RAFT polymerization, ATRP, CROP and AROP. For the polymerization method and the applied monomer, specific prerequisite must be fulfilled to be considered as possible candidates. The used monomers should ideally be commercially available and if not easy to synthesize, preferably in a single step. An important prerequisite for the polymerization method is the possibility of CE after modification or else no multiblock copolymer is possible. Furthermore, the functional group used in the PPM reaction must not interact with the active end of the polymer chain otherwise side reactions may occur, limiting the application of the system. **Scheme 19** depicts the difference between the “traditional” approach, where multiple monomers are necessary to create a sequence-controlled multiblock copolymer and the approach of this thesis, in which a single functional monomer is used.

Traditional approach



This work



Scheme 19: Comparison between the “traditional” and the approach presented in this thesis to synthesize a sequence-controlled triblock copolymer. The former uses three different monomers (A, B, C) to introduce properties into the polymer, while the latter uses a single monomer in combination with reactants. This allows to simplify the synthesis by bypassing laborious and time-consuming monomer syntheses.

4. Results and Discussion

This part of the thesis is intended to provide insight into the work carried out, their results and discussion in logical order.

The first chapter will include all applied polymerization techniques with each subchapter addressing the topic of the monomer procurement, polymerization, modification reaction and CE. Finally, a brief summary of the chapter and the subsequent consequences are presented.

The second chapter is about seeking the limits of the found system by decreasing the number of repeating units to an average of one, creating “sequence-defined”-like polymers. Herein, a macroinitiator is used as a precipitation agent, simplifying the purification process.

Detailed synthetic procedures for each synthesis with corresponding analytical data are presented in *chapter 6.3 Synthetic Procedures*.

4.1. Synthesis of Multiblock Copolymers by Combining CE and PPM reactions

This chapter is split into multiple subchapters dealing with the general prerequisites for the monomer and the synthesis of multiblock copolymer systems using a combination of CE and PPM reactions. Each subchapter is about a different polymerization technique and a functional monomer.

4.1.1. General Prerequisites for the Choice of Monomer

For a monomer to be perceived as a suitable candidate for the synthesis of sequence-controlled multiblock copolymers, specific prerequisites need to be fulfilled, which can be split into four main categories: (i) commercial availability or simple synthesis, (ii) a reactive group allowing for further modification reactions, (iii) polymerization via living/controlled polymerization and (iv) no interference with the polymerization or CE step.

In scope of this thesis four different monomers were investigated, which meet those criteria, namely pentafluorophenyl acrylate (PFPA), pentafluorophenyl methacrylate (PFPPMA), α -allyl-caprolactone (ACL) and allyl glycidyl ether (AGE).

The acrylate- and methacrylate-based monomers PFPA and PFPMA are commercially available or can be synthesized in a single step from (meth)acryloyl chloride with pentafluorophenol,^{165,166} making both easily accessible monomers. The acrylate as well as the methacrylate are both well-known to be polymerizable using RDRP techniques (such as RAFT polymerization and ATRP)^{165,167,168} allowing for polymers with defined structures and possible CE reactions by using the obtained polymer as macroinitiator. Additionally, both monomers count to the class of active esters, which can react almost quantitatively with amines under mild conditions (e.g., ambient temperature),³² making it perfect candidates for PPM reactions.

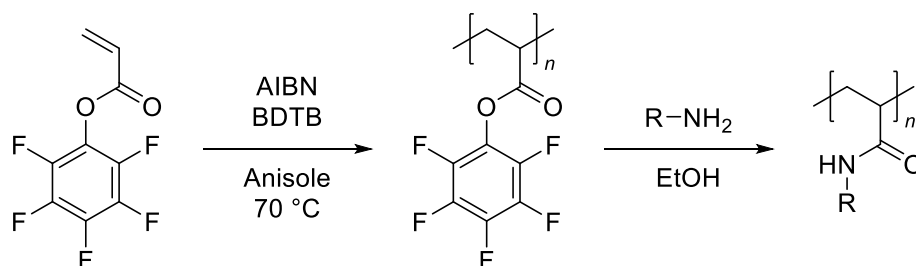
On the contrary, ACL and AGE are cyclic monomers with pendant C=C double bonds as reactive groups, which can be polymerized via ionic ring-opening polymerization in a living manner. One feature this polymerization method has is the similarity of the reactive group of the used initiator with the obtained polymer. In both cases a hydroxy group can be found, which means the synthesized macromolecule could be used as a macroinitiator again. Due to the ring-opening procedure of the polymerization, the pendant allyl group does not participate in any side reactions (e.g., crosslinking) and is available for PPM reactions. As mentioned previously, this particular reactive group can undergo different PPM reactions, such as the highly effective “*click*”-like thiol-ene reaction or IV, enabling the preparation of polymers with a variety of properties. Similar to PFPA and PFPMA, both monomers are also easily available. While ACL can be synthesized in a single step,¹⁶⁹ AGE is commercially available, making both monomers suitable candidates.

Based on the mentioned benefits, these molecules were chosen as possible monomers for the synthesis of sequence-controlled multiblock copolymer built from a single monomer.

4.1.2. Multiblock Copolymer Synthesis via RAFT Polymerization

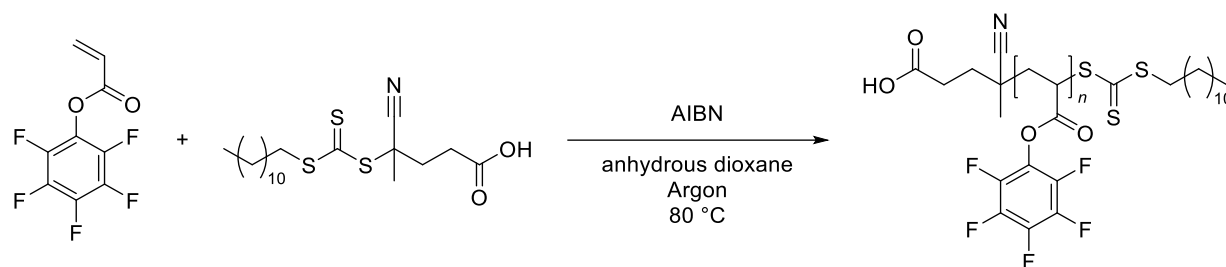
The first step for the synthesis of multiblock copolymers was to choose a fitting polymerization method. As mentioned above, a polymerization technique in a controlled manner and the ability to easily extend a polymer chain after its synthesis is necessary to create multiblock copolymers built from a single monomer. With the synthesis of low \bar{D} polymers with a defined chain length and the possibility to initiate polymerizations by macroinitiators to obtain multiblock systems, RAFT polymerization is a suitable candidate matching the necessary criteria.

As the first monomer to be studied was the active ester PFPA. As mentioned in the previous chapter, PFPA is well known to be easily polymerizable via RAFT polymerization¹⁶⁵ and can be modified using nucleophiles such as amines or alcohols (see **Scheme 20**).



Scheme 20: RAFT polymerization of PFPA with subsequent PPM using a primary amine. Redrawn after reference.¹⁶⁵

Even though the monomer is commercially available, PFPA was synthesized in a single step based on published literature.¹⁶⁵ The structure and the successful synthesis were confirmed via ¹H and ¹⁹F nuclear magnetic resonance (NMR) spectroscopy (see *chapter 6.3 Synthetic Procedures* for analytical data). Subsequently, a polymerization was conducted using PFPA and the RAFT agent 4-cyano-4-[(dodecylsulfanylthiocarbonyl)sulfanyl]pentanoic acid (CDTPA) (refer to **Scheme 21**).



Scheme 21: Reaction equation of the RAFT polymerization of PFPA using CDTPA and AIBN in anhydrous dioxane under inert atmosphere at 80 °C.

After 30 minutes a sample was taken directly from the reaction mixture and a ^{19}F NMR spectrum was recorded, showing a conversion of approximately 60 %, while 94 % conversion had been reached after 80 minutes. The size exclusion chromatogram (displayed in **Figure 1**) of the obtained polymer showed a single sharp peak with a \bar{M}_w of 1.07. However, with a number average molar mass (M_n) of approximately $8,000 \text{ g mol}^{-1}$, the experimentally acquired value was less than the targeted molar mass of approximately $9,000 \text{ g mol}^{-1}$ at a conversion of 94 %. This difference in molar mass can be explained by the structural difference of the used polystyrene calibration standard and PPFPA. Additionally, a small shoulder at the higher molar mass side indicated a small degree of side reactions, such as dimerization. By comparing the ^{19}F NMR spectrum of the monomer with the polymer a significant change in signal shape and chemical shift was visible. The previously defined ortho, meta and para signals of the monomer at -152.60, -162.32 and -157.94 ppm respectively got significantly broader and undefined after the polymerization, which is typical for polymeric material. The ^1H NMR spectrum showed the vanishment of the vinyl signals in the range of 6.75 - 6.00 ppm, confirming the absence of the monomer after the polymerization. Additionally, some signals overlapped with others making a proper signal assignment difficult.

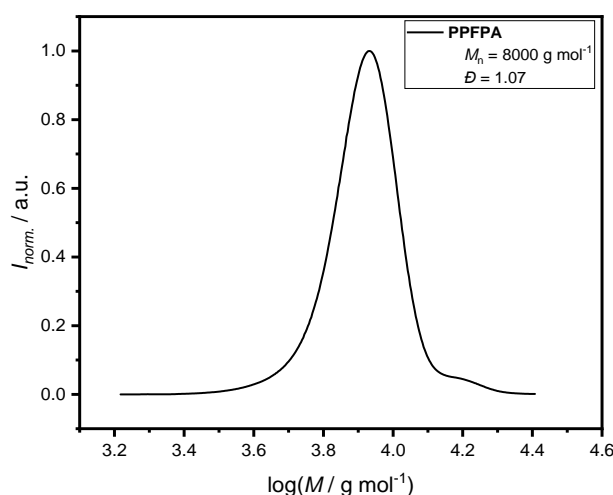
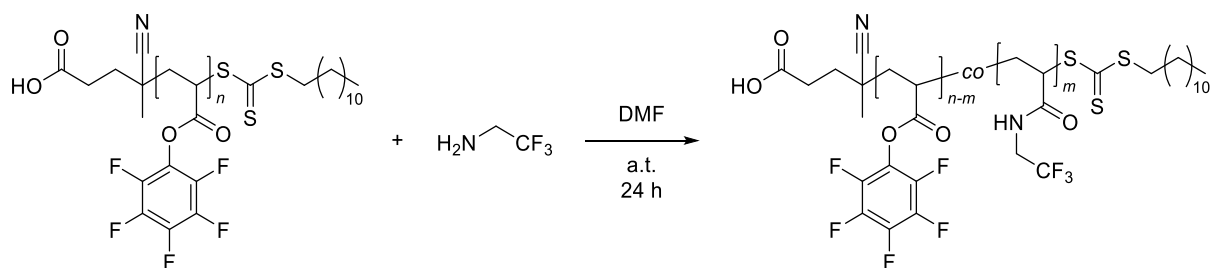


Figure 1: Size exclusion chromatogram of PPFPA synthesized via RAFT polymerization.

After the successful polymerization, the next step was to modify the polymer with a suitable nucleophile. First attempts were done using the fluorinated amine 2,2,2-trifluoroethylamine, because of the high electronegativity and its characteristic signals in the ^{19}F NMR spectrum. For total conversion an excess of amine in comparison to the active ester group should be used, but this might lead to complications. The trithiocarbonate group of the RAFT agent is prone to aminolysis, which would lead to the cleavage of the RAFT agent and a permanently terminated chain.¹⁷⁰ However, in a previous study done by Roth et al.¹⁷¹ to synthesize an heterotelechelic α,ω dye-functionalized polymer, a pentafluorophenyl ester at the α position and a dithioester at the ω site could be orthogonally modified. This was achieved by using stoichiometric amounts of amine in respect to the pentafluorophenyl ester, doing no harm to the RAFT end group. Therefore, to prevent an aminolysis of the PPFPA's RAFT endgroup during the modification, 0.6 eq. of amine in respect to the ester group was used (depicted in **Scheme 22**).



Scheme 22: Reaction equation of the partial PPM of PPFPA with 2,2,2 trifluoroethylamine in DMF at ambient temperature for 24 hours.

The modification reaction was conducted at ambient temperature and without the additional use of base, otherwise an increase in imide formation might be noticeable.¹⁷² Noteworthy was the immediate change of color of the orange/reddish reaction mixture to colorless after the addition of the amine.

By comparing the ^{19}F NMR spectra before and after the modification, the appearance of two new signals at -72.61 and -69.71 ppm was visible. While the larger peak at -72.61 ppm represented the desired amide group, the smaller peak at -69.71 ppm could be assigned to the respective imide, based on comparison to the literature.¹⁷² This leads to the conclusion that even without the addition of supplementary base the formation of imide could not be prevented, at best reduced. However, with a ratio of 0.14:1.47:1 of the imide:amide:ester signals, approximately 38 % of the ester groups remained, which was in range of the expected value for the total consumption of the amine. The size exclusion chromatograms (see **Figure 2**) of the precursor (gray) and the modified polymer (red), showed a decrease in molar mass of approximately 31 % which was in line with the expected value of 34 % for complete modification, without the imide considered. Additionally, an increase in \bar{D} from 1.07 to 1.13 could be observed while maintaining the general shape of the peak.

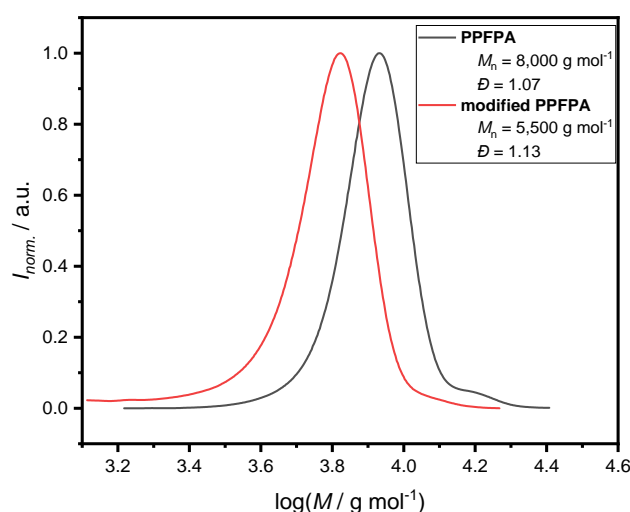
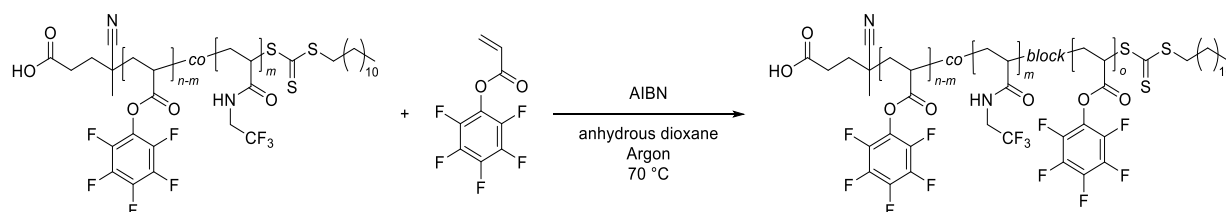


Figure 2: Size exclusion chromatograms of PPFPA before (gray) and after (red) the partial PPM with 2,2,2- trifluoroethylamine. A decrease in M_n and increase in \bar{D} is visible, indicating the success of the modification.

The newly appearing signals in the ^{19}F NMR spectrum and the change to lower molar mass in the size exclusion chromatogram were both indications for the success of the PPM of PPFPA leading to the next step, the first CE.

The conditions for the extension were similar to the first polymerization but instead of CDTPA, the modified polymer was used as a macro-RAFT agent, the temperature was decreased from 80 to 70 °C and the reaction time was increased from approx. 1.5 to 4.5 hours to ensure total conversion (refer to **Scheme 23**).



Scheme 23: Reaction equation of the first CE of the modified PPFA with PFFA and AIBN in anhydrous dioxane under inert atmosphere at 70 °C.

After 4.5 hours, the reaction was stopped and the polymer subsequently purified via precipitation. The product was again analyzed via ^{19}F NMR spectroscopy and size exclusion chromatography (SEC). If the CE was successful, a change in the previously determined imide:amide:ester ratio should be observable in the ^{19}F NMR spectrum. However, with a ratio of 0.15:1.45:1 no significant change could be detected, indicating an unsuccessful CE. This presumption got further supported by the size exclusion chromatogram (displayed in **Figure 3**) in which the newly synthesized polymer (red) was compared to the precursor (gray), the amine-modified polymer. With an identical M_n of approx. $5,500 \text{ g mol}^{-1}$ and a \bar{D} of 1.13 no change could be observed.

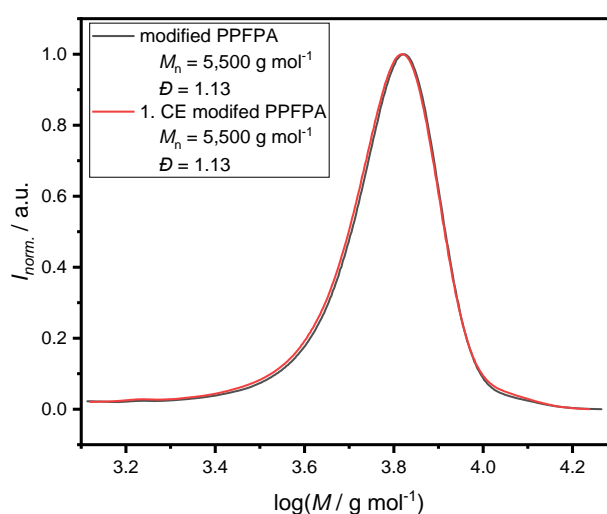
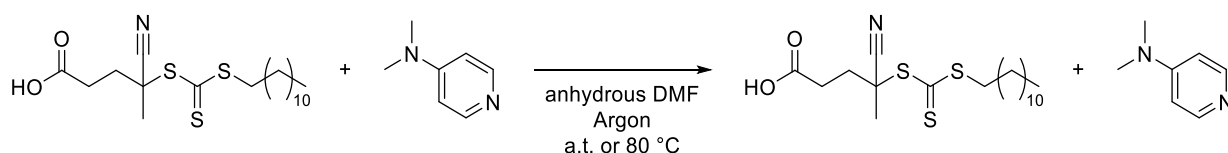


Figure 3: Size exclusion chromatograms of modified PPFA before (gray) and after (red) the CE with PFFA. No noticeable change was observed, suggesting an unsuccessful reaction.

This suggests that the decolorization after the amine addition might be due to the cleavage of the trithiocarbonate RAFT end group by aminolysis. With this in mind, it can be assumed that the amine reinitiates in the modification after the cleavage of the trithiocarbonate, which would explain the observed conversion in the previous modification step. Nevertheless, the termination of the CTA would lead to a terminated chain end making this RAFT system an unsuited candidate for the synthesis of multiblock copolymers.

To avoid aminolysis, the PPM procedure was consequently switched to transesterification and the fluorinated amine was replaced with a less nucleophilic molecule, namely 2,2,2-trifluoroethanol, which should minimize the RAFT end group cleavage. Even though PPFPA is demanded as unsuited for transesterification, Das et al.¹⁷³ presented a procedure under mild conditions in which the transesterification of PPFPA was successful by using 4-dimethylaminopyridine (DMAP) as catalyst and applying only stoichiometric amounts of alcohol.

However, before the modification was conducted, a base compatibility test (see **Scheme 24**) of the used RAFT agent with DMAP was conducted to investigate a possible RAFT agent cleavage. Therefore, a high excess of DMAP was added to the RAFT agent in anhydrous dimethylformamide (DMF) at two different temperatures (ambient temperature and 80 °C) under inert atmosphere for 48 hours.

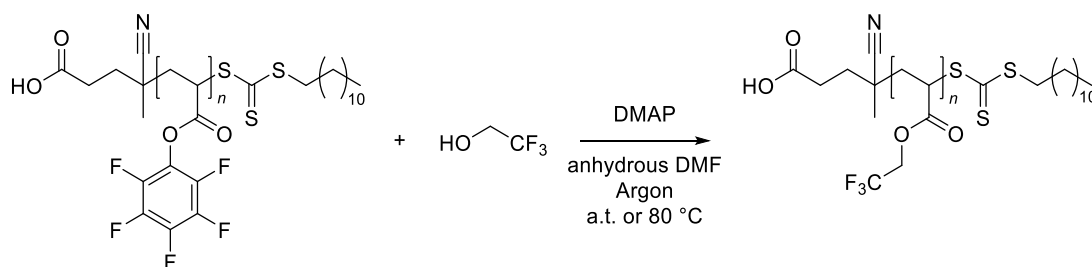


Scheme 24: Reaction equation of the base compatibility test reactions of CDTPA with DMAP in anhydrous DMF under inert atmosphere at ambient temperature and 80 °C.

In case of the reaction conducted at 80 °C, a visible change in color of the reaction mixture was noticeable, changing from previously yellow to orange. This change was not visible in the case of the reaction done at ambient temperature. By comparing the signals of the dodecane's methyl end group with the methyl group opposite of the nitrile in the ¹H NMR spectra of both reactions, decomposition of the RAFT agent was noticeable. In case of the reaction done at ambient temperature 53 % of the RAFT group were still intact, while after the reaction at 80 °C only 15 % were left. To reduce

decomposition, it is therefore advisable to conduct the reaction at lower temperatures and for less than 48 hours.

Therefore, based on the work of Das et al.¹⁷³ and the test reactions, two PPM reactions with 2,2,2-trifluoroethanol and DMAP were conducted overnight, one at ambient temperature with three equivalent of the alcohol, the other at 80 °C with two equivalents (refer to **Scheme 25**).



Scheme 25: Reaction equation of the transesterification PPFPA and 2,2,2-trifluoroethanol using DMAP in anhydrous DMF under inert atmosphere at ambient temperature or 80 °C.

¹⁹F NMR spectra (see **Figure 4**) of both reactions showed the appearance of a new peak at approx. -74 ppm of the newly added CF₃-group after completion. However, while the reaction conducted at 80 °C showed no other signals, indicating the total conversion of the active ester, the reaction done at ambient temperature only reached 93 % conversion.

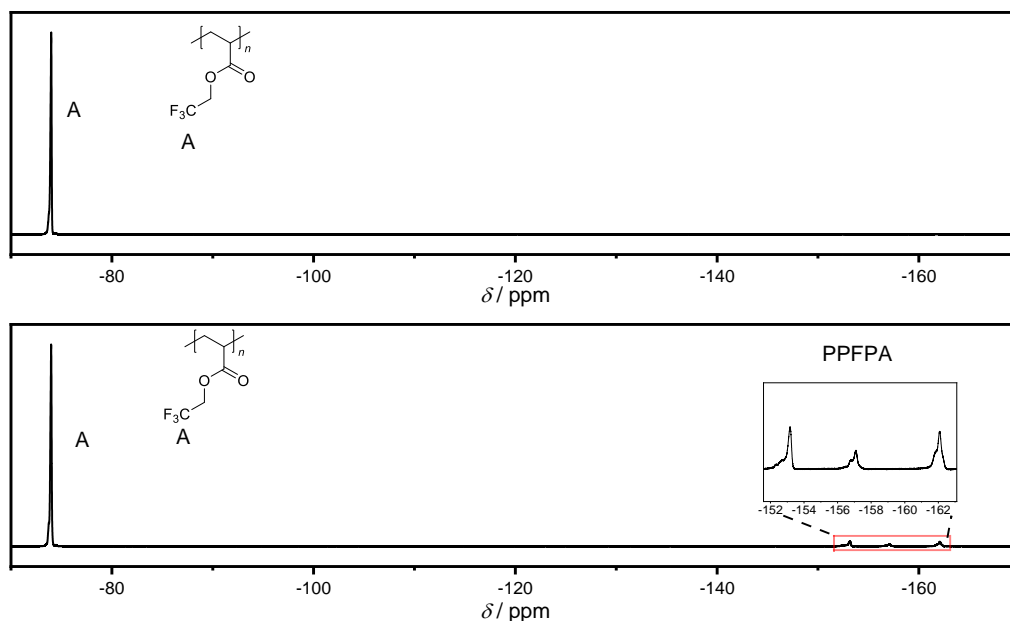


Figure 4: ^{19}F NMR spectra of the transesterification of PPFPA with 2,2,2-trifluoroethanol at ambient temperature (bottom) and at 80 °C (top). The reaction done at ambient temperature still has unreacted PPFPA moieties present. Solvent: CDCl_3 .

A representative size exclusion chromatogram (depicted in **Figure 5**) of this transesterification reaction showed a single symmetrical peak with a M_n of approx. 5,600 g mol^{-1} after (red) the modification, which was a slight decrease of approx. 300 g mol^{-1} in comparison to the precursor polymer (gray) while improving the \bar{D} faintly (1.08 to 1.05). Furthermore, the peak's shape and lack of further peaks indicated the absence of undesired side reactions, leading in combination with the NMR spectra to the assumption that the modification was successful.

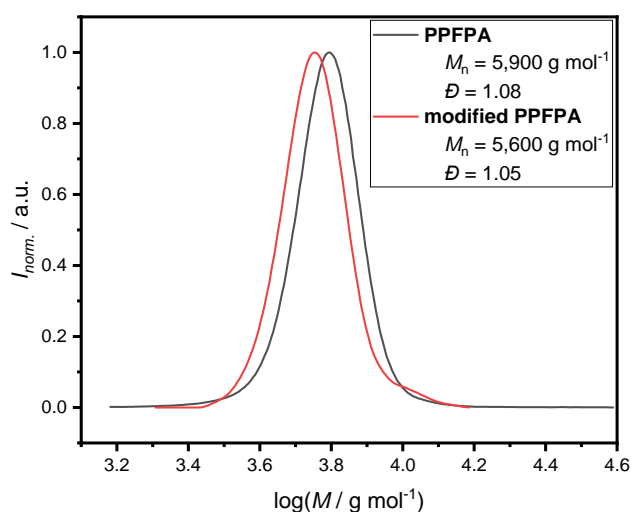
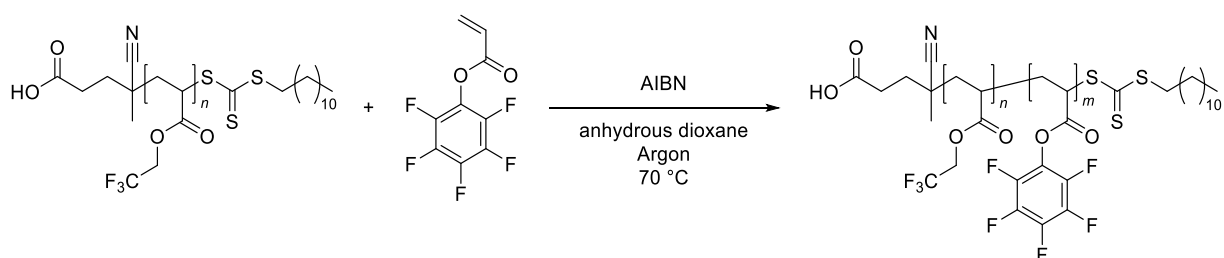


Figure 5: Size exclusion chromatograms of PPFPA before (gray) and after (red) the transesterification with 2,2,2-trifluoroethanol. A slight decrease in M_n and \bar{D} is visible, indicating a change in the structure.

Following from this, another CE attempt was conducted, similar to the first one, but with increased monomer equivalents to 140 (see **Scheme 26**). However, this time the ^{19}F NMR spectrum showed the appearance of the PPFPA signal as desired, but small amounts of monomer were still present, indicating an incomplete polymerization. This statement got further supported by the fact that the determined macroinitiator:PPFPA ratio was 1:118 and therefore below the targeted ratio of 1:140. Nevertheless, the presence of the PPFPA signals confirmed a successful polymerization of PFPA, even though the polymerization was incomplete.



Scheme 26: Reaction equation of the CE of modified PPFPA with PFPA and AIBN in anhydrous dioxane under inert atmosphere at 70 °C.

But instead of a single peak, which would be expected, the corresponding size exclusion chromatogram (refer to **Figure 6**) showed two overlapping peaks, a larger one with a peak molar mass (M_p) of approx. 47,900 g mol^{-1} and a smaller one at 6,800 g mol^{-1} with a combined \bar{D} of 1.95 and a M_n of 23,300 g mol^{-1} . The appearance

of a second peak confirmed the presence of a second polymeric species in the product. By comparing the M_p of the precursor polymer, which was approx. $5,600 \text{ g mol}^{-1}$, with the M_p of the smaller peak ($6,800 \text{ g mol}^{-1}$), an increase of $1,200 \text{ g mol}^{-1}$ could be determined, indicating a small degree of CE. However, due to the larger peak in the chromatogram, most of the monomer participated in an undesired uncontrolled free radical polymerization of PFPA, resulting in insufficient results.

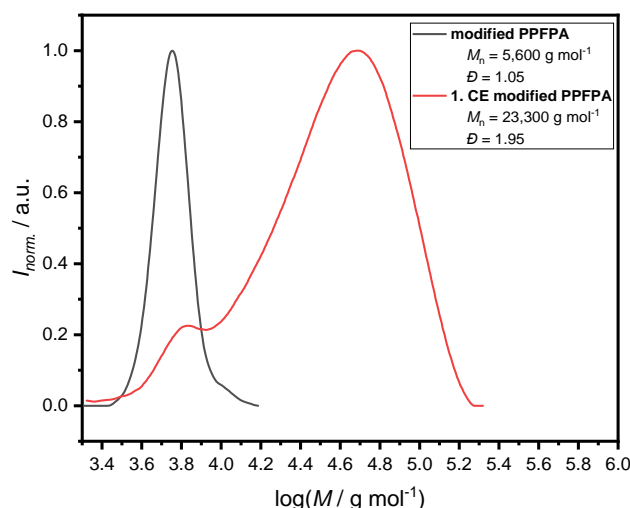


Figure 6: Size exclusion chromatograms of modified PPFA before (gray) and after (red) the CE with PFPA. Two peaks are visible after the reaction, a smaller one with a similar M_p as the precursor polymer and a larger one at approx. $47,900 \text{ g mol}^{-1}$. Additionally, an increase in \bar{D} to almost 2 could also be observed.

In summary, the attempts to synthesize sequence-controlled multiblock copolymers using a RAFT polymerization of the active ester monomer PFPA in combination with PPM were unsuccessful. After the successful polymerization and modification reaction via amidation, the necessary CE step failed, due to cleavage of the CTA, resulting in an unreactive polymer chain end. To exclude a possible amidation of the end group, the type of PPM was switched from amidation to transesterification. However, after the successful modification, an uncontrolled free radical reaction of PFPA during the first CE reaction could be observed, resulting in no development in terms of CE. To improve the results and to possibly use RAFT polymerization as method for the synthesis of sequence-controlled multiblock copolymer, further research needs to be done. One possibility would be the investigation of different CTAs, such as dithiosters, but also the use of different monomers. However, due to the insufficient results in given time, the RAFT approach was paused and a different RDRP, namely ATRP, was investigated.

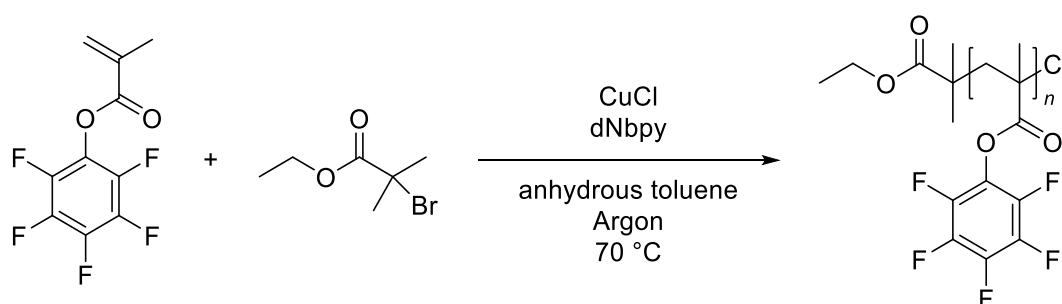
4.1.3. Multiblock Copolymer Synthesis via ATRP

As mentioned above, ATRP is another RDRP technique to obtain polymers with tailored molar masses, defined chain length and low \bar{D} and is therefore a possible polymerization technique to synthesize sequence-controlled multiblock copolymers.

For this RDRP method, the monomer of choice was switched from PFPA to the methacrylate derivative PFPMA, which is well known to be polymerizable using ATRP.^{167,168}

As mentioned before, PFPMA is commercially available but can also be synthesized in a single step, which was done in this thesis based on a known procedure.¹⁶⁶ The ^1H and ^{19}F NMR spectra were in accordance with the literature, confirming the successful synthesis (see *chapter 6.3 Synthetic Procedures* for analytical data).

Based on a published polymerization procedure of Lee et al.^{167,168} in which Cu(I)Cl instead of Cu(I)Br was used, a polymerization was conducted.



Scheme 27: Reaction equation of the ATRP of PFPMA and EBiB using dNbpy and Cu(I)Cl in anhydrous toluene under inert atmosphere at $70\text{ }^\circ\text{C}$.

After 4 hours at $70\text{ }^\circ\text{C}$, the polymerization was stopped and the polymer precipitated into cold methanol. The ^1H and ^{19}F NMR spectra were in accordance with the literature, confirming a successful synthesis of PFPMA. Moreover, the size exclusion chromatogram (see **Figure 7**) of the product showed a single peak with a M_n of approx. $12,000\text{ g mol}^{-1}$, a \bar{D} of 1.22 and a long tailing at the lower molar mass side, also confirming the polymeric nature of the product.

In summary, both characterization methods, the NMR spectroscopy and SEC, confirmed the successful synthesis of PFPMA, which led to the next step, the PPM reaction.

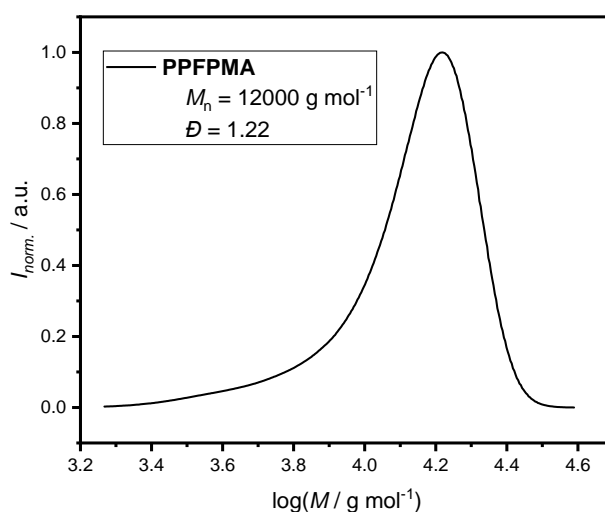
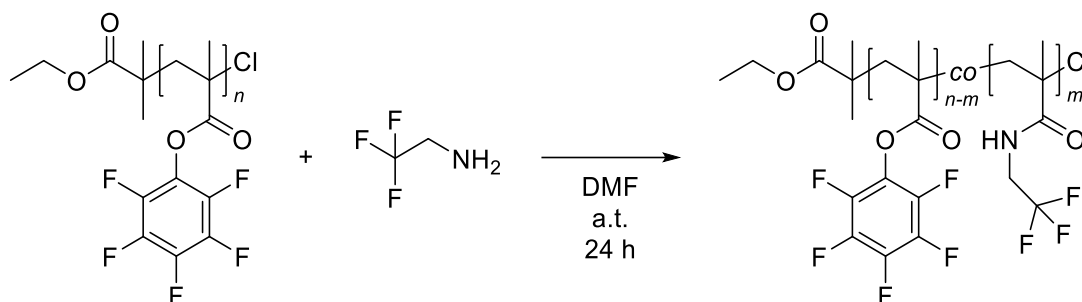


Figure 7: Size exclusion chromatogram of PPFMA synthesized via ATRP. A long tailing at the lower molar mass side is visible.

The first PPM reaction was conducted in a similar way to the PPM of PPFPA, with 2,2,2-trifluoroethylamine being the reactant of choice, due to the characteristic signals in the ^{19}F NMR spectrum (see **Scheme 28**).



Scheme 28: Reaction equation of the partial PPM of PPFMA with 2,2,2-trifluoroethylamine in DMF at ambient temperature.

The ^{19}F NMR spectrum after the modification showed no clear change in comparison to the one of the precursor polymer, except for multiple small signals between -68 and -73 ppm, which could represent the newly added 2,2,2-trifluoroethylamine group. However, if the actual ^{19}F NMR spectrum is similar to the one of the 2,2,2-trifluoroethylamine modified PPFPA, a single signal instead of multiple ones would be expected, which was not the case. The integral ratio between the para fluor signal of the monomer and the multiple ones was 1:0.03 which is negligible and therefore indicated an unsuccessful modification. Additionally, the size exclusion

chromatogram (depicted in **Figure 8**) of PFPMA before (gray) and after (red) the modification showed only a small increase in the molar mass (approx. 800 g mol^{-1}) as well as an improvement in \bar{D} from 1.22 to 1.14. If the modification would have been successful, a more prominent change in the chromatogram should have been visible, similar to the difference observed for the acrylate derivative PFFPA (see **Figure 2**), which was not the case. Therefore, both analytical methods (^1H NMR spectroscopy and SEC) indicated a failed modification.

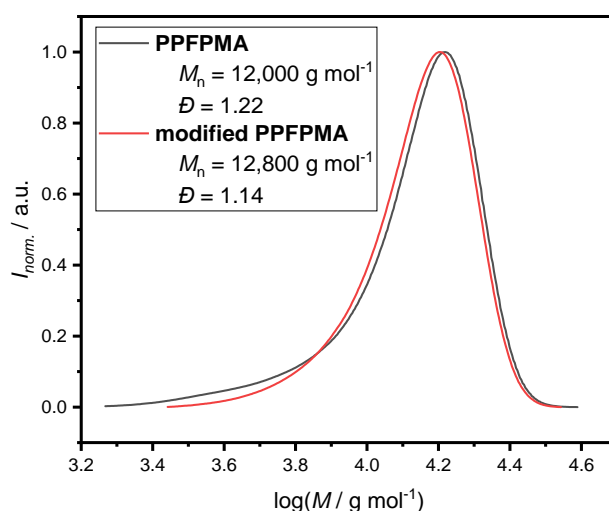
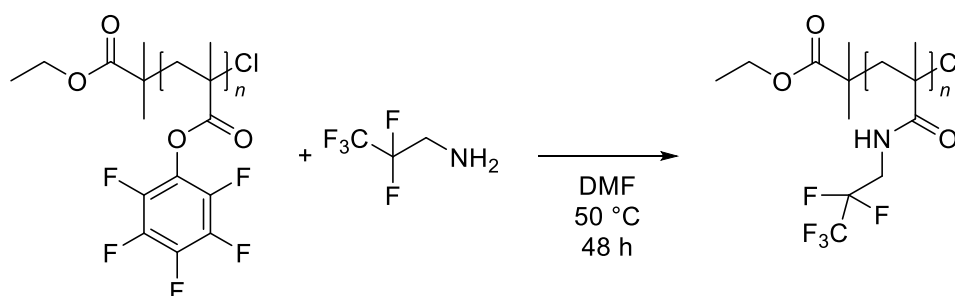


Figure 8: Size exclusion chromatogram of PFPMA before (gray) and after (red) the partial PPM with 2,2,2-trifluoroethylamine. A small increase in M_n is visible, as well as an improvement in the \bar{D} .

To exclude a possible failure of the modification due to the choice of monomer, a PPM reaction with a different amine (2,2,3,3,3-pentafluoropropylamine) was conducted, to see if improved results could be achieved. Additionally, the reaction temperature and amine equivalents were increased (ambient temperature to 50°C) and the reaction time (24 to 48 hours) extended, to ensure a higher conversion (**Scheme 29**).



Scheme 29: Reaction equation of the PPM of PFPMA with 2,2,3,3,3-pentafluoropropylamine in DMF at 50°C for 48 hours.

After 48 hours at 50 °C, the crude ^{19}F NMR spectrum (displayed in **Figure 9**) of the polymerization showed no change, which is why triethylamine (TEA) was added to the reaction mixture to accelerate the modification reaction, even though imide formation could be the consequence. However, even after the addition of the base no improvement could be achieved, leading to an unsuccessful attempt once again.

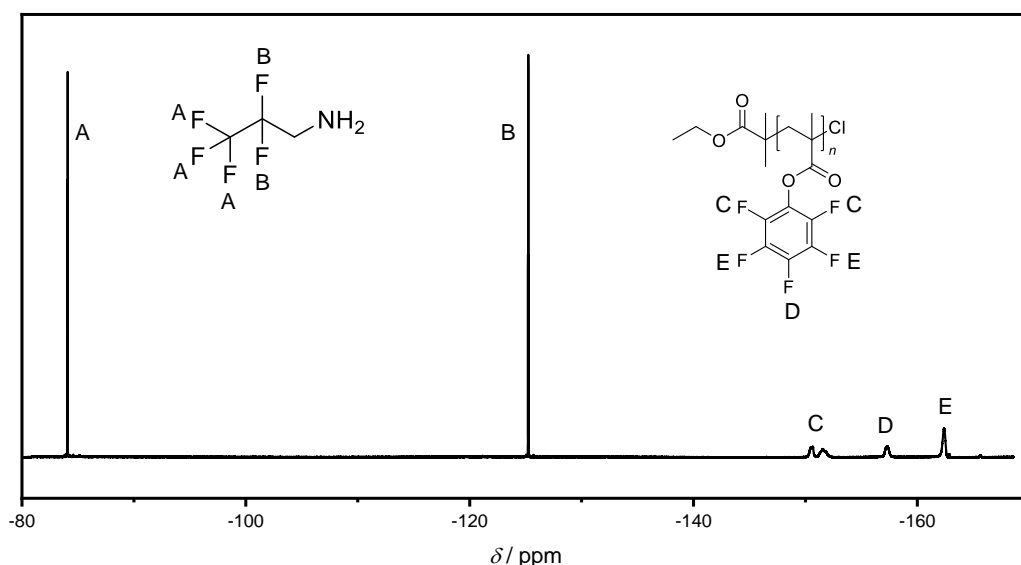


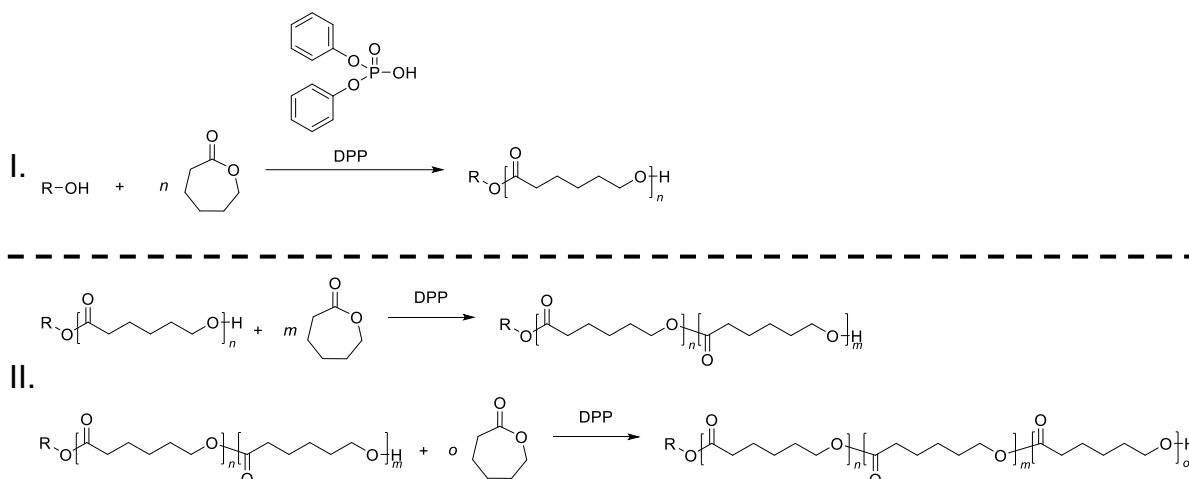
Figure 9: Crude ^{19}F NMR spectrum of the PPM of PFPMA with 2,2,3,3,3-pentafluoropropylamine after 48 hours. The still present PFPMA signals indicate an unsuccessful PPM. Solvent: CDCl_3 .

In summary, the synthesis of sequence-controlled multiblock copolymers via ATRP of PFPMA, the methacrylate derivative of PFPA, with PPM was investigated, which remained unsuccessful. After the successful synthesis of PFPMA, this attempt failed at the modification step. A change in conditions, reactant and even base addition resulted in no improvement. To possibly use ATRP as a method to synthesize sequence-controlled multiblock copolymers, further research needs to be done, such as using different reactants during the modification process, changing the type of monomer as well as pursuing a different PPM method.

Consequently, similar to the RAFT approach, the ATRP technique was discarded due to insufficient results and a different system was investigated. Instead of continuing the trend of achieving multiblock copolymers via a RDRP method, the focus was changed to ionic polymerization techniques, namely CROP and AROP.

4.1.4. Multiblock Copolymer Synthesis via CROP

As mentioned in a previous chapter, CROP is a special case of cationic polymerization, in which cyclic monomers such as cyclic ethers, lactones and lactams can be polymerized. An interesting CROP is the polymerization of CL to PCL, using an alcohol as initiator and diphenyl phosphate (DPP) as organocatalyst (displayed in **Scheme 30**; I.).¹⁷⁴



Scheme 30: I. General reaction equation of the polymerization of CL using a primary alcohol and DPP. II. General reaction equation of the second and third CE of PCL with CL in presence of DPP.

As visible in **Scheme 30**, this polymerization technique allows for the preparation of polymers which have the same functional groups as the initiator (in this case a hydroxy group) for their end group and can therefore act as macroinitiators themselves (see **Scheme 30**; II.). To prove this idea, CL was first polymerized using benzyl alcohol as initiator and DPP as catalyst, and subsequently used as a macro initiator for CE reactions. The number of repeating units for each polymerization and CE was aimed to be approx. 20, which should be confirmed via SEC and ¹H NMR spectroscopy. The size exclusion chromatograms (depicted in **Figure 10**) of PCL and two further CE displayed each one distinct peak, which shifted to higher molar masses with each follow-up reaction, from 4,200 g mol⁻¹ to 7,500 g mol⁻¹ and finally 9,900 g mol⁻¹. The determined values exceed the theoretical ones, which could be explained by the difference in the structure of the used polystyrene (PS) standard to PCL. For the first two reactions, the absence of further peaks after each polymerization indicated no second growing species aside from the desired polymer structure. However, after the last extension, a broadening of the peak as well as a formation of two shoulders, one

at the lower molar mass the other at the higher side was visible, indicating small side reactions. The shoulder at the higher molar mass side was with approx. $18,600 \text{ g mol}^{-1}$ almost twice the value of the main peak, suggesting a recombination of two chains. This might be the result of oxygen in the reaction flask caused by insufficient purging during the polymerization preparation. The smaller peak around $4,000 \text{ g mol}^{-1}$ might be to a small side polymerization initiated by impurities (e.g., water).

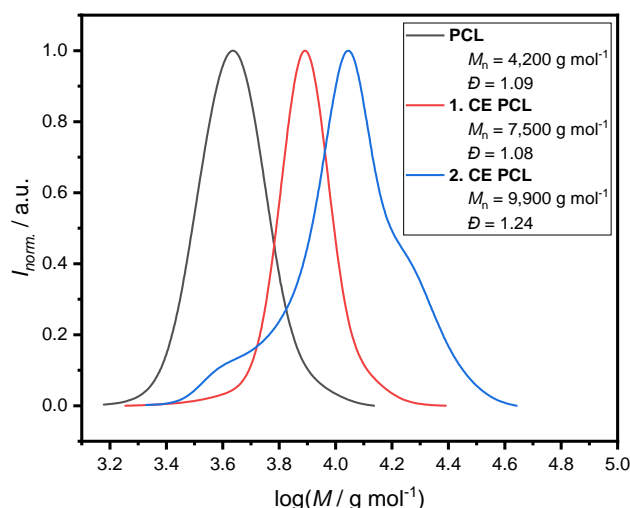
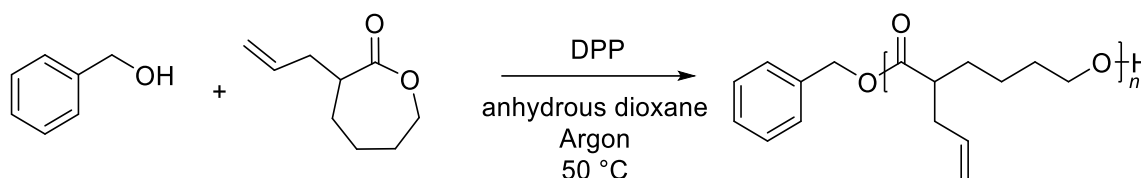


Figure 10: Size exclusion chromatograms of PCL (gray) and the first (red) and second (blue) CE with CL. After each reaction a shift to higher M_n is visible, indicating a successful extension of the chain.

The ^1H NMR spectra for each polymerization were also in accordance with the spectra found in literature¹⁷⁵ for PCL. To confirm the extension of the chain, the ratio of the $-\text{CH}_2-$ signal of the benzyl alcohol initiator was compared to the $-\text{CH}_2\text{-O}-$ signal of the PCL backbone. After each reaction an increase of approx. 20 repeating units per addition could be established, confirming the successful extensions.

However, even though PCL might be suited for CE reactions, the lack of reactive groups for PPM reactions excludes it as a possible candidate for the synthesis of multiblock copolymers. In contrast to CL, α -allyl-caprolactone (ACL) has a pendant allyl group, which allows for PPM reactions such as thiol-ene reaction and can be synthesized from CL in a single step, based on a known procedure.¹⁶⁹

The successful synthesis of the monomer ACL was confirmed via NMR spectroscopy (see chapter 6.3 *Synthetic Procedures* for analytical data) and the first polymerization attempt was conducted under similar conditions to the polymerization for CL.



Scheme 31: Reaction equation of the CROP of ACL with benzyl alcohol and DPP in anhydrous dioxane under inert atmosphere at 50 °C.

However, in contrast to CL, no polymer could be obtained after the same time which led to a change in the reaction conditions as the reaction time was increased (48 hours) but the temperature was lowered (50 °C) (displayed in **Scheme 31**). After 48 hours, the total conversion of the monomer could be confirmed via ^1H NMR spectroscopy, in which the remaining signals equaled those found in literature.¹⁶⁹

Even though ^1H NMR spectroscopy proved complete monomer consumption, no polymer was obtained, which was confirmed via SEC. The chromatogram (see **Figure 11**) showed multiple sharp peaks, which is more akin to oligomeric behavior than polymeric.

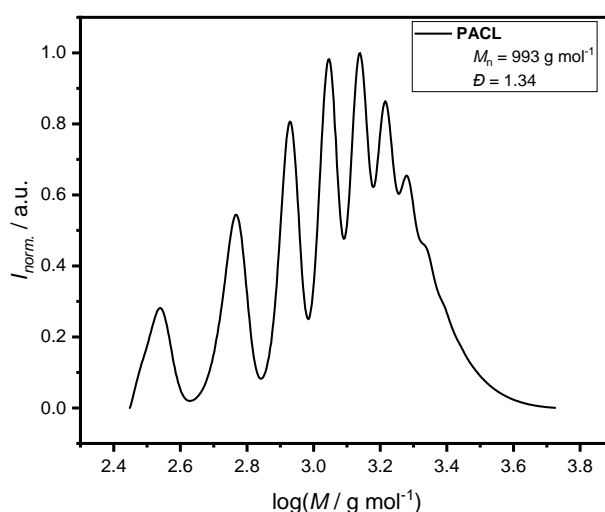
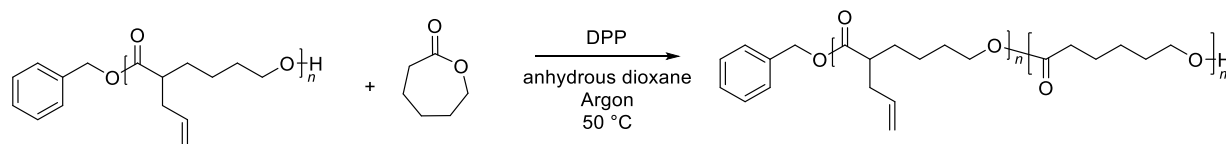


Figure 11: Size exclusion chromatogram of PACL. Multiple sharp peaks are visible, indicating an oligomeric material.

This assumption got further supported by the small but similar differences in M_p between each peak (approx. 3,000 g mol⁻¹) and the overall low M_n of approx. 1,000 g mol⁻¹ (\bar{D} of 1.34), while the theoretical value was about 3,100 g mol⁻¹. Nevertheless, this oligomer was further used as a macro initiator in a CE reaction, to see if it is even possible to extend PACL, before further optimization was done. Due to

the better polymerization results of CL in previous reactions, CL was used as monomer instead of the functional monomer ACL. The polymerization was conducted once again with DPP as organocatalyst at 50 °C for 48 hours, identical to the conditions of PACL.



Scheme 32: Reaction equation of the first CE of PACL with CL using DPP in anhydrous dioxane under inert atmosphere at 50 °C.

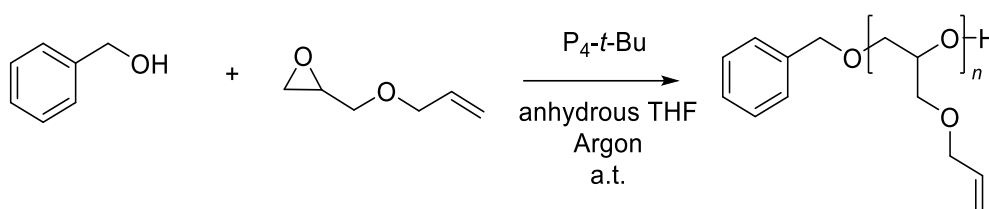
The ^1H NMR spectrum of the obtained material showed no evidence of the presence of ACL in the structure but was in accordance with the expected spectrum of PCL. This indicated a side reaction in which CL was initiated by impurities in the reaction mixture or self-initiated by DPP to form PCL instead of the desired CE of the oligomeric ACL chain, resulting in a failed attempt.

In summary, primary attempts were made in synthesizing sequence-controlled multiblock copolymers via CROP of lactones. First tests were conducted with the commercially available CL to investigate the suitability of CROP for CE reactions, because the obtained polymer carries the same functional group as the initiator and should therefore work as a macroinitiator itself. This idea could be confirmed by successfully chain extending PCL twice. However, due to the lack of functionality in the structure, the allyl containing derivative ACL was chosen as a possible candidate. The synthesis of the monomer was successful, but during polymerization attempts only oligomers could be obtained. Nevertheless, a CE reaction of the oligomeric species was conducted to investigate if an extension would be even possible. Due to the better results in previous reactions, the monomer was changed to CL for those reactions. However, no chain extended polymer could be obtained, indicating a failed reaction. To possibly use CROP and ACL as a system to synthesize sequence-controlled multiblock copolymers, further investigations are necessary, such as changing the catalyst from DPP to another one.

Due to the poor performance of this system, this approach was discarded and a more promising system was investigated, the AROP of AGE.

4.1.5. Multiblock Copolymer Synthesis via AROP

Parallel to the CROP of CL and ACL, a different kind of ring-opening polymerization was investigated in which the propagating species was also of ionic nature, but anionic instead of cationic. While for the CROP a functional monomer had to be synthesized, a suitable monomer, AGE, is commercially available for the AROP as mentioned above. Similar to ACL, AGE carries a pendant C=C double bond making it accessible for “click”-like modification reactions. Based on the polymerization system by Ree’s group,⁵⁰ first polymerization attempts of AGE with benzyl alcohol as initiator and P₄-t-Bu as promoter were conducted at mild conditions (ambient temperature) for 4 hours (refer to **Scheme 33**).



Scheme 33: Reaction equation of the AROP of AGE with benzyl alcohol using P₄-t-Bu in anhydrous THF under inert atmosphere at ambient temperature.

The obtained material was characterized via ¹H NMR spectroscopy and SEC to confirm the polymeric nature. The ¹H NMR spectrum (see **Figure 12**) was in accordance with the ones found in literature⁵⁰ and showed a clear change in comparison to the spectrum of AGE. The signal at 4.53 ppm could be assigned to the -CH₂- of the benzyl alcohol and could therefore be used to calculate the ratio between initiator and repeating units. With approx. 25 repeating units instead of the targeted 50, the conversion was about 50 %, which was viewed as insufficient. Therefore, subsequent polymerization attempts were conducted at a longer reaction time (7 hours), which resulted in an almost quantitative polymerization and a yield of 76 %.

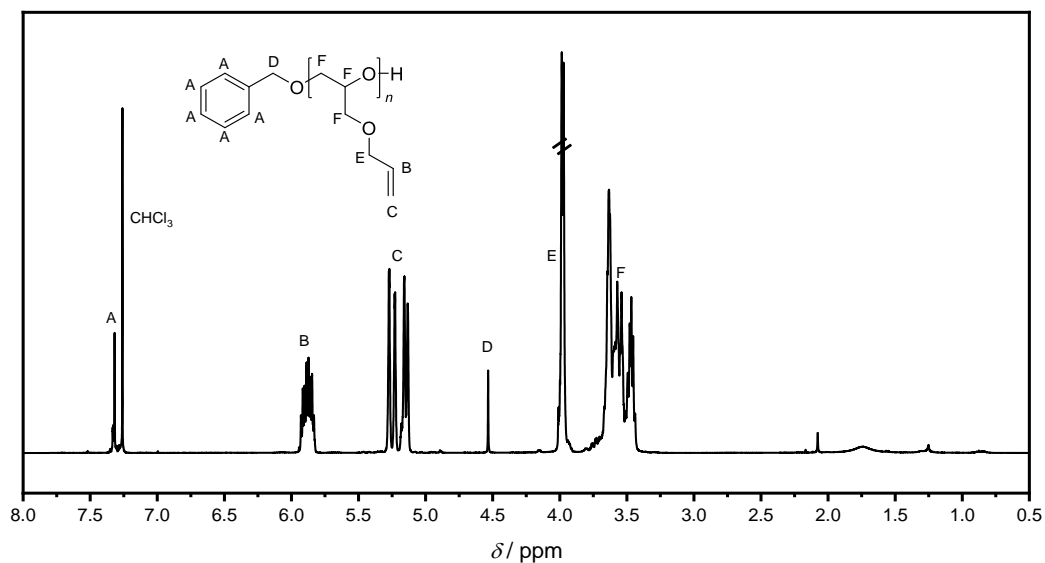


Figure 12: ^1H NMR spectrum of PAGE. Solvent: CDCl_3 .

The size exclusion chromatogram (depicted in **Figure 13**) of the polymerization confirmed the synthesis of PAGE by showing a single peak with a M_n of approx. $3,700 \text{ g mol}^{-1}$, a \bar{D} of 1.13 and a small shoulder at a higher molecular weight, indicating a slight degree of dimerization.

Overall, the ^1H NMR spectrum as well as the size exclusion chromatogram confirmed the successful synthesis of the polymer which should further be used in PPM reactions.

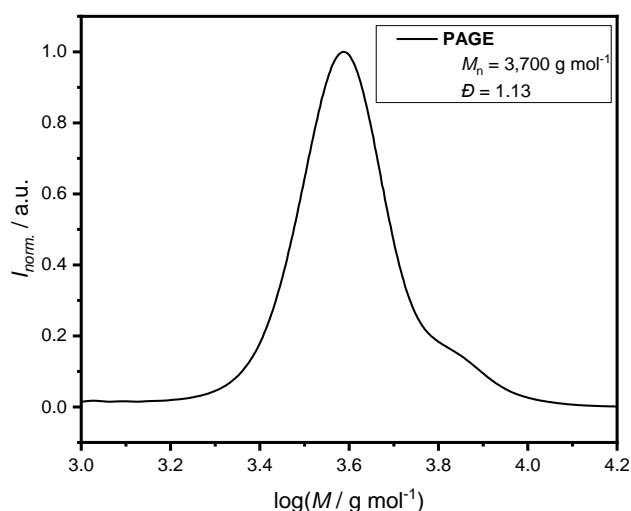
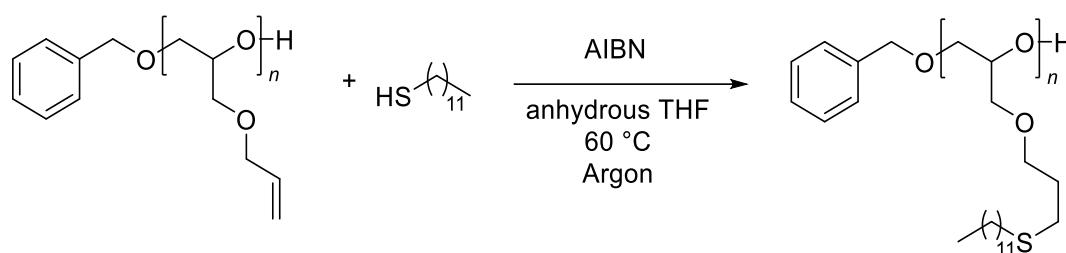


Figure 13: Size exclusion chromatogram of PAGE. A single peak with a small shoulder at its higher molar mass side is visible.

The first PPM reaction was conducted in form of a thiol-ene reaction using 1-dodecanethiol and AIBN at 60 °C overnight (refer to **Scheme 34**) resulting in a yield of 80 %. This particular thiol was chosen for two reasons: (i) to introduce an alkyl group as the first “functional” group and (ii) to investigate possible influences of the pendant group on CE reactions, such as shielding the active center. To prevent undesired crosslinking of the pendant group initiated by the radical source AIBN, a high excess of thiol in comparison to the C=C double bond of 4:1 was used.



Scheme 34: Reaction equation of the thiol-ene reaction of PAGE and 1-dodecanethiol with AIBN in anhydrous THF under inert atmosphere at 60 °C.

The ¹H NMR spectrum (see **Figure 14**) confirmed a successful modification of the precursor polymer by displaying the loss of the characteristic double bond signals in the range of 6.00 – 5.00 ppm while new signals e.g., the one around 0.8 ppm, appeared, which belong to the long alkyl chain of the added 1-dodecanethiol.

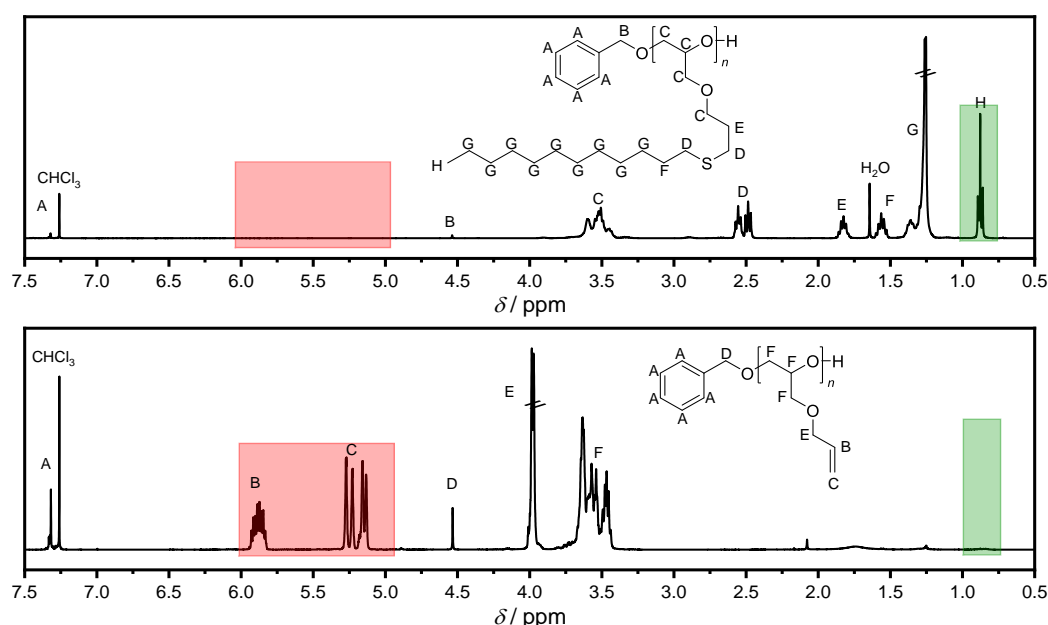


Figure 14: Comparison of the ¹H NMR spectra of PAGE before (bottom) and after (top) the PPM with 1-dodecanethiol. After the modification the disappearance of the H₂C=CH-R signals of AGE (red) and the appearance of the thiol signals (green) could be observed, confirming a change in the structure.

The size exclusion chromatograms (see **Figure 15**) of the precursor and the modified polymer also confirmed a successful modification by presenting a significant shift in the molar mass ($3,700 \text{ g mol}^{-1}$ to $7,700 \text{ g mol}^{-1}$) and an improvement of the \bar{D} (1.13 to 1.08). The absence of any further peaks at a lower molar mass indicated no precursor polymer was left and only the modified polymer remained. Additionally, any form of crosslinking could be excluded because no peak broadening or additional shoulder formation was observed.

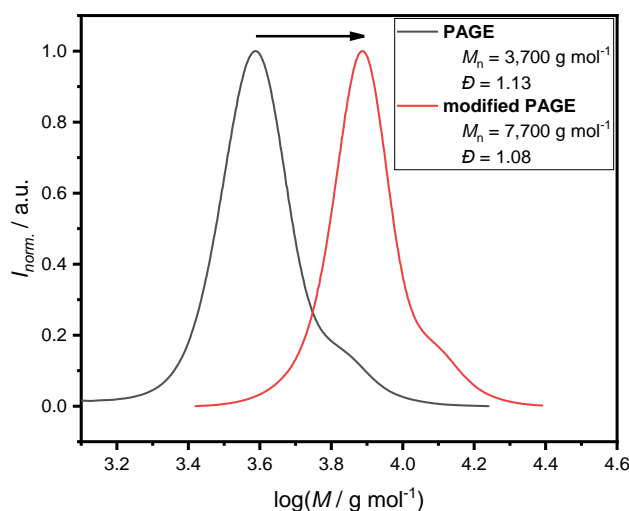
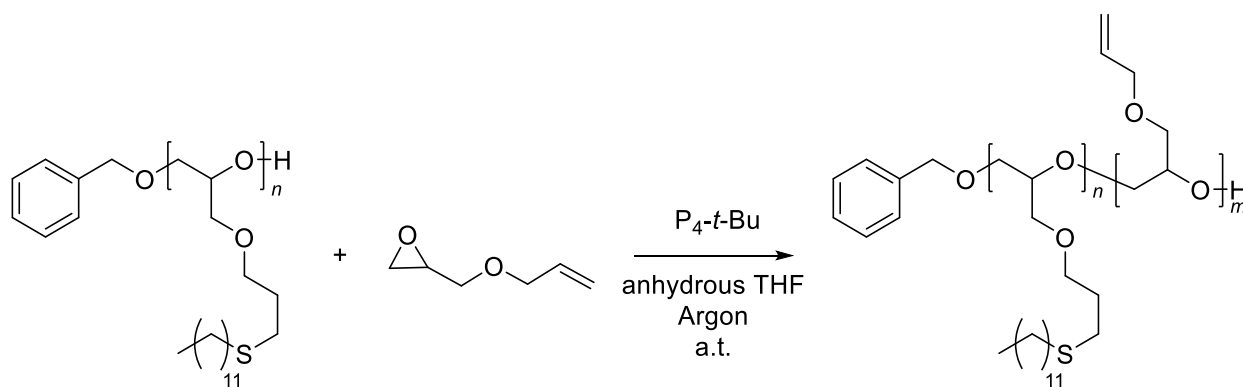


Figure 15: Size exclusion chromatograms of PAGE before (gray) and after (red) the PPM with 1-dodecanethiol. After the modification a shift to higher molar masses is noticeable, indicating a change in the structure of the chain.

After successfully modifying PAGE via thiol-ene reaction, the next step was to conduct the first CE reaction. Because the polymerization of AGE was done at ambient temperature, the first attempt for CE was conducted at similar conditions (refer to **Scheme 35**).



Scheme 35: Reaction equation of the first CE of modified PAGE with AGE using P_4 - t -Bu in anhydrous THF under inert atmosphere at ambient temperature.

After 22 hours, the polymerization was stopped and a crude ^1H NMR spectrum (depicted in **Figure 16**) was recorded to calculate the conversion by comparing the ratio of a monomer and a polymer signal. For the monomer the signal at 3.11 ppm was picked, whereas for the polymer the signal at 5.85 ppm, representing the C=C double bond, was chosen. While the monomer signal is not interfering with any other signals, the polymer one was also overlapping with the C=C double bond signal of the monomer. Therefore, it was important to subtract the monomer's value of the total integral so only the polymer signal remained. This led to the determination of a monomer conversion of approx. 58 %.

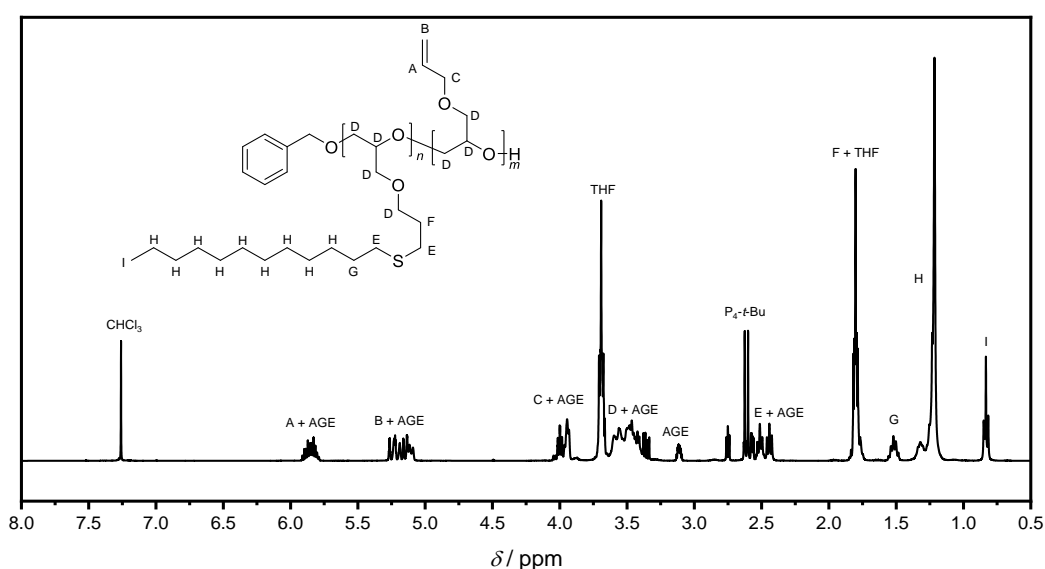
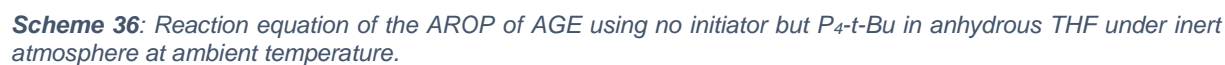


Figure 16: Crude ^1H NMR spectrum of the CE reaction of modified PAGE with AGE at ambient temperature. Solvent: CDCl_3 .

However, the size exclusion chromatogram (depicted in **Figure 17**) after the extension showed no shift to higher molar masses compared to the precursor polymer, but even a small decrease. This observation was in contrast to the one obtained by NMR spectroscopy and indicates a failed CE. An explanation which brings both results into harmony is the occurrence of a side reaction in form of an homopolymerization resulting in PAGE, which is soluble in the precipitation solvent during the purification process. Therefore, the conversion of the monomer was visible in the ^1H NMR spectrum but no peak shift could be observed in the size exclusion chromatogram. Additionally, due to the solubility of the homopolymer during the precipitation procedure, no second peak appeared in the chromatogram after the purification process. Because no further initiator besides the modified PAGE was intentionally



To prove this assumption, a polymerization was conducted at similar conditions to the previous reaction, except no initiator was added (see **Scheme 36**). And indeed, after 4 hours a monomer conversion of approx. 96 % could be achieved, determined via ¹H NMR spectroscopy.



After purification, the ^1H NMR spectrum resembled the one of PAGE initiated by benzyl alcohol but lacking the characteristic benzyl signals. Furthermore, no other signal except for impurities e.g., water and $\text{P}_4\text{-}t\text{-Bu}$ could be detected (**Figure 18**).

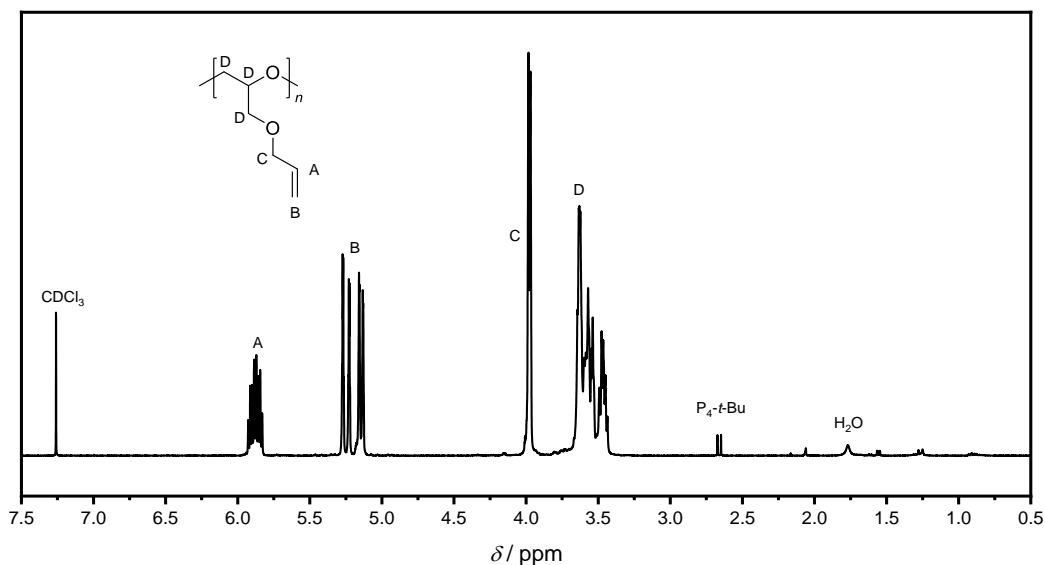


Figure 18: ^1H NMR spectrum of PAGE after the synthesis without an initiator. Solvent: CDCl_3 .

The associated size exclusion chromatogram (displayed in **Figure 19**) of the purified polymer showed two overlapping peaks with a long tailing at the lower molar mass side. The overall shape of the peak indicates a polymerization in a more uncontrolled behavior than a controlled one. The achieved M_n of approx. $10,500 \text{ g mol}^{-1}$ and \bar{D} of 1.31 indicate 92 repeating units, even though this value should be taken into account with skepticism, due to the structural difference of the used PS standard and PAGE.

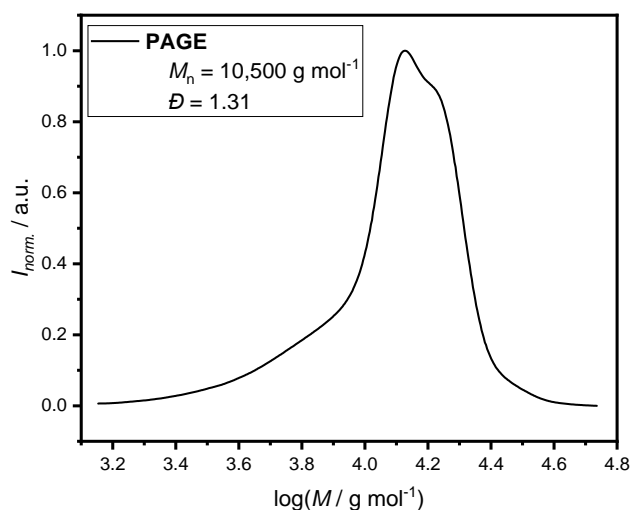


Figure 19: Size exclusion chromatogram of PAGE synthesized without additional initiator. A broad peak with a \bar{D} of 1.31 is visible, indicating an uncontrolled polymerization.

The results of this experiment supported the assumption of an uncontrolled homopolymerization of AGE during the CE reaction, leading to a failed attempt. By comparing the previous polymerization of AGE using benzyl alcohol as initiator with the CE reaction in which the modified polymer is used as initiator, a difference is noticeable. Even though both reactions utilize the same functional group as starting point of the polymerization, the benzyl alcohol carries a primary hydroxy group, while the modified polymer has a secondary one, which is less reactive. Therefore, to achieve a CE of the modified polymer, a higher activation energy might be necessary, which can be achieved by increasing the reaction temperature.

Thus, another extension attempt was conducted at an increased temperature of 50 °C in comparison to the previously used ambient temperature. After 5 hours, a sample to determinate the monomer conversion via ^1H NMR spectroscopy was taken, in which no monomer signals were left, indicating a total conversion. During the precipitation process in methanol, two fractions, a soluble and an insoluble one, could be obtained. While the ^1H NMR spectrum (see **Figure 20**) of the insoluble product showed the desired signals of the added AGE, e.g., the $\text{H}_2\text{C}=\text{CH}-\text{R}$ signals between 6.00 – 5.00 ppm, as well as the benzyl signals, the spectrum of the soluble product showed only the $\text{H}_2\text{C}=\text{CH}-\text{R}$ signals, but no benzyl ones.

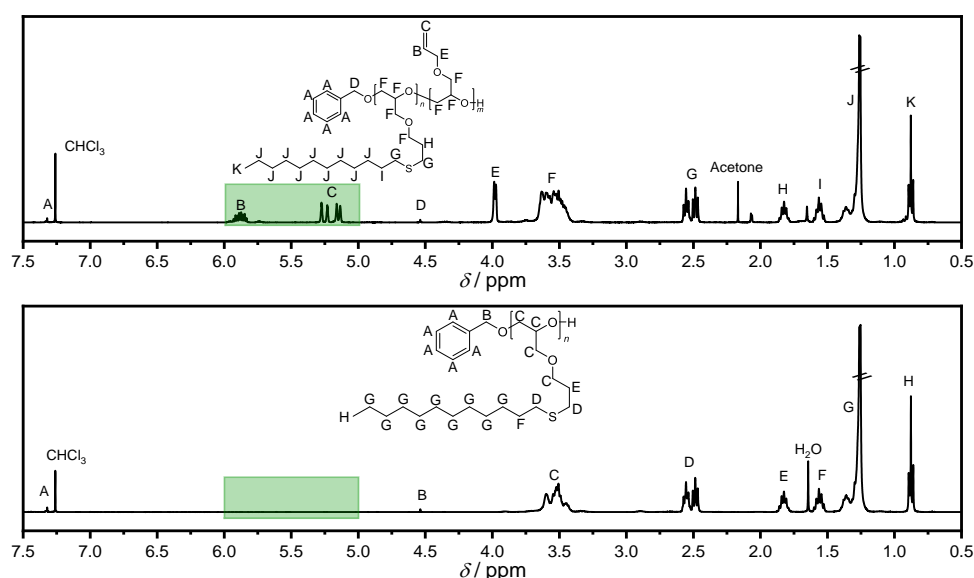


Figure 20: Comparison of the ^1H NMR spectra of modified PAGE before (bottom) and after (top) the CE with AGE at 50 °C. After the reaction, the $\text{H}_2\text{C}=\text{CH}-\text{R}$ signals of the attached AGE units in the range of 6.00 – 5.00 ppm (green area) could be observed. Solvent: CDCl_3 .

This indicated a successful CE of the modified polymer for the first time, while a homopolymerization happened nevertheless, which resulted in shorter chain than desired and a yield of 66 %. The size exclusion chromatogram (refer to **Figure 21**) of the crude polymer before purification showed two peaks, a smaller one at an approx. M_n of $3,700 \text{ g mol}^{-1}$ (\bar{D} of 1.07) and a much larger one at an approx. M_n of $11,200 \text{ g mol}^{-1}$ (\bar{D} of 1.07). After the purification via precipitation in MeOH, the smaller peak which represented the homopolymer, vanished from the chromatogram and only the larger peak, the chain extended modified polymer, remained, confirming the solubility of the lower molecular weight fraction.

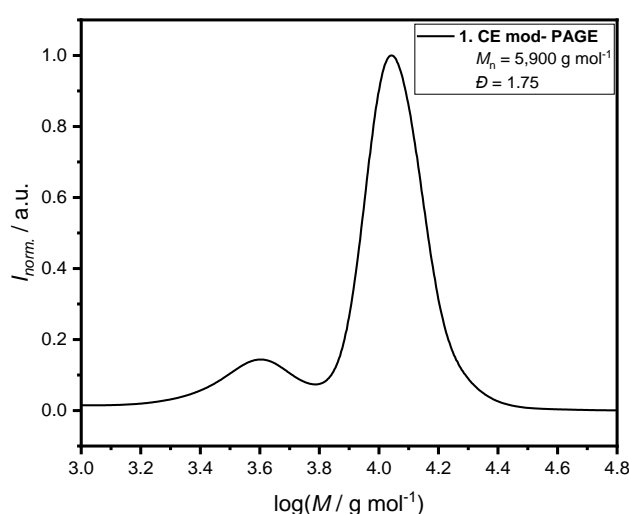


Figure 21: Crude size exclusion chromatogram of the first CE of modified PAGE with AGE. Two peaks are visible, a smaller one at $M_p = 3,700 \text{ g mol}^{-1}$ and a larger one at $M_p = 11,200 \text{ g mol}^{-1}$.

By comparing the peak before the extension (see **Figure 22**) with the peak afterwards, a clear shift towards higher molar masses ($7,700$ to $11,100 \text{ g mol}^{-1}$) and a small improvement in the \bar{D} (1.08 to 1.07) was visible. This, in combination with the results provided via ^1H NMR spectroscopy proved the successful CE of the modified polymer. Already, this structure could be seen as a diblock copolymer due to the different pendant groups. However, to truly synthesize a multiblock copolymer with different functionalities further modifications and CEs are necessary.

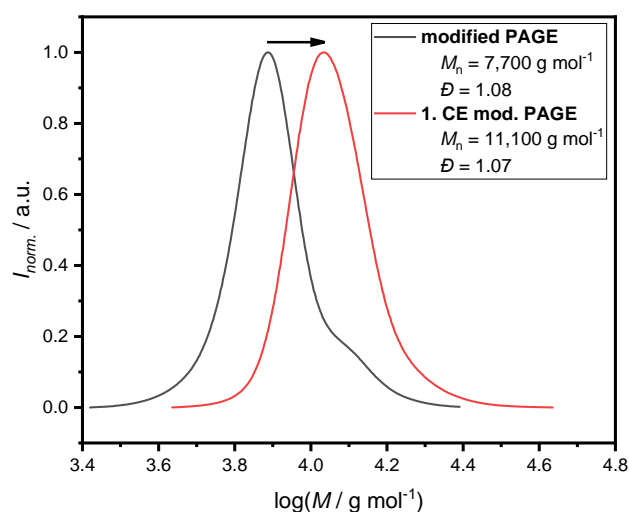
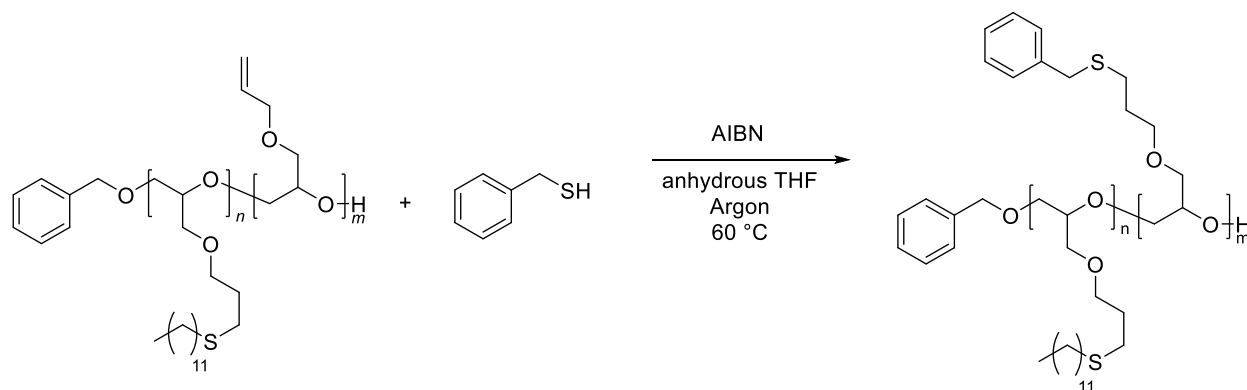


Figure 22: Size exclusion chromatograms of modified PAGE before (gray) and after (red) the first CE with AGE. After the reaction, a noticeable shift of the peak to a higher molar mass could be observed, indicating a change of the chain structure.

Therefore, a second modification of the now extended 1-dodecanethiol-modified PAGE was conducted using a different thiol, namely benzyl mercaptan (depicted in **Scheme 37**).



Scheme 37: Reaction equation of the thiol-ene reaction of once chain extended PAGE and benzyl mercaptan with AIBN in anhydrous THF under inert atmosphere at 60 °C.

With this, the polymer will incorporate two different kinds of pendant groups, one with a long alkyl chain, the other with a short aromatic system. The reaction conditions of this thiol-ene reaction were similar to the modification using 1-dodecanethiol and the obtained product (yield: 65 %) was characterized via ^1H NMR spectroscopy and SEC to prove the success of the modification. After the reaction, the ^1H NMR spectrum (displayed in **Figure 23**) of the purified product showed no characteristic $\text{H}_2\text{C}=\text{CH}-\text{R}$ signals in the area of 6.00 - 5.00 ppm anymore, confirming a full conversion of the

double bonds. Meanwhile, around 7.25 – 7.15 ppm a new signal appeared, which could be assigned to the phenyl ring of the newly added benzyl mercaptan. However, this signal was overlapping with the signal of the initiator as well as the solvent peak making a clear assignment difficult. The signal of the $-\text{CH}_2-$ unit could be determined to be in the range of 3.79 – 3.30 ppm, also overlying with other signals. Additionally, the general spectrum was in accordance with the expected one and all signals could be assigned. Those results indicated a successful modification of the precursor polymer.

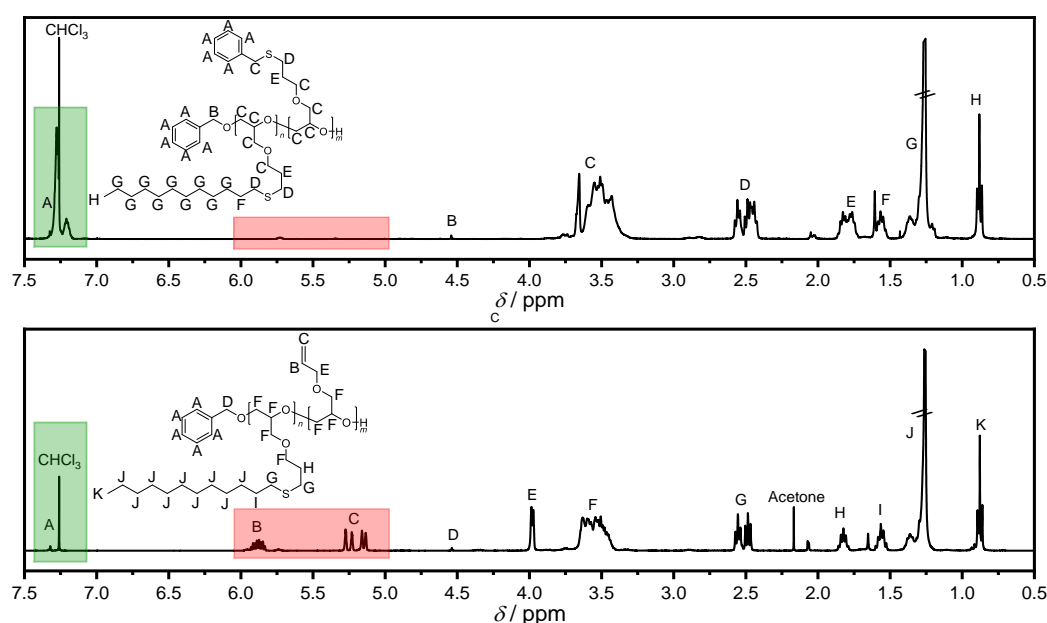


Figure 23: ^1H NMR spectra of once chain extended modified PAGE before (bottom) and after (top) the second PPM via thiol-ene reaction using benzyl thiol. Solvent: CDCl_3 .

The size exclusion chromatogram (see **Figure 24**) of the polymer after the thiol-ene reaction showed a single peak with a M_n of approx. $13,000 \text{ g mol}^{-1}$ which was an increase of $1,900 \text{ g mol}^{-1}$ to the precursor polymer, while the \bar{D} slightly worsened (1.07 to 1.10). The shift to a higher molar mass as well as the absence of any further peaks indicated a successful modification of the chain extended 1-dodecanethiol-modified PAGE.

Herewith, a diblock copolymer with a long alkyl chain and an aromatic system as its pendant groups could be successfully synthesized, confirming the usability of the investigated system of CE and PPM reactions. To further confirm its usefulness as a

toolbox system, further CEs and modifications were done to create a longer system but also different structures, such as a crosslinked one.

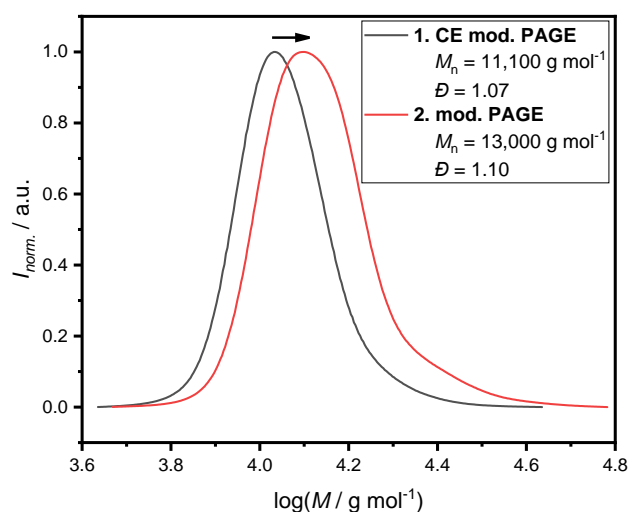
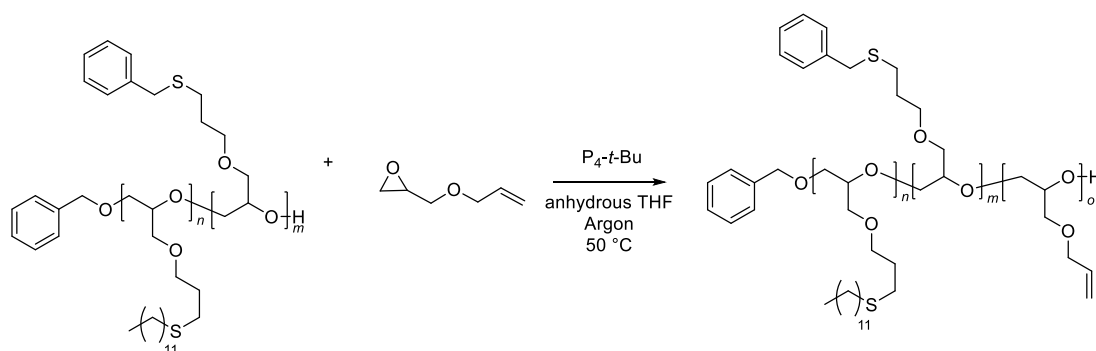


Figure 24: Size exclusion chromatograms of once chain extended modified PAGE before (gray) and after (red) the PPM via thiol-ene reaction with benzyl thiol.

After the second modification of the polymer, a further CE was conducted to obtain a triblock copolymer (refer to **Scheme 38**), which was used to synthesize a crosslinked structure, as well as a linear polymer with methyl-3-mercaptopropionate to introduce an ester as a functional group to the chain.



Scheme 38: Reaction equation of the second CE of modified PAGE with AGE using P_4-t-Bu in anhydrous THF under inert atmosphere at 50 °C.

The success of the CE was confirmed via ^1H NMR spectroscopy and SEC. Again, the ^1H NMR spectrum (see **Figure 25**) showed the desired $\text{H}_2\text{C}=\text{CH}-\text{R}$ signals around 6.00 – 5.00 ppm, confirming the presence of AGE in the structure. Because the characteristic monomer signal at 3.10 ppm was absent, it could be assumed that no

monomer was left in the purified product and the determined AGE units were part of the chain. All the other signals could also be assigned to their respective protons accordingly. The number of repeating units was determined by comparing the signal of the methyl group of the 1-dodecanethiol at 0.88 ppm with the proton signal of the double bond at approx. 5.87 ppm. As in the previous extensions, the determined number of repeating units was lower than the targeted one, indicating a side reaction in form of a homopolymerization leading to a yield of only 22 %.

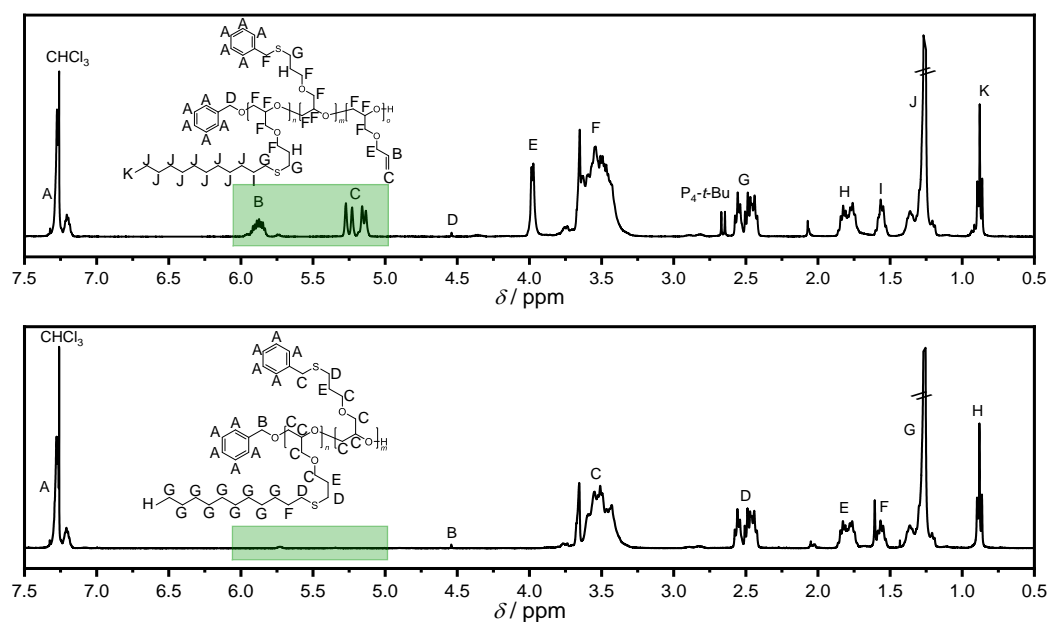


Figure 25: ¹H NMR spectra of twice modified PAGE before (bottom) and after (top) the second CE with AGE. After the reaction, the H₂C=CH-R signals of the AGE in the range of 6.00 – 5.00 (green area) could be observed, indicating a successful CE. Solvent: CDCl₃.

The size exclusion chromatogram (displayed in **Figure 26**) of the polymer after the reaction showed a single peak with a M_n of approx. 18,600 g mol⁻¹, a \bar{D} of 1.44 and a long tailing at the higher molar mass side. The fact that the tailing is at the higher molar mass side indicated the occurring of a side reaction such as dimerization which could have been a result of oxygen contamination due to incomplete atmosphere purging. With a bigger increase from 1.10 to 1.44 in the \bar{D} , the broadening of the peak is also visible. However, in comparison to the precursor peak a clear shift to higher molar masses from 13,000 to 18,600 g mol⁻¹ was noticeable, confirming the extension of the polymer chain.

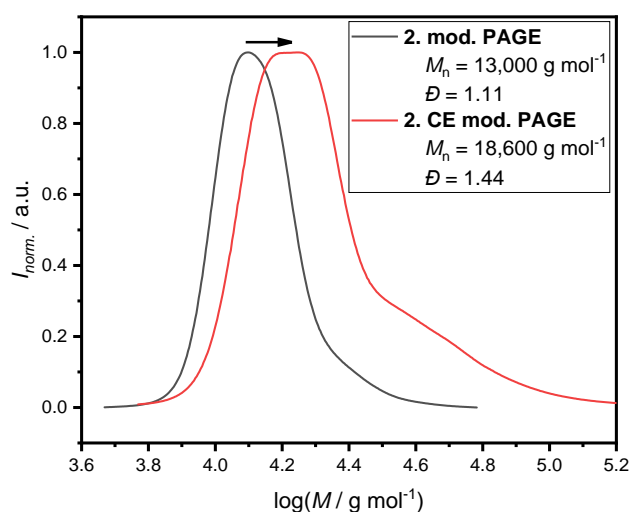
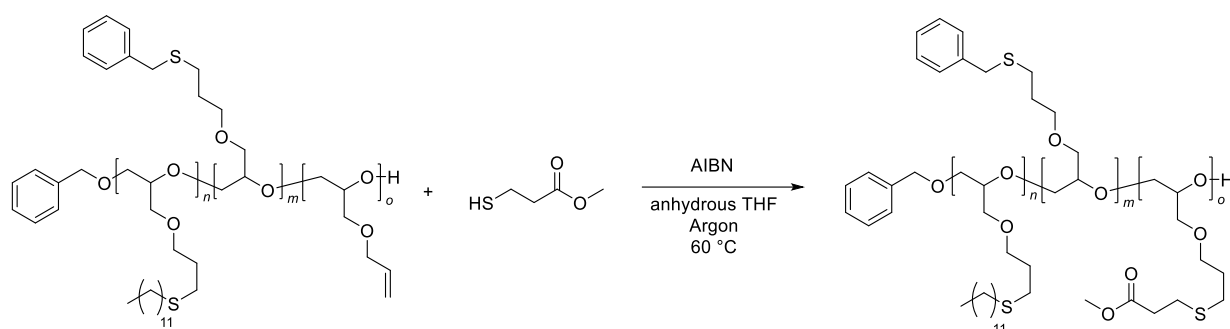


Figure 26: Size exclusion chromatograms of twice modified PAGE before (gray) and after (red) the second CE with AGE. After the reaction, a shift to higher molar mass was observed, indicating the success of the reaction.

Overall, the size exclusion chromatogram and the NMR spectrum confirmed the success of the second CE of PAGE, while side reactions could not be prevented.

The next PPM reaction using the ester group containing methyl-3-mercaptopropionate was done under similar conditions as the previous thiol-ene reactions (displayed in **Scheme 39**) and the product was characterized via ^1H NMR spectroscopy and SEC.



Scheme 39: Reaction equation of the thiol-ene reaction of twice chain extended PAGE methyl-3-mercaptopropionate with AIBN in anhydrous THF under inert atmosphere at 60 °C.

The crude NMR spectrum (see **Figure 27**) of the product showed no $\text{H}_2\text{C}=\text{CH}-\text{R}$ signals around 6.00 – 5.00 ppm, indicating a total conversion of the double bond. Additionally, new signals around 3.80 – 3.27 ppm and 2.97 – 2.39 ppm appeared, belonging to the newly added thiol.

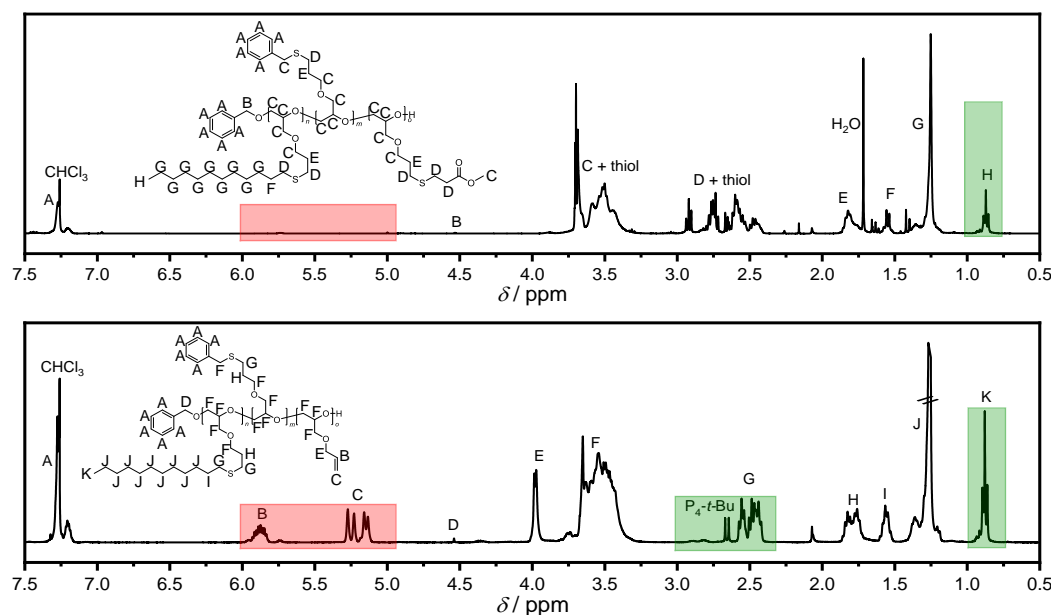


Figure 27: Crude ^1H NMR spectra of twice chain extended modified PAGE before (bottom) and after (top) the third PPM via thiol-ene reaction using methyl-3-mercaptopropionate. After the reaction, the disappearance of the $\text{H}_2\text{C}=\text{CH-R}$ signal of the AGE (6.00 – 5.00 ppm; red area) as well as the appearance of the newly added thiol signals (e.g., 2.97 – 2.39 ppm; green area).

The size exclusion chromatogram (refer to **Figure 28**) after the reaction showed a single peak with a M_n of approx. 21,600 g mol^{-1} , a D of 1.66 and a prominent shoulder at the higher molar mass side. With a M_p of approx. 42,700 g mol^{-1} , the molar mass of the shoulder was almost twice as high as the M_p of the main peak (19,500 g mol^{-1}). This indicated a slight degree of branching in the form of dimerization of two chains. Nevertheless, a shift to higher molar masses in comparison to the precursor polymer from 18,600 to 21,600 g mol^{-1} was visible, confirming the extension of the chain. This observation in combination with the results of the NMR spectroscopy confirmed the third modification of PAGE, introducing an ester as a functional group to the already alkyl and aromatic modified system.

A summary of all size exclusion chromatograms and ^1H NMR spectra for all conducted CE and PPM reactions until now are displayed in **Figure 29** and **Figure 30**. In case of the chromatograms, a change to a higher molar mass after each reaction is visible, while for the ^1H NMR spectra the appearance of the $\text{H}_2\text{C}=\text{CH-R}$ signal after each extension and its disappearance after the modifications can be noticed.

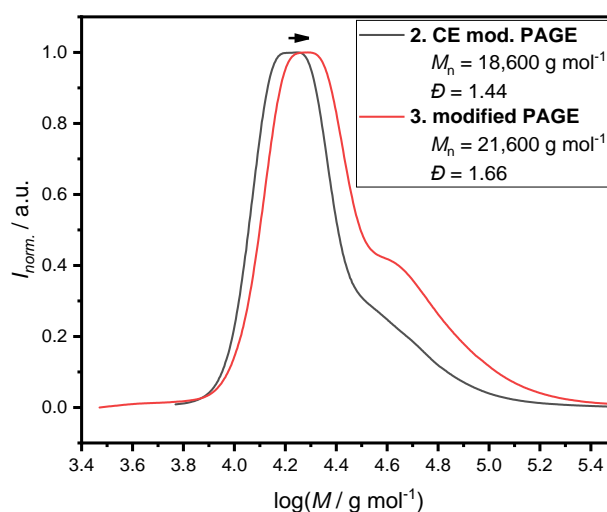


Figure 28: Size exclusion chromatograms of twice chain extended modified PAGE before (gray) and after (red) the third PPM via thiol-ene reaction using methyl-3-mercaptopropionate. After the reaction a small shift to higher molar mass as well as the formation of a shoulder could be observed.

It is worth noting, that due to the presence of an homopolymerization during each CE, as well as the precipitation after each step, the over yield of the products is moderate. To improve the yield, a different purification method could be used and the reactions could be conducted using reactants and solvents which are freshly purified/dried before use, preventing a possible homopolymerization initiated by impurities. However, due to the fast forward approach of this method, those changes were neglected. In **Table 1** an overview of the polymerization of AGE with each CE and PPM including the equivalents of monomer, equivalents of thiol, M_n and \bar{D} is displayed.

Table 1: Overview of the polymerization of AGE with each CE and PPM, including equivalents of monomer, equivalents of thiol, M_n and \bar{D} .

Entry	Eq. of AGE	Eq. of thiol ^{*1}	M_n / g mol ⁻¹	\bar{D}
PAGE	50	-	3,700	1.13
1. CE	50	-	11,100	1.07
2. CE	50	-	18,600	1.44
1. PPM	-	4	7,700	1.08
2. PPM	-	4	13,000	1.10
3. PPM	-	4	21,600	1.66

^{*1}: Equivalents of thiol in respect to one available double bond in the pendant chain.

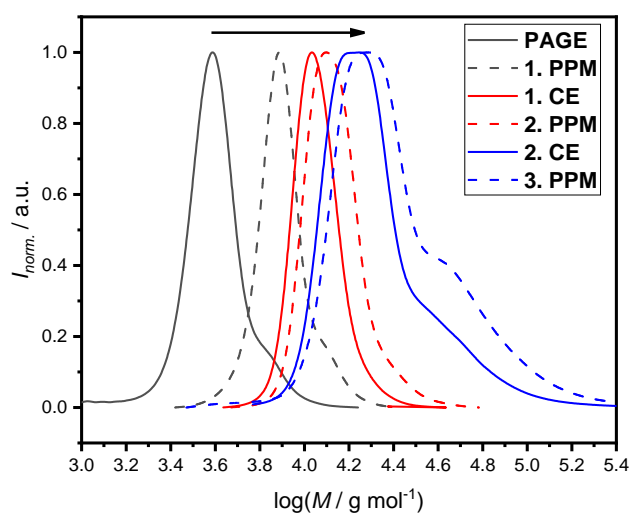


Figure 29: Collection of all size exclusion chromatograms for each CE and PPM reaction of PAGE. A clear shift in the molar mass from the beginning (PAGE; gray) to the last modification (3. PPM; yellow) can be observed.

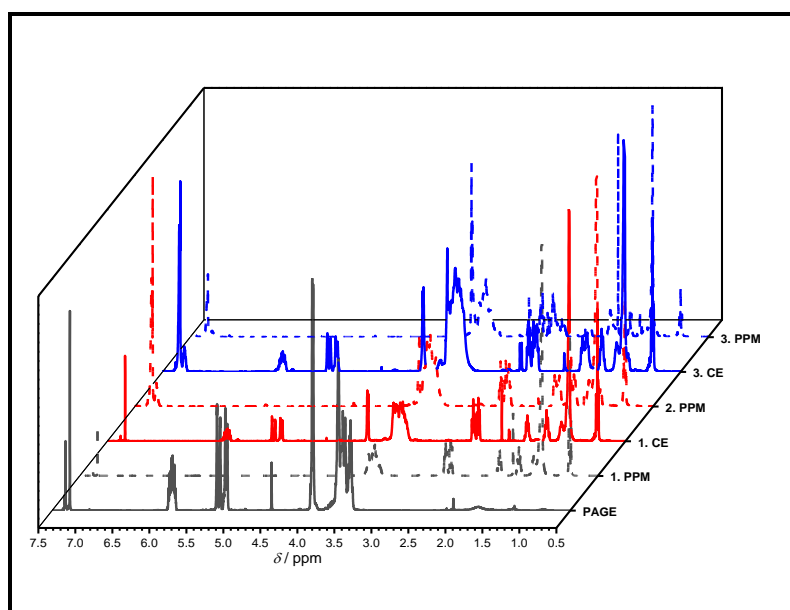
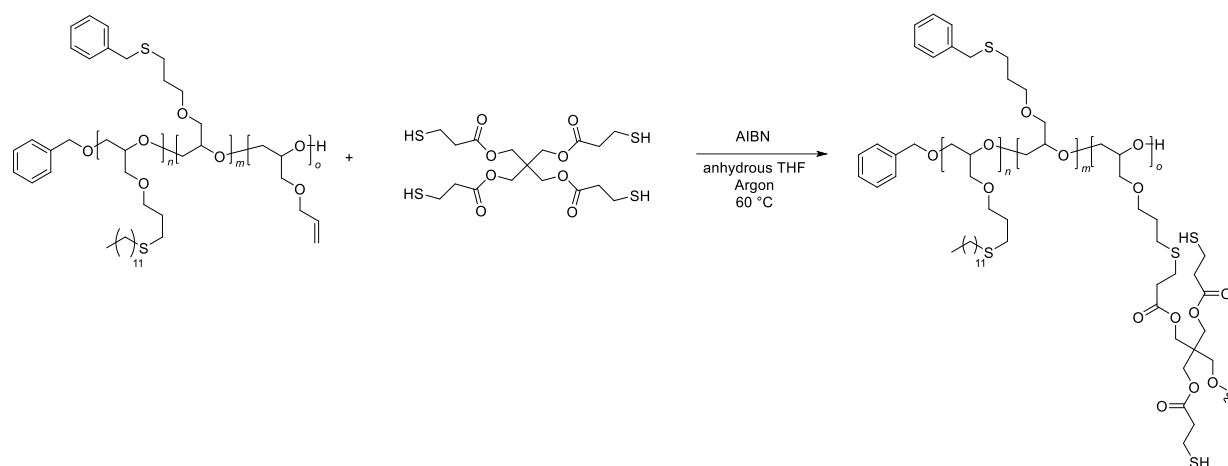


Figure 30: Collection of all ^1H NMR spectra for each CE and PPM reaction of PAGE. With each reaction, the appearance and disappearance of the $\text{H}_2\text{C}=\text{CH-R}$ signal of the AGE units can be observed.

4.1.5.1. Synthesis of a Sequence-Controlled Network

Besides the synthesis of linear sequence-controlled multiblock copolymers, sequence-controlled networks could be of high interest. Due to the PEG-like backbone of the synthesized multiblock copolymer and the well-known biocompatibility and medical application of PEG,¹⁷⁶ a generated sequence-controlled PAGE-network could find use in similar biomedical applications. What could set this network apart from the well-known ones is the possibility to generate a network with desired properties by introducing different functionalities to the system via PPM before crosslinking in the final step.

Therefore, a first attempt to synthesize a network was conducted based on the previously synthesized twice chain extended PAGE and tetrathiol pentaerythritol tetrakis(3-mercaptopropionate). For each available double bond in the polymer, 0.5 equivalents of the thiol were used, which should result in a crosslinked structure with two thiol groups remaining per tetrathiol. The reaction conditions were similar to the previous thiol-ene reactions (displayed in **Scheme 40**).



Scheme 40: Reaction equation of the thiol-ene reaction of twice chain extended PAGE using pentaerythritol tetrakis(3-mercaptopropionate) with AIBN in anhydrous THF under inert atmosphere at 60 °C.

In comparison to previous modifications, a noticeable increase in viscosity could be observed, which got to the point where the stirring bar stopped moving. This phenomenon was an indication for the formation of a crosslinked structure. However, after the reaction time the product could be dissolved in THF, which was only possible after treating the sample multiple times with the solvent. In case of a complete crosslinked system this phenomenon should not be observable, suggesting a branched structure instead of the desired crosslinked one. The ¹H NMR spectrum

(depicted in **Figure 31**) of the product was in accordance with the expected one, showing no signs of the $\text{H}_2\text{C}=\text{CH-R}$ signals, indicating the total conversion of the pendant double bond.

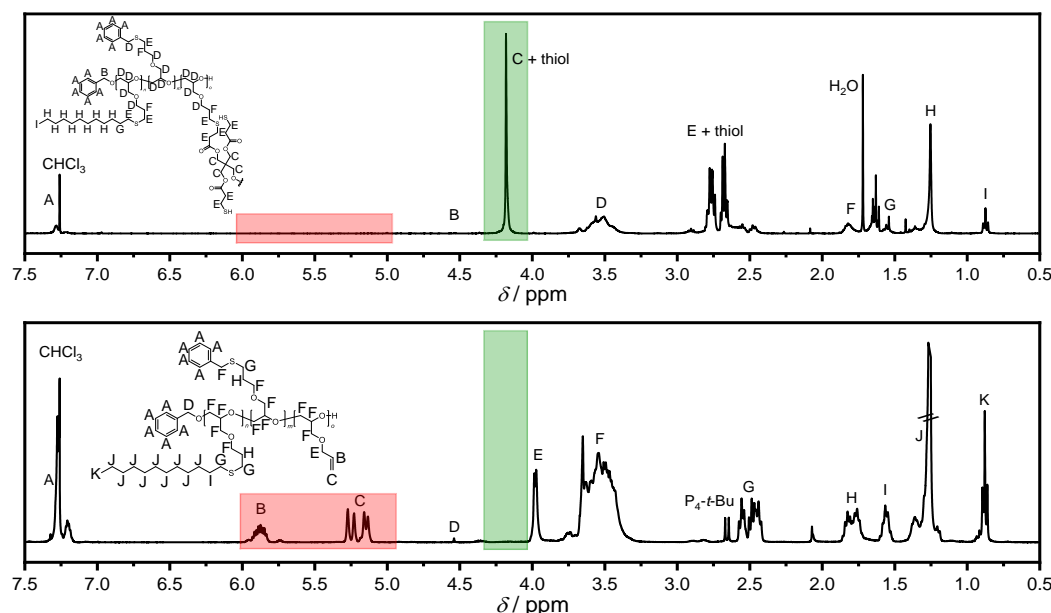


Figure 31: ^1H NMR spectra of twice chain extended modified PAGE before (bottom) and after (top) the PPM via thiol-ene reaction using pentaerythritol tetrakis(3-mercaptopropionate). After the reaction, the disappearance of the $\text{H}_2\text{C}=\text{CH-R}$ signals of the AGE (6.00 – 5.00 ppm; red area) and the appearance of the thiol signals (e.g., 4.17 ppm; green area) could be observed. Solvent: CDCl_3 .

During the SEC sample preparation, a different behavior in contrast to the previous modification reaction could be observed. While the previous reactions pass through syringe filters without any problem, the system with the tetrathiol clogged the filter almost immediately. This phenomenon is often observed by crosslinked or branched systems, which would confirm the success of the modification. After multiple filters and high pressure, enough sample was obtained for a SEC measurement of which the chromatogram can be seen in **Figure 32**. Herein, a broad peak system with a \bar{D} of 101 and a M_n of approx. $25,000 \text{ g mol}^{-1}$ can be seen. In total, 5 main peaks can be identified, with the largest one being at approx. $14,800 \text{ g mol}^{-1}$, followed by $24,000 \text{ g mol}^{-1}$ and $9,100 \text{ g mol}^{-1}$. The two other prominent peaks are situated at the higher molar mass side at approx. $490,000 \text{ g mol}^{-1}$ and $7,943,000 \text{ g mol}^{-1}$. However, the determined values for the molar masses were the ones originating from the parts of the modified polymer which could pass through the filter. Therefore, it can be

assumed that the residue in the filter has an even higher molar mass than the determined $7,943,000 \text{ g mol}^{-1}$.

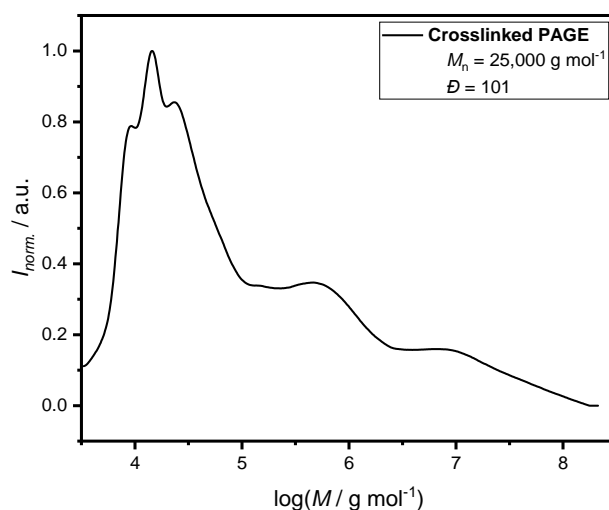


Figure 32: Size exclusion chromatogram of crosslinked modified PAGE. Multiple peaks and shoulder are visible with an overall \bar{D} of 101 and molar masses up to $7,943,000 \text{ g mol}^{-1}$.

The ^1H NMR spectrum as well as the size exclusion chromatogram indicated a successful modification of the polymer, however not a totally crosslinked structure, but a branched system. Still, the high \bar{D} of 101 and determined molar masses up to $7,943,000 \text{ g mol}^{-1}$ could be seen as evidence for a beginning network formation at least. To improve the results and obtain a totally crosslinked system, the ratio of thiol groups to double bonds needs to be tuned to be lower than 1:1, which for example can be achieved by reducing the amount of tetrathiol.

In conclusion of this main chapter, novel ways to synthesize sequence-controlled multiblock copolymers using a single monomer were investigated. In comparison to the more traditional method in which multiple different monomers are necessary, the utilization of a single monomer should reduce the amount of monomer syntheses, which sometimes can be laborious, time-consuming and costly. The main concept of those new systems was the combination of CE reactions via living/controlled polymerization methods with PPM reactions. Therefore, different polymerization techniques and monomer systems were investigated, i.e. the RAFT polymerization of PFPA, the ATRP of PFPMA and the CROP of ACL. After those attempts failed, promising results could be achieved by polymerizing the commercially available AGE

via AROP using the *Schwesinger* base P_4 -*t*-Bu as promoter. In a series of CEs with subsequential thiol-ene reactions, a linear triblock copolymer with aliphatic, aromatic and ester group as functionalities could be successfully synthesized. Additionally, a slightly crosslinked triblock copolymer network could be achieved by using a tetrathiol in the last PPM step. The success of each step could be confirmed by NMR spectroscopy and SEC.

4.2. AROMA - Anionic Ring-Opening Monomer Addition

Parts of this chapter and the related parts in the experimental section were adapted with permission from a publication¹⁷⁷ written by the author of this thesis (Sven Schneider), published in *Programmable Materials*. Additionally, parts of the evaluation and synthesis were conducted in cooperation with Benedikt L. Schwalm in context of a bachelor's thesis under the supervision of the author (Sven Schneider).

After the successful synthesis of a sequence-controlled triblock copolymer using the newly established system based on the repeated AROP of AGE with subsequential thiol-ene reactions, the limits of this system should be explored. Due to the benefits of the living character of AROP, e.g., low \bar{D} and chains with tailored length, the reduction of the average number of repeating units, which was previously 20 to 50 units, to an average number of one should be possible. Thereby, it should be possible to synthesize sequence-controlled polymers, which approach the precision of sequence-defined polymers.

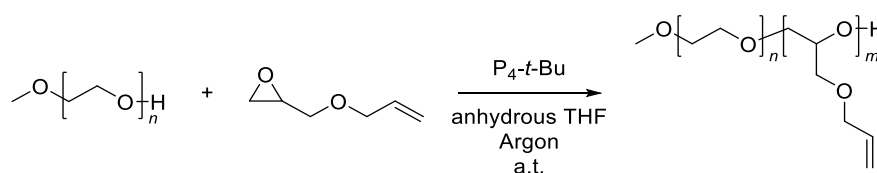
Therefore, this chapter of the thesis deals with the possible expansion of the already available options to synthesize sequence-defined polymers using polymerization techniques, similar to the already known RDRP ones. However, instead of relying on radical active chain ends, this approach will use an anionic species.

4.2.1. Anionic Ring-opening Monomer Addition of AGE to Methoxy Polyethylene Glycol

As mentioned above, the in this thesis established method of combining CEs of AGE with PPM via thiol-ene reactions was employed to achieve the synthesis of sequence-controlled multiblock copolymer with an average repeating unit of one.

In theory, benzyl alcohol could be used as the initiator for this synthesis once again, but it was replaced by methoxy polyethylene glycol with an average molar mass of $1,900 \text{ g mol}^{-1}$ (mPEG-1900) out of convenience. In case of the benzyl alcohol, the obtained molecules cannot be precipitated and need to be purified using a more laborious methods, such as column chromatography, while mPEG-1900 can be precipitated easily. Therefore, mPEG-1900 was used as a precipitation agent.

Before any single monomer addition reaction was conducted, a polymerization with 20 equivalents of AGE under inert atmosphere at ambient temperature for 2.5 hours were done to investigate the suitability of mPEG-1900 as initiator (refer to **Scheme 41**).



Scheme 41: Reaction equation of the AROP of AGE with mPEG-1900 using P_4 -t-Bu in anhydrous THF under inert atmosphere at ambient temperature.

The ^1H NMR spectrum (depicted in **Figure 33**) associated to this polymerization showed the $\text{H}_2\text{C}=\text{CH}-\text{R}$ signals of AGE in the range of 6.00 – 5.00 ppm as well as the characteristic signals of mPEG, e.g., the methyl group at 3.37 ppm. Additionally, the signals of the promoter, the *Schwesinger base*, were visible due to insufficiency during the purification process. In general, the spectrum was in accordance with the expected one and all signals could be assigned to their associated protons, indicating a successful polymerization using mPEG-1900 as initiator.

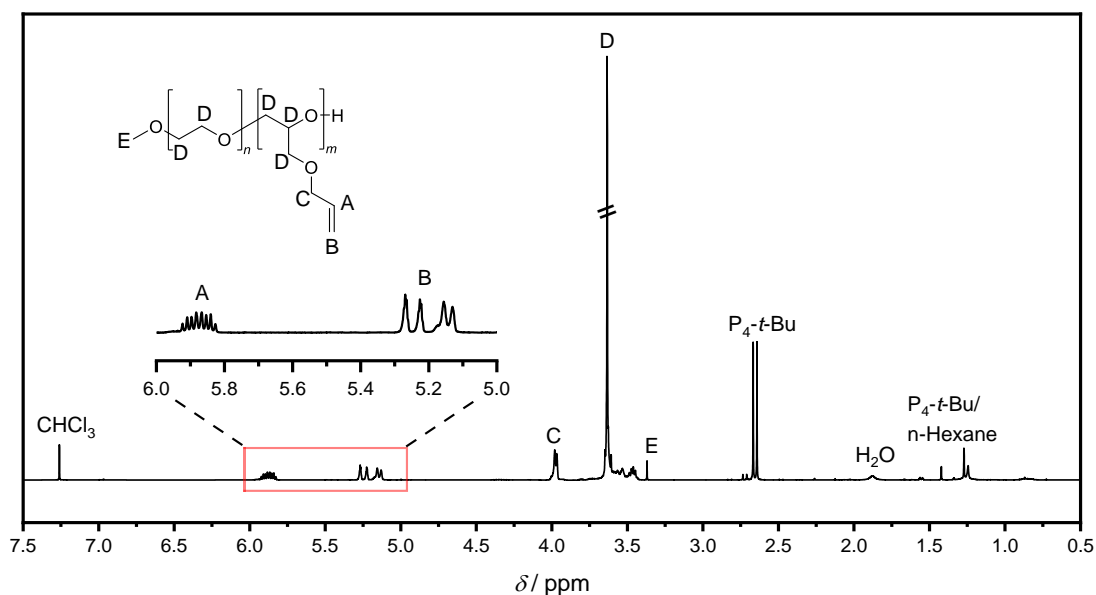


Figure 33: ^1H NMR spectrum of PAGE using mPEG-1900 as initiator. Solvent: CDCl_3 .

The assumption of a successful polymerization got further supported by the single symmetrical peak with a M_n of approx. $5,000 \text{ g mol}^{-1}$ and a \bar{D} of 1.03 in the corresponding size exclusion chromatogram (**Figure 34**). Furthermore, the absence of a second peak suggested the total conversion of the initiator mPEG-1900, confirming the suitability of this molecule for the reaction.

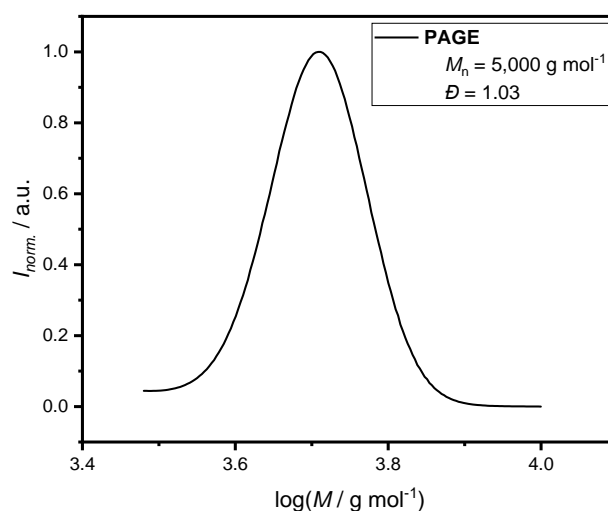


Figure 34: Size exclusion chromatogram of PAGE using mPEG-1900 as initiator. A single symmetrical peak could be observed.

After the successful polymerization of AGE using the mPEG-initiator, two different approaches for the synthesis of sequence-controlled polymers with a number average of one were investigated; (*i*) making use of the living character of the polymerization and (*ii*) a slight excess of monomer. Both approaches will be addressed in detail in the following sections.

4.2.2. Anionic Ring-Opening Monomer Addition via Kinetic Approach

For the first approach, the linear increase of $\ln([M]_0/[M])$ with the reaction time, which is typical for a polymerization in a living manner, was used to calculate the exact moment a single unit is added to the chain. The necessary equation¹⁷⁸ is the following:

$$\ln \frac{[M]_0}{[M]} = k_p \cdot t$$

$[M]_0$ is the monomer concentration at the start of the polymerization, $[M]$ the monomer concentration at the given time t and k_p the propagation constant, for the case of a constant concentration of the active propagating species over the entire period.¹⁷⁸

In theory, the moment of the single monomer addition can be determined by knowing the exact conversion at which a single unit should be added, if k_p is also known, which can be determined experimentally. In case of a polymerization with a monomer:initiator ratio of 20:1, the desired chain length of a single unit should be at 5 % conversion. To get k_p , a kinetic study (**K1**) was conducted, in which samples were taken after 0.5, 1, 2.5, 3.5 and 5 hours to calculate the conversion of the monomer by comparing the integrals of the monomer signal at 3.12 ppm with the ones of polymer signal at 5.85 ppm in the ¹H NMR spectrum. Because the signal at 5.85 ppm overlapped with one of the monomer signals, the overall integral needed to be reduced by the integral of the latter. By plotting the resulted values of $\ln([M]_0/[M])$ against the time and applying a linear fit, k_p represents the slope of the fit. The plot is shown in **Figure 35** while a list of all times with the associated monomer conversion is shown in **Table 2**.

Table 2: Reaction time, monomer conversion and $\ln([M]_0/[M])$ of the kinetic study (**K1**) of the polymerization of AGE using untreated mPEG-1900 as initiator.

<i>Time / min</i>	<i>Conversion / %</i>	<i>$\ln([M]_0/[M])$</i>
30	15.9	0.174
60	22.9	0.260
150	30.4	0.363
210	36.4	0.452
300	37.5	0.470

Noticeable was the flatten of $\ln([M]_0/[M])$ at longer reaction times, instead of the linear increase, making a linear fit impossible. This might be due to a decrease in the active propagating species during the reaction, resulting from side reactions such as the termination of the chain ends induced by impurities (e.g., water). Due to the high affinity of mPEG towards water a second approach (**K2**) was done to investigate this presumption. However, this time the initiator was treated before use by drying under reduced pressure at 40 °C. Additionally, because a conversion of 16 % was already reached after 30 minutes for the first reaction, another sample after 15 minutes was taken for the second study, to achieve better result for the linear fit. The conversion values for each time are displayed in **Table 3**.

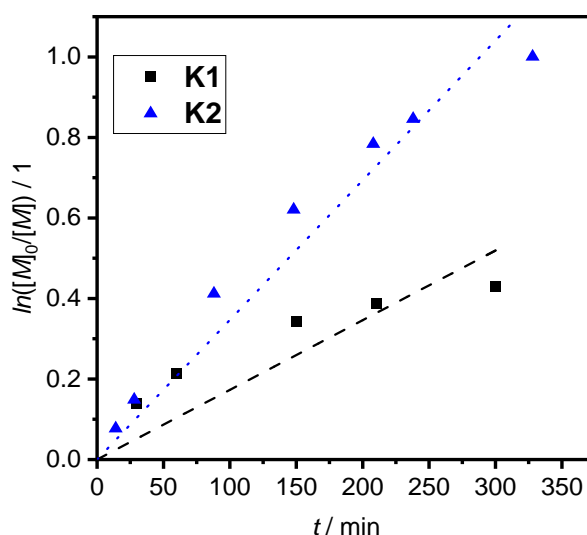


Figure 35: Kinetic study of the polymerization of AGE using untreated (black, **K1**) and pre-dried (blue, **K2**) mPEG-1900 as initiator. In case of the untreated initiator, a clear flattening of the curve with longer reaction time could be observed.

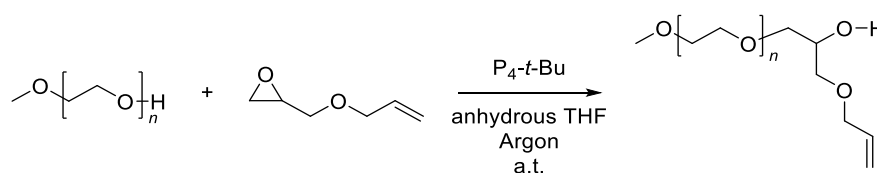
Table 3: Reaction time, monomer conversion and $\ln([M]_0/[M])$ of the kinetic study (**K2**) of the polymerization of AGE using pre-dried mPEG-1900 as initiator.

<i>Time / min</i>	<i>Conversion / %</i>	<i>$\ln([M]_0/[M])$</i>
14	7.41	0.0770
28	13.8	0.148
88	33.8	0.412
148	46.2	0.621
208	54.1	0.779
238	56.9	0.842
328	63.2	1.001

In comparison to the first study (**K1**; untreated initiator), the second one (**K2**; treated initiator) resulted in a plot of a more linear manner with a higher conversion at the same time (displayed in **Figure 35**). This confirmed the presumption that water indeed caused side reaction during the first reaction, which could now be reduced but not eliminated. Moreover, this confirmed the importance of dry and purified chemicals for these polymerization techniques to obtain a polymerization in a living manner.

This time, a conversion of approx. 7 % could be reached after 15 minutes, getting closer to the desired 5 %. Because the relevant part for this approach is in the first minutes of the polymerization, the linear fit was applied to the 3 first values, resulting in the determination of $k_p = 0.00476 \pm 1.48 \cdot 10^{-4} \text{ min}^{-1}$. If the corresponding values are inserted into the abovementioned equation, the moment of the single addition can be calculated to be approx. 11 minutes (10 minutes and 46 seconds).

With this information, first reactions to add a single unit to the initiator were conducted at ambient temperature (refer to **Scheme 42**).



Scheme 42: General reaction equation of the first CE of mPEG-1900 with AGE via the kinetic approach, using P₄-t-Bu in anhydrous THF under inert atmosphere at ambient temperature.

Due to the anionic ring-opening character of the reaction and the addition of a single monomer, the method was named *Anionic Ring-Opening Monomer Addition*, short *AROMA*. It is important to mention that the displayed polymer structures of those AROMA-polymers are depicted with a single repeating unit, even though the actual repeating unit is an average of one.

After the calculated reaction time, the polymerization was stopped and the polymer purified. The exact number of added AGE units was determined via ¹H NMR spectroscopy, comparing the H₂C=CH-R signals of the C=C double bond at 5.87 ppm with the methyl group at 3.36 ppm of the mPEG-initiator. The average repeating unit was determined to be 2.075 ± 0.065 , which was twice as high as the targeted value. Possible reasons for that were imprecise weighing of reactants, which would lead to a deviation in the calculated time, or an inaccurate linear fit. While the first could be easily avoided by using proper working techniques and effective instrumental devices, the

latter can be solved by improving the fit with more measuring points. Therefore, another study (**K3**) was done with a tighter timing between each sample, namely every 2 minutes. The associated plot and a list of times with the corresponding monomer conversions are shown in **Figure 36** and **Table 4**.

Noticeable is an outlier at 4 minutes, which is due to a late quenching of the sample. If excluded from the calculation, a rather linear fit with a slope of $0.00851 \pm 1.52 \cdot 10^{-4} \text{ min}^{-1}$ could be obtained, leading to an estimated reaction time of approx. 7 minutes (7 minutes and 25 seconds) for the addition of a single unit.

Table 4: Reaction time, monomer conversion and $\ln([M]_0/[M])$ of the kinetic study (**K3**) of the polymerization of AGE using pre-dried mPEG-1900 as initiator.

<i>Time / min</i>	<i>Conversion / %</i>	<i>$\ln([M]_0/[M])$</i>
2	1.96	0.0198
4	4.76	0.0488
6	4.76	0.0488
8	6.54	0.0677
10	8.26	0.0862

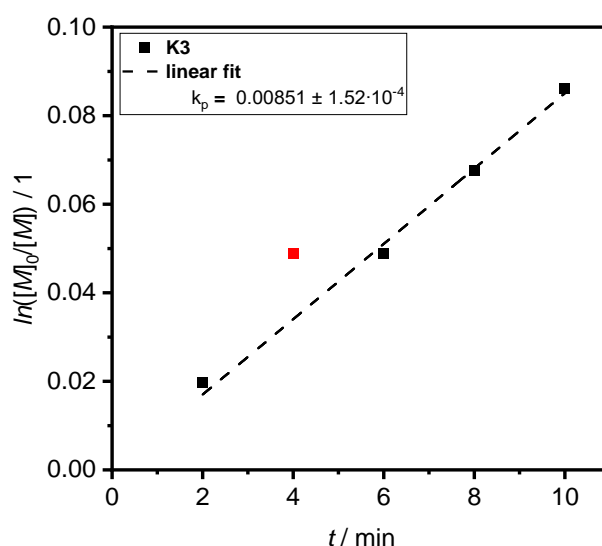


Figure 36: Kinetic study of the polymerization of AGE using pre-dried mPEG-1900 as initiator for a shorter time frame. At 4 minutes, an outlier due to late quenching is visible.

Afterwards, a new polymerization was conducted with a reaction time of 7 minutes and 25 seconds, leading to a mPEG-1900 with an average AGE repeating unit of 1.28. This result was an improvement to its predecessors, but still too high and inaccurate. An

overview of each kinetic study with their respective k_p , estimated addition time and the resulted average repeating unit is shown in (Table 5).

Table 5: Overview of each kinetic study with their respective k_p , estimated addition time and the resulted average repeating unit.

Entry	k_p / min^{-1}	Est. addition time	Average repeating unit
K1	$0.00173 \pm 2.36 \cdot 10^{-4}$	-	-
K2	$0.00476 \pm 1.48 \cdot 10^{-4}$	10 min, 46 s	2.075 ± 0.065
K3	$0.00851 \pm 1.52 \cdot 10^{-4}$	7 min, 25 s	1.28

Even after the development in regards of the linear fit, the obtained number of repeating units was still insufficient, leading to the assumption that the inaccuracy of the weighing seems to be a bigger issue than expected. While the weighing process of the reactants and solvents was done as accurately as possible, even a small difference in equivalents in addition to the error margins of the applied apparatus results in a change in concentration and therefore in a deviation of the fit. Therefore, the achievement of an average repeating unit of one with this method is a difficult undertaking and needs further research. However, due to a limited time schedule it was decided to take some distance from this approach and focus on the second tactic, which is based on utilizing only a small feed excess of the monomer.

4.2.3. Anionic Ring-Opening Monomer Addition via Monomer Excess Approach

Instead of focusing on the start of the polymerization and trying to use the linear increase of $\ln([M]_0/[M])$ with time, the second approach focused on the end of the polymerization. By plotting the monomer conversion vs. reaction time (displayed in **Figure 37**), the decrease of the monomer incorporation rate into the backbone over the course of the polymerization becomes visible.

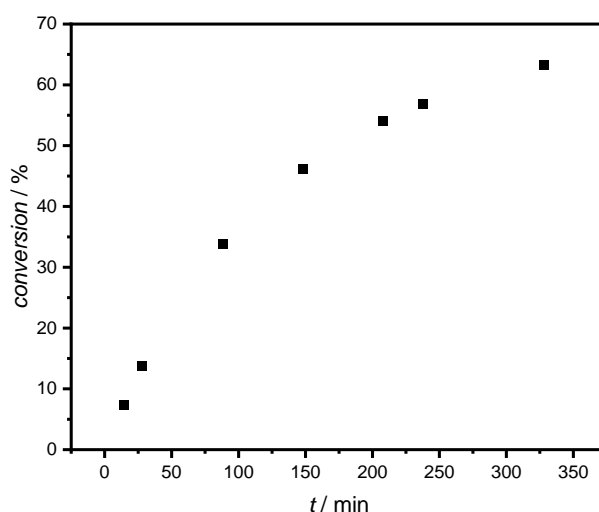
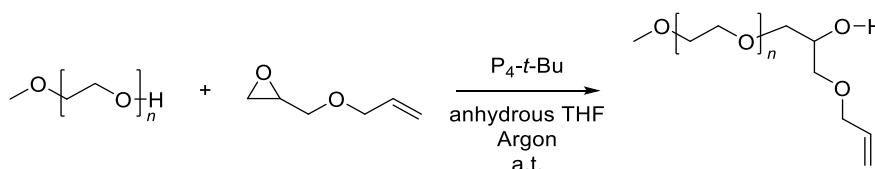


Figure 37: Monomer conversion vs. time of the polymerization of AGE using pre-dried mPEG-1900 as initiator. With increasing reaction time, a flattening of the curve is noticeable.

In theory, the time span between the incorporation of a further unit should be bigger at the end of the polymerization than at its start, reducing the error margin. Therefore, multiple polymerizations of AGE using a small feed excess of 1.25 eq. in relation to the mPEG-initiator were conducted at ambient temperature for 5 hours, resulting in a yield of 89 % (refer to **Scheme 43**).



Scheme 43: Reaction equation of the first CE of mPEG-1900 with AGE via the small excess approach, using $\text{P}_4\text{-t-Bu}$ in anhydrous THF under inert atmosphere at ambient temperature.

To determine the number of repeating units, the integrals in the ^1H NMR spectrum of the proton signals of the double bond at 5.88 ppm were compared to the ones of the methyl group at 3.36 ppm (see **Figure 38**; II.). With an average repeating unit of 1.02 ± 0.07 , the determined value improved in comparison to the first method (1.28 repeating units) and was in close proximity of the targeted value of one. It is crucial to stated, that due to the applied method, which is based on the anionic polymerization technique, polymeric systems with low \bar{D} (values between $1.01 - 1.1^{12}$) can be achieved, but never monomodal systems. Additionally, due to the already polymeric character of the initiator, a value of \bar{D} greater than one is already set from the start. A size exclusion chromatogram (displayed in **Figure 38**; I.) of this “AROMA-polymer” showed a single symmetrical peak with a \bar{D} of 1.05 and a M_n of $3,200 \text{ g mol}^{-1}$, indicating no side reaction such as crosslinking.

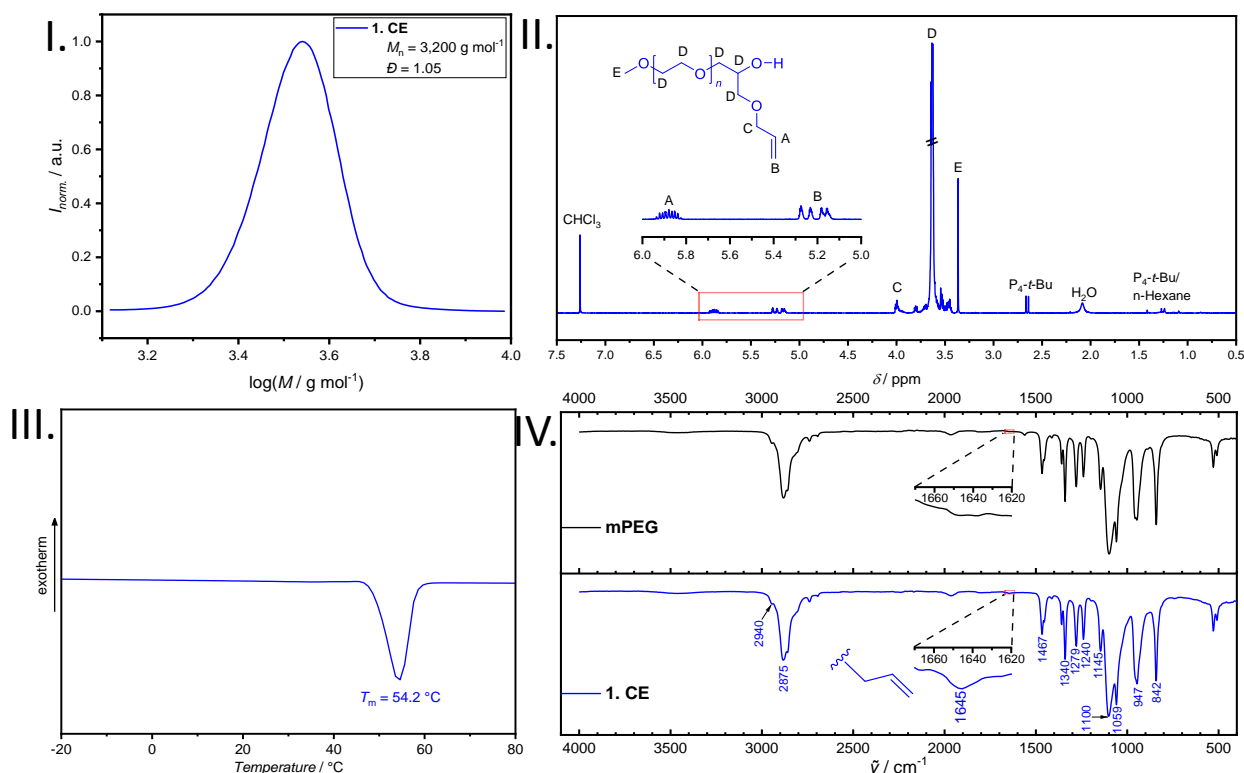


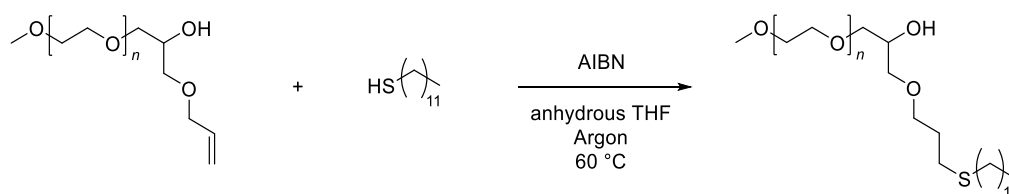
Figure 38: I. Size exclusion chromatogram after the first CE of mPEG-1900 with AGE. II. ^1H NMR spectrum of the AGE chain extended mPEG-1900. The new signals between 6.00 – 5.00 ppm confirm a successful CE. Solvent: CDCl_3 . III. DSC thermogram (heating curve; 2. cycle) of AGE chain extended mPEG with a visible T_m at 54.2°C . IV. ATR FT-IR spectrum of mPEG-1900 (black) and the first CE (blue). After the CE a new signal at $1,645 \text{ cm}^{-1}$ appears, which could be assigned to the $\text{C}=\text{C}$ double bond of the AGE.

To further confirm the presence of AGE in the polymer, attenuated total reflection Fourier-transform infrared (ATR FT-IR) spectroscopy was conducted. Comparing the spectrum (see **Figure 38**; IV.) of precursor polymer (mPEG-1900) with the

AROMA-polymer, a minimal change at $1,645\text{ cm}^{-1}$ was noticeable. This signal is characteristic for the C=C double bond's stretching vibration¹⁷⁹ and confirmed the presence of AGE in the system. The low intensity of the signal can be explained by the small share of the newly added AGE unit to the overall molecular structure. In addition to the already mentioned characterization methods, a fourth one, the differential scanning calorimetry (DSC), was used to determine the glass transition temperature (T_g) and/or melting temperature (T_m) of the AROMA-polymer. The thermogram (displayed **Figure 38**; *III.*) showed a single T_m at $54.2\text{ }^\circ\text{C}$. This value will be used as a reference temperature to see if any further modifications influence the T_m in any way. In summary, an average repeating unit of AGE of 1.02 ± 0.07 could be determined via ^1H NMR spectroscopy, which is in close proximity of the targeted value of one. Furthermore, ATR FT-IR spectroscopy confirmed the presence of AGE in the system as well by showing the characteristic C=C double bond's stretching vibration at $1,645\text{ cm}^{-1}$ while the SEC excluded any crosslinking of the system.

After those promising results, first PPM reactions with 1-dodecanethiol were conducted to truly synthesize sequence-defined-like polymers and to investigate the influence of the side chain on the active center, similar to the previous tests done in the first project. Furthermore, it was important to confirm the viability of the system to add an average repeating unit of one to the system multiple times.

The thiol-ene reaction with 1-dodecanethiol was conducted at similar conditions (refer to **Scheme 44**) as the previous reactions (yield: 67 %) and characterized via ^1H NMR spectroscopy, SEC and ATR FT-IR spectroscopy and DSC.



Scheme 44: Reaction equation of the first PPM of the AROMA-polymer using 1-dodecanethiol and AIBN in anhydrous THF under inter atmosphere at $60\text{ }^\circ\text{C}$.

By comparing the ^1H NMR spectra of the AROMA-polymer before (see **Figure 38**; *II.*) and after the modification (displayed in **Figure 39**; *II.*), changes were visible. Firstly, in the range of $6.00 - 5.00\text{ ppm}$ the $\text{H}_2\text{C}=\text{CH}-\text{R}$ signal of AGE vanished, while secondly, new ones emerged (e.g., 0.87 ppm), which could be assigned to the 1-dodecanethiol,

confirming a successful modification. With a ratio of $1:1 \pm 0.01$ of the methyl group of the mPEG (3.37 ppm) and the methyl group of the 1-dodecanethiol (0.87 ppm), the relation between the initiator and the thiol was in accordance with the desired value of approx. 1.02.

In addition to this, the size exclusion chromatogram (refer to **Figure 39; I.**) after the reaction showed the shift of a single symmetrical peak with a \bar{D} of 1.05 and a M_n of $3,800 \text{ g mol}^{-1}$ to a higher molar mass, in comparison to its precursor (\bar{D} of 1.05 and a M_n of $3,200 \text{ g mol}^{-1}$). The difference in molar mass between the determined and the theoretical value ($3,400 \text{ g mol}^{-1}$) can be explained by the structural difference of the used polymer standard to the AROMA-polymer. Furthermore, the absence of any second peak or shoulder formation excluded the occurrence of side reactions such as crosslinking.

The DSC thermogram (see **Figure 39; III.**) of the 1-dodecanethiol modified polymer showed a small increase of 1°C in the T_m (54.2 to 55.2°C), which is probably due to the error margin of the device instead of structural change. However, the exothermic peak of a cold crystallization at 44.6°C (T_{cc}) could be observed, which is initiated by the long alkyl chains of the newly added 1-dodecanethiol moiety and therefore indicate a structural change after the reaction.

Another change between the polymer before and after the thiol-ene reaction can be seen in the ATR FT-IR spectrum (depicted in **Figure 39; IV.**). The previous signal at $1,645 \text{ cm}^{-1}$, which was assigned to the C=C double bond's stretching vibration of the AGE, disappeared after the modification, indicating a structural change.

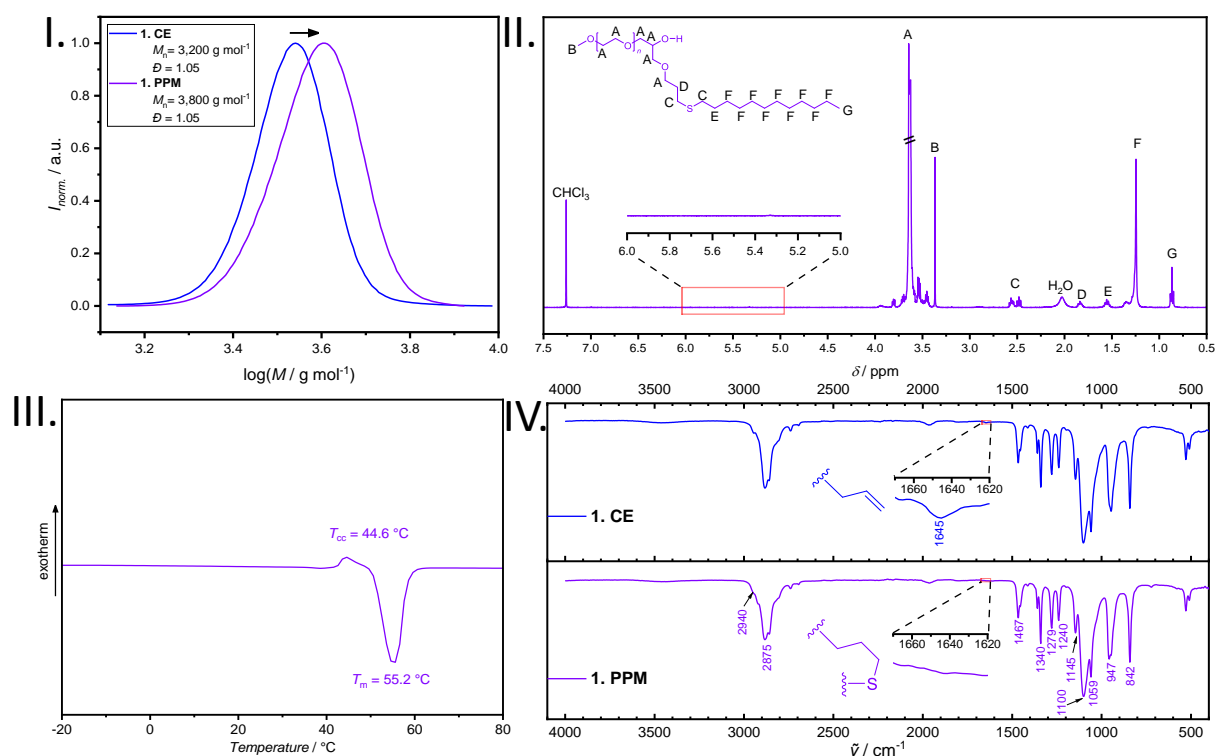
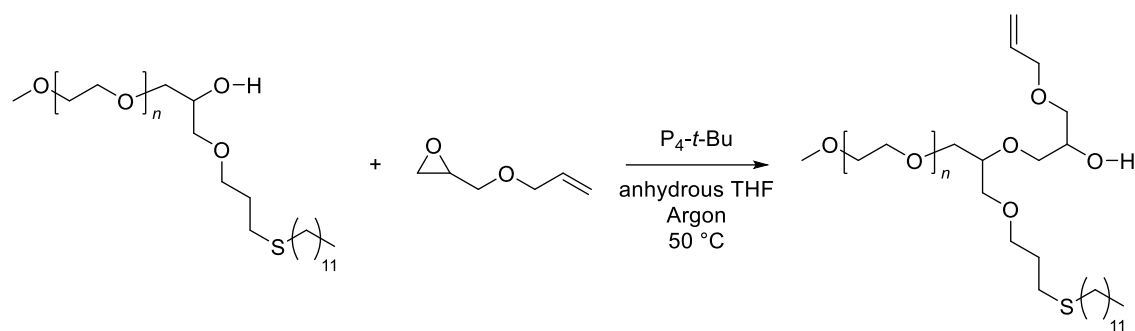


Figure 39: I. Size exclusion chromatogram of chain extended mPEG-1900 before (blue) and after (violet) the first PPM via thiol-ene reaction using 1-dodecanethiol. After the modification, a shift to higher molar masses is visible in comparison to the previous polymer. II. ^1H NMR spectrum of chain extended mPEG-1900 after the thiol-ene reaction with 1-dodecanethiol. After the reaction the signals of the double bond between 6.00 – 5.00 ppm disappeared and the thiol signals (e.g., 0.87 ppm) appeared, confirming a successful modification reaction. Solvent: CDCl_3 . III. DSC thermogram (heating curve; 2. cycle) of 1-dodecanethiol modified chain extended mPEG-1900 with a visible T_m at 55.2°C . IV. ATR FT-IR spectrum of once chain extended mPEG-1900 (blue) and the 1-dodecanethiol modified polymer (violet). After the modification the signal at $1,645 \text{ cm}^{-1}$ disappeared, confirming a successful modification.

In summary, characterization done for the 1-dodecanethiol modified AROMA-polymer via ^1H NMR spectroscopy, SEC and ATR FT-IR spectroscopy and DSC, confirmed the addition of the thiol to the polymer and therefore a successful modification. As mentioned above, this modified polymer should be further used as a macroinitiator for additional AROMA reactions, confirming the viability of the AROMA method for the synthesis of sequence-controlled polymers with an average repeating unit of one. Due to the knowledge gained in the previous project in regards of changing from a primary alcohol to a secondary one, the second CE was conducted with 1.25 eq. of monomer in relation to the initiator at a higher temperature (50°C) than the previous AROMA reaction, resulting in a yield of 77 % (see **Scheme 45**).



Scheme 45: Reaction equation of the second CE of mPEG-1900 with AGE via the small excess approach, using P_4 - t -Bu in anhydrous THF under inert atmosphere at 50 °C.

To confirm the success of the reaction, ^1H NMR spectroscopy, SEC, ATR FT-IR spectroscopy and DSC were used once again. After the purification of the polymer, the ^1H NMR spectrum (displayed in **Figure 40**; II.) showed the familiar $\text{H}_2\text{C}=\text{CH}-\text{R}$ signals in the range of 6.00 – 5.00 ppm, indicating the presence of AGE in the chain. By checking the ratio between initiator and AGE, an average repeating unit of 1.02 ± 0.06 could be determined, which was almost identical to the previous AROMA reaction and confirming a successful reaction. The size exclusion chromatogram of the CE (refer to **Figure 40**; I.) displayed a single symmetrical peak with a \bar{D} of 1.05 and a M_n of $4,100 \text{ g mol}^{-1}$, which was a slight increase in molar mass in comparison to the precursor polymer ($M_n = 3,800 \text{ g mol}^{-1}$). Similar to the first extension or PPM, the lack of further peaks or shoulders indicate the absence of side reactions e.g., crosslinking. The DSC thermogram (see **Figure 40**; III.) of the twice chain extended polymer showed a small decrease in T_m of $2.2 \text{ }^\circ\text{C}$ (55.2 to $53 \text{ }^\circ\text{C}$) as well as a cold crystallization at $43.6 \text{ }^\circ\text{C}$. Once again, this small change can be explained by two points, (i) the error margin of the device and (ii) the small share of AGE to the overall structure of the polymer chain, which should have a small influence on the T_m . The ATR FT-IR spectrum (displayed in **Figure 40**; IV.) of the twice chain extended polymer showed similar to the first extension the appearance of the monomer's characteristic $\text{C}=\text{C}$ double bond's stretching vibration at $1,645 \text{ cm}^{-1}$, confirming the presence of AGE in the chain. Once again, the intensity of the signal was extremely low due to the small share of the AGE to the overall polymer chain.

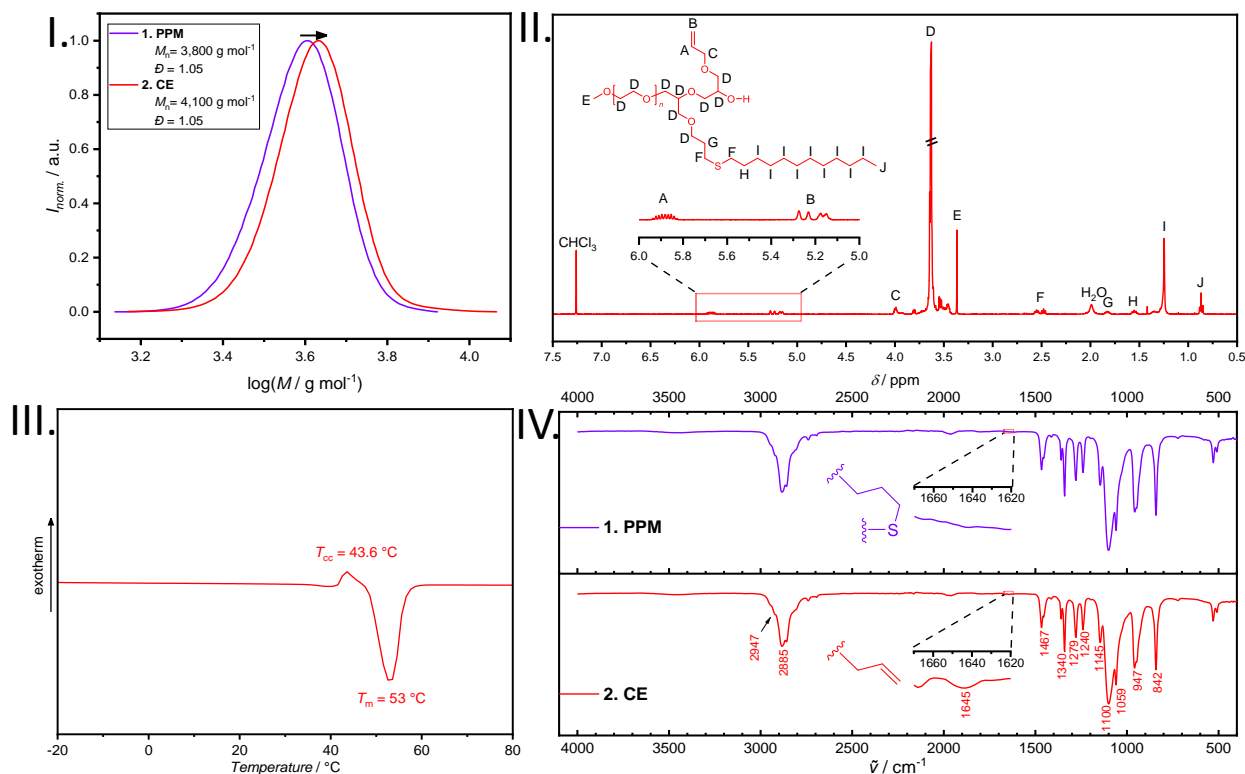
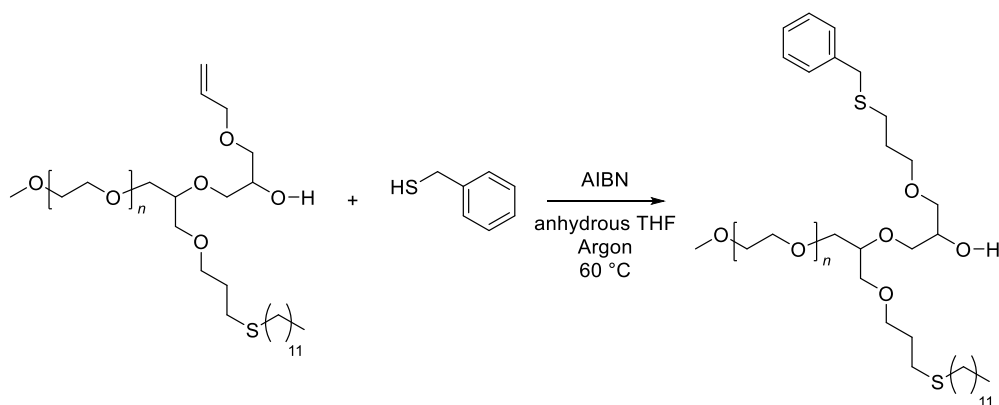


Figure 40: I. Size exclusion chromatogram of modified mPEG-1900 before (violet) and after (red) the second CE with AGE. After the extension, a shift to higher molar masses is visible. II. ^1H NMR spectrum of the twice chain extended mPEG-1900. Again, the signals of the double bond between 6.00 – 5.00 ppm are visible, confirming a successful CE. III. DSC thermogram (heating curve; 2. cycle) of twice chain extended mPEG-1900 with a visible T_m at 53 $^{\circ}\text{C}$. IV. ATR FT-IR spectrum of once modified mPEG-1900 (violet) and twice chain extended mPEG-1900 (red). After the CE a new signal at 1,645 cm^{-1} appears, which could be assigned to the C=C double bond of the AGE.

All in all, the presence of AGE in the chain with an average repeating number of 1.02 ± 0.06 could be verified via multiple characterization methods, namely ^1H NMR spectroscopy, SEC, ATR FT-IR spectroscopy and DSC, confirming the success of the second AROMA reaction.

After the second CE, a second PPM reaction to synthesize a functional sequence-controlled copolymer was conducted at similar reaction conditions to the preceding PPM reaction of 1-dodecanethiol and the AROMA-polymer (see **Scheme 46**). Once again, benzyl thiol was chosen as thiol to introduce an aromatic moiety to the already alkyl containing system.



Scheme 46: Reaction equation of the second PPM of the AROMA-polymer using benzyl mercaptan and AIBN in anhydrous THF under inter atmosphere at 60 °C.

Because of the low intensity of the AGE signal in the ATR FT-IR spectrum and the minimal change of the T_m in the DSC thermogram, ^1H NMR spectroscopy and SEC were the main characterization methods of choice for the next reactions. Those two methods are important, because ^1H NMR spectroscopy is a fast and easy way to determine the number of repeating units added to the polymer chain, while SEC is useful to gather information about possible side reactions e.g., crosslinking. The ^1H NMR spectrum (displayed in **Figure 41**) showed the disappearance of the $\text{H}_2\text{C}=\text{CH}-\text{R}$ signals of AGE in the range between 6.00 – 5.00 ppm, as well as the appearance of the benzyl thiol signals at 7.30 and 3.50 ppm. As the signals of the benzyl thiol were overlapping with the ones of the solvent (CDCl_3) and the mPEG-initiator, an exact determination of the thiol amount was not possible. The size exclusion chromatogram (refer to **Figure 42**) showed a slight increase in the molar mass of 100 g mol^{-1} in comparison to the precursor polymer by maintaining an identical \bar{D} of 1.05. More important than the change in molar mass was the shape of the peak, which remained symmetrical without any shoulder formation. This indicated the absence of side reactions such as crosslinking, which got further supported by the lack of any other peak in the chromatogram.

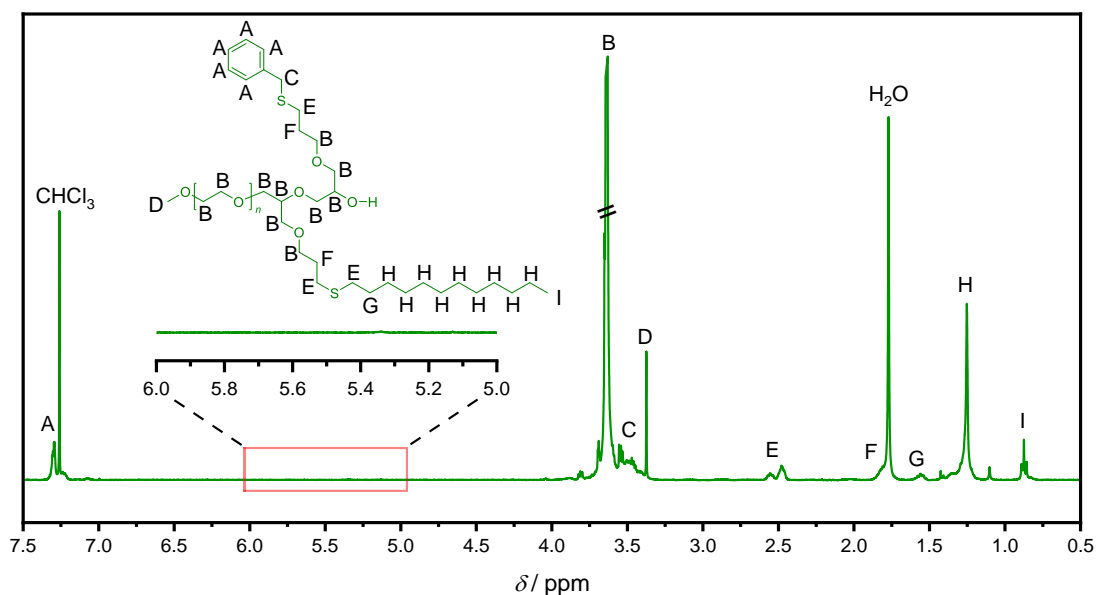


Figure 41: ^1H NMR spectrum of twice chain extended mPEG-1900 after the PPM via thiol-ene reaction using benzyl mercaptan. After the reaction, the disappearance of the $\text{H}_2\text{C}=\text{CH}-\text{R}$ signals of AGE (6.00 – 5.00 ppm) and appearance of the thiol signals could be observed. Solvent: CDCl_3 .

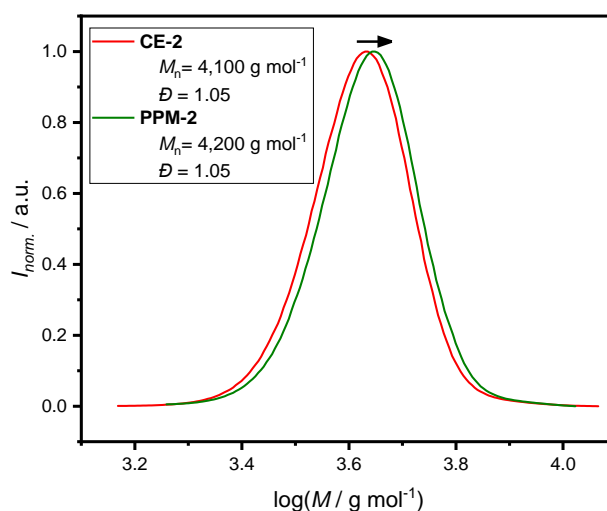
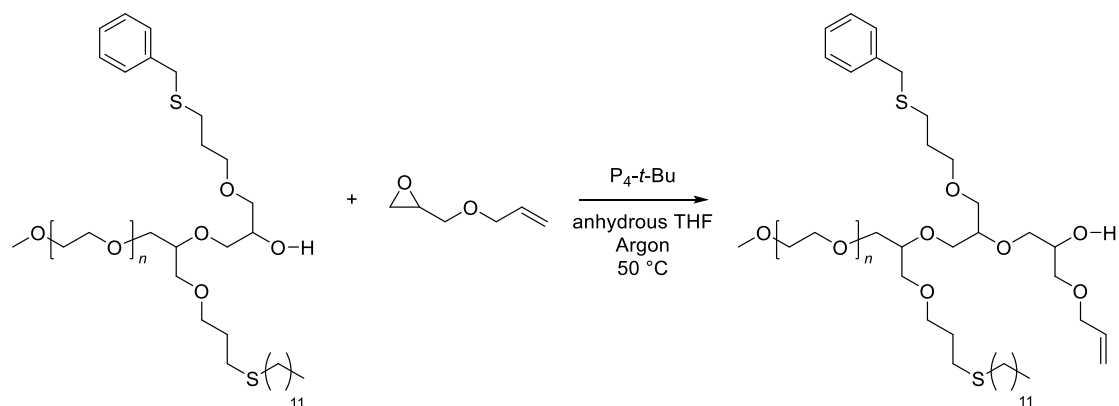


Figure 42: Size exclusion chromatogram of twice chain extended mPEG-1900 before (red) and after (green) the PPM via thiol-ene reaction using benzyl mercaptan. After the reaction, a minimal shift in the molar mass is noticeable.

To sum up, the appearance of benzyl signals and the disappearance of the double bond signals in the ^1H NMR spectrum as well as the absence of any further peaks or shoulders in the size exclusion chromatogram confirmed the incorporation of benzyl thiol in the polymer structure without any side reactions.

This modified polymer was further used in one final AROMA reaction to obtain a sequence-controlled triblock copolymer, even a tetrablock copolymer if the

mPEG-initiator is taken into account. The reaction conditions were similar to the second CE, using 1.25 eq. of AGE in respect to the polymer initiator and at 50 °C under inert atmosphere, resulting in a yield of 73 % (displayed in **Scheme 47**).



Scheme 47: Reaction equation of the third CE of mPEG-1900 with AGE via the small excess approach, using P_4-t-Bu in anhydrous THF under inert atmosphere at 50 °C.

The corresponding 1H NMR spectrum (see **Figure 43**) to the polymer showed the familiar appearance of the $H_2C=CH-R$ signals in the range of 6.00 – 5.00 ppm, confirming a successful addition. This time, the number of AGE units could not be determined by comparing the ratio of the AGE and initiator integrals as previously done, due to the overlapping of the initiator's methyl group with the CH_2 group of the benzyl thiol. Therefore, the methyl group of the 1-dodecanethiol at 0.87 ppm was chosen as reference leading to an average repeating unit of AGE of approx. 0.88, which falls behind the targeted value of one unit. Possible explanations are for example (i) the change in the determination method by going from the initiator to the thiol signal, which could lead to inaccurate values, but also (ii) a lower amount of *Schwesinger* base during the reaction. The latter may happen due to protonic impurities in the reaction mixture, quenching small amounts of the base and therefore reducing the overall concentration of active catalyst in the mixture. This might lead to a decrease in the propagation speed of the reaction and a lower monomer conversion at the end of the reaction.

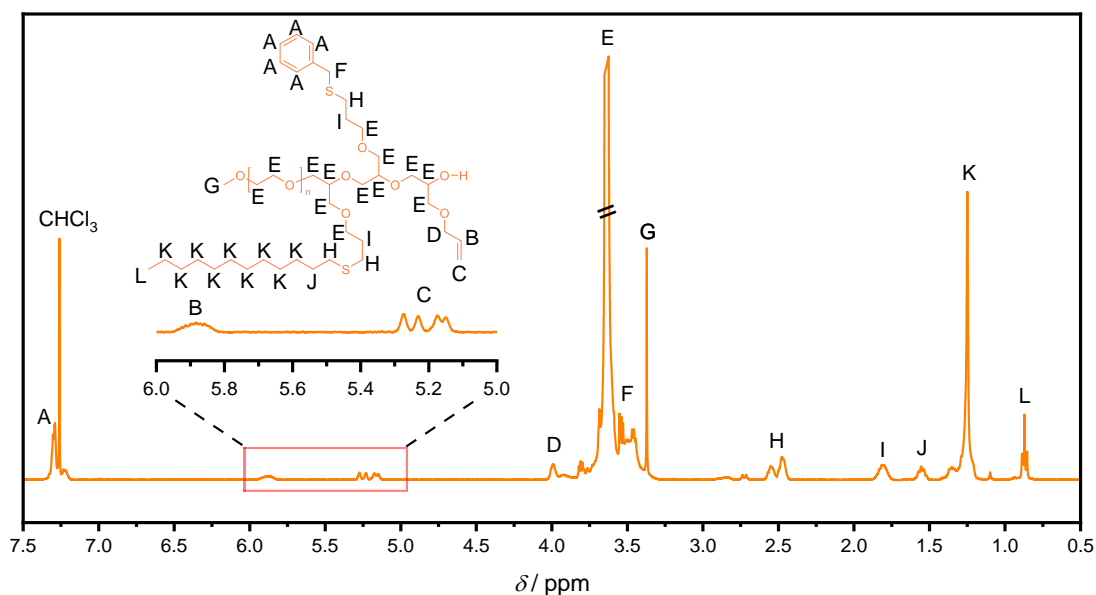


Figure 43: ^1H NMR spectrum of twice modified mPEG-1900 after the third CE with AGE. After the reaction, the appearance of the $\text{H}_2\text{C}=\text{CH}-\text{R}$ signals of AGE between 6.00 – 5.00 ppm could be observed, confirming the addition of the monomer to the chain. Solvent: CDCl_3 .

The size exclusion chromatogram (refer to **Figure 44**) of the reaction displayed a single symmetrical peak with a minimal shift to the higher molar mass side ($4,300 \text{ g mol}^{-1}$ to $4,400 \text{ g mol}^{-1}$) and a slight improvement in \bar{D} of 0.01, from 1.06 to 1.05. The lack of further peaks or shoulder suggested the absence of undesired side reactions e.g., crosslinking.

All things considered a third CE was successfully executed while not being perfect. In contrast to previous AROMA reactions, the average unit of one could not be reached precisely. One possible reason was the change in the determination process for the average number of the repeating unit, in which due to an overlapping of signals the previously used initiator signal was unavailable and the methyl group of the 1-dodecanethiol had to be used. Another possible reason for the result could be the decrease of the amount of *Schwesinger base* in the reaction mixture due to protonic impurities. A lower amount of promotor would result in a lower propagation rate and therefore in a lower monomer conversion at the end of the polymerization.

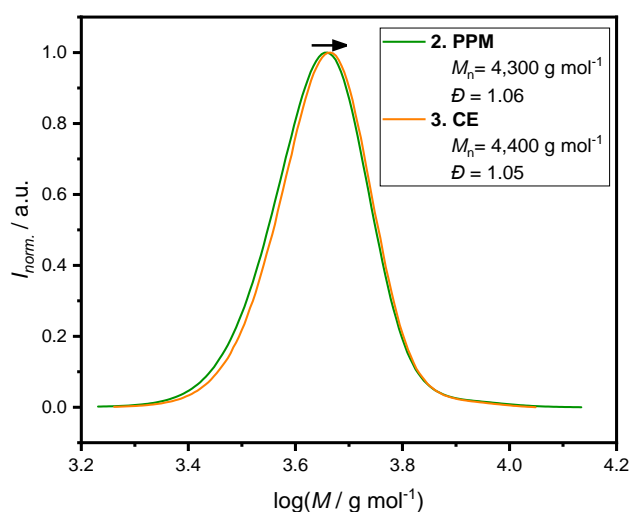
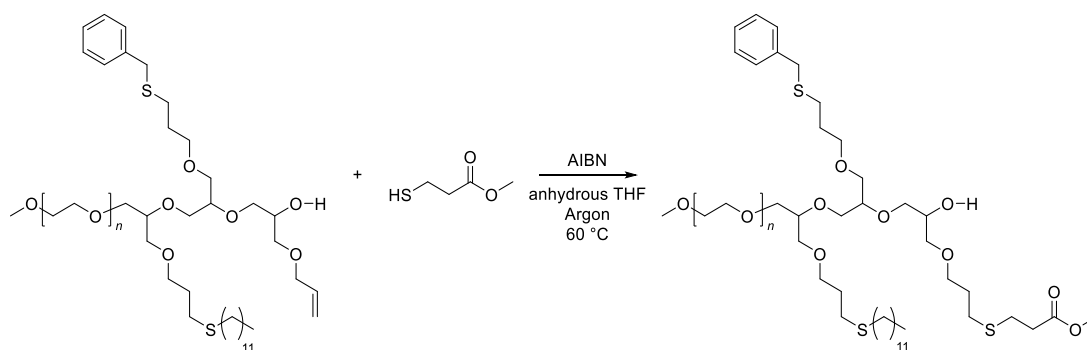


Figure 44: Size exclusion chromatogram of twice modified mPEG-1900 before (green) and after (orange) the third CE with AGE. A slight shift in the molar mass and an improvement of the \bar{D} could be observed.

Nevertheless, this polymer was used in a final thiol-ene reaction with methyl-3-mercaptopropionate as reactant of choice to synthesize a sequence-controlled triblock copolymer (refer to **Scheme 48**). The reaction conditions were similar to the previous two thiol-ene reactions (yield: 78 %) and the success of the reaction was confirmed via ^1H NMR spectroscopy and SEC.



Scheme 48: Reaction equation of the third PPM of the AROMA-polymer using methyl-3-mercaptopropionate and AIBN in anhydrous THF under inert atmosphere at 60 °C.

As before, the ^1H NMR spectrum (see **Figure 45**) indicated a total conversion of the AGE moiety in the chain, by displaying no characteristic $\text{H}_2\text{C}=\text{CH}-\text{R}$ signal in the range of 6.00 – 5.00 ppm. The general spectrum was in accordance with the expected one and all present signals could be assigned to their respective protons in the polymer chain, confirming a successful modification.

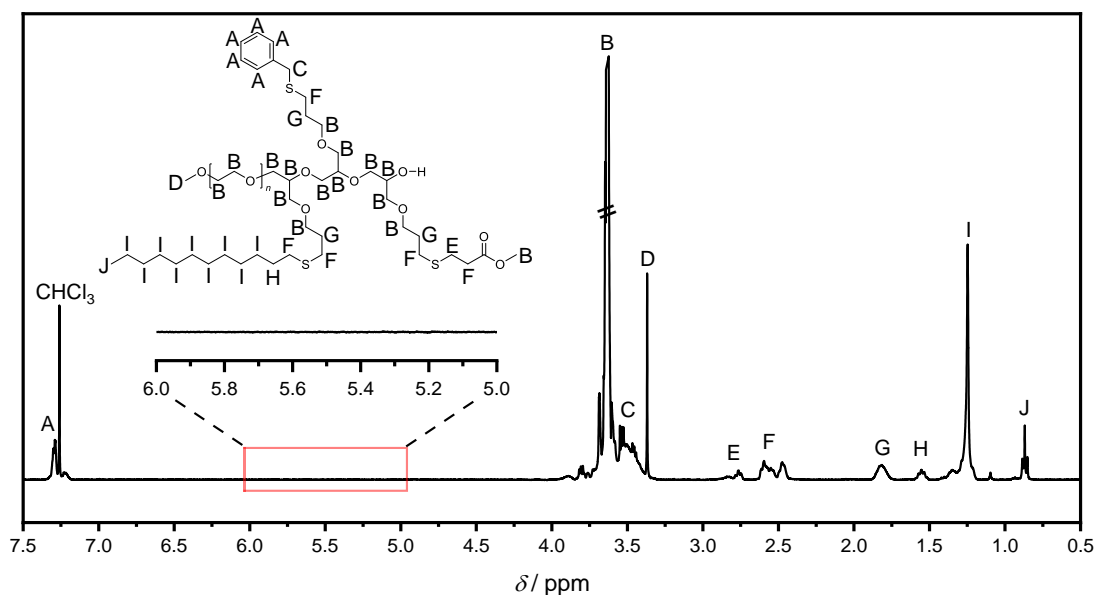


Figure 45: ^1H NMR spectrum of thrice chain extended mPEG-1900 after the PPM via thiol-ene reaction using methyl-3-mercaptopropionate. After the reaction, the disappearance of the $\text{H}_2\text{C}=\text{CH}-\text{R}$ signals of AGE between 6.00 – 5.00 ppm could be observed. Solvent: CDCl_3 .

In case of the size exclusion chromatogram (depicted in **Figure 46**), a symmetrical peak with a higher M_n than its precursor ($4,400 \text{ g mol}^{-1}$ to $4,800 \text{ g mol}^{-1}$) could be observed. However, a slight second peak at the higher molar mass side of the main peak could be observed for the first time. With approx. twice the molar mass of the main peak, the second peak indicated the occurrence of side reactions during the modification reaction in form of dimerization, initiated by the radical source AIBN, which also resulted in an increase in \bar{D} from 1.05 to 1.08. As a consequence, some double bonds become unavailable for the reaction with the thiol via thiol-ene reaction, reducing the overall yield of methyl-3-mercaptopropionate in the polymer. Nevertheless, the success of the modification could also be confirmed via SEC.

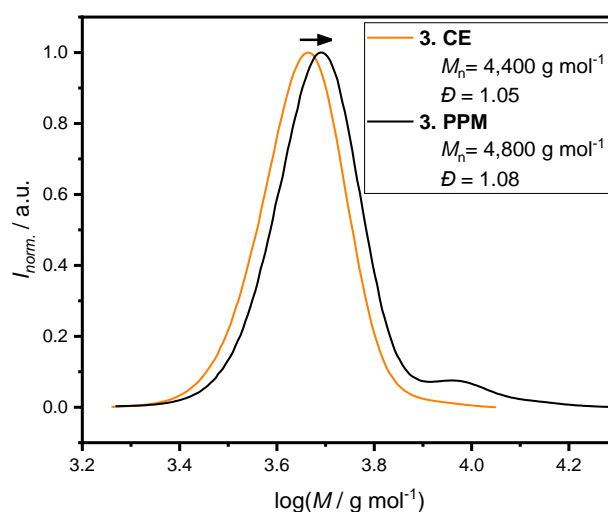


Figure 46: Size exclusion chromatogram of thrice chain extended mPEG-1900 before (orange) and after (black) the PPM via thiol-ene reaction using methyl-3-mercaptopropionate. After the reaction, a shift to higher molar masses could be observed, indicating the success of the reaction.

In summary, the third and final PPM reaction was successfully conducted, confirmed via ^1H NMR spectroscopy and SEC. However, for the first time a slight dimerization initiated by the radical source could be observed, which could decrease the overall number of methyl-3-mercaptopropionate in the chain.

An overview of each CE and PPM including equivalents, reaction time, temperature, M_n , \bar{D} and the average repeating unit is displayed in **Table 6**.

Table 6: Overview of each CE and PPM including equivalents, reaction time, temperature, M_n , \bar{D} and the average repeating unit.

<i>Entry</i>	<i>Eq. AGE</i>	<i>Eq. thiol</i>	<i>Time / h</i>	<i>Temp.</i>	$M_n / \text{g mol}^{-1}$	\bar{D}	<i>average repeating unit</i>
1. CE	1.25	-	5	a.t.	3,200	1.05	1.02 ± 0.07
2. CE	1.25	-	5.5	50 °C	4,100	1.05	1.02 ± 0.06
3. CE	1.25	-	5.5	50 °C	4,400	1.05	0.88
1. PPM	-	4.00	24	60 °C	3,800	1.05	-
2. PPM	-	4.00	20	60 °C	4,200	1.05	-
3.PPM	-	4.00	20	60 °C	4,800	1.08	-

To summarize this chapter, a successful attempt was made to synthesize sequence-controlled multiblock copolymers with an average repeating unit of one, approaching the precision of sequence-defined polymers. The method of choice was the in the previous chapter established system of combining CEs (AROP) with PPM (thiol-ene) reactions. Two different approaches were investigated to achieve this goal, one based on the living character of the used anionic polymerization technique, while the other relies on a small excess of monomer. After some tests, the second approach seemed to be the more promising one, resulting in the successful synthesis of a sequence-controlled polymer with 3 “blocks” possessing different pendant groups (aliphatic, aromatic and ester), with an average repeating unit for each “block” of 1.02 ± 0.07 , 1.02 ± 0.06 and 0.88, respectively. Due to the anionic character of the reaction and the addition of a single unit, the method was called *Anionic Ring-Opening Monomer Addition*, short *AROMA*.

5. Conclusion and Outlook

Topic of this thesis was the investigation of new synthetic ways to synthesize sequence-controlled multiblock copolymers and ideally simplify them. Traditionally, each block of a multiblock copolymers is formed by a different monomer, which makes it necessary to have multiple different monomers available. Depending on the number of blocks and the desired functionality the monomers should introduce to the overall polymer structure, laborious, time-consuming and costly monomer syntheses can be required, based on the complexity of the molecules. Aside from the synthetic efforts, the reactivity of each monomer in comparison to the previously added monomer plays a significant role for the success of the CE reaction, because incompatibility can lead to side reactions or even failure of the synthesis. Therefore, to evade those difficulties, a system consisting of a single commercially available monomer would be desirable and ideal.

To achieve the goal of sequence-controlled multiblock copolymers built from a single monomer, new systems based on a combination of CE reactions via living/controlled polymerization techniques with PPM reactions were investigated in the first part of the thesis. Therefore, the polymerization of a variety of monomers based on (meth)acrylates, lactones and epoxides via different RDRP and ionic polymerization techniques were studied. In the beginning, the focus was on the RAFT polymerization of the functional active ester monomer PFPA. After the successful monomer synthesis, first polymerization attempts were conducted, whose success could be confirmed via NMR spectroscopy and SEC. Afterwards, this polymer was used in a subsequential PPM step via amidation using 2,2,2-trifluoroethylamine. The success of the modification could also be confirmed via NMR spectroscopy and SEC. The next step was the CE of the modified polymer with PFPA, which failed due to aminolysis of the RAFT agent during the PPM process, leading to a “dead” polymer and no visible shift in the size exclusion chromatogram. To prevent the cleavage of the RAFT end group, the modification type was switched from amidation to transesterification and 2,2,2-trifluoroethanol was used as reactant of choice. Similar to the previous attempt, the PPM was successful (confirmed via NMR spectroscopy and SEC), but the CE failed again.

Consequently, the applied polymerization technique was changed to a different one, namely ATRP. In comparison to the RAFT polymerization, the monomer was switched

from PFPA to the methacrylate derivate, PFPMA, which is known to polymerize via ATRP. After the successful monomer synthesis, first polymerization attempts were conducted, which led to a successful synthesis, confirmed via NMR spectroscopy and SEC. Next step was to modify the polymer via amidation using 2,2,2-trifluoroethylamine, which was unsuccessful. Even after the change to a different amine (2,2,3,3,3-pentafluoropropylamine) and the additional use of TEA, no improvement could be achieved. Due to the insufficient results and a limited time frame, this approach was abandoned as well and new polymerization techniques were investigated.

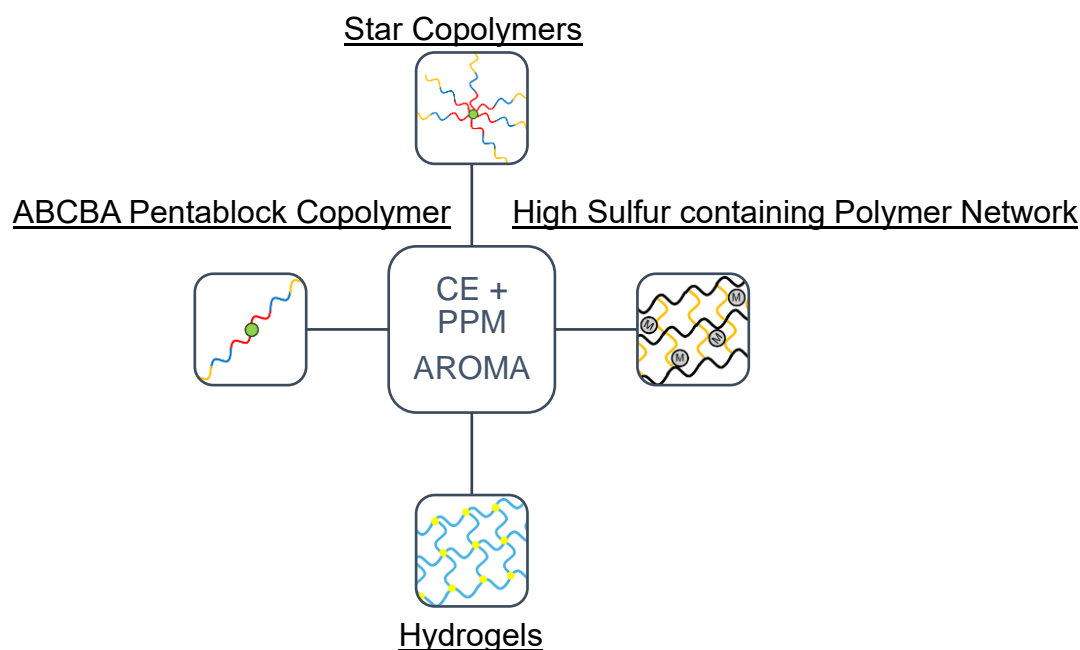
Instead of sticking to RDRP techniques, the new systems were of ionic nature, namely CROP and AROP. For CROP, an allyl-containing lactone was synthesized and investigated, while for AROP the commercially available AGE was the monomer of choice. After some tests, the AROP of AGE promoted by the *Schwesinger Base* P₄-*t*-Bu showed the most promising results and was further pursued. In a series of CE reactions via AROP with subsequent PPM reactions via thiol-ene reaction using different thiols, a sequence-controlled triblock copolymer with different pendant groups (aliphatic, aromatic, ester) based on a single monomer, could be successfully synthesized. The success of each step could be confirmed via NMR spectroscopy and SEC.

The second part of this thesis dealt with the investigation of the newly established method's limits. Target was to reduce the average repeating unit of each added "block" to one, what would lead to well-defined sequence-controlled macromolecules, which approach the precision of sequence-defined polymers. To achieve this goal, two different approaches were tested, (i) a kinetic approach founded on the living character of the applied polymerization technique and another one (ii) based on a small feed excess of the monomer. While the first approach led to an average repeating unit twice as high (2.075 ± 0.065) as the desired one, the second approach was able to achieve the set goal of approximately one. In combination with subsequent thiol-ene reactions, precise macromolecules with different functional groups (aliphatic, aromatic, ester) could be synthesized, confirmed by a variety of characterization methods (¹H NMR spectroscopy, SEC, ATR FT-IR spectroscopy and DSC). Due to the anionic ring-opening character of the applied polymerization technique as well as the addition of a single monomer, this method was called *anionic ring-opening monomer addition*, short AROMA.

With that, a new method to synthesize sequence-controlled multiblock copolymer has been successfully developed. As mentioned, this system relies on a commercially available single functional monomer, instead of multiple different ones, simplifying the synthetic procedure by avoiding possible complex, time consuming and costly monomer syntheses. Additionally, by applying only a small excess of monomer in relation to the initiator, this system was used to synthesize sequence-controlled macromolecular structures with an average repeating unit of one, approaching the precision of sequence-defined polymers.

The toolbox-like structure of this system allows for the creation of polymers for different and interesting applications in the future. One example would be the syntheses of structures such as sequence-controlled ABCBA pentablock and multiarm copolymers by switching from a monofunctional to a di-, tri or even tetra functionalized initiators.

In the present work, first steps were done in regards of network formation by using a tetrathiol. Due to the PEG-like backbone of PAGE, further research in this topic could lead to sequence-controlled hydrogels with tailored functionalities and a possible biomedical application. By applying a different PPM method like inverse vulcanization, the present pendant C=C double bond could be used to generate polymeric networks with high sulfur content for possible metal uptake applications (see **Scheme 49**).



Scheme 49: Possible applications for the newly established system: I. Synthesis of sequence-controlled multiarm (star) copolymers; II: High sulfur containing polymer networks; III. Sequence-controlled hydrogels; IV: Sequence-controlled ABCBA pentablock copolymers.

6. Experimental Part

Herein, the instruments and materials used are listed as well a detailed description of the synthetic procedures of each product with their corresponding analytical data.

6.1. Instruments

6.1.1. Nuclear Magnetic Resonance (NMR) Spectroscopy

^1H , ^{13}C and ^{19}F NMR spectra were recorded on a *Bruker Ascend III* 400 MHz spectra at a frequency of $\nu = 400$ MHz, $\nu = 101$ MHz and $\nu = 377$ MHz, respectively. Chloroform- d_1 and dichloromethane- d_2 was used as the deuterated solvents of choice for all samples. The solvent used for each spectrum is listed in the corresponding caption.

6.1.2. Size Exclusion Chromatography (SEC)

Size Exclusion Chromatography was carried out in THF (HPLC grade with 0.55 g BHT per 2.5 L THF) on three different devices:

1. *Agilent Technologies 1260 Infinity II* equipped with a 5 μm *PSS SDV Lux 1000 Å* column (8 x 300 mm) and a 5 μm *PSS SDV Lux 100.000 Å* column (8 x 300 mm). The operation temperature was set to 35 °C with a flow rate of 1 mL min $^{-1}$. The system was calibrated via PS standards ranging from 370 to 2.52×10^6 g mol $^{-1}$ and PMMA standards ranging from 800 to 2.20×10^6 g mol $^{-1}$.
2. *Agilent Technologies 1200 Series* equipped with a 5 μm *Agilent PLgel Mixed-C 3x* and a 5 μm *Agilent PLgel Mixed-E 1x*. The operation temperature was set to 35 °C with a flow rate of 1 mL min $^{-1}$. The system was calibrated via PS standards ranging from 370 to 2.52×10^6 g mol $^{-1}$ and PMMA standards ranging from 800 to 2.20×10^6 g mol $^{-1}$.
3. *Agilent Technologies 1200 Series* equipped with a 5 μm *PSS SDV Lux 1000 Å* column (8 x 300 mm) and a 5 μm *PSS SDV Lux 100.000 Å* column (8 x 300 mm). The operation temperature was set to 35 °C with a flow rate of 1 mL min $^{-1}$. The system was calibrated via PS standards ranging from 370 to 2.52×10^6 g mol $^{-1}$ and PMMA standards ranging from 800 to 2.20×10^6 g mol $^{-1}$.

6.1.3. Attenuated Total Reflection Fourier-Transform Infrared (ATR FT-IR) Spectroscopy

ATR FT-IR measurements were recorded on a *Bruker Alpha II* equipped with an ATR unit. The spectra were measured at a range from 4,000 - 400 cm^{-1} .

6.1.4. Differential Scanning Calorimetry (DSC)

All DSC thermograms were recorded on a *Netzsch DSC 214* ranging from -50 to 100 °C with a scanning rate of 10 K min^{-1} . For all experiments the second heat cycle was used.

6.2. Chemicals

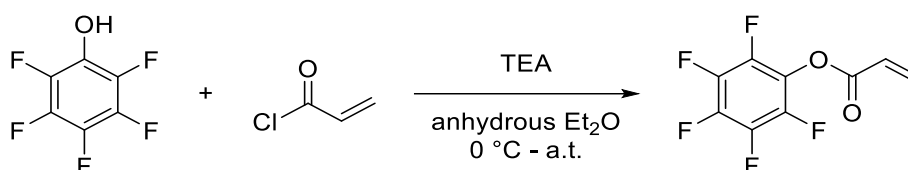
Acetic acid (100 %, Carl Roth), Acetone (VWR), Acetonitrile (99.9%, extra dry, Acros Organics), Acryloyl chloride (96%, abcr) Allyl bromide (99%, Sigma-Aldrich), Allyl glycidyl ether (AGE, 99+ %, Acros Organics), Aluminium oxide (Alox, neutral, Brockmann I, 50-200 μ m, 60A, Acros Organics), Ammonium chloride (NH₄Cl, p.a., Acros Organics), 2,2'-Azobis(2-methylpropionitrile) (AIBN, 98 %, Sigma-Aldrich), Benzyl alcohol (>99%, TCI), Benzyl mercaptan (99%, Alfa Aesar), ϵ -Caprolactone (99%, Alfa Aesar), Chloroform-d₁ (CDCl₃, 99.8 %, Eurisotop), Copper(I) bromide (Cu(I)Br, 98%, Sigma-Aldrich), Copper(I) chloride (Cu(I)Cl, 99.99%, Acros Organics), 4-Cyano-4-[(dodecylsulfanylthiocarbonyl)sulfanyl]pentanoic acid (CDTPA, 97%, Sigma-Aldrich), Dichloromethane (DCM, 99.8%, extra dry, Acros Organics), Dichloromethane-d₂ (DCM-d₂, 99.8%, Eurisotop), Diethyl ether (Et₂O, 99.5% extra dry, Acros Organics; 100 %, VWR Chemicals), 4-Dimethylaminophenol (DMAP, 99%, Acros Organics), 1,3-Dimethyl-1,3-diazinan-2-one (DMPU, \geq 99%, Sigma-Aldrich), N,N-Dimethylformamide (DMF, 99.8%, extra dry, Acros Organics), 4,4'-Dinonyl-2,2'-dipyridyl (dNbpy, 97%, Sigma-Aldrich), Diphenyl Phosphate (DPP, >99%, TCI), 1-Dodecanethiol (\geq 98%, Sigma-Aldrich), 1,4-Dioxane (99.5%, extra dry, thermo scientific), Ethyl α -bromoisobutyrate (EBiB, 98%, abcr), Ethanol (EtOH, 96%, VWR), Lithium diisopropylamide solution (LDA, 1.0 M in THF/hexanes, Sigma-Aldrich), 2,6-Lutidine (Sigma-Aldrich), Magnesium sulphate (MgSO₄, \geq 99%, Carl Roth), Methacryloyl chloride (95%, 200 ppm MEHQ, Acros Organics), Methanol (MeOH, \geq 98.5%, technical, VWR), Methyl 2-bromopropionate (MBP, 98%, Sigma-Aldrich), Petroleum ether (PE, VWR), 2,2,3,3,3-pentafluoropropylamine (>97%, TCI), N,N,N',N'',N''-Pentamethyldiethylenetriamine (PMDTA, 98+%, Acros Organics), Sodium chloride (NaCl, \geq 99.8%, Carl Roth), 1-tert-Butyl-4,4,4-tris(dimethylamino)-2,2-bis[tris(dimethylamino)-phosphoranylideneamino]-2 λ 5,4 λ 5-catenadi(phosphazene) (P₄-*t*-Bu, 0.8 M in hexane, Sigma-Aldrich), Tetrahydrofuran (THF, 99.5 % extra dry, Acros Organics), Toluene (99.85%, extra dry, Acros Organics), Triethylamine (TEA, \geq 99%, fisher scientific), 2,2,2-Trifluoroethylamine (>97%, TCI), 2,2,2-Trifluoroethanol (99+%, Alfa Aesar), Pentaerythritol tetrakis(3-mercaptopropionate) (>95%, Sigma-Aldrich), Pentafluorophenol (PFP, 99%, abcr) were used as received. If mentioned, methoxy poly(ethylene glycol) 1900 (mPEG-1900, Alfa Aesar) was dried at 40 °C at reduced pressure.

6.3. Synthetic Procedures

This part of the thesis describes the procedures for the various monomer syntheses, kinetic studies, polymerizations and post-polymerization modification reactions in detail with their corresponding analytical data.

6.3.1. Synthetic Procedures for “Multiblock Copolymer Synthesis via RAFT Polymerization”

6.3.1.1. Synthesis of Pentafluorophenyl Acrylate



This synthetic procedure is based on previously published studies.¹⁶⁵

In a 100 ml round bottom flask PFP (2.5 g, 13.6 mmol, 1.00 eq.) and TEA (2.27 mL, 1.65 g, 16.3 mmol, 1.20 eq.) were dissolved in anhydrous Et₂O (50.0 mL). Under cooling (ice bath), acryloyl chloride (1.32 mL, 1.48 g, 16.3 mmol, 1.20 eq.) was added dropwise to the reaction mixture. After stirring overnight at ambient temperature, the precipitated salt was removed by filtration. The organic phase was washed four times with water and the aqueous phase was extracted twice with Et₂O. Afterwards, the organic phases were combined and dried over MgSO₄. The solvent was removed under reduced pressure, obtaining a slightly yellow liquid. The crude product was purified by column chromatography using petrol ether as solvent to give a colorless liquid (1.37 g; 77 %).

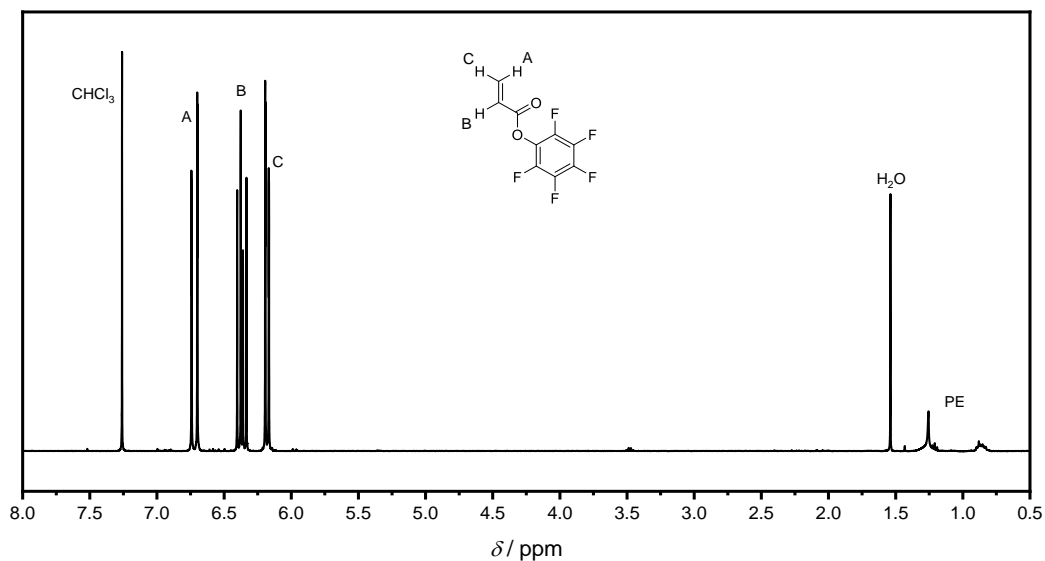


Figure 47: ^1H NMR spectrum of PFPA. Solvent: CDCl_3 .

^1H NMR (400 MHz, CDCl_3) δ = 6.73 (dd, J = 1.0 Hz, J = 17.3 Hz, 1H, A), 6.39 (dd, J = 10.6 Hz, J = 17.3 Hz, 1H, B), 6.19 (dd, J = 1.0 Hz, J = 10.5 Hz, 1H, C).

Impurities:

- 1.54 ppm: H_2O
- 1.36 – 0.78 ppm: PE

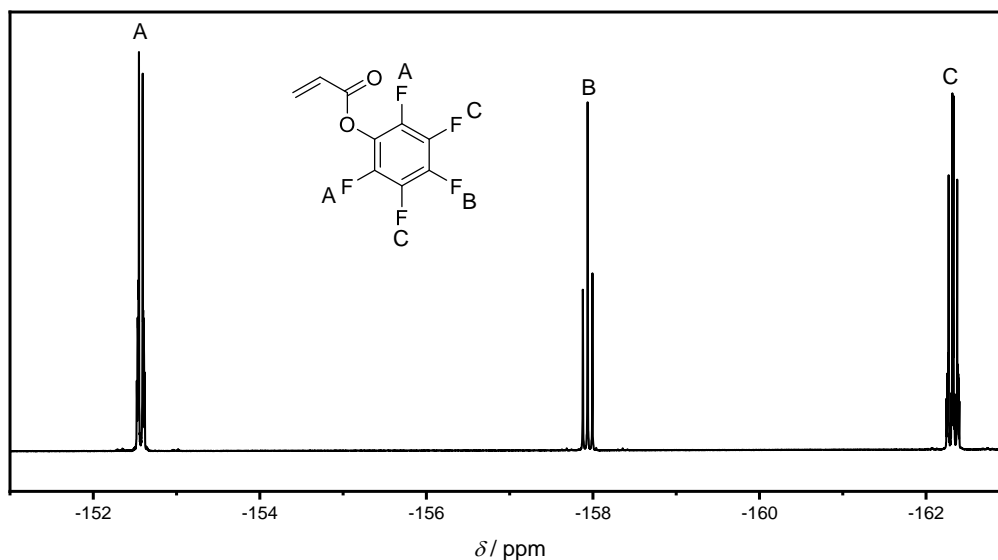
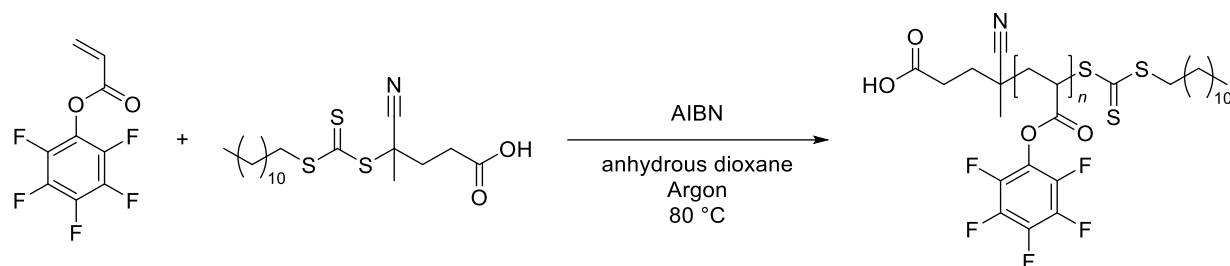


Figure 48: ^{19}F NMR spectrum of PFPA. Solvent: CDCl_3 .

^{19}F NMR (377 MHz, CDCl_3) δ = -152.47 - -152.69 (m, 2F, A), -157.94 (t, J = 21.5 Hz, 1F, B), -162.20 - -162.47 (m, 2F, C).

6.3.1.2. *Reversible Addition-Fragmentation Chain Transfer*
Polymerization of PFPA with CDTPA



PFPA (163 μL , 236 mg, 991 μmol , 40.0 eq.) and CDTPA (10.0 mg, 27.4 μmol , 1.00 eq.) was given into a 5 mL flask. Afterwards, AIBN (610 μg , 3.72 μmol , 0.15 eq.) and anhydrous dioxane (400 μL) were added and the reaction mixture was purged with argon for 10 minutes in a water bath. Then, the flask was given into a preheated oil bath at 80 °C. After 80 minutes the reaction was quenched by cooling with an ice bath and contact to oxygen. The yellow residue was dissolved in small amounts of THF and given dropwise into cold methanol. The precipitation procedure was repeated three times with methanol before it was dried in a vacuum oven at 40 °C. An off-white, slightly yellow solid was obtained (58.7 mg; 22 %).

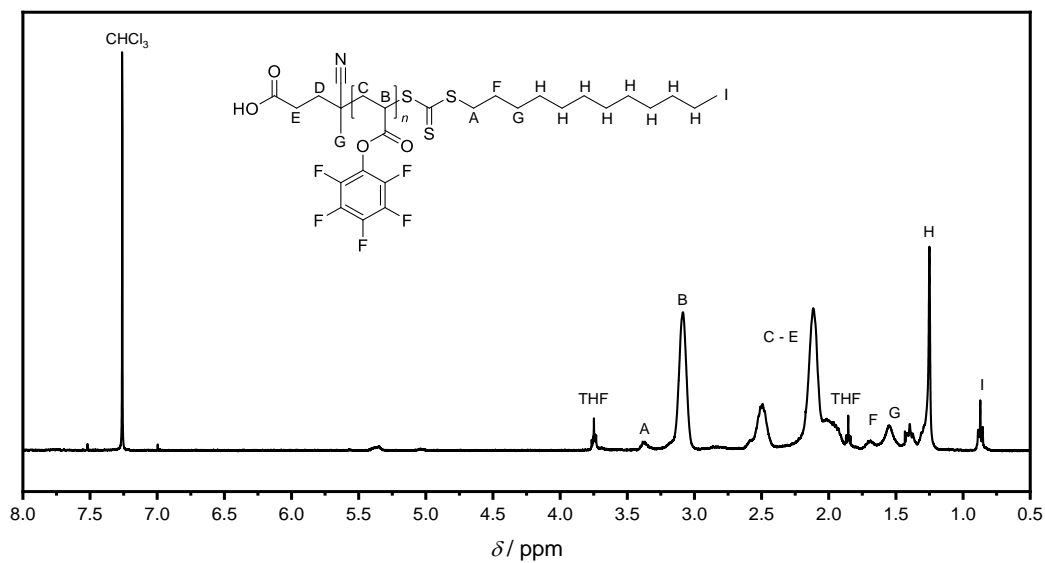


Figure 49: ^1H NMR spectrum of PPFPA. Solvent: CDCl_3 .

^1H NMR (400 MHz, CDCl_3) δ = 3.42 – 3.29 (m, 2H, A), 3.23 – 2.98 (m, 33H, B), 2.64 – 1.89 (m, 68H, C - E), 1.76 – 1.63 (m, 2H, F), 1.62 – 1.46 (m, 2H, G), 1.35 – 1.19 (m, 16H, H), 0.87 (t, J = 6.8 Hz, 3H, I).

Impurities:

- 3.75 ppm: THF
- 1.85 ppm: THF

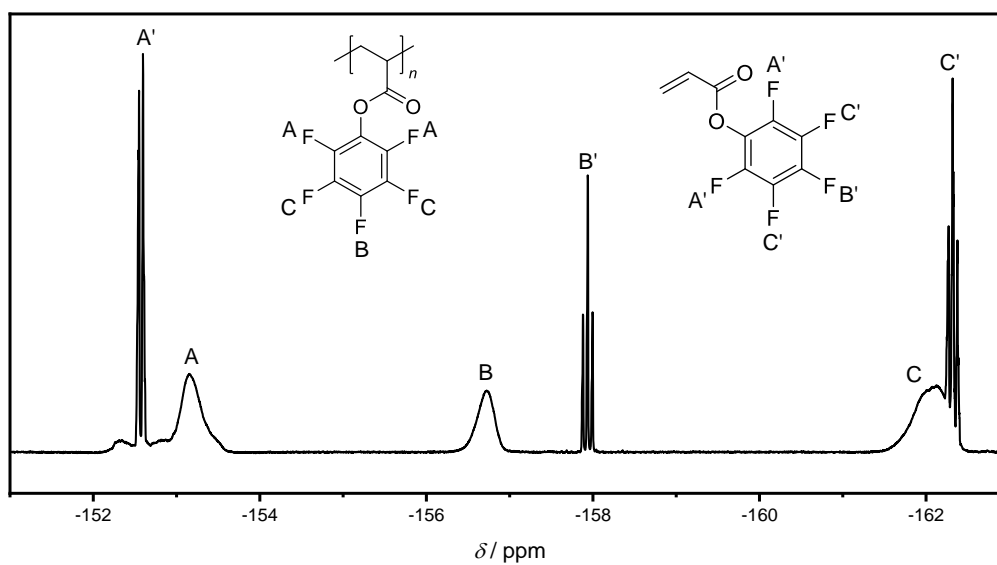


Figure 50: ^{19}F NMR spectrum of the RAFT polymerization of PFPA after 30 minutes. Solvent: CDCl_3 .

^{19}F NMR (377 MHz, CDCl_3) δ = -152.72 - -153.66 (m, 2F, A), -156.31 - -157.02 (m, 1F, B), -161.40 - -162.49 (m, 2F, C).

Impurities:

- -152.60 ppm: PFPA
- -157.94 ppm: PFPA
- -162.32 ppm: PFPA

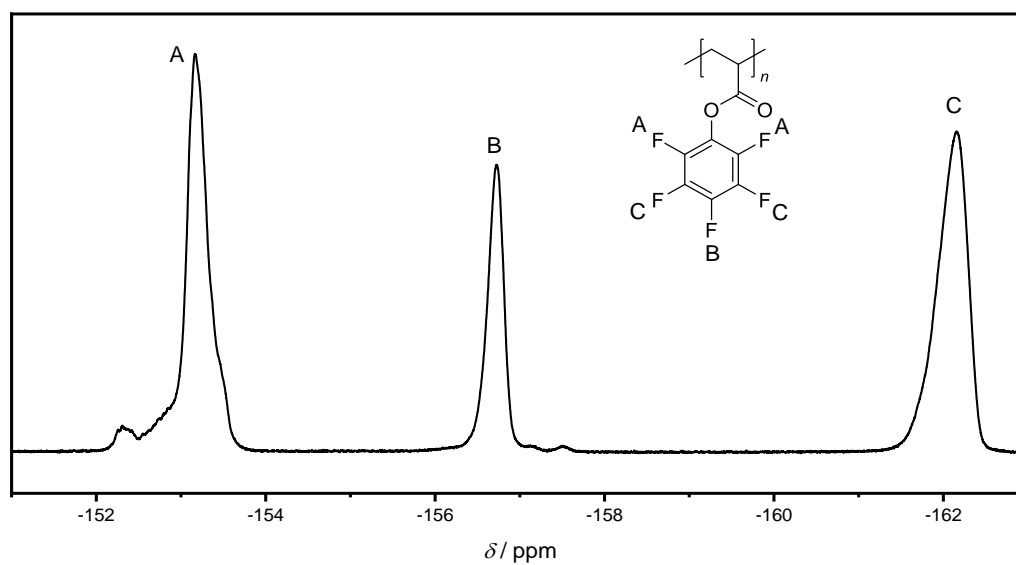


Figure 51: ^{19}F NMR spectrum of PPFPA. Solvent: CDCl_3 .

^{19}F NMR (377 MHz, CDCl_3) δ = -151.96 - -153.87 (m, 2F, A), -155.86 - -157.81 (m, 1F, B), -161.20 - -162.86 (m, 2F, C).

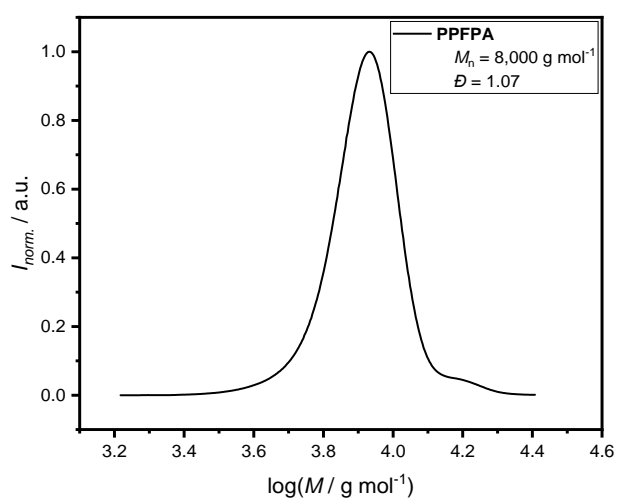
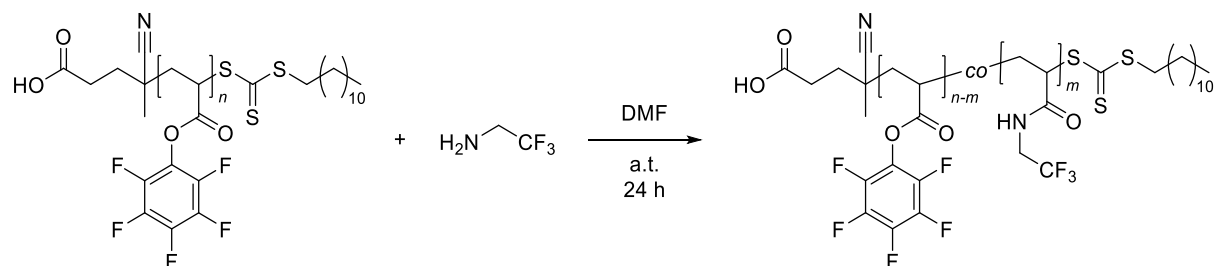


Figure 52: Size exclusion chromatogram of PPFPA.

6.3.1.3. Post-Polymerization Modification of PPFPA with 2,2,2-Trifluoroethylamine



PPFPA (70 mg, approx. 281 μmol of repeating units, 1.00 eq.) was dissolved in DMF (1.75 mL) and put aside for further use. 2,2,2-trifluoroethylamine (13.2 μL , 16.7 mg, 168 μmol , 0.60 eq.) was given into a 5 mL peach flask and the DMF/PPFPA mixture was added immediately. The flask was sealed and stirred overnight at ambient temperature. The next day, the solvent was removed under reduced pressure and the residue was dissolved in acetone. The polymer was precipitated three times in cold PE before the solvent was removed under reduced pressure at 40 $^{\circ}\text{C}$. A solid white/slightly yellow solid was obtained (39.6 mg; 71 %).

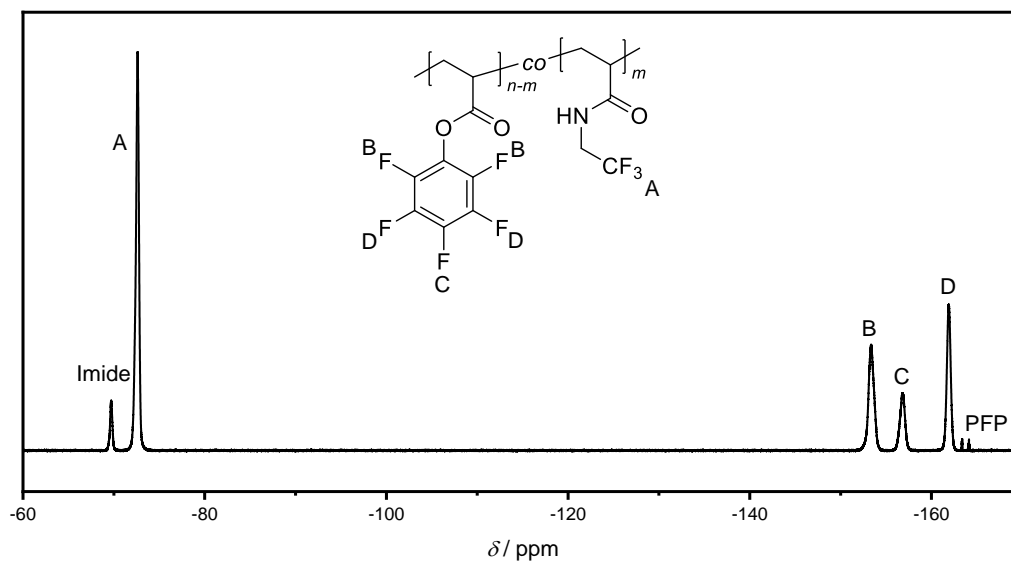


Figure 53: ^{19}F NMR spectrum of partially modified PPFPA. Solvent: CDCl_3 .

^{19}F NMR (377 MHz, CDCl_3) δ = -71.57 - -73.52 (m, 4.40F, A), -152.41 - -154.49 (m, 2F, B), -156.18 - -157.69 (m, 1F, C), -161.01 - -162.88 (m, 2F, D).

Impurities:

- -69.72 ppm: Imide
- -163.39 ppm: PFP
- -164.13 ppm: PFP
- -168.98 ppm: PFP

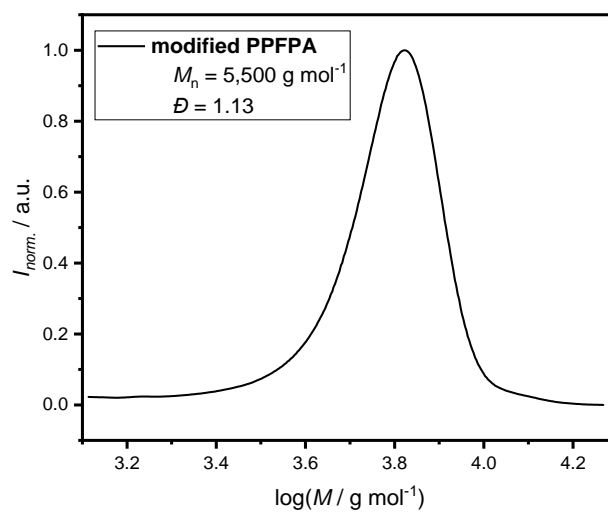
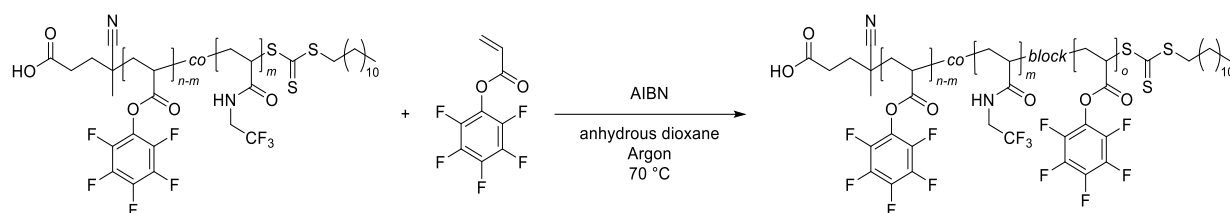


Figure 54: Size exclusion chromatogram of partially modified PPFPA.

6.3.1.4. Chain Extension Reaction of Modified PPFPA with PFPFA



PPFA (24.8 μL , 35.9 mg, 151 μmol , 50.0 eq.) was given into a flask, followed by the macro-RAFT agent (20 mg, 3.02 μmol , 1.00 eq.) in anhydrous dioxane (200 μL). Afterwards, AIBN (198 μg , 1.21 μmol , 0.40 eq.) was added and the flask was purged for 5 min with argon. In the end, the flask was put into a preheated oil bath at 70 °C for 4.5 hours. The reaction was stopped by cooling the reaction mixture and exposure to air. The solvent was removed under reduced pressure, the residue was dissolved in THF and precipitated 3 times in cold PE. The final product was dried under reduced pressure at 40 °C, leading to a white solid (5.5 mg; 55 %).

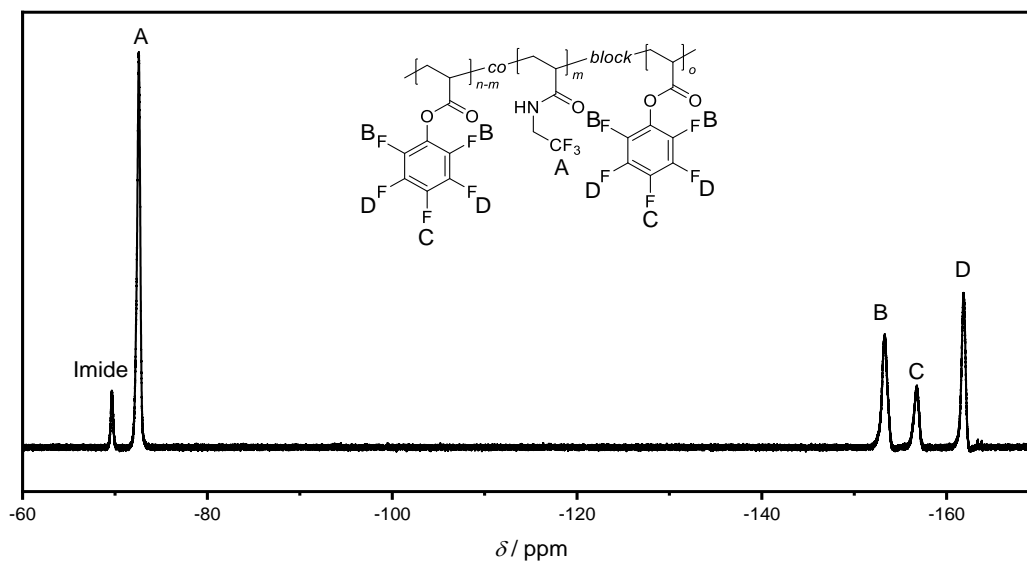


Figure 55: ^{19}F NMR spectrum of the chain extended modified PPFA. Solvent: CDCl_3 .

^{19}F NMR (377 MHz, CDCl_3) δ = -71.44 - -73.77 (m, 4.36F, A), -152.00 - -154.57 (m, 2F, B), -155.70 - -157.61 (m, 1F, C), -160.64 - -162.87 (m, 2F, D).

Impurities:

- -69.64 ppm: Imide

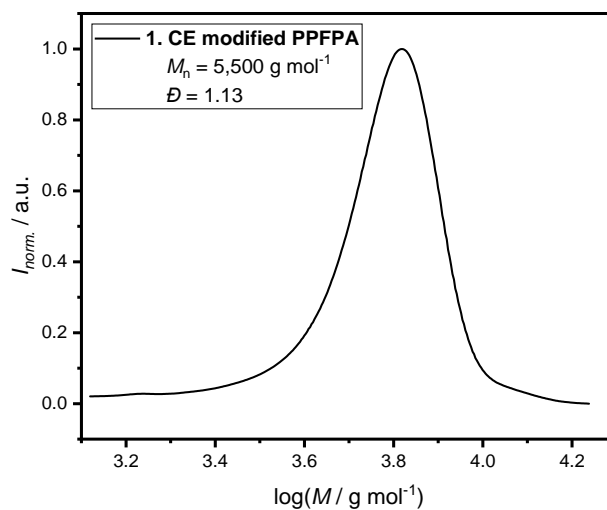
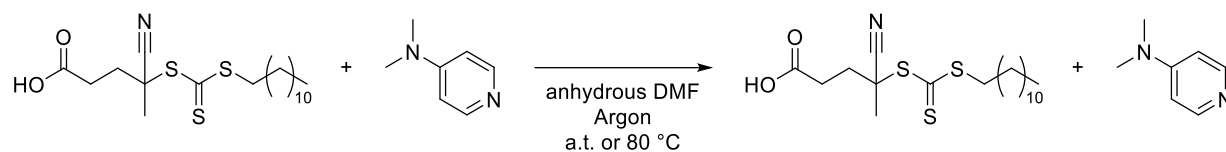


Figure 56: Size exclusion chromatogram of once chain extended modified PPFA.

6.3.1.5. Base Stability Test of CDTPA with DMAP



CDTPA (10.0 mg, 24.8 μmol , 1.00 eq.) and DMAP (15.1 mg, 124 μmol , 5.00 eq.) was given into a 5 mL flask and the atmosphere was changed to argon. Afterwards, anhydrous DMF (1.10 mL) was added and the mixture was stirred for 48 hours at ambient temperature or 80 °C. Every 24 hours samples were taken directly from the reaction mixture and investigated via ^1H NMR spectroscopy to check the progress.

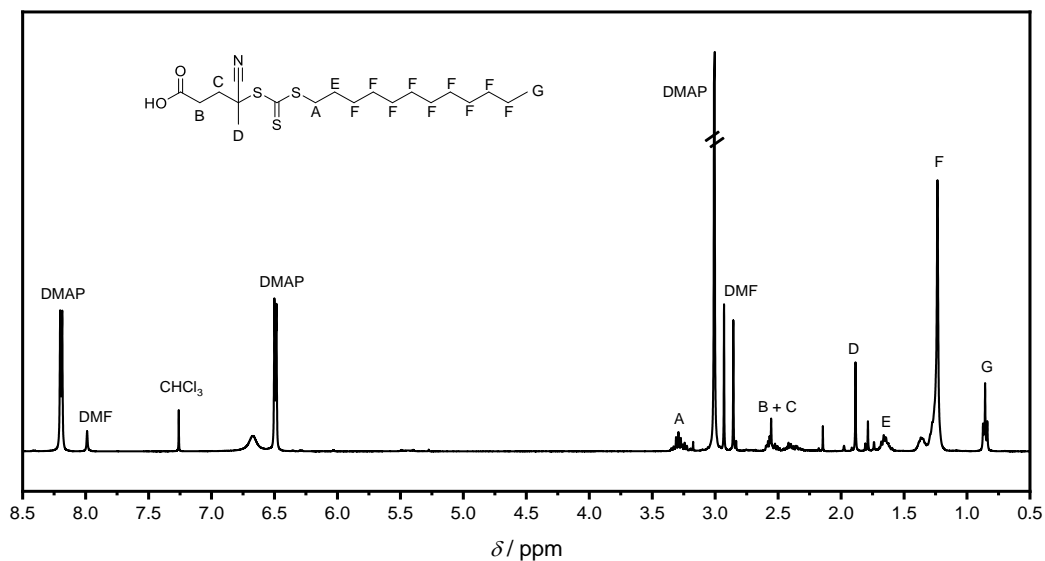


Figure 57: ^1H NMR spectrum of the base stability test of CDTPA with DMAP at ambient temperature after 48 hours. Solvent: CDCl_3 .

^1H NMR (400 MHz, CDCl_3) δ = 3.37 – 3.15 (m, 2H, A), 2.62 – 2.30 (m, 3.5H, B + C), 1.88 (s, 1.5 H, D), 1.71 – 1.58 (m, 2H, E), 1.41 – 1.17 (m, 18H, F), 0.86 (t, J = 6.7 Hz, 3H, G).

Impurities:

- 8.20 ppm: DMAP
- 7.99 ppm: DMF
- 6.49 ppm: DMAP
- 3.00 ppm: DMAP
- 2.93 ppm: DMF
- 2.86 ppm: DMF

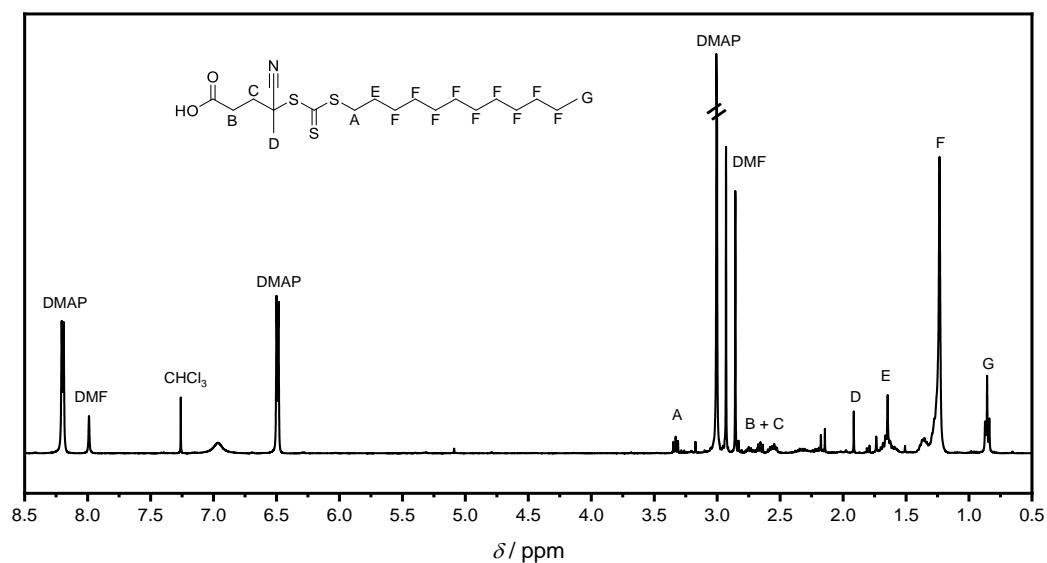


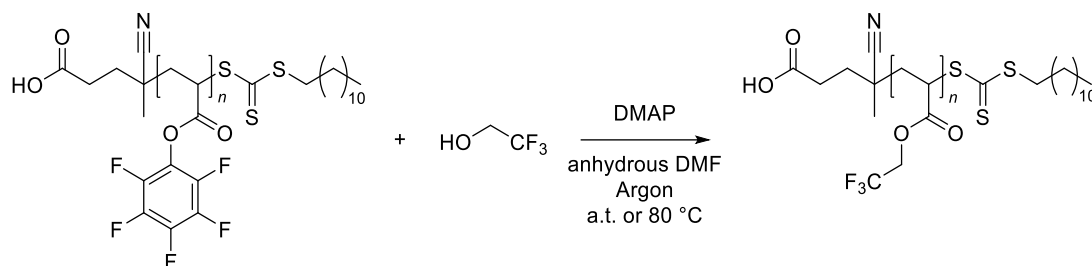
Figure 58: ^1H NMR spectrum of the base stability test of CDTPA with DMAP at 80 °C after 48 hours. Solvent: CDCl_3 .

^1H NMR (400 MHz, CDCl_3) δ = 3.37 – 3.30 (m, 1H, A), 2.77 – 2.48 (m, 2H, B + C), 1.91 (s, 0.44 H, D), 1.75 – 1.52 (m, 4H, E), 1.43 – 1.15 (m, 18H, F), 0.86 (t, J = 6.7 Hz, 3H).

Impurities:

- 8.20 ppm: DMAP
- 7.99 ppm: DMF
- 6.49 ppm: DMAP
- 3.00 ppm: DMAP
- 2.93 ppm: DMF
- 2.85 ppm: DMF

6.3.1.6. Post-Polymerization Modification of PPFPA with 2,2,2-Trifluoroethanol



PPFPA (**a.t.**: 156 mg, approx. 612 μmol of repeating units, 1.00 eq.; **80 °C**: 70.0 mg, approx. 281 μmol of repeating units, 1.00 eq.) was dissolved in anhydrous DMF (**a.t.**: 583 μL ; **80 °C**: 268 μL) and added with DMAP (**a.t.**: 15.0 mg, 122 μmol , 0.20 eq.; **80 °C**: 6.87 mg, 56.0 μmol , 0.20 eq.) into a 5 mL flask. Afterwards, 2,2,2-trifluoroethanol (**a.t.**: 20.3 μL , 28.1 mg, 281 μmol , 3.00 eq.; **80 °C**: 40.5 μL , 56.2 mg, 562 μmol , 2.00 eq.) was given into the mixture and the flask was sealed, purged with argon for 10 minutes and stirred overnight at ambient temperature or 80 °C. The next day, the solvent was removed under reduced pressure and the residue was dissolved in acetone. The polymer was precipitated in cold PE leading to a black oil (**a.t.**: 6.20 mg, 16 %; **80 °C**: 35.9 mg, 86 %).

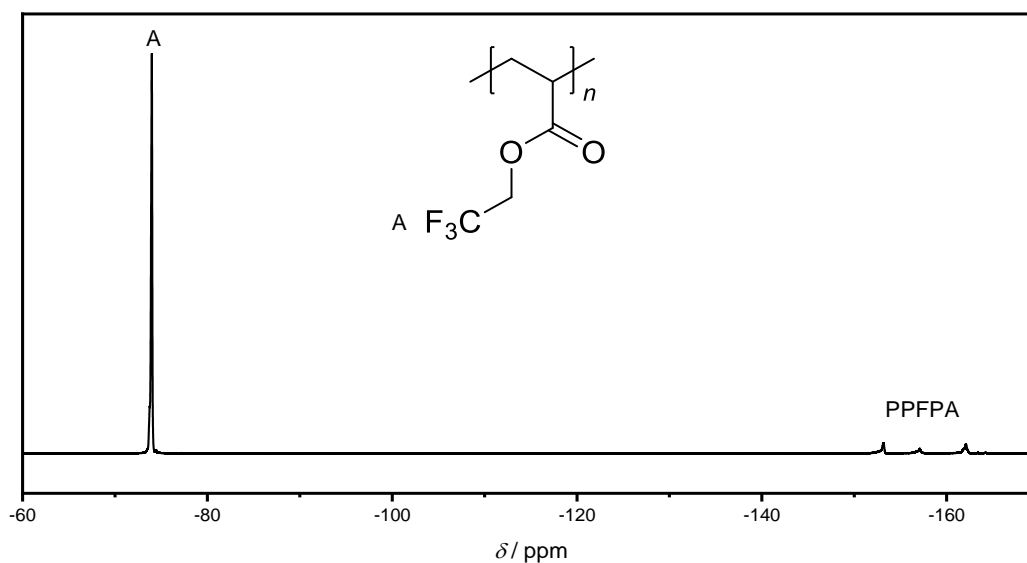


Figure 59: ^{19}F NMR of the transesterification of PPFPA with 2,2,2-trifluoroethanol at ambient temperature. Solvent: CDCl_3 .

^{19}F NMR (377 MHz, CDCl_3) $\delta = -74.03$ (s, 3F, A).

Impurities:

- -153.17 ppm: PPFPA
- -157.12 ppm: PPFPA
- -162.08 ppm: PPFPA

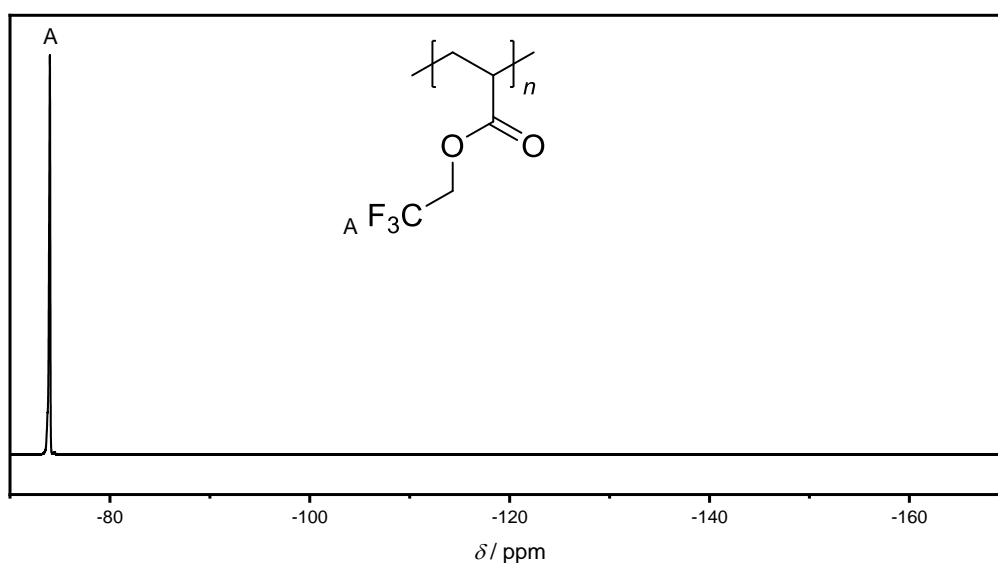


Figure 60: ^{19}F NMR spectrum of the transesterification of PPFPA with 2,2,2-trifluoroethanol at 80 °C. Solvent: CDCl_3 .

^{19}F NMR (377 MHz, CDCl_3) $\delta = -73.99$ (s, 3F, A).

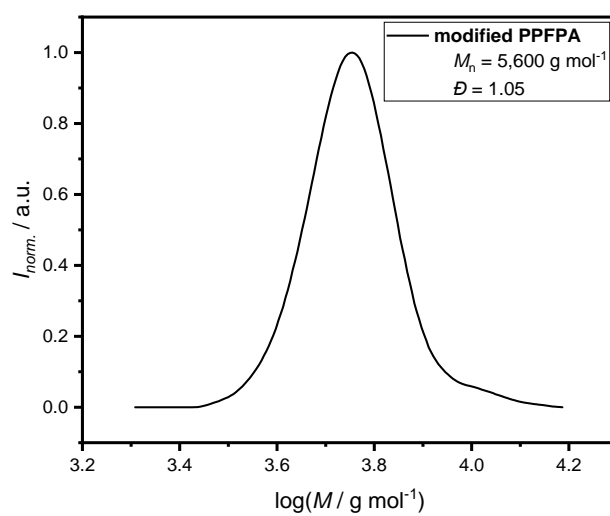
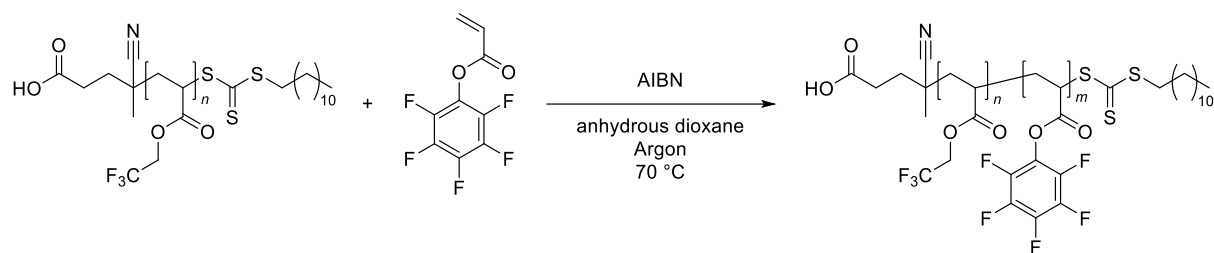


Figure 61: Size exclusion chromatogram of PPFPA after the transesterification with 2,2,2-trifluoroethanol at ambient temperature.

6.3.1.7. Chain Extension Reaction of Modified PPFA with PFPA



PFPA (119 μL , 172 mg, 724 μmol , 140 eq.) was given into a flask followed by the macro-RAFT agent (30.0 mg, 5.17 μmol , 1.00 eq.) in anhydrous dioxane (300 μL). Afterwards, AIBN (679 μg , 4.14 μmol , 0.80 eq.) was added and the flask was put into a water bath and purged for 10 min with argon. In the end, the flask was put into a preheated oil bath at 70 °C and the reaction was done overnight. The next day, the reaction was stopped by cooling the reaction mixture and exposure to oxygen.

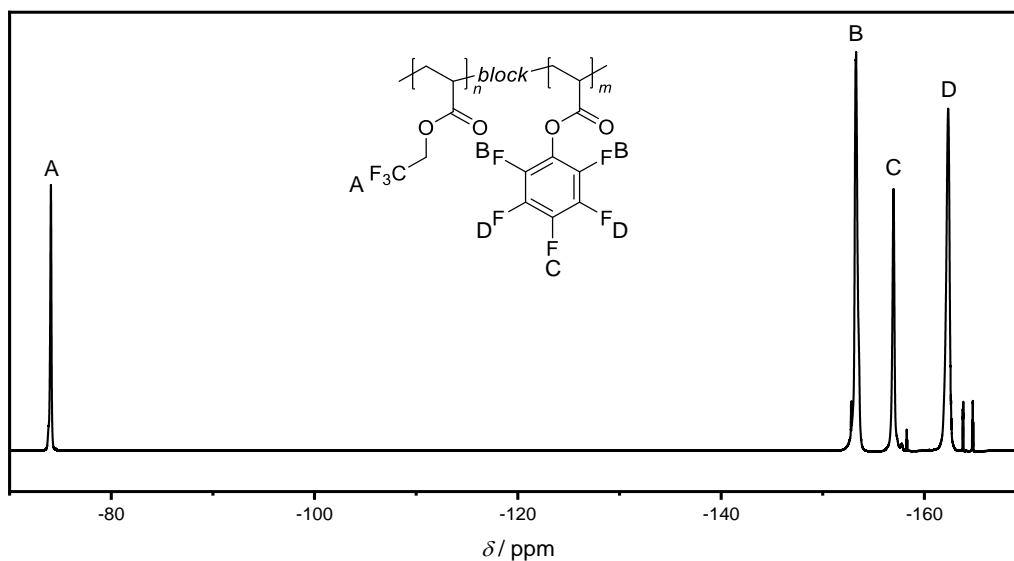


Figure 62: ^{19}F NMR spectrum of the first CE of 2,2,2-trifluoroethanol modified PPFPA. Solvent: CDCl_3 .

^{19}F NMR (377 MHz, CDCl_3) δ = -77.06 (s, 3F, A), -152.00 - -154.02 (m, 10F, B), -156.04 - -158.03 (m, 5F, C), -160.72 - -163.26 (m, 10F, D).

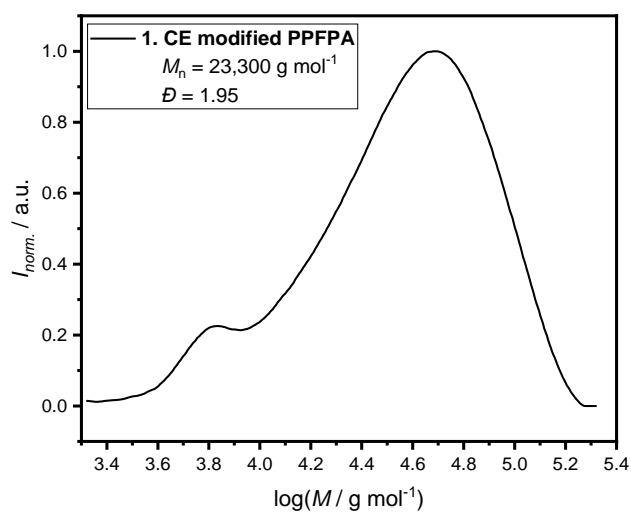
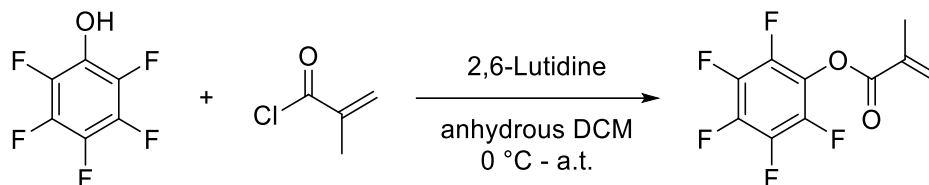


Figure 63: Size exclusion chromatogram of once chain extended 2,2,2-trifluoroethanol modified PPFPA.

6.3.2. Synthetic Procedures for “Multiblock Copolymer Synthesis via ATRP”

6.3.2.1. Synthesis of Pentafluorophenyl Methacrylate



This synthetic procedure is based on previously published studies.¹⁶⁶

In a 50 mL round bottom flask PFP (3.00 g, 16.3 mmol, 1.00 eq.) and 2,6-Lutidine (2.08 mL, 1.92 g, 17.9 mmol, 1.10 eq.) were dissolved in anhydrous DCM (27.8 mL) and methacryloyl chloride (1.75 mL, 1.87 g, 17.9 mmol, 1.10 eq.) was added dropwise under cooling with an ice bath. A white precipitation was visible. The next day, the precipitated salt was filtrated and the reaction mixture was washed four times with water, while the aqueous phase was extracted twice using ethyl acetate. Afterwards, the combined organic phases were dried with MgSO₄. The solvent was removed at ambient temperature under reduced pressure. A yellowish oil was obtained and purified via column chromatography using PE as solvent. After the solvent removal under reduced pressure at ambient temperature, a colorless oil was obtained (2.32 g; 56 %).

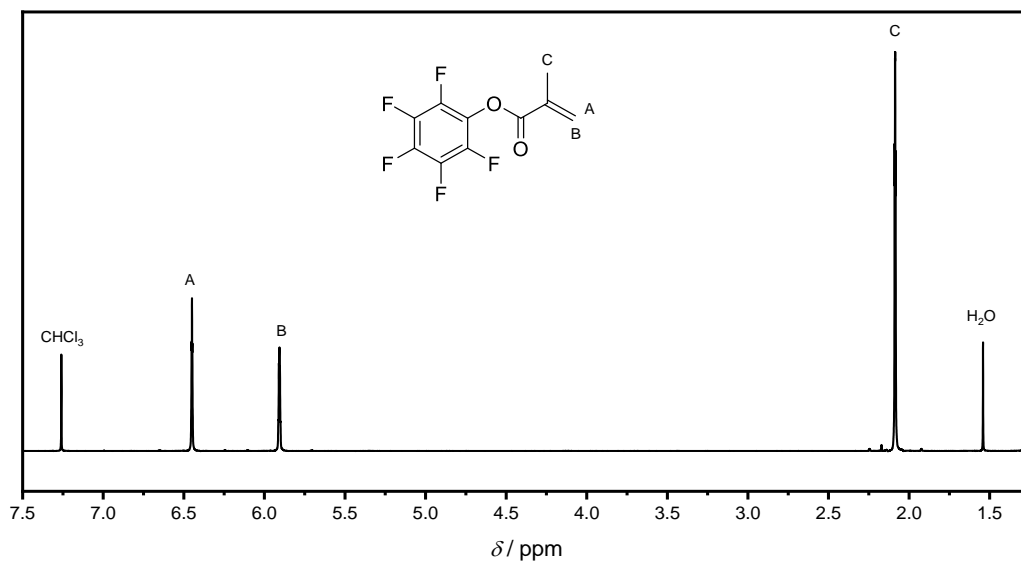


Figure 64: ^1H NMR spectrum of PFPMA. Solvent: CDCl_3 .

^1H NMR (400 MHz, CDCl_3) δ = 6.45 (s, 1H, A), 5.91 (s, 1H, B), 2.09 (s, 3H, C).

Impurities:

- 1.55 ppm: H_2O

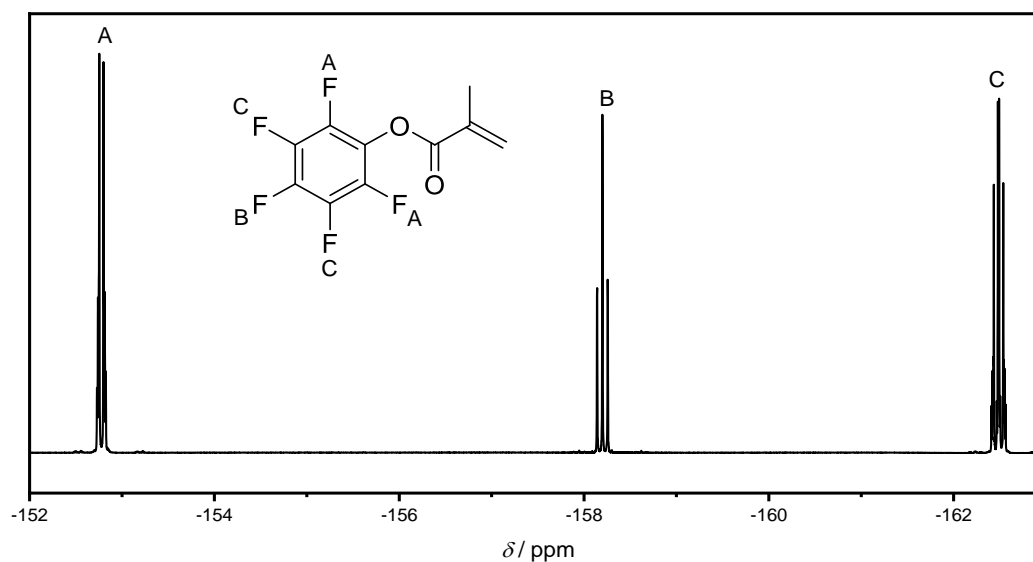
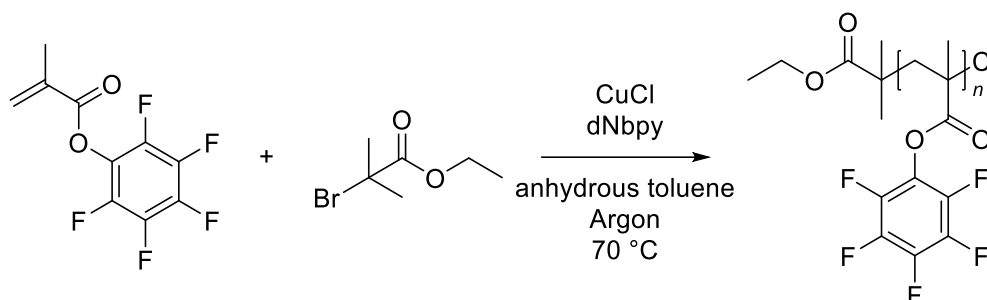


Figure 65: ^{19}F NMR spectrum of PFPMA. Solvent: CDCl_3 .

^{19}F NMR (377 MHz, CDCl_3) δ = -152.68 - -152.95 (m, 2F, A), -158.20 (t, J = 21.6 Hz, 1F, B), -162.35 - -162.65 (m, 2F, C).

6.3.2.2. Atom Transfer Radical Polymerization of PFPMA with EBiB and dNbpy



Cu(I)Cl (3.37 mg, 34.1 μmol , 0.50 eq.) and dNbpy (27.8 mg, 68.1 μmol , 1.00 eq.) were given into a 5 mL flask and the atmosphere was changed to argon. Afterwards, PFPMA (859 mg, 616 μL , 3.41 mmol, 50.0 eq.) and anhydrous toluene (61.6 μL) were added under cooling of an ice bath and argon purging. After the addition of EBiB (10.0 μL , 13.3 mg, 68.1 μmol , 1.00 eq.) to the mixture, the flask was given into a preheated oil bath (70 °C). After 4 hours, no movement of the stirring bar was visible anymore and the polymerization was stopped. THF was added and the reaction mixture was passed through a short neutral alox column to remove the copper catalyst. Afterwards, the polymer was precipitated three times in cold methanol and the solvent was removed under reduced pressure at 40 °C (301 mg; 35 %).

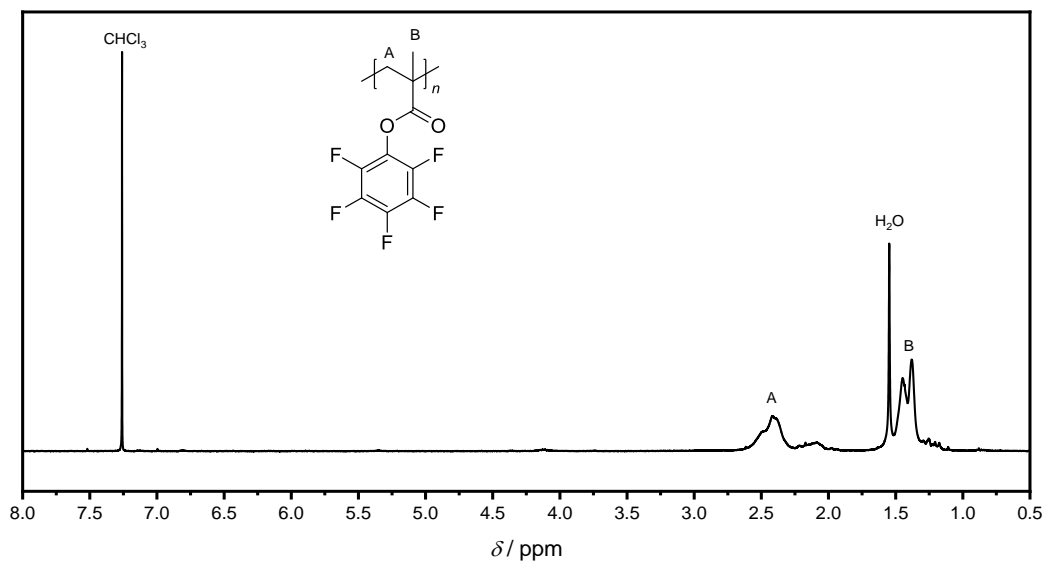


Figure 66: ^1H NMR of PPFMA. Solvent: CDCl_3 .

^1H NMR (400 MHz, CDCl_3) $\delta = 2.70 - 1.92$ (m, 2H, A), $1.66 - 1.07$ (m, 3H, B).

Impurities:

- 1.54 ppm: H_2O

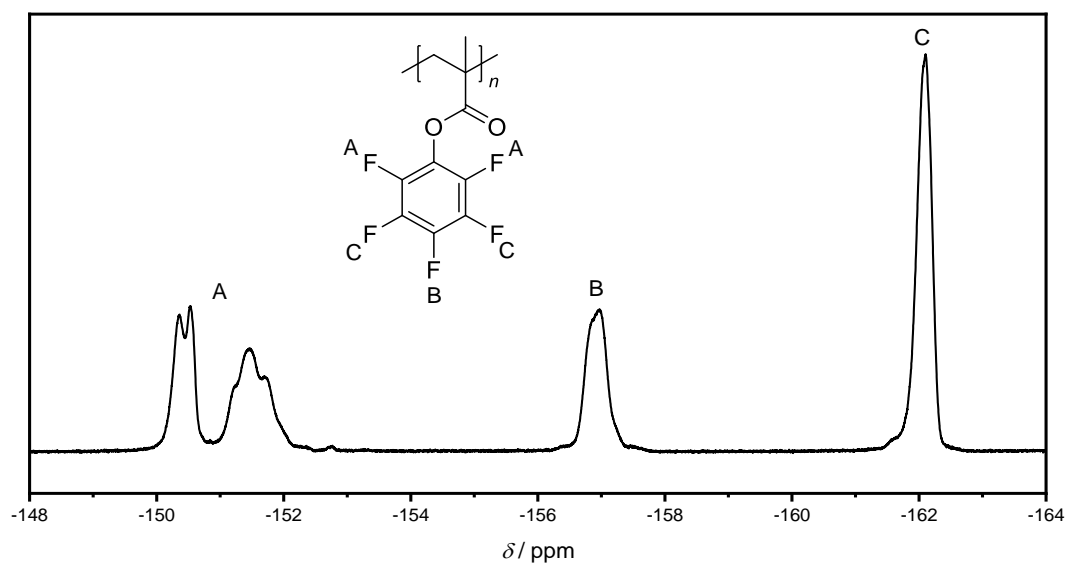


Figure 67: ^{19}F NMR spectrum of PPFMA. Solvent: CDCl_3 .

^{19}F NMR (377 MHz, CDCl_3) $\delta = -149.76 - -152.55$ (m, 2F, A), $-156.26 - -157.69$ (m, 1F, B), $-161.45 - -162.62$ (m, 2F, C).

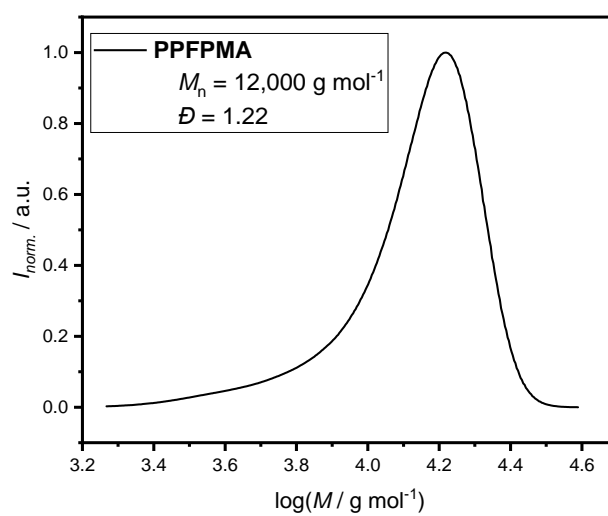
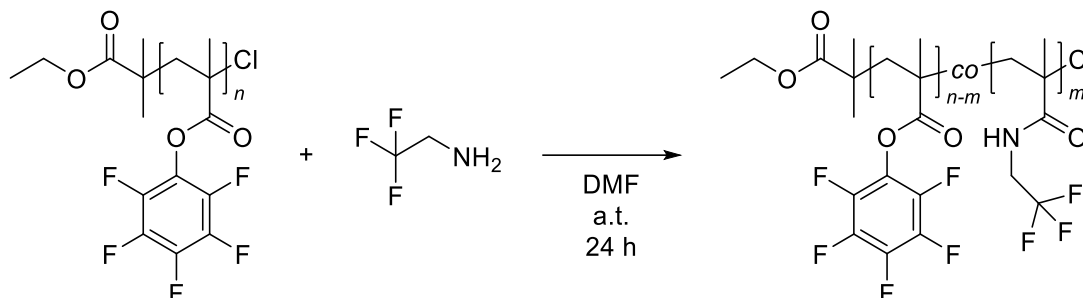


Figure 68: Size exclusion chromatogram of PFPMA.

6.3.2.3. Post-Polymerization Modification of PPFMA with 2,2,2-Trifluoroethylamine



PPFPMA (70.0 mg, approx. 273 μmol of repeating units, 1.00 eq.) was dissolved in DMF (1.80 mL) under heating and put aside for further use. 2,2,2-Trifluoroethylamine (12.9 μL , 16.2 mg, 164 μmol , 0.60 eq.) was given into a 5 mL peach flask and the DMF/PPFPA mixture was immediately added. The flask was sealed and stirred overnight at ambient temperature. The next day, the solvent was removed under reduced pressure, the residue dissolved in acetone and precipitated three times in cold PE. Afterwards, the solvent was removed under reduced pressure at 40 $^{\circ}\text{C}$, leading to a white solid product (33.6 mg; 77 %).

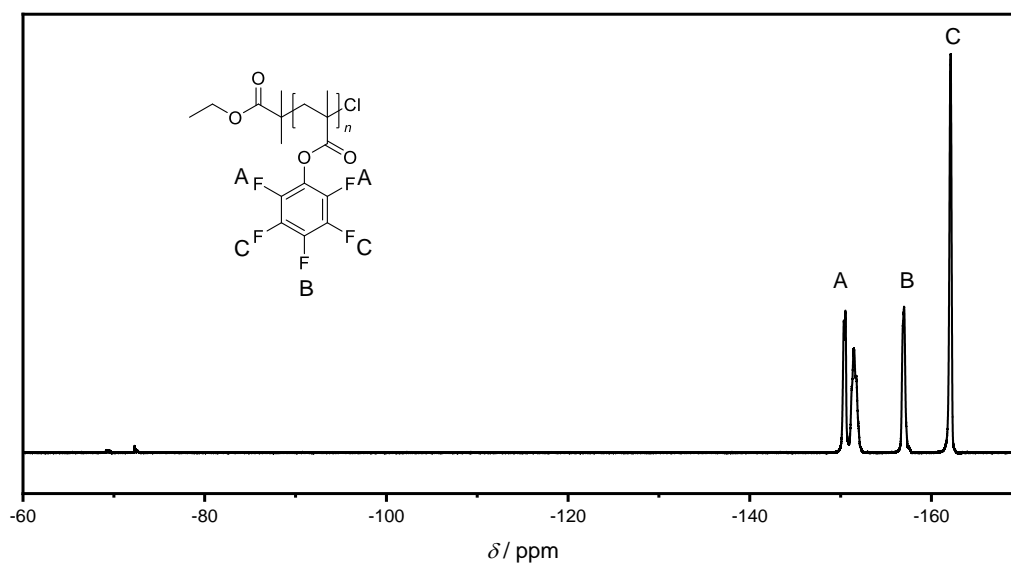


Figure 69: ^{19}F NMR spectrum of the PPM of PPFMA with 2,2,2-trifluoroethanol. No modification could be observed. Solvent: CDCl_3 .

^{19}F NMR (377 MHz, CDCl_3) δ = -149.83 - -152.37 (m, 2F, A), -156.30 - -157.94 (m, 1F, B), -161.11 - -162.73 (m, 2F, C).

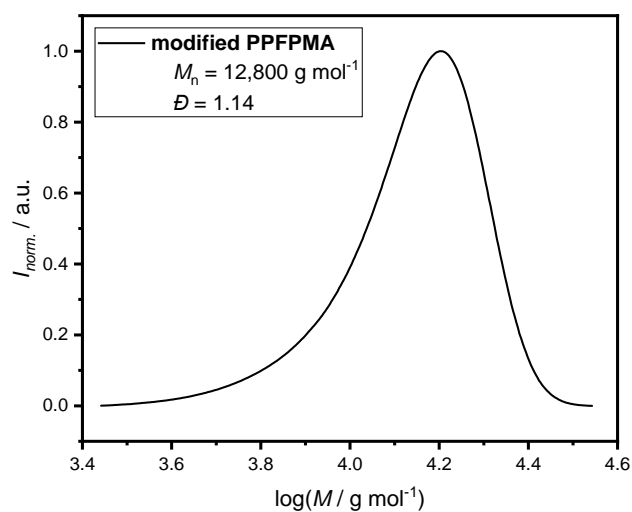
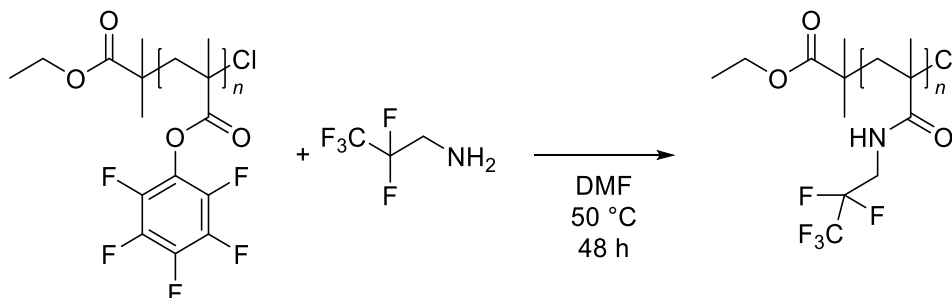


Figure 70: Size exclusion chromatogram of the PPM of PPFMA with 2,2,2-trifluoroethanol.

6.3.2.4. Post-Polymerization Modification of PFPMA with 2,2,3,3,3-Pentafluoropropylamine



PFPMA (70.0 mg, approx. 273 μmol of repeating units, 1.00 eq.) was dissolved in DMF (1.80 mL). Afterwards, 2,2,3,3,3-pentafluoropropylamine (58.2 μL , 81.4 mg, 546 μmol , 2.00 eq.) was added to the reaction mixture and stirred for two days at 50 °C. An NMR sample was taken to determine the conversion. However, the ^{19}F NMR spectrum showed no conversion. Therefore, TEA (77.4 μL) was added to the reaction mixture, but no improvement could be observed.

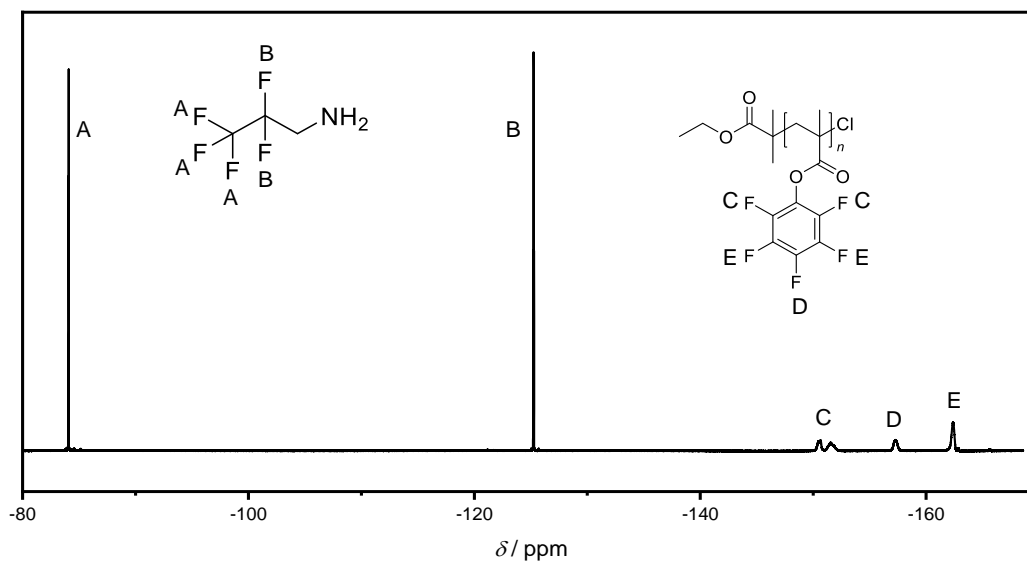
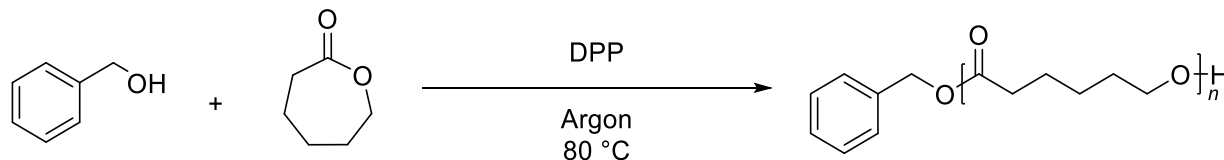


Figure 71: Crude ^{19}F NMR of the PPM of PPFMA with 2,2,3,3,3-pentafluoropropylamine after 48 hours. The still present PPFMA signals indicate an unsuccessful PPM. Solvent: CDCl_3 .

^{19}F NMR (377 MHz, CDCl_3) δ = -84.05 - -84.11 (m, 3F, A), -125.24 (t, J = 15.6 Hz, 2F, B), -149.94 - -152.30 (m, 2F, C), -156.88 - -157.88 (m, 1F, D), -161.79 - -162.92 (m, 2F, E).

6.3.3. Synthetic Procedures for “Multiblock Copolymer Synthesis via CROP”

6.3.3.1. Cationic Ring-Opening Polymerization of CL



CL (2.03 mL, 2.20 g, 19.2 mmol, 20.0 eq.) was given in a dry flask with a stirring bar under argon. Afterwards, BnOH (10.0 μ L, 104 mg, 961 μ mol, 1.00 eq.) was added, followed by DPP (12.0 mg, 48.1 μ mol, 0.05 eq.). The flask was put into a preheated oil bath at 80 °C. After almost 1 hour, the stirring bar did not move anymore and the reaction was stopped by precipitating the polymer three times in cold MeOH. After the solvent was removed under reduced pressure at 40 °C, a white solid was obtained (1.56 g; 68 %).

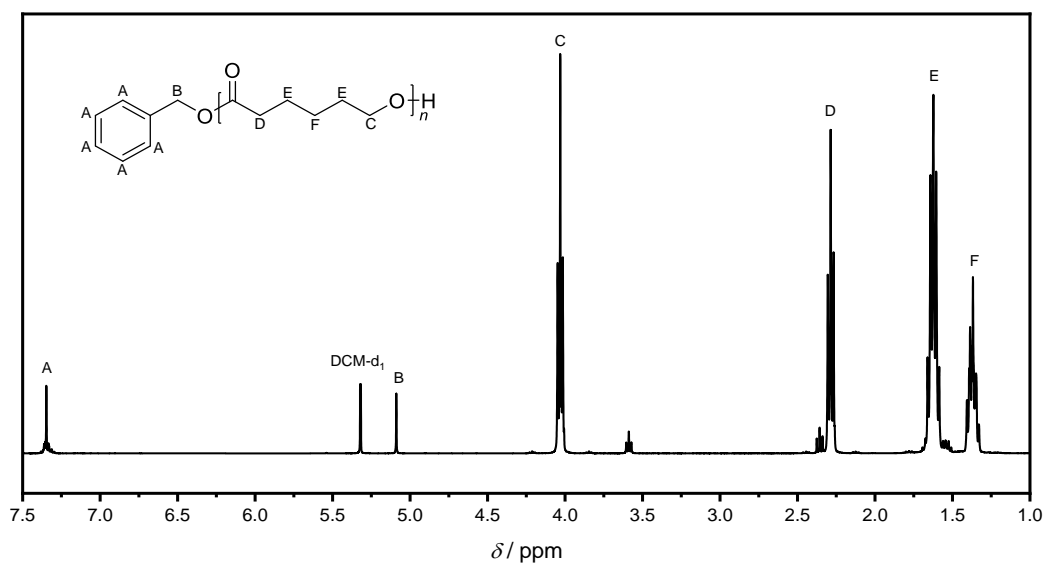


Figure 72: ^1H NMR spectrum of PCL. Solvent: DCM-d_2 .

^1H NMR (400 MHz, DCM-d_2) $\delta = 7.39 - 7.26$ (m, 5H, A), 5.09 (s, 2H, B), 4.03 (t, $J = 6.7$ Hz, 40H, C), 2.29 (t, $J = 7.5$ Hz, 40H, D), 1.62 (p, $J = 7.7$ Hz, 80H, E), 1.45 – 1.08 (m, 40H, F).

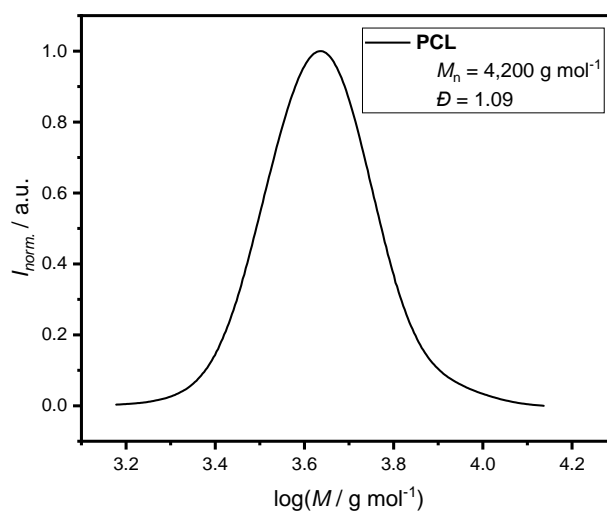
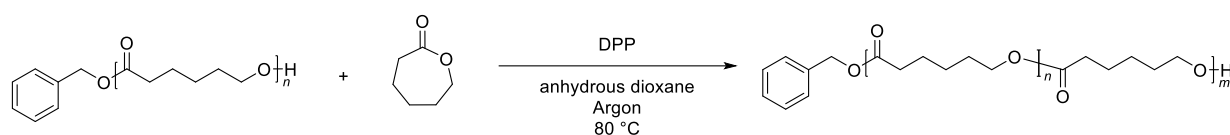


Figure 73: Size exclusion chromatogram of PCL.

6.3.3.2. First Chain Extension Reaction of PCL with CL



CL (396 μL , 428 mg, 3.75 mmol, 30.0 eq.) was given in a dry flask with a stirring bar under argon. Afterwards, PCL (300 mg, 125 μmol , 1.00 eq.) in anhydrous dioxane (600 μL) was added, followed by DPP (1.56 mg, 6.25 μmol , 0.05 eq.). The flask was put into a preheated oil bath at 80 °C and the polymerization was stopped after 2.5 hours by precipitating the polymer three times in cold MeOH. After the solvent was removed under reduced pressure at 40 °C, a white solid was obtained.

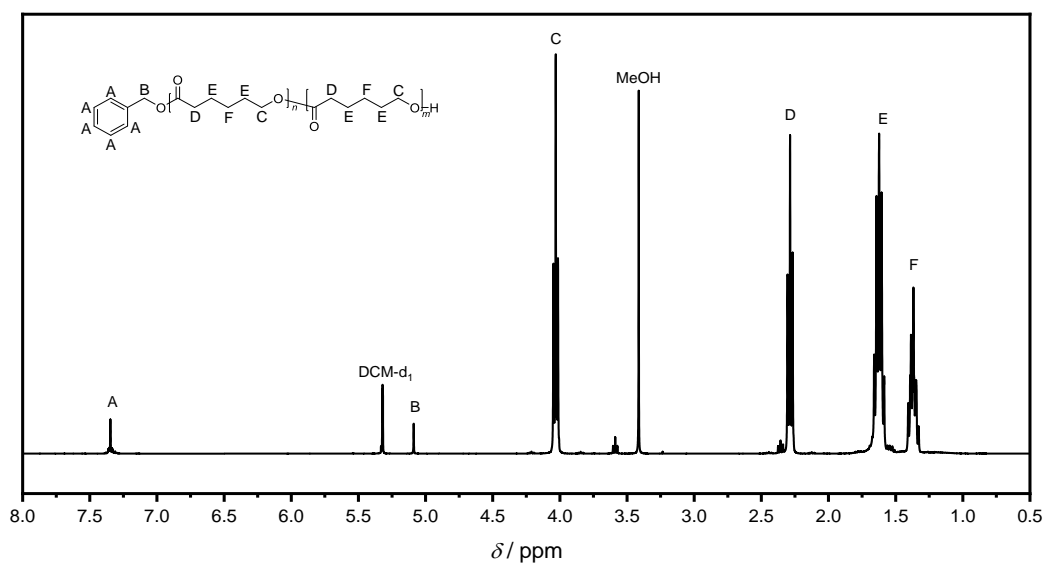


Figure 74: ^1H NMR spectrum of once chain extended PCL. Solvent: DCM-d_2 .

^1H NMR (400 MHz, DCM-d_2) δ = 7.40 – 7.28 (m, 5H, A), 5.09 (s, 2H, B), 4.03 (t, J = 6.7 Hz, 72H, C), 2.29 (t, J = 7.5 Hz, 72H, D), 1.70 – 1.57 (m, 140H, E), 1.43 – 1.31 (m, 70H, F).

Impurities:

- 3.36 ppm: MeOH

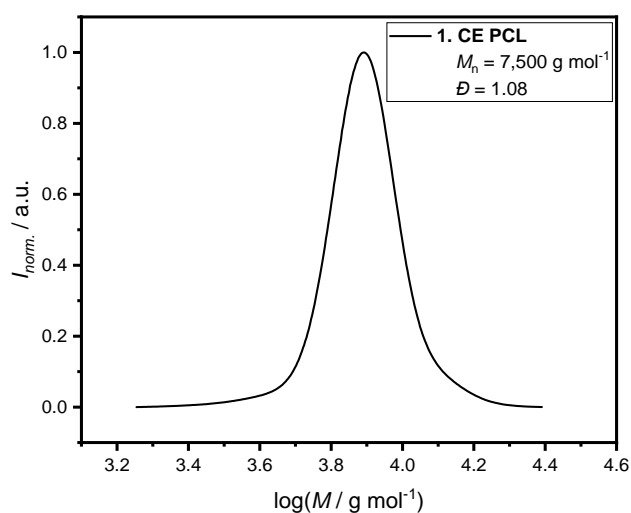
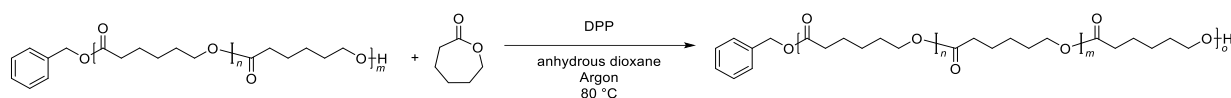


Figure 75: Size exclusion chromatogram of once chain extended PCL.

6.3.3.3. Second Chain Extension Reaction of PCL with CL



CL (139 μL , 150 mg, 1.32 mmol, 20.0 eq.) was given in a dry flask with a stirring bar under argon. Afterwards, chain extended PCL (300 mg, 65.8 μmol , 1.00 eq.) in anhydrous dioxane (400 μL) was added, followed by DPP (820 μg , 3.29 μmol , 0.05 eq.). The flask was put into a preheated oil bath at 80 $^{\circ}\text{C}$ and the polymerization was stopped by precipitating the polymer three times in cold MeOH. A white solid was obtained.

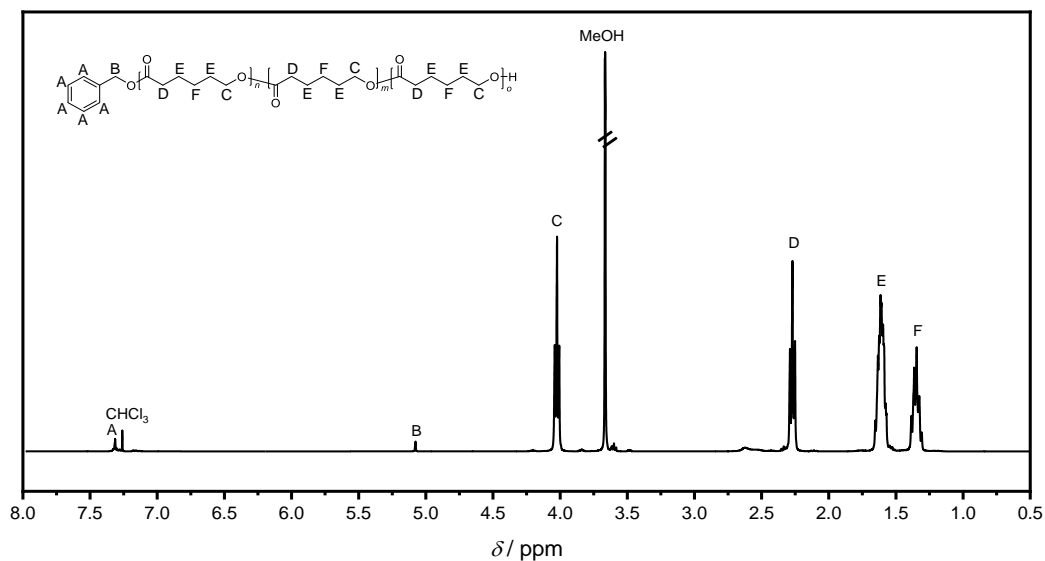


Figure 76: ^1H NMR spectrum of twice chain extended PCL. Solvent: CDCl_3 .

^1H NMR (400 MHz, CDCl_3) δ = 7.33 – 7.24 (m, 5H, A), 5.04 (s, 2H, B), 3.99 (t, J = 6.7, 1.5 Hz, 118H, C), 2.24 (t, J = 7.5, 1.4 Hz, 119H, D), 1.66 – 1.50 (m, 236H, E), 1.37 – 1.22 (m, 118H, F).

Impurities:

- 3.63 ppm: MeOH

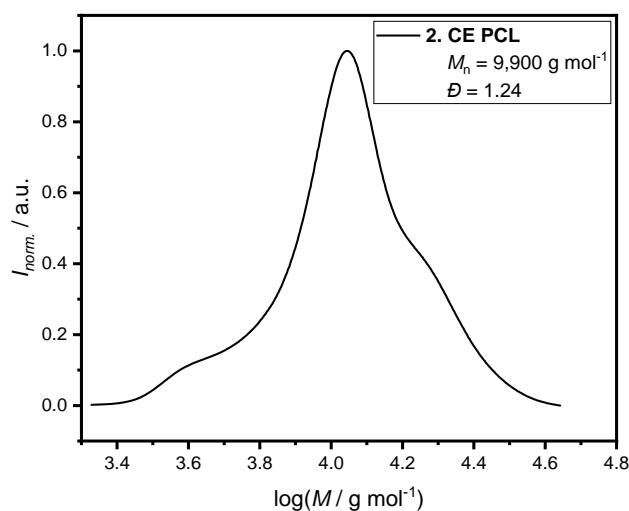
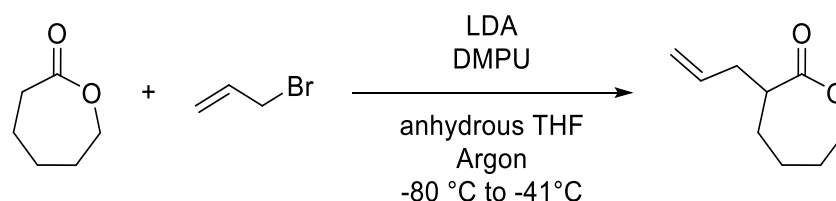


Figure 77: Size exclusion chromatogram of twice chain extended PCL.

6.3.3.4. Synthesis of α -Allyl-Caprolactone



This synthetic procedure is based on previously published studies.¹⁶⁹

Anhydrous THF (50.0 mL) was given into a dry flask under argon. Afterwards, the flask was put into a $-80\text{ }^\circ\text{C}$ cooling bath (acetone/ $\text{CO}_2(\text{s})$) and a 1 M LDA solution (22.8 mL, 2.44 g of LDA, 22.8 mmol, 1.30 eq.) was added slowly into the flask. Afterwards, CL (1.94 mL, 2.00 g, 17.5 mmol, 1.00 eq.) in anhydrous THF (15.0 mL) was added over the course of one hour to the system. The mixture was stirred for another hour before allyl bromide (1.97 mL, 2.76 g, 22.8 mmol, 1.30 eq.) in DMPU (5.00 mL) was added slowly. The temperature was slowly increased to $-41\text{ }^\circ\text{C}$ (acetonitrile/ CO_2) and stirred for another two hours, before the reaction was quenched by addition of saturated NH_4Cl solution. The next day, the organic phase was washed three times with brine and saturated NH_4Cl solution. The aqueous phase was extracted twice with THF. The organic phase was concentrated under reduced pressure and given into cold Et_2O . Afterwards, the precipitated solid was removed by filtration and the remaining mixture was dried over MgSO_4 . The solvent was removed under reduced pressure at $40\text{ }^\circ\text{C}$ and the crude monomer was purified via column chromatography (7:3 PE:EE). Once again, the solvent was removed under reduced pressure and a yellow oil was obtained (689 mg; 26 %; Rf: 0.5).

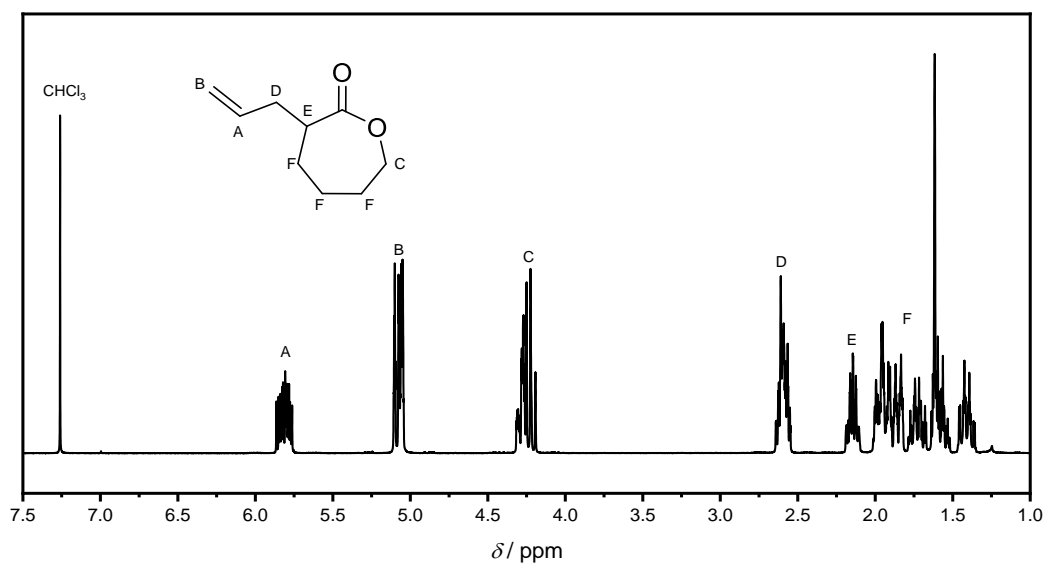
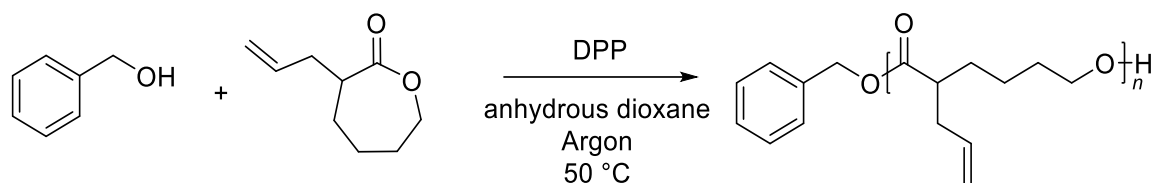


Figure 78: ^1H NMR spectrum of α -allyl-caprolactone. Solvent: CDCl_3 .

^1H NMR (400 MHz, CDCl_3) δ = 5.88 – 5.74 (m, 1H, A), 5.13 – 4.98 (m, 2H, B), 4.34 – 4.15 (m, 2H, C), 2.68 – 2.52 (m, 2H, D), 2.20 – 2.08 (m, 1H, E), 2.02 – 1.32 (m, 6H, F).

6.3.3.5. Cationic Ring-Opening Polymerization of ACL



ACL (297 μ g, 1.92 mmol, 20.0 eq.) and anhydrous dioxane (1.70 mL) were given into a dry flask with a stirring bar under argon. Afterwards, BnOH (10.0 μ L, 10.4 mg, 96.1 μ mol, 1.00 eq.) was added, followed by DPP (48.1 mg, 192 μ mol, 2.00 eq.). The flask was put into a preheated oil bath at 50 °C. After two days, the polymerization was stopped by precipitating the mixture into cold MeOH. No polymer but only oligomers were obtained.

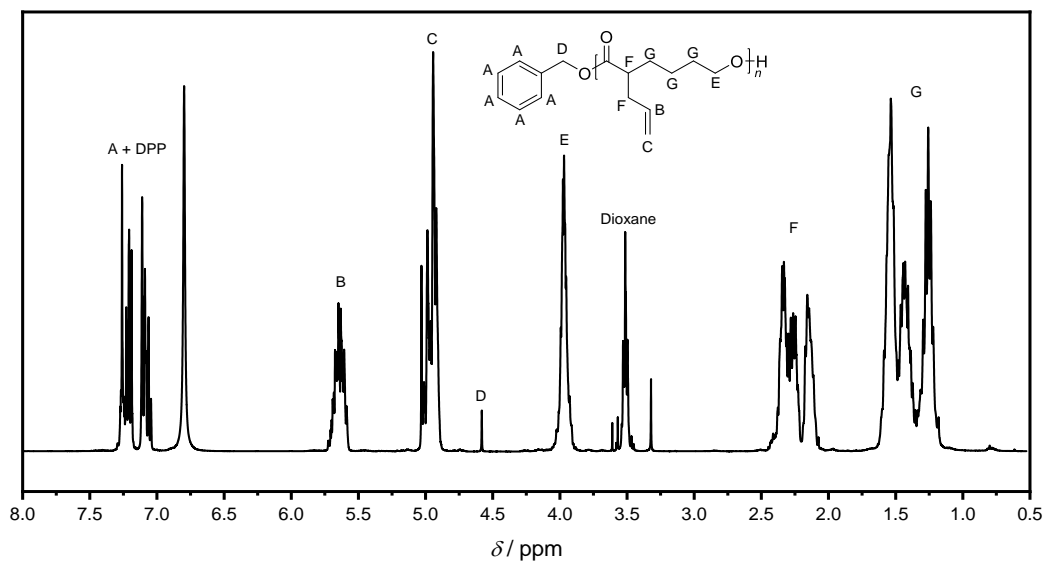


Figure 79: Crude ^1H NMR spectrum of PACL. Solvent: CDCl_3 .

^1H NMR (400 MHz, CDCl_3) δ = 7.30 – 7.01 (m, 149H, A), 5.76 – 5.56 (m, 93H, B), 5.05 – 4.85 (m, 200H, C), 4.57 (s, 2H, D), 4.07 – 3.89 (m, 134H, E), 2.46 – 2.03 (m, 284H, F), 1.68 – 1.04 (m, 581H, G).

Impurities:

- 3.51 ppm: Dioxane

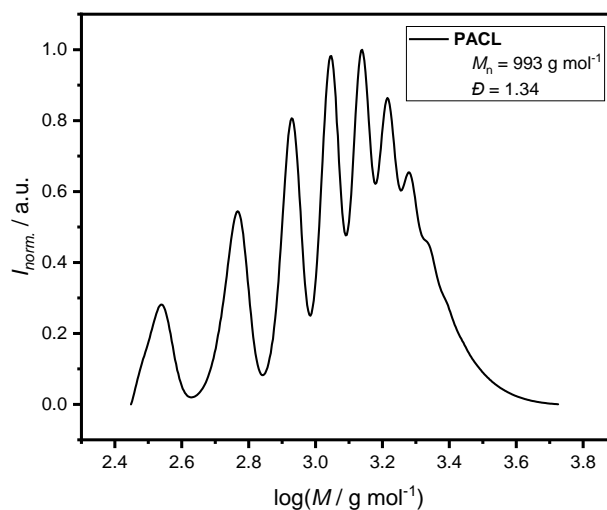
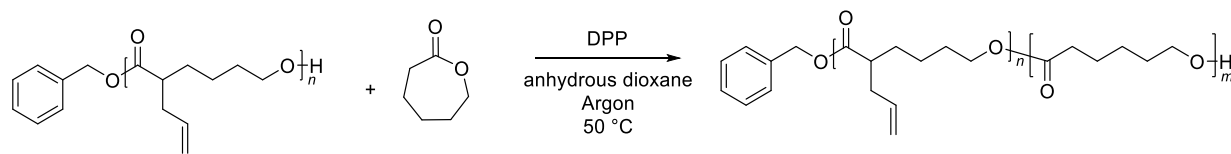


Figure 80: Size exclusion chromatogram of PACL.

6.3.3.6. First Chain Extension Reaction of PACL with CL



CL (426 μ L, 439 mg, 3.85 mmol, 50.0 eq.) was given in a dry flask with anhydrous dioxane (3.20 mL) and a stirring bar under argon. Afterwards, PACL (100 mg, 76.9 μ mol, 1.00 eq.) followed by DPP (96.2 mg, 384 μ mol, 5.00 eq.) were added. The flask was put into a preheated oil bath at 50 °C. After 48 hours, the polymerization was stopped by precipitating the polymer three times in cold MeOH. A white solid was obtained.

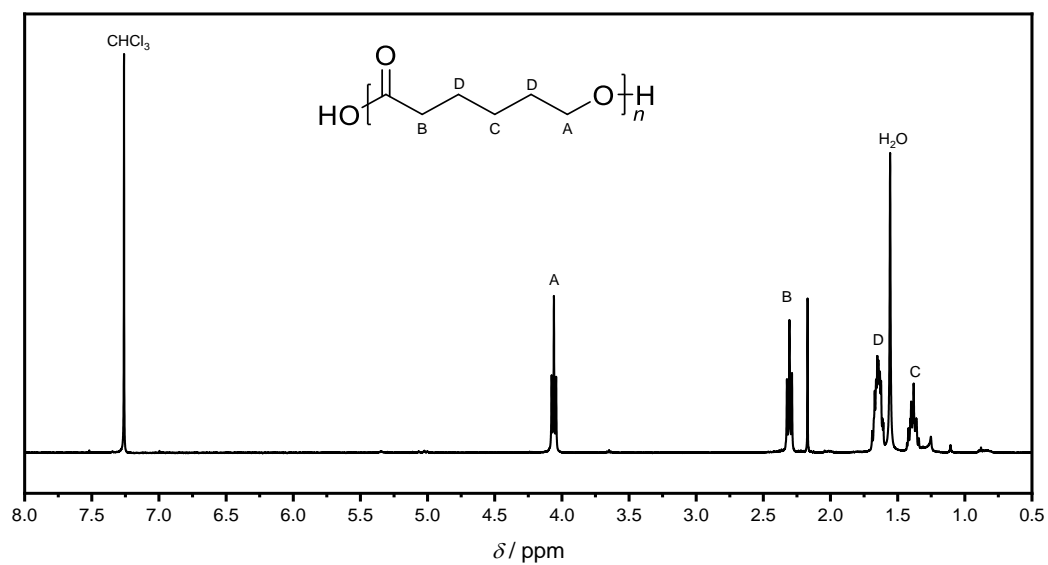


Figure 81: ^1H NMR spectrum of the first CE of PACL with ϵ -caprolactone. No CE could be observed, only the formation of PCL. Solvent CDCl_3 .

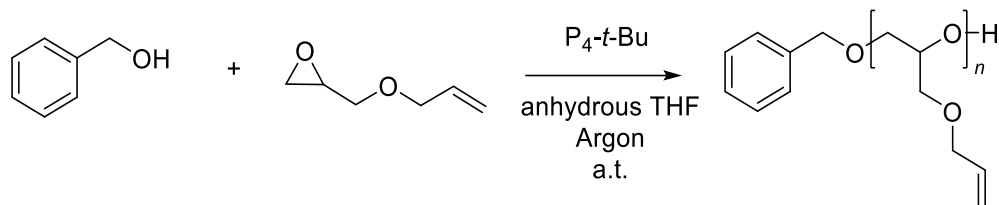
^1H NMR (400 MHz, CDCl_3) δ = 4.06 (t, J = 6.7 Hz, 2H, A), 2.31 (t, J = 7.5 Hz, 2H, B), 1.71 – 1.59 (m, 4H, C), 1.44 – 1.21 (m, 2H, D).

Impurities:

- 1.55 ppm: H_2O

6.3.4. Synthetic Procedures for “Multiblock Copolymer Synthesis via AROP”

6.3.4.1. Anionic Ring-Opening Polymerization of AGE using P_4 -*t*-Bu



AGE (566 μL , 549 mg, 4.81 mmol, 50.0 eq.) was given into a flask with anhydrous THF (2.77 mL). After 10 minutes of argon purging a 0.8 M P_4 -*t*-Bu solution (120 μL , equals 60.9 mg pure P_4 -*t*-Bu, 96.2 μmol , 1.00 eq.) was added, followed by BnOH (10.0 μL , 10.4 mg, 96.2 μmol , 1.00 eq.). The polymerization was stopped by adding acetic acid (1.00 mL) after 7 hours. To remove the catalyst the polymer was dissolved in ethyl acetate and washed three times with water. Afterwards, the solvent was removed under reduced pressure at 40 $^\circ\text{C}$, leading to a yellow oil (425 mg; 76 %).

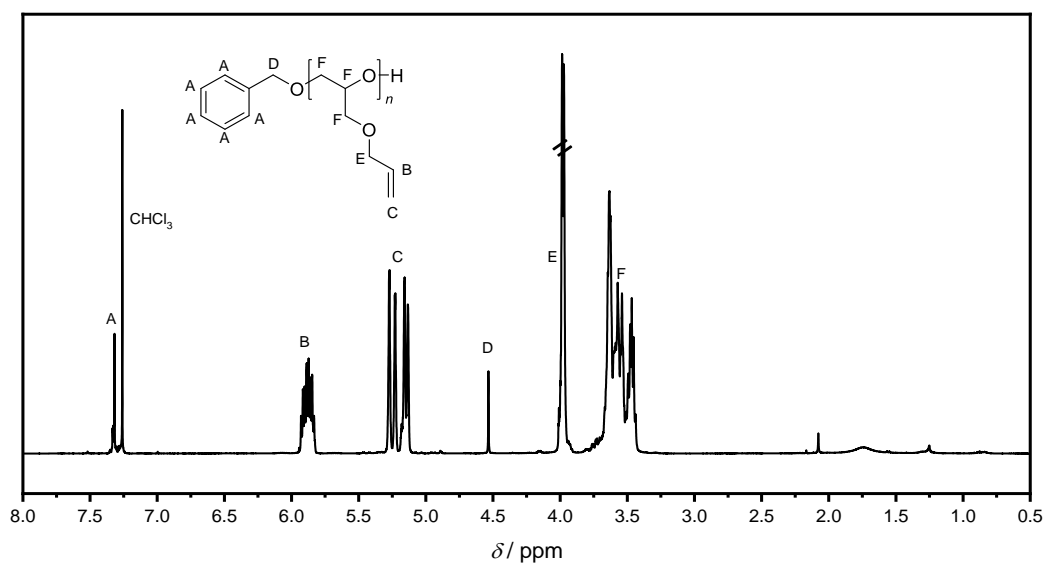


Figure 82: ^1H NMR spectrum of PAGE. Solvent: CDCl_3 .

^1H NMR (400 MHz, CDCl_3) δ = 7.36 – 7.20 (m, 5H, A), 5.96 – 5.79 (m, 23 H, B), 5.31 – 5.07 (m, 46H, C), 4.53 (s, 2H, D), 4.03 – 3.88 (m, 46, E), 3.82 – 3.36 (m, 115H, F).

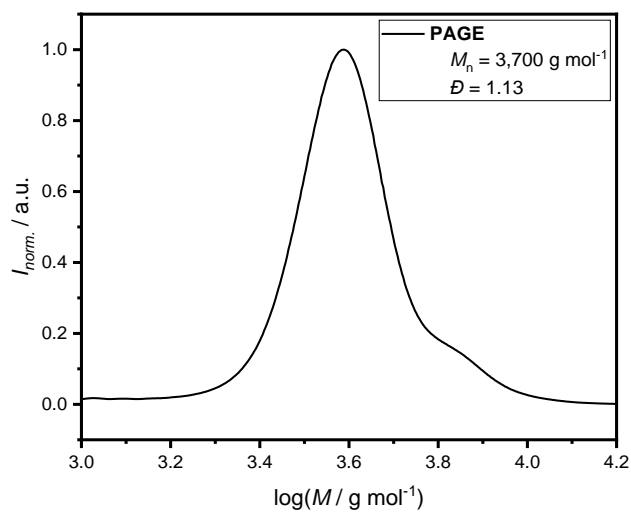
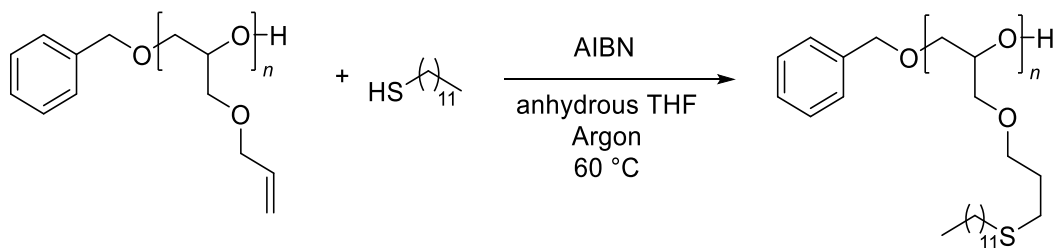


Figure 83: Size exclusion chromatogram of PAGE.

6.3.4.2. Post-Polymerization Modification of PAGE via Thiol-ene reaction using 1-Dodecanethiol



PAGE (150 mg, approx. 1.26 mmol of the repeating units, 1.00 eq.) was given into a flask with anhydrous THF (2.50 mL) followed by 1-dodecanethiol (1.20 mL, 1.02 g, 5.05 mmol, 4.00 eq.) and AIBN (104 mg, 631 μ mol, 0.50 eq.). Afterwards, the reaction mixture was purged for 10 minutes with argon and then put into a preheated oil bath (60 °C). The next day, the solvent was removed under reduced pressure and the reaction mixture was precipitated in cold EtOH and washed three times. The solvent was removed under reduced pressure at 40 °C, leading to a yellow oil (326 mg; 80 %).

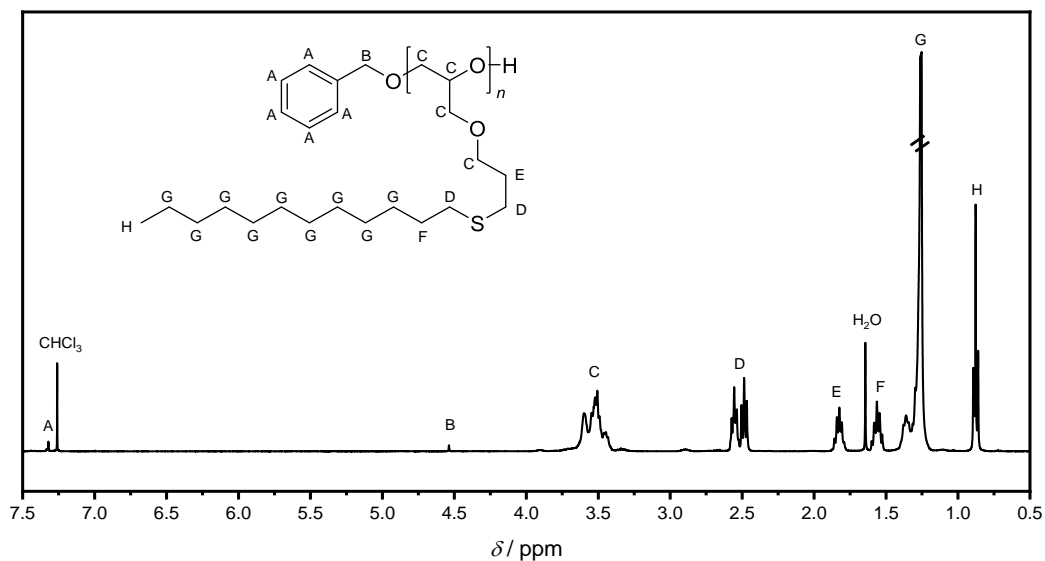


Figure 84: ^1H NMR spectrum of 1-dodecanethiol modified PAGE. Solvent: CDCl_3 .

^1H NMR (400 MHz, CDCl_3) δ = 7.35 – 7.29 (m, A), 4.53 (s, B), 3.76 – 3.26 (m, 7H, C), 2.63 – 2.42 (m, 4, D), 1.90 – 1.70 (m, 2H, E), 1.59 – 1.46 (m, 2H, F), 1.42 – 1.16 (m, 18H, G), 0.91 – 0.77 (m, 3 H, H).*

*Due to the low intensity of signals A and B, signal H is used as reference for proton determination.

Impurities:

- 1.63 ppm: H_2O

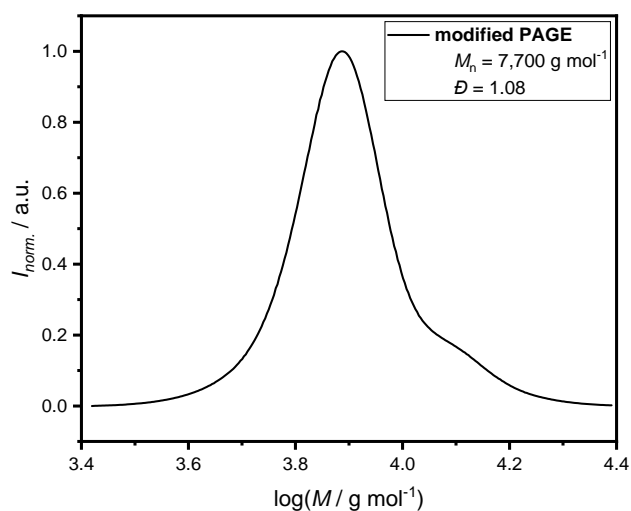
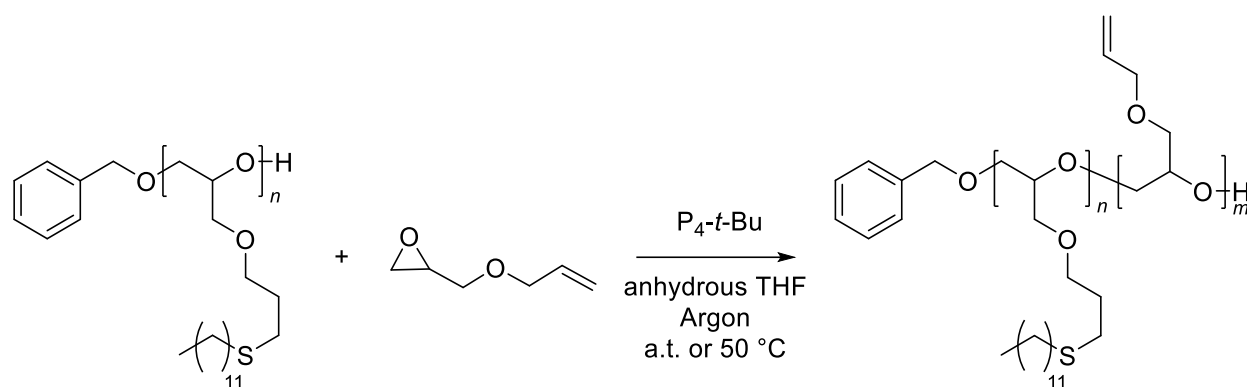


Figure 85: Size exclusion chromatogram of 1-dodecanethiol modified PAGE.

6.3.4.3. First Chain Extension of Modified PAGE with AGE and P₄-t-Bu



Once modified PAGE (216 mg, 29.7 μmol , 1.00 eq.) was given into a flask with anhydrous THF (2.00 mL) and 0.8 M P₄-t-Bu solution (37.1 μL , 18.8 mg of pure P₄-t-Bu, 29.7 μmol , 1.00 eq.). The reaction mixture was purged for 10 minutes with argon before AGE (175 μL , 24.9 mg, 1.97 mmol, 50.0 eq.) was added and the flask was stirred at ambient temperature or given into a preheated oil bath (50 °C). In case of the reaction at ambient temperature, the CE was stopped after 21 hours by adding acetic acid (1.00 mL) to the mixture, while the reaction at 50 °C was stopped after 5.5 hours. The product was precipitated into cold MeOH and washed three times. In the end, the solvent was removed under reduced pressure at 40 °C, leading to a yellowish oil (50 °C: 144 mg; 66 %).

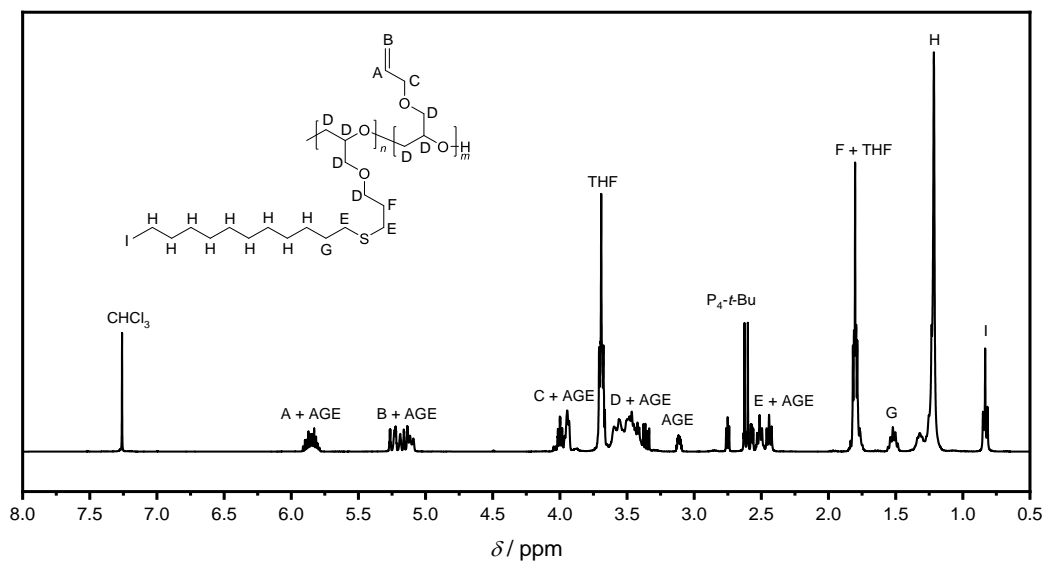


Figure 86: Crude ^1H NMR spectrum of the CE reaction of modified PAGE with AGE at ambient temperature. Solvent: CDCl_3 .

^1H NMR (400 MHz, CDCl_3) δ = 5.94 – 5.77 (m, 2H, A), 5.30– 5.06 (m, 4H, B), 4.06 – 3.81 (m, 4H, C), 3.62 – 3.30 (m, 12H, D), 2.55 – 2.39 (m, 3H, E), 1.81 – 1.72 (m, 10H, F), 1.56 – 1.45 (m, 2H, G), 1.36 – 1.13 (m, 18H, H), 0.87 – 0.79 (m, 3H, I).

Impurities:

- 5.85 ppm: AGE
- 5.17 ppm: AGE
- 4.00 ppm: AGE
- 3.69 ppm: THF
- 3.35 ppm: AGE
- 3.12 ppm: AGE
- 2.61 ppm: $\text{P}_4\text{-t-Bu}$
- 2.51 ppm: AGE
- 1.80 ppm: THF

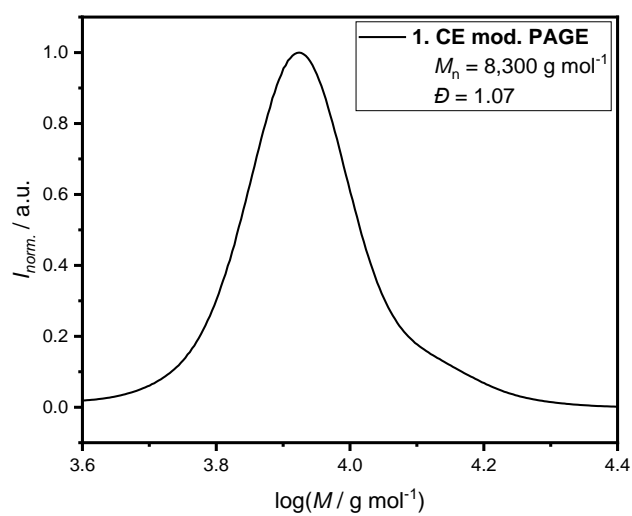


Figure 87: Size exclusion chromatogram of the first CE of modified PAGE with AGE at ambient temperature.

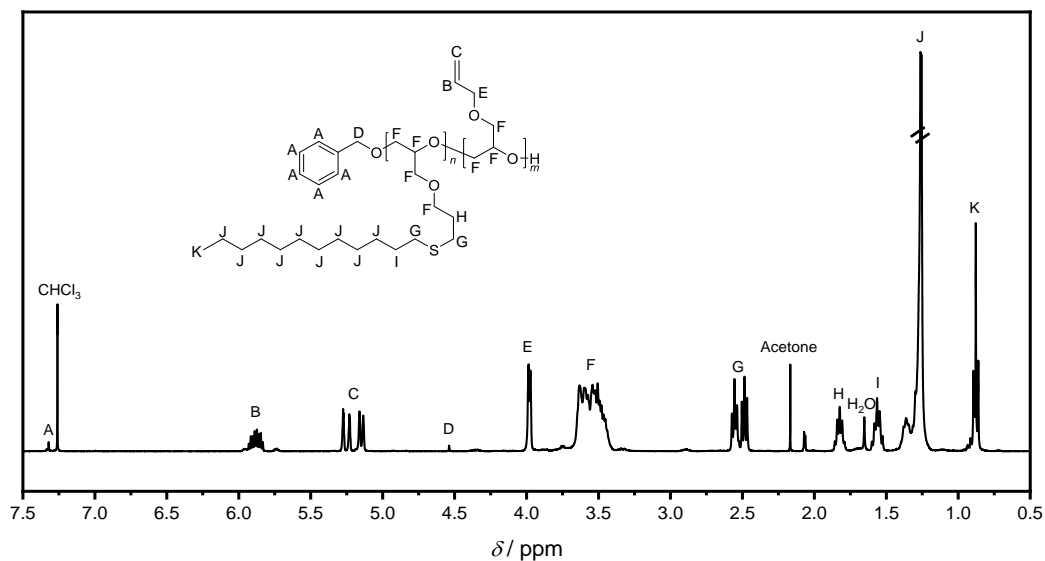


Figure 88: ^1H NMR spectrum of the CE reaction of modified PAGE with AGE at 50 °C. Solvent: CDCl_3

^1H NMR (400 MHz, CDCl_3) δ = 7.33 – 7.28 (m, A), 6.00 – 5.80 (m, 25H, B), 5.31 – 5.08 (m, 49H, C), 4.54 (s, D), 4.05 – 3.86 (m, 50H, E), 3.84 – 3.28 (m, 280H, F), 2.58 – 2.40 (m, 77H, G), 1.89 – 1.76 (m, 39H, H), 1.60 – 1.50 (m, 47H, I), 1.44 – 1.16 (m, 385H, J), 0.96 – 0.76 (m, 69H, K).*

*Due to the low intensity of signals A and D, signal K is used as reference for proton determination.

Impurities:

- 2.16 ppm: Acetone
- 1.65 ppm: H_2O

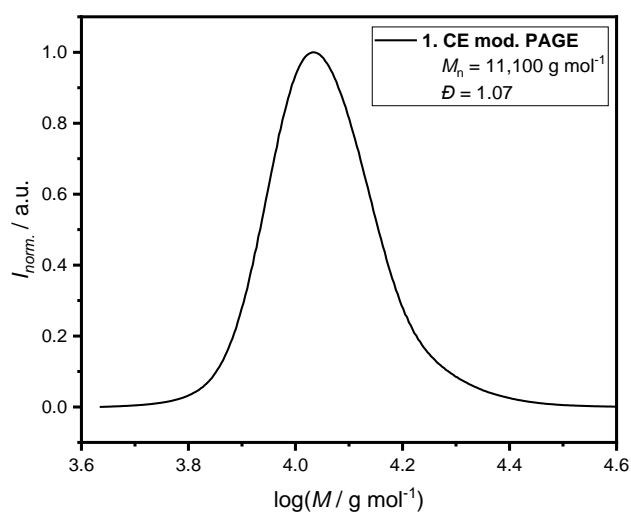


Figure 89: Size exclusion chromatogram of once chain extended modified PAGE at 50 °C.

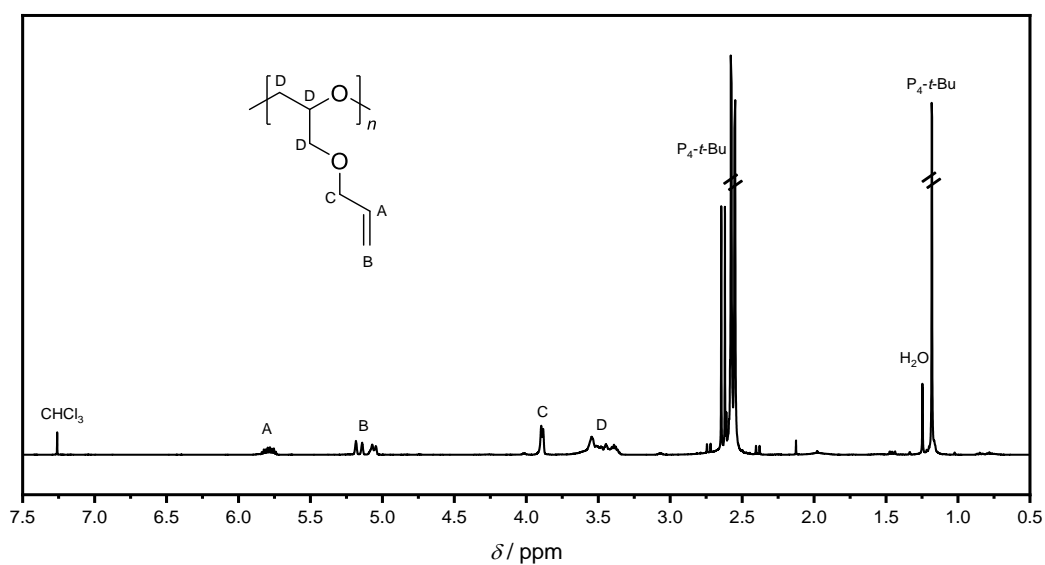


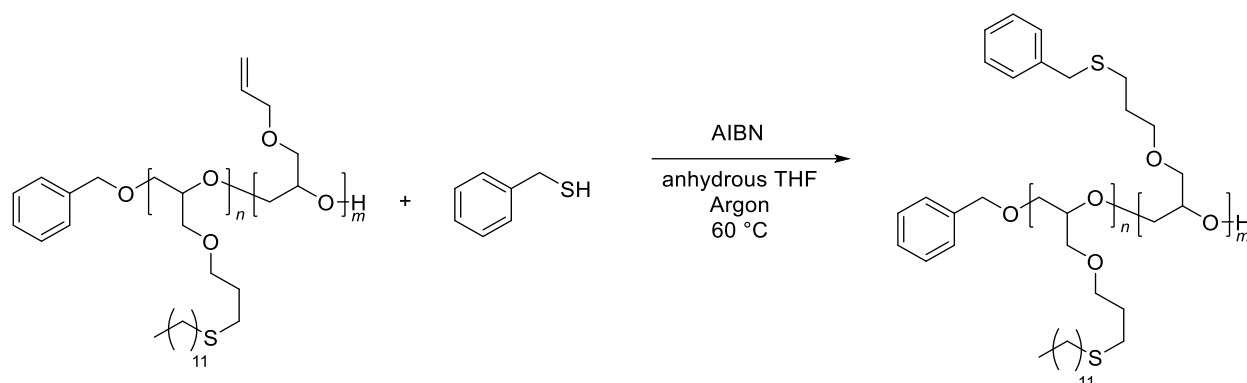
Figure 90: ^1H NMR spectrum of the residue in MeOH after the first CE reaction of modified PAGE with AGE at 50 °C. The spectrum matches the one of PAGE. Solvent: CDCl_3 .

^1H NMR (400 MHz, CDCl_3) δ = 5.92 – 5.73 (m, 1H, A), 5.28 – 5.00 (m, 2H, B), 3.97 – 3.80 (m, 2H, C), 3.71 – 3.32 (m, 5H, D).

Impurities:

- 2.60 ppm: $\text{P}_4\text{-t-Bu}$
- 1.25 ppm: H_2O
- 1.18 ppm: $\text{P}_4\text{-t-Bu}$

6.3.4.4. Post-Polymerization Modification of Once Chain Extended PAGE via Thiol-ene reaction using Benzyl Mercaptan



Once chain extended PAGE (118 mg, approx. 321 μ mol of the repeating units, 1.00 eq.) was given into a flask with anhydrous THF (2.00 mL), followed by benzyl mercaptan (150 μ L, 159 mg, 1.28 mmol, 4.00 eq.) and AIBN (26.4 mg, 161 μ mol, 0.50 eq.). Afterwards, the reaction mixture was purged for 10 minutes with argon and then put into a preheated oil bath (60 °C). The next day, the solvent was removed with compressed air, the reaction mixture was precipitated in cold MeOH and washed three times. The solvent was removed under reduced pressure at 40 °C, leading to a slightly yellow oil (102 mg; 65 %).

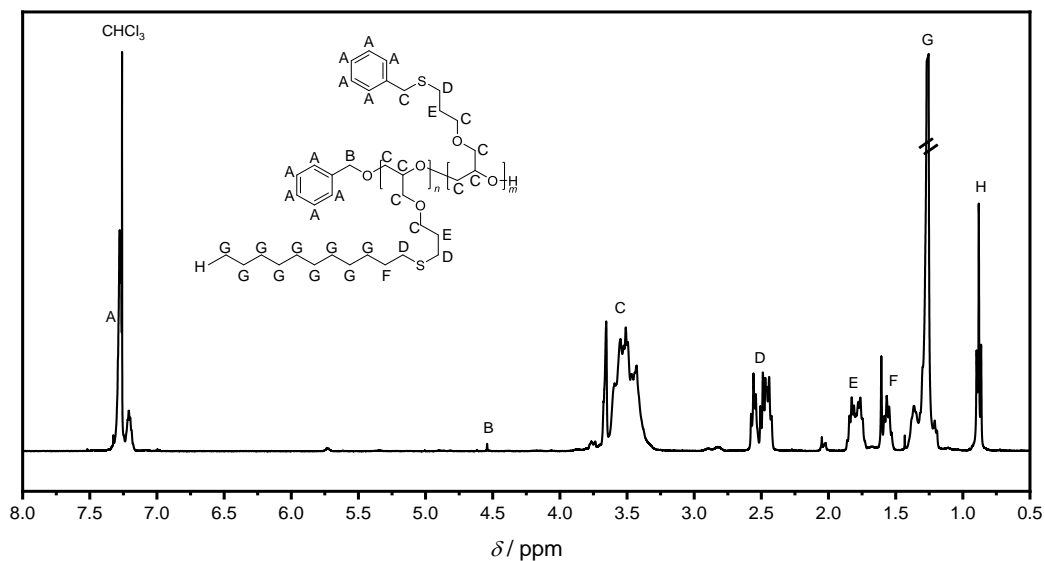


Figure 91: ^1H NMR spectrum of once chain extended PAGE after the thiol-ene reaction with benzyl mercaptan. Solvent: CDCl_3 .

^1H NMR (400 MHz, CDCl_3) δ = 7.33 – 7.16 (m, 146H, A), 4.55 (s, B), 3.88 – 3.22 (m, 396H, C), 2.60 – 2.37 (m, 121H, D), 1.89 – 1.70 (m, 81H, E), 1.64 – 1.51 (m, 56H, F), 1.43 – 1.17 (m, 401H, G), 0.96 – 0.80 (m, 69H, H).*

*Due to the low intensity of signal B, signal H is used as reference for proton determination.

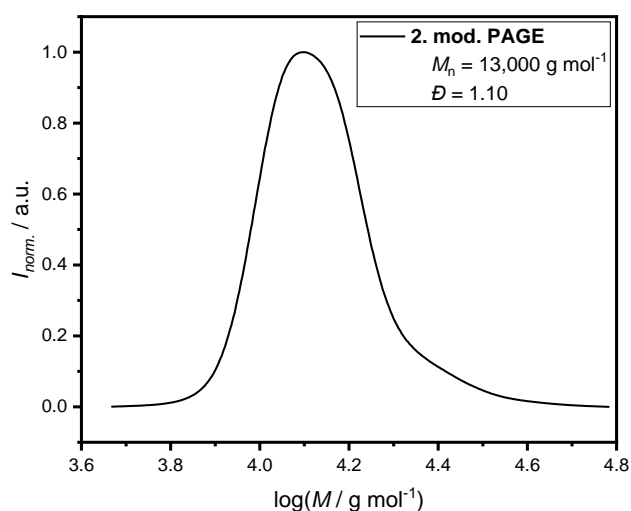
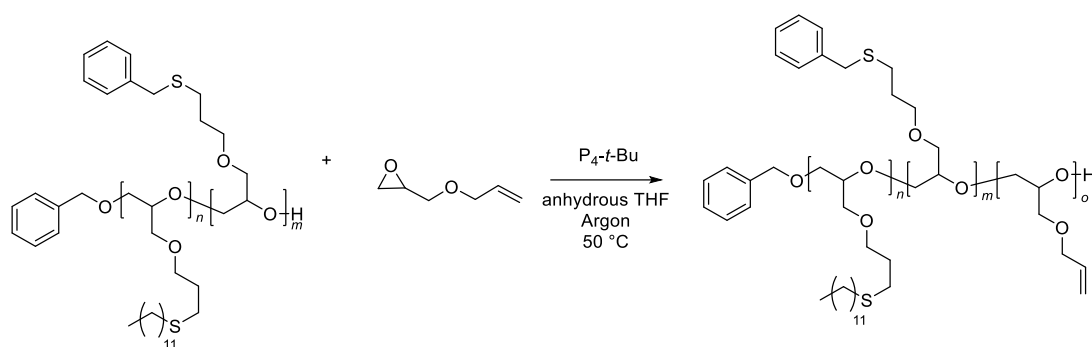


Figure 92: Size exclusion chromatogram of once chain extended PAGE after the thiol-ene reaction with benzyl mercaptan.

6.3.4.5. Second Chain Extension of Modified PAGE with AGE and P₄-t-Bu

Twice modified PAGE (87.5 mg, 6.46 μmol , 1.00 eq.) was given into a flask with anhydrous THF (1.00 mL) and 0.8 M P₄-t-Bu solution (8.07 μL , 4.09 mg of pure P₄-t-Bu, 6.46 μmol , 1.00 eq.). The reaction mixture was purged for 10 minutes with argon before AGE (38.0 μL , 36.8 mg, 323 μmol , 50.0 eq.) was added and the flask was given into a preheated oil bath (50 °C) overnight. The next day, the polymerization was stopped by adding acetic acid (1.00 mL) to the reaction mixture. The polymer was precipitated into cold MeOH and washed three times before the solvent was removed under reduced pressure at 40 °C, leading to a yellow oil (19.5 mg; 22 %).

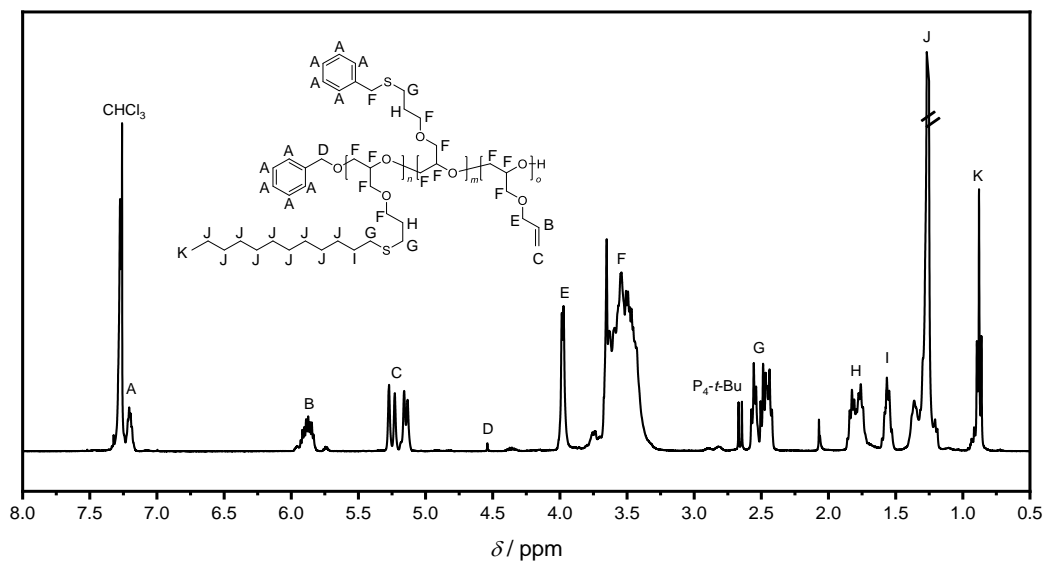


Figure 93: ^1H NMR spectrum of twice chain extended PAGE with AGE. Solvent: CDCl_3 .

^1H NMR (400 MHz, CDCl_3) δ = 7.36 – 7.15 (m, 129H, A), 5.98 – 5.78 (m, 34H, B), 5.29 – 5.09 (m, 65H, C), 4.54 (s, D), 4.03 – 3.88 (m, 69H, E), 3.82 – 3.21 (m, 561H, F), 2.59 – 2.36 (m, 116H, G), 1.88 – 1.63 (m, 86H, H), 1.62 – 1.47 (m, 48H, I), 1.42 – 1.14 (m, 384H, J), 0.98 – 0.77 (m, 69H, K).*

*Due to the low intensity of signal D, signal K is used as reference for proton determination.

Impurities:

- 2.65 ppm: P_4 -*t*-Bu

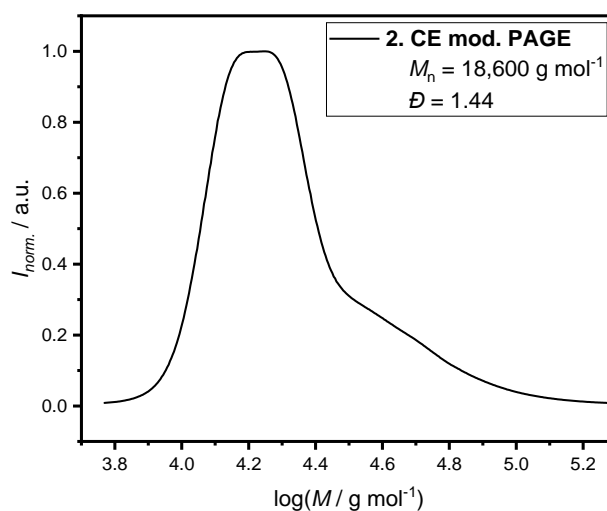
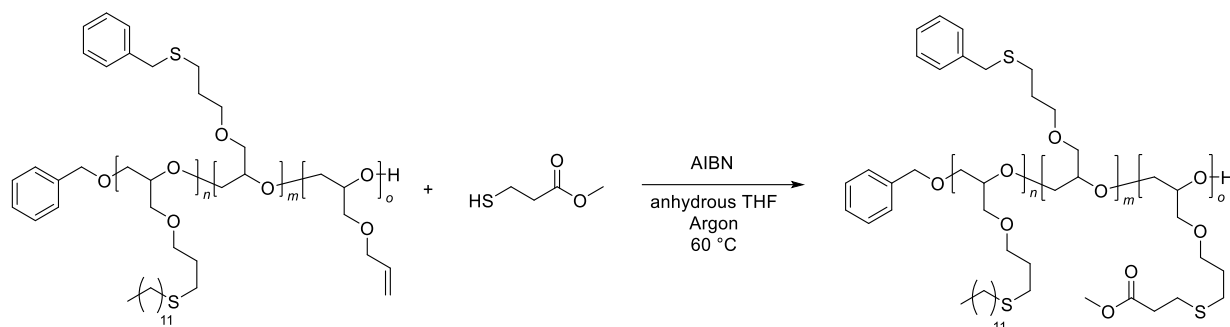


Figure 94: Size exclusion chromatogram of twice chain extended PAGE with AGE.

6.3.4.6. Post-Polymerization Modification of Twice Chain Extended PAGE via Thiol-ene Reaction using Methyl-3-mercaptopropionate



Twice chain extended PAGE (19.5 mg, approx. 37.8 μ mol of the repeating units, 1.00 eq.) was given into a flask with anhydrous THF (1.00 mL) followed by methyl-3-mercaptopropionate (20.9 μ L, 22.7 mg, 189 μ mol, 5.00 eq.) and AIBN (3.10 mg, 18.9 μ mol, 0.50 eq.). Afterwards, the reaction mixture was purged for 10 minutes with argon and then put into a preheated oil bath (60 °C). The next day, the reaction was stopped by cooling and exposure to oxygen. Afterwards, the solvent was removed under reduced pressure at 40 °C leading to a yellow oil.

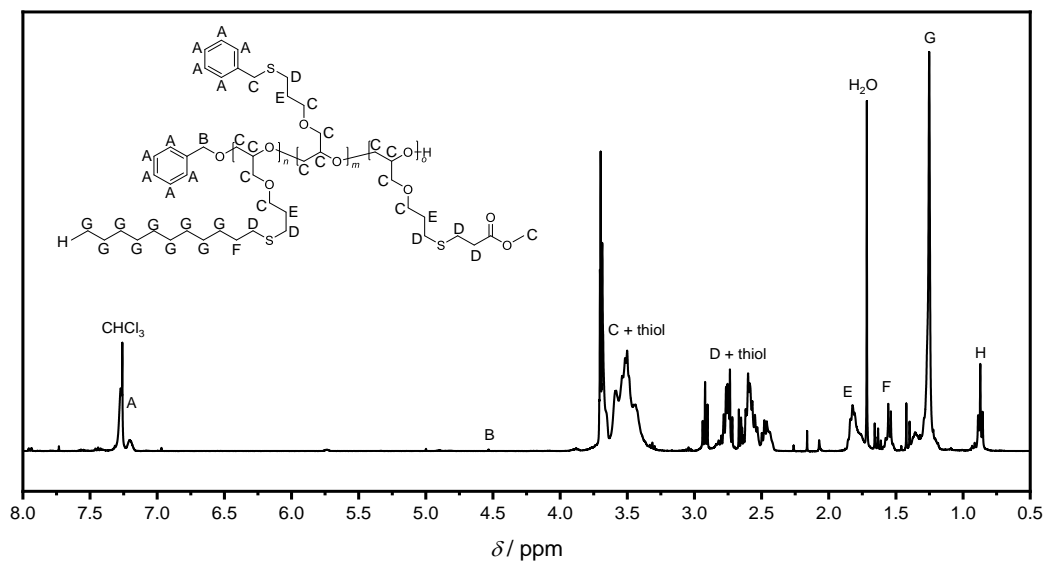


Figure 95: Crude ^1H NMR spectrum of twice chain extended PAGE after the thiol-ene reaction with methyl-3-mercaptopropionate. Solvent: CDCl_3 .

^1H NMR (400 MHz, CDCl_3) δ = 7.35 – 7.15 (m, 109H, A), 4.54 (s, B), 3.80 – 3.27 (m, 813H, C), 2.99 – 2.37 (m, 456H, D), 1.88 – 1.72 (m, 126H, E), 1.59 – 1.50 (m, 49H, F), 1.41 – 1.15 (m, 407H, G), 0.94 – 0.79 (m, 69H, H).*

*Due to the low intensity of signal B, signal H is used as reference for proton determination.

Impurities:

- 3.53 ppm: thiol
- 2.72 ppm: thiol
- 1.71 ppm: H_2O

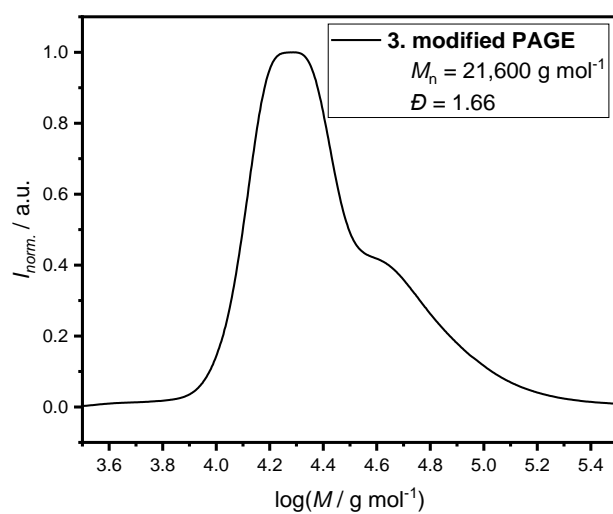
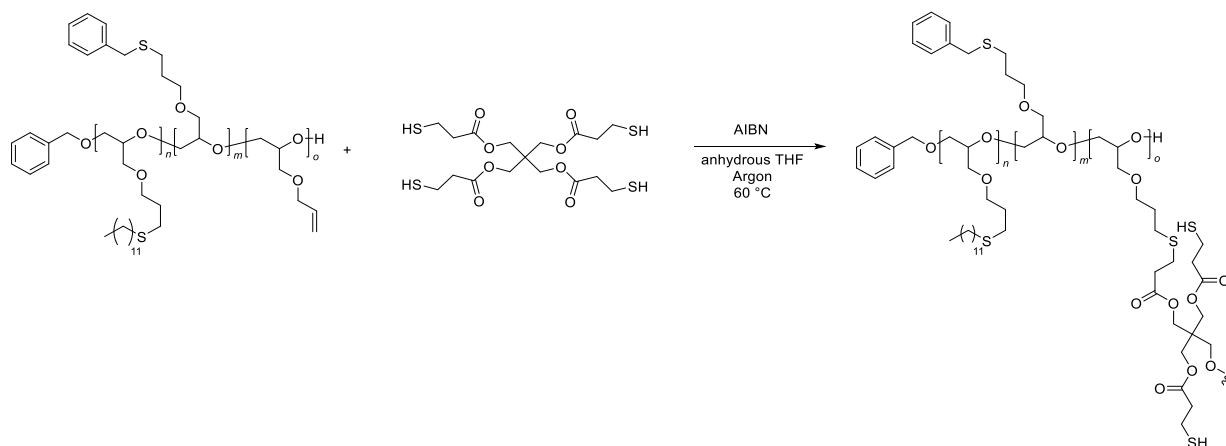


Figure 96: Crude size exclusion chromatogram of twice chain extended PAGE after the thiol-ene reaction with methyl-3-mercaptopropionate.

6.3.4.7. Post-Polymerization Modification of Twice Chain Extended PAGE via Thiol-ene Reaction using Pentaerythritol tetrakis(3-mercaptopropionate)



Twice chain extended PAGE (134 mg, approx. 333 μmol of the repeating units, 1.00 eq.) was given into a flask with anhydrous THF (1.30 mL), followed by pentaerythritol tetrakis(3-mercaptopropionate) (63.6 μL , 81.4 mg, 167 μmol , 0.50 eq.) and AIBN (27.4 mg, 167 μmol , 0.50 eq.). Afterwards, the reaction mixture was purged for 10 minutes with argon and then put into a preheated oil bath (60 °C). The next day, the reaction was stopped by cooling and exposure to oxygen. Afterwards, the solvent was removed under reduced pressure at 40 °C. The product was hardly soluble in common organic solvents (e.g., THF).

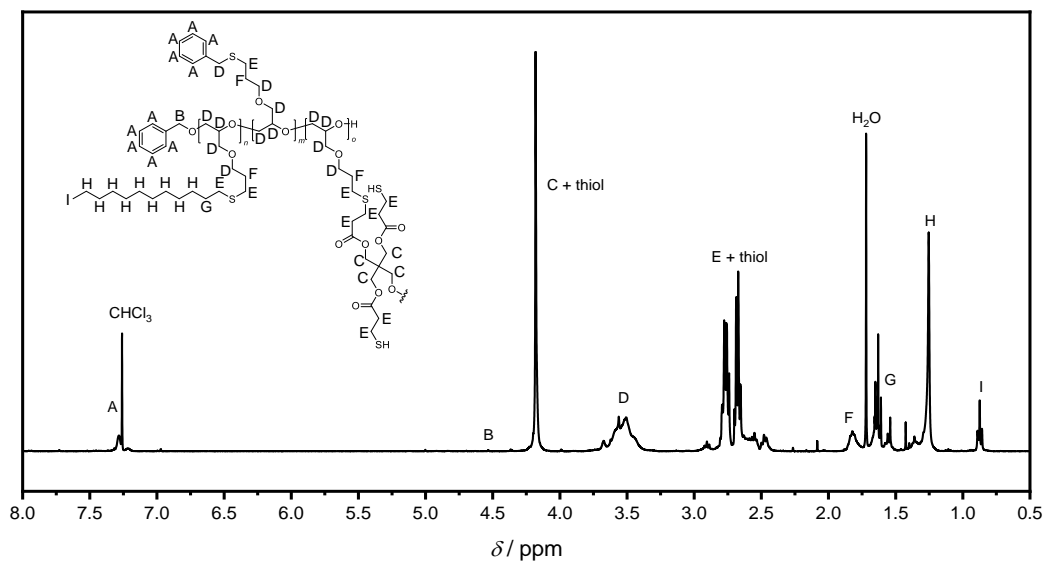


Figure 97: Crude ^1H NMR spectrum of twice chain extended PAGE after the thiol-ene reaction with pentaerythritol tetrakis(3-mercaptopropionate). Solvent: CDCl_3 .

^1H NMR (400 MHz, CDCl_3) δ = 7.36 – 7.17 (m, A), 4.54 (s, B), 4.17 (s, 894H, C), 3.74 – 3.35 (m, 945H, D), 2.87 – 2.38 (m, 2100H, E), 1.87 – 1.72 (m, 236H, F), 1.59 – 1.48 (m, 143H, G), 1.40 – 1.18 (m, 956H, H), 0.96 – 0.80 (m, 150H, I).*

*Due to the low intensity of signal B, signal I is used as reference for proton determination.

Impurities:

- 4.17 ppm: thiol
- 2.68 ppm: thiol
- 1.72 ppm: H_2O

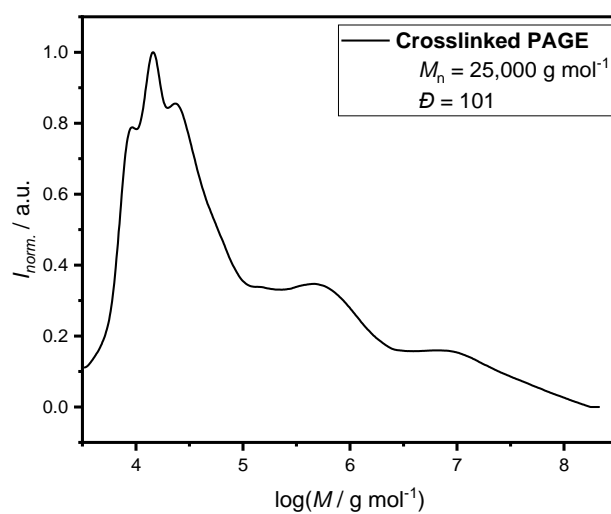
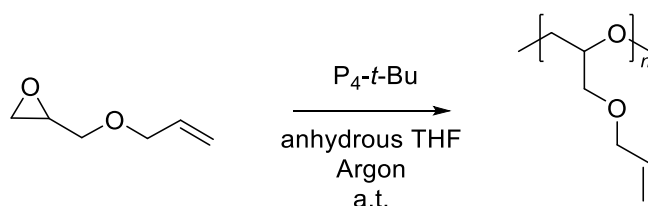


Figure 98: Crude size exclusion chromatogram of twice chain extended PAGE after the thiol-ene reaction with pentaerythritol tetrakis(3-mercaptopropionate).

6.3.4.8. Anionic Ring-Opening Polymerization of AGE using P_4 -*t*-Bu without Initiator



0.566 mL allyl glycidyl ether (0.549 g, 4.81 mmol, 50 eq.) was given into a flask with 1.85 mL THF. After 10 minutes of argon purging 0.120 mL of a 0.8 M P_4 -*t*-Bu solution (equals 60.9 mg P_4 -*t*-Bu, 9.61716E-05 mol, 1 eq.) was added. After 4 hours the polymerization was stopped by adding acetic acid. To remove the catalyst, the reaction mixture was put through a short alox column. Afterwards, the solvent was removed under reduced pressure leading to a yellow oil.

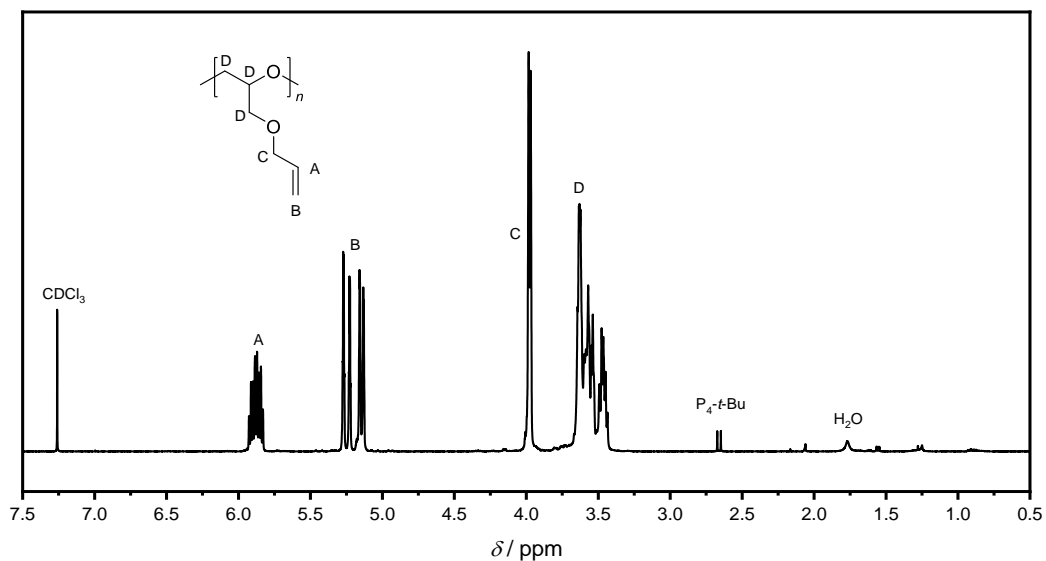


Figure 99: ^1H NMR spectrum of PAGE synthesized without additional initiator. Solvent: CDCl_3 .

^1H NMR (400 MHz, CDCl_3) δ = 5.96 – 5.79 (m, 1H, A), 5.31 – 5.07 (m, 2H, B), 4.03 – 3.88 (m, 2H, C), 3.82 – 3.36 (m, 5H, D).

Impurities:

- 2.65 ppm: $\text{P}_4\text{-}t\text{-Bu}$
- 1.77 ppm: H_2O

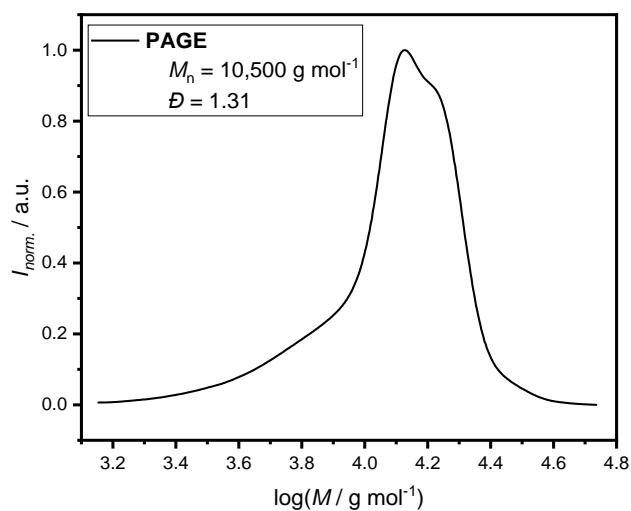
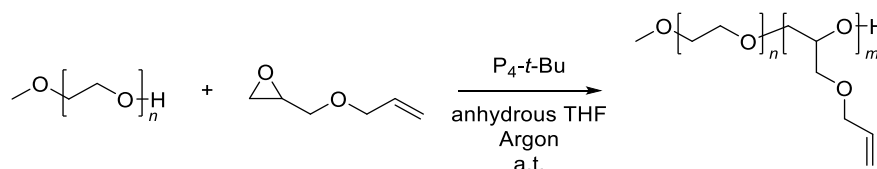


Figure 100: Size exclusion chromatogram of PAGE synthesized without additional initiator.

6.3.5. Synthetic Procedure for “AROMA – Anionic Ring-Opening Monomer Addition”

6.3.5.1. Anionic Ring-Opening Polymerization of AGE using P_4 -*t*-Bu with mPEG-1900 as Initiator



mPEG-1900 (200 mg, 105 μ mol, 1.00 eq.) and a stirring bar were given into a 5 mL round-bottom flask and the atmosphere was changed to argon. Afterwards, anhydrous THF (2.00 mL) and AGE (248 μ L, 240 mg, 2.11 mmol, 20.0 eq.) were added to the flask, followed by a 0.8 M P_4 -*t*-Bu solution (132 μ L, 105 μ mol of pure P_4 -*t*-Bu, 1.00 eq.). After 5 hours the reaction was stopped by the addition of acetic acid. The solvent was removed under reduced pressure and the residue was dissolved in THF. After precipitation in cold Et₂O (three times), the polymer was dried at 40 °C under reduced pressure overnight. A white solid was obtained.

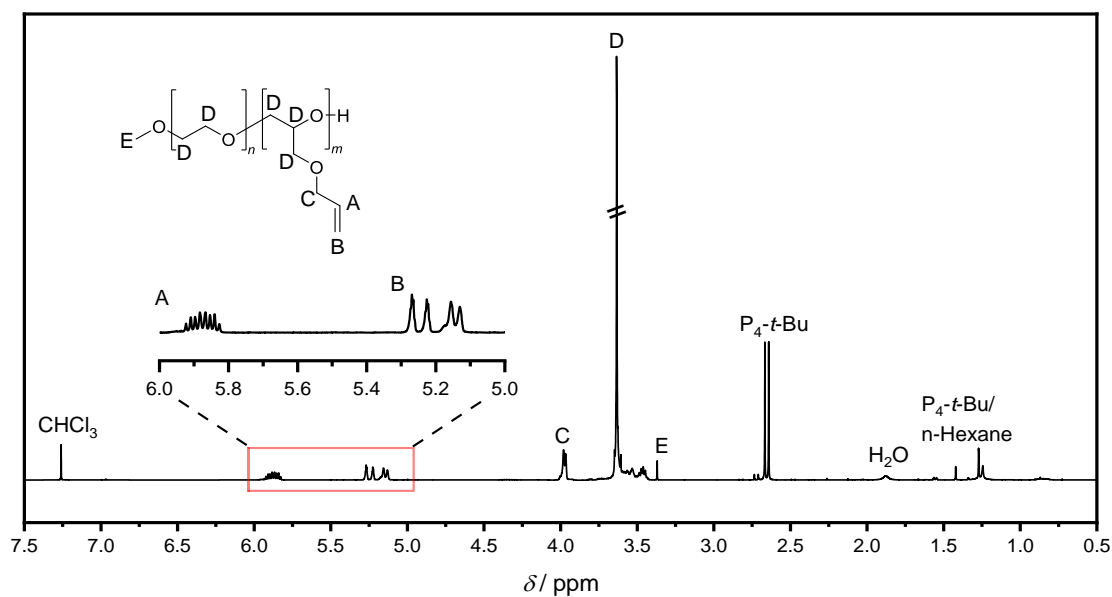


Figure 101: ^1H NMR spectrum of the AROP of AGE using mPEG-1900 as initiator. Solvent: CDCl_3 .

^1H NMR (400 MHz, CDCl_3) δ in ppm: 5.96 – 5.80 (m, 20H, A), 5.30 – 5.09 (m, 40H, B), 4.03 – 3.95 (m, 40H, C), 3.83 – 3.42 (m, 272H, D), 3.37 (s, 3H, E).

Impurities:

- 2.65 ppm: P_4 -*t*-Bu
- 1.88 ppm: H_2O
- 1.27 ppm: P_4 -*t*-Bu/*n*-Hexane

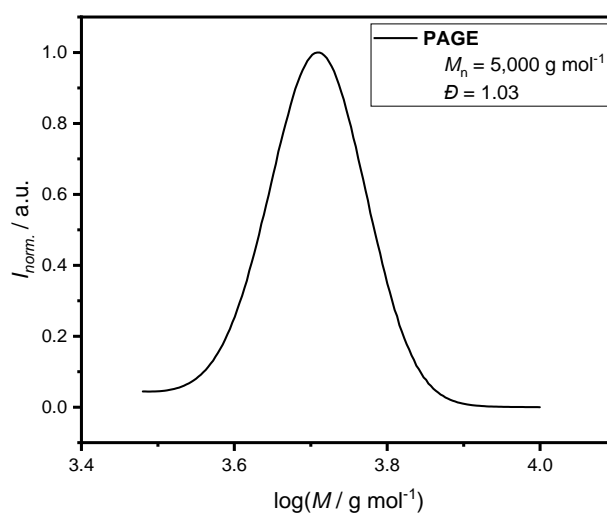
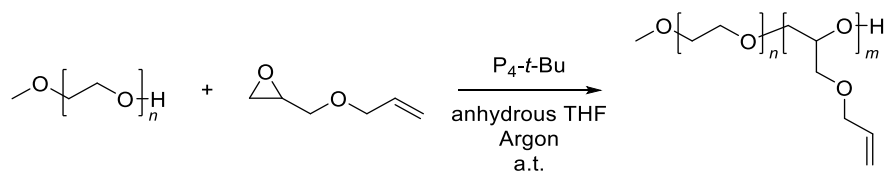


Figure 102: Size exclusion chromatogram of the AROP of AGE using mPEG-1900 as initiator.

6.3.5.2. Kinetic Studies of the Polymerization of AGE using mPEG-1900 as Initiator

General procedure for the kinetic studies of the polymerization of AGE using mPEG-1900 as initiator.



(Un)treated mPEG-1900 (200 mg, 105 μmol , 1.00 eq.) and a stirring bar were given into a 5 mL round-bottom flask and the atmosphere was changed to argon. Afterwards, anhydrous THF (2.00 mL) and AGE (248 μL , 240 mg, 2.11 mmol, 20.0 eq.) were added to the flask, followed by a 0.8 M P_4-t-Bu solution (132 μL , 105 μmol of pure P_4-t-Bu , 1.00 eq.). Over the course of time, the reaction turned from a yellow to an amber colored mixture. Samples for ^1H NMR measurements were taken directly from the flask to specific times, quenched with small amounts of acetic acid and dissolved with chloroform- d_1 . After the addition of the acid the mixture turned to a pale yellow.

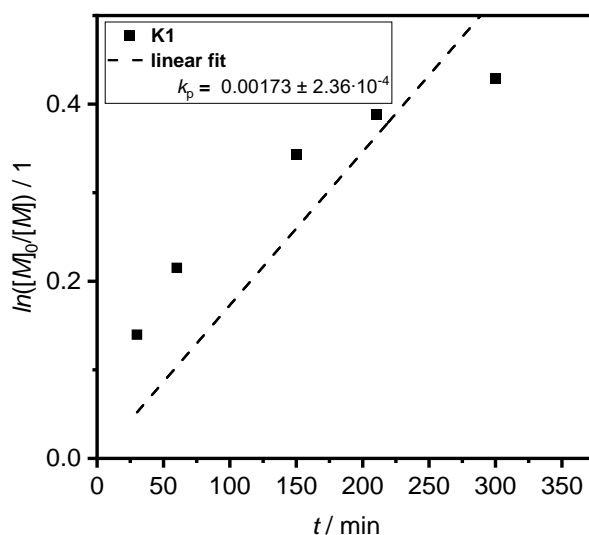


Figure 103: Kinetic study of the polymerization of AGE using untreated mPEG-1900 as initiator. A clear flattening of the curve with longer reaction time could be observed.

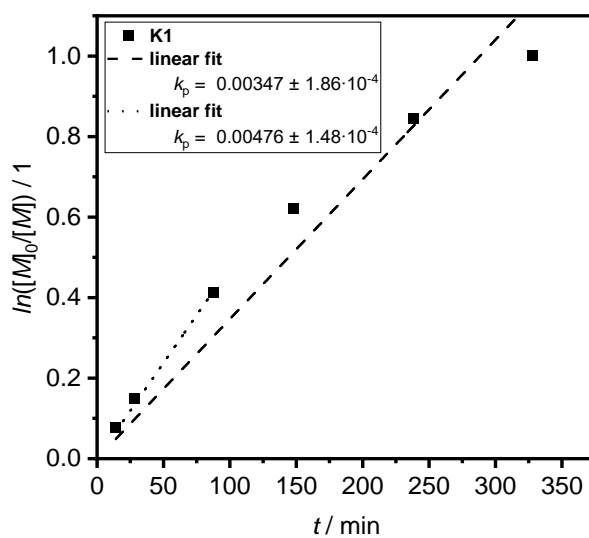
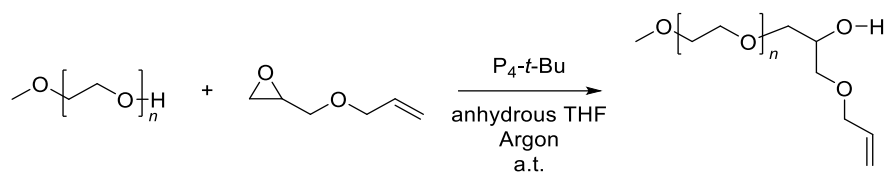


Figure 104: Kinetic study of the polymerization of AGE using pre-dried mPEG-1900 as initiator. An almost linear behavior with longer reaction time could be observed.

6.3.5.3. 1. Method: Chain Extension Reaction of mPEG-1900 with AGE using P_4 -*t*-Bu based on the Kinetic Approach



mPEG-1900 (200 mg, 105 μ mol, 1.00 eq.) and a stirring bar were given into a 5 mL round-bottom flask and the atmosphere was changed to argon. Afterwards, anhydrous THF (2.00 mL) and AGE (248 μ L, 240 mg, 2.11 mmol, 20.0 eq.) were added to the flask, followed by a 0.8 M P_4 -*t*-Bu solution (132 μ L, 105 μ mol of pure P_4 -*t*-Bu, 1.00 eq.). After a specific time, the reaction was stopped by addition of acetic acid. The solvent was removed under reduced pressure and the residue was dissolved in THF. After precipitation in cold Et₂O (three times), the polymer was dried at 40 °C under reduced pressure overnight. A white solid was obtained (162 mg; 77 %).

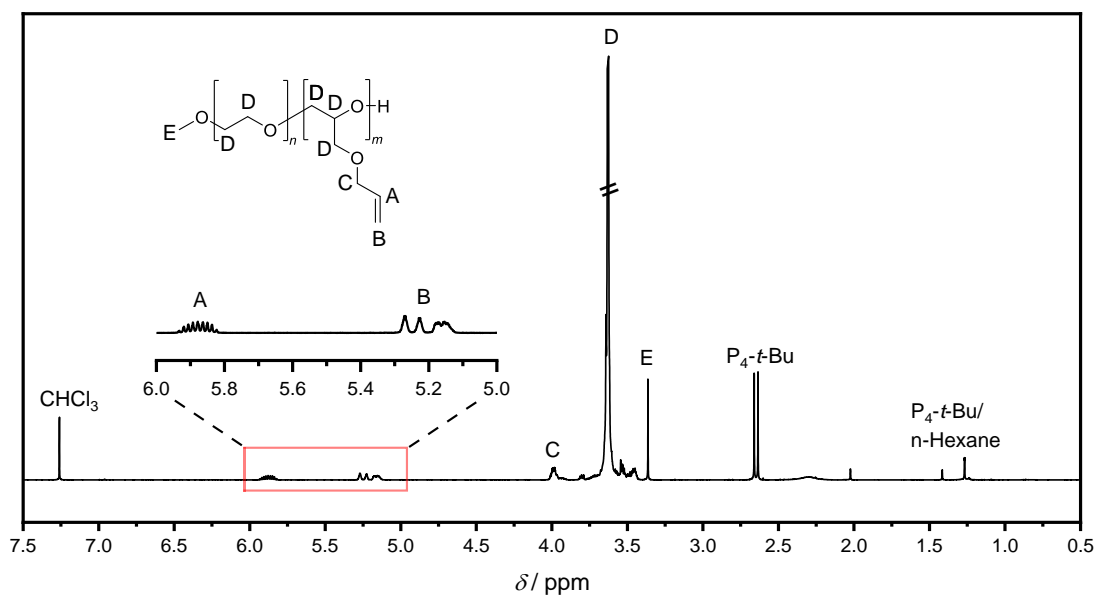


Figure 105: ^1H NMR spectrum of once chain extended mPEG-1900 with AGE based on the kinetic approach after 10 minutes and 46 seconds. The repeating unit of AGE is 2.01. Solvent: CDCl_3 .

^1H NMR (400 MHz, CDCl_3) δ in ppm: 5.96 – 5.80 (m, 2.01H, A), 5.30 – 5.09 (m, 4H, B), 4.03 – 3.95 (m, 4H, C), 3.83 – 3.42 (m, 203H, D), 3.37 (s, 3H, E).

Impurities:

- 2.65 ppm: P₄-t-Bu
- 1.27 ppm: P₄-t-Bu/n-Hexane

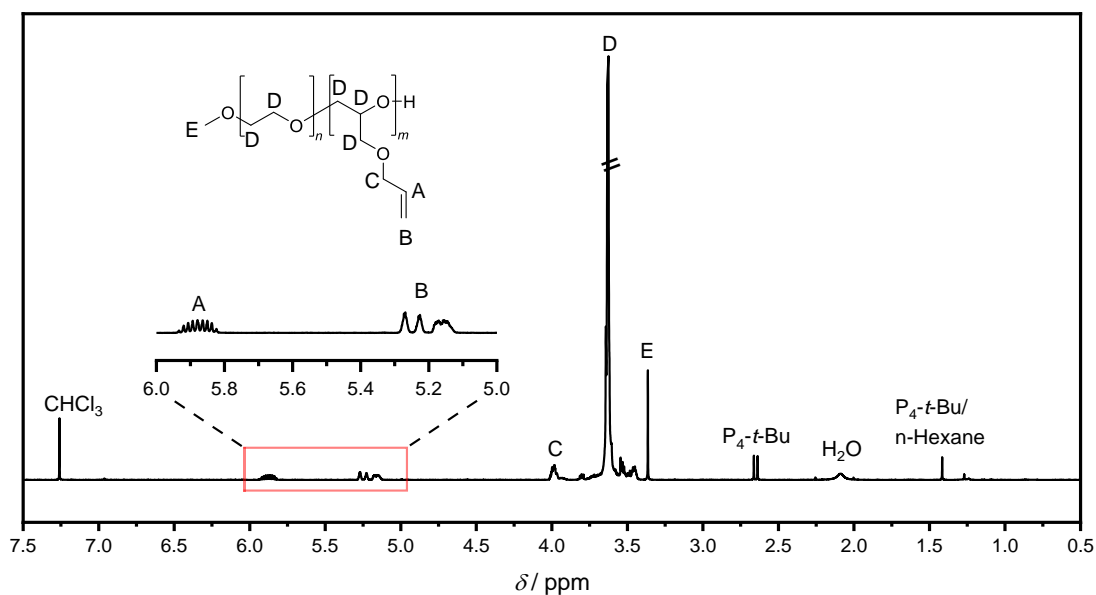


Figure 106: ^1H NMR spectrum of once chain extended mPEG-1900 with AGE based on the kinetic approach after 10 minutes and 46 seconds. The repeating unit of AGE is 2.14. Solvent: CDCl_3

^1H NMR (400 MHz, CDCl_3) δ in ppm: 5.96 – 5.80 (m, 2.14H, A), 5.30 – 5.09 (m, 4H, B), 4.03 – 3.95 (m, 4H, C), 3.83 – 3.42 (m, 203H, D), 3.37 (s, 3H, E).

Impurities:

- 2.65 ppm: $\text{P}_4\text{-}t\text{-Bu}$
- 1.27 ppm: $\text{P}_4\text{-}t\text{-Bu/n-Hexane}$
- 2.07 ppm: H_2O

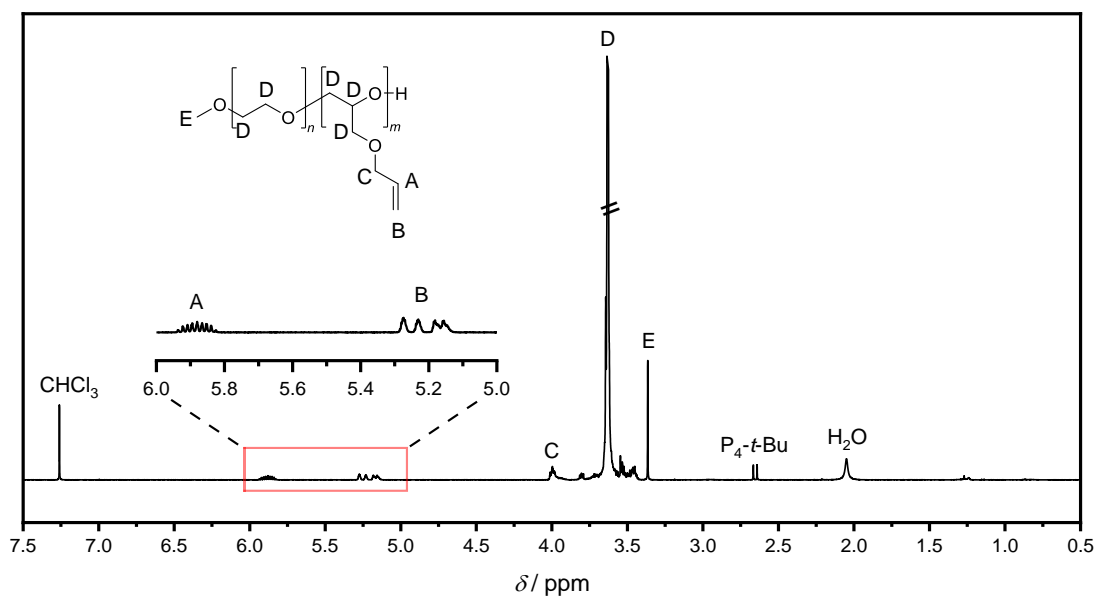


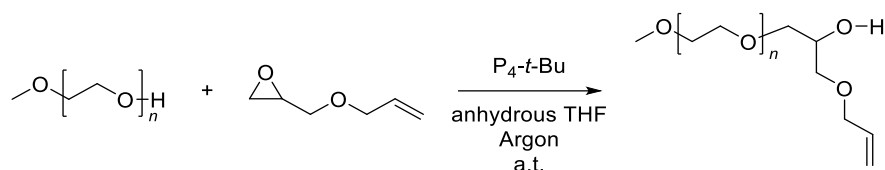
Figure 107: ^1H NMR spectrum of once chain extended mPEG-1900 with AGE based on the kinetic approach after 7 minutes and 25 seconds. The repeating unit of AGE is 1.28. Solvent: CDCl_3

^1H NMR (400 MHz, CDCl_3) δ in ppm: 5.96 – 5.80 (m, 1.28H, A), 5.30 – 5.09 (m, 2H, B), 4.03 – 3.95 (m, 2H, C), 3.83 – 3.42 (m, 193H, D), 3.37 (s, 3H, E).

Impurities:

- 2.65 ppm: $\text{P}_4\text{-}t\text{-Bu}$
- 2.05 ppm: H_2O

6.3.5.4. 2. Method: Chain Extension Reaction of mPEG-1900 AGE using P₄-t-Bu based on Small Monomer Excess Approach (1. AROMA)



mPEG-1900 (200 mg, 105 μ mol, 1.00 eq.) and a stirring bar were given into a 5 mL round-bottom flask and the atmosphere was changed to argon. Afterwards, anhydrous THF (2.00 mL) and AGE (15.4 μ L, 15.0 mg, 132 μ mol, 1.25 eq.) were added to the flask, followed by a 0.8 M P₄-t-Bu solution (132 μ L, 105 μ mol of pure P₄-t-Bu, 1.00 eq.). After 5 hours the reaction was stopped by the addition of acetic acid. The solvent was removed under reduced pressure and the residue was dissolved in THF. After precipitation in cold Et₂O (three times), the polymer was dried at 40 °C under reduced pressure overnight. A white solid was obtained (188 mg; 89%).

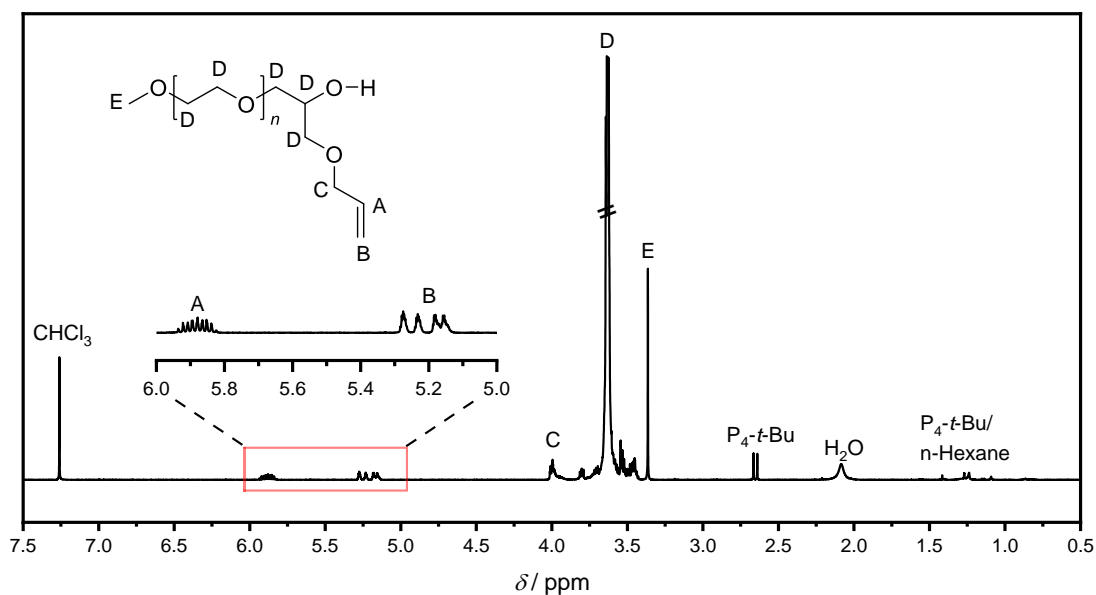


Figure 108: ^1H NMR spectrum of mPEG-1900 after the first CE with AGE. The new signals between 6.00 – 5.00 ppm confirm a successful CE. Solvent: CDCl_3 .

^1H NMR (400 MHz, CDCl_3) δ in ppm: 5.98 – 5.81 (m, 1H, A), 5.32 – 5.10 (m, 2H, B), 4.09 – 3.90 (m, 2H, C), 3.88 – 3.42 (m, 178H, D), 3.36 (s, 3H, E).

Impurities:

- 2.08 ppm: H_2O
- 1.26 ppm: $\text{P}_4\text{-}t\text{-Bu}$, $n\text{-Hexane}$

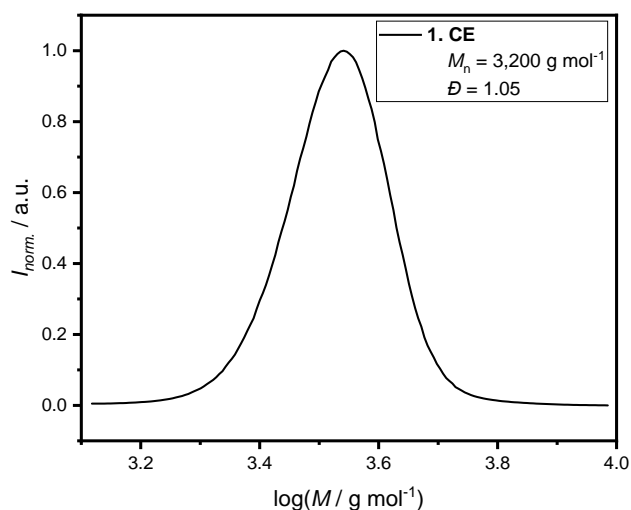


Figure 109: Size exclusion chromatogram after the first CE of mPEG-1900 with AGE.

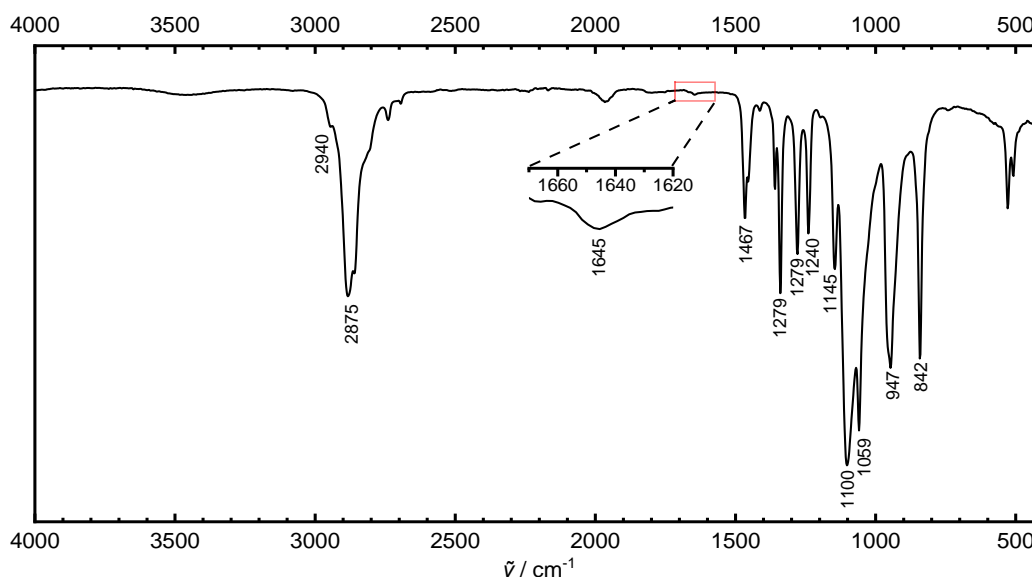


Figure 110: ATR FT-IR spectrum of once chain extended mPEG-1900 with AGE. After the CE a new signal at $1,645\text{ cm}^{-1}$ appears, which could be assigned to the C=C double bond of the AGE.

IR Assignment (based on literature):^{179–181}

- C–O, C–C stretching, CH₂ rocking at 842 cm^{-1}
- CH₂ rocking, CH₂ twisting at 947 cm^{-1}
- C–O, C–C stretching, CH₂ rocking at $1,059\text{ cm}^{-1}$
- C–O, C–C stretching at $1,100\text{ cm}^{-1}$
- C–O stretching, CH₂ rocking at $1,145\text{ cm}^{-1}$
- CH₂ twisting at $1,240$ and $1,279\text{ cm}^{-1}$
- CH₂ wagging at $1,340\text{ cm}^{-1}$
- CH₂ scissoring at $1,467\text{ cm}^{-1}$
- C=C double bond's stretching vibration at $1,645\text{ cm}^{-1}$
- Symmetric and asymmetric stretching vibration bands of the methylene group C–H bonds at $2,875$ and $2,940\text{ cm}^{-1}$

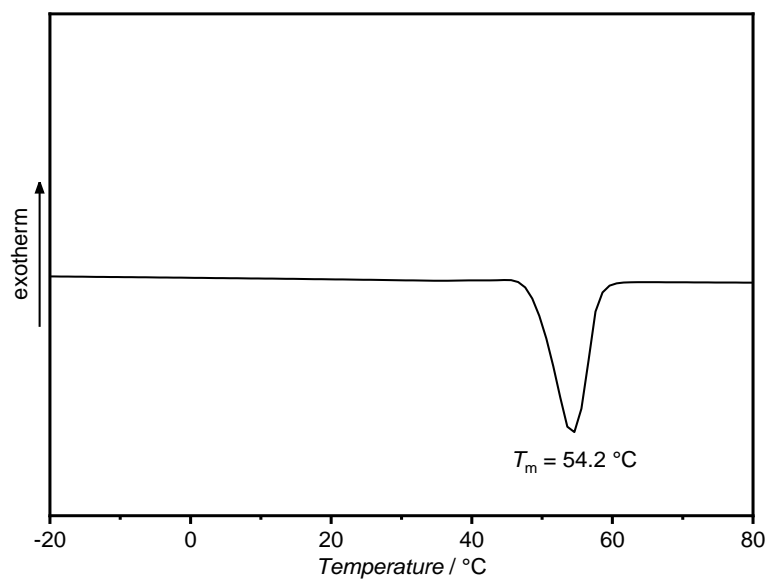
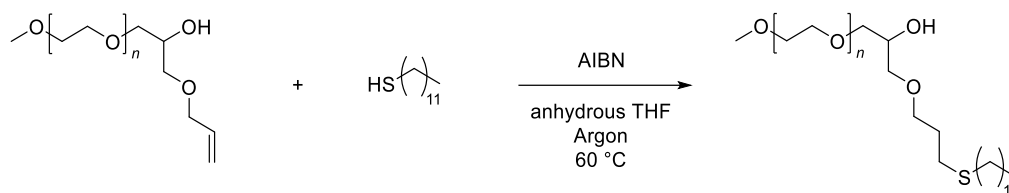


Figure 111: DSC thermogram (heating curve; 2. cycle) of AGE chain extended mPEG-1900 with a visible T_m at 54.2 °C.

6.3.5.5. Post-Polymerization Modification of Once Chain Extended mPEG-1900 via Thiol-ene Reaction using 1-Dodecanethiol



Once chain extended mPEG-1900 (150 mg, 74.5 μmol , 1.00 eq.) was given into a 5 mL round-bottom flask, followed by AIBN (6.11 mg, 37.2 μmol , 0.50 eq.) and anhydrous THF (2.00 mL). Afterwards, 1-dodecanethiol (70.9 μL , 60.3 mg, 29.8 mmol, 4.00 eq.) was added and the atmosphere was changed to argon. The flask was placed into a preheated oil bath (60 °C) and stirred for 24 hours. The next day, the system was quenched by contact to air and cooling. The solvent was removed under reduced pressure and the residue was dissolved in THF. After the precipitation in cold Et₂O (three times), the product was dried under reduced pressure at 40 °C overnight. A white solid was obtained (111 mg; 67 %).

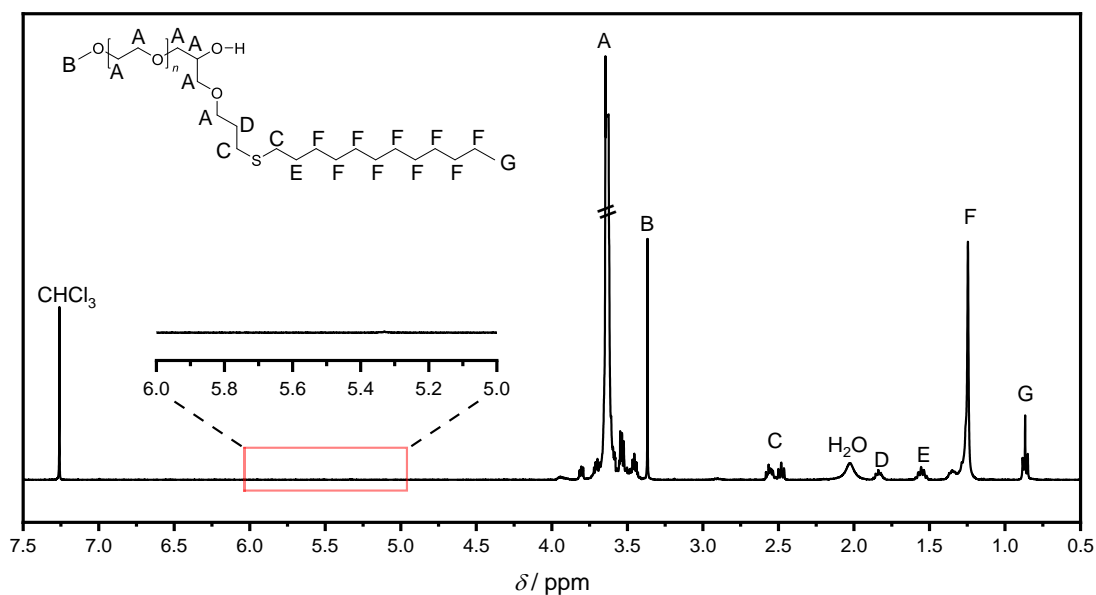


Figure 112: ^1H NMR spectrum of once chain extended mPEG-1900 after the thiol-ene reaction with 1-dodecanethiol. After the reaction, the signals of the double bond between 5.00 – 6.00 ppm disappeared and the thiol signals (e.g., around 0.8 ppm) appeared, confirming a successful modification reaction. Solvent: CDCl_3 .

^1H NMR (400 MHz, CDCl_3) δ in ppm: 3.86 – 3.41 (m, 179H, A), 3.37 (s, 3H, B), 2.64 – 2.43 (m, 4H, C), 1.91 – 1.78 (m, 2H, D), 1.63 – 1.49 (m, 2H, E), 1.44 – 1.13 (m, 18H, F), 0.86 (t, 3H, G).

Impurities:

- 2.03 ppm: H_2O

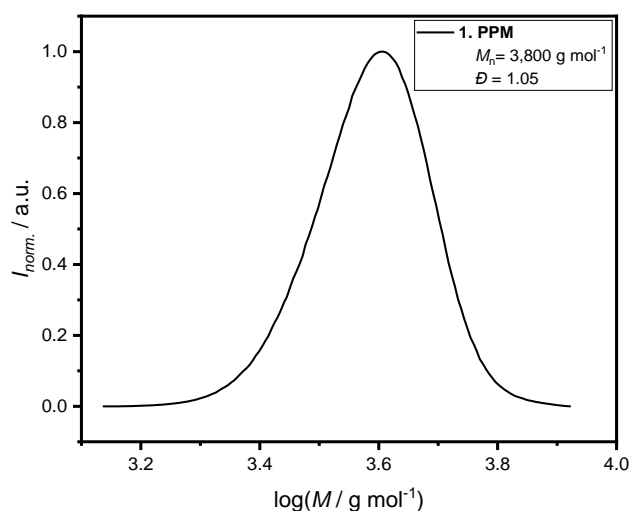


Figure 113: Size exclusion chromatogram of once chain extended mPEG-1900 after the thiol-ene reaction with 1-dodecanethiol.

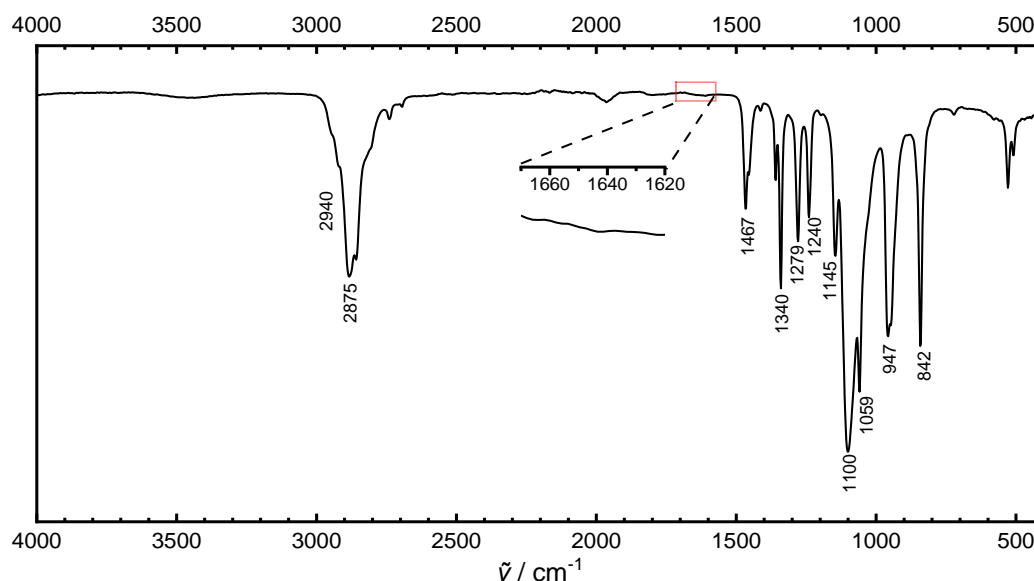


Figure 114: ATR FT-IR spectrum of once chain extended mPEG-1900 after the thiol-ene reaction with 1-dodecanethiol. After the modification the signal at $1,645\text{ cm}^{-1}$ disappeared, which confirms a successful modification.

IR Assignment (based on literature)^{180,181}

- C–O, C–C stretching, CH₂ rocking at 842 cm^{-1}
- CH₂ rocking, CH₂ twisting at 947 cm^{-1}
- C–O, C–C stretching, CH₂ rocking at $1,059\text{ cm}^{-1}$
- C–O, C–C stretching at $1,100\text{ cm}^{-1}$
- C–O stretching, CH₂ rocking at $1,145\text{ cm}^{-1}$
- CH₂ twisting at $1,240$ and $1,279\text{ cm}^{-1}$
- CH₂ wagging at $1,340\text{ cm}^{-1}$
- CH₂ scissoring at $1,467\text{ cm}^{-1}$
- Symmetric and asymmetric stretching vibration bands of the methylene group C–H bonds at $2,875$ and $2,940\text{ cm}^{-1}$

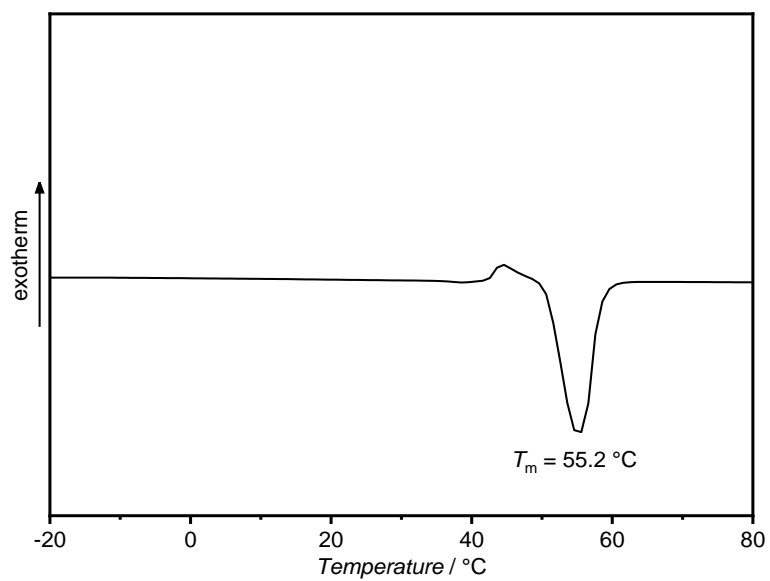
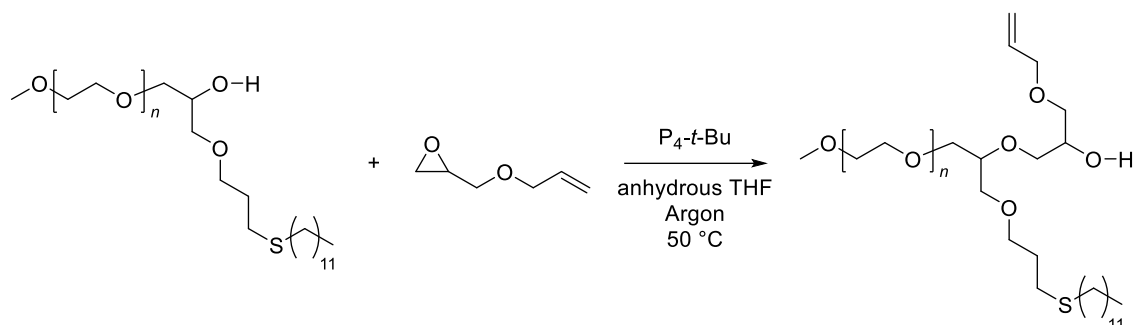


Figure 115: DSC thermogram (heating curve; 2. cycle) of once chain extended mPEG-1900 after the thiol-ene reaction with 1-dodecanethiol with a visible T_m at 55.2 °C.

6.3.5.6. Second Chain Extension Reaction of mPEG-1900 with AGE using P₄-t-Bu (2. AROMA)



Once modified mPEG-1900 (57.0 mg, 25.7 μmol , 1.00 eq.) and a stirring bar were given into a 5 mL round-bottom flask and the atmosphere was changed to argon. Afterwards, anhydrous THF (2.00 mL) and AGE (3.78 μL , 3.67 mg, 32.1 μmol , 1.25 eq.) were added to the flask, followed by a 0.8 M P₄-t-Bu solution (32.2 μL , 25.8 μmol of pure P₄-t-Bu, 1.00 eq.). The flask was placed in a preheated oil bath (50 °C). After 5.5 hours the reaction was stopped by the addition of acetic acid. The solvent was removed under reduced pressure and the residue was dissolved in THF. After precipitation in cold Et₂O (three times), the polymer was dried at 40 °C under reduced pressure overnight. A white solid was obtained (46.1 mg; 77 %).

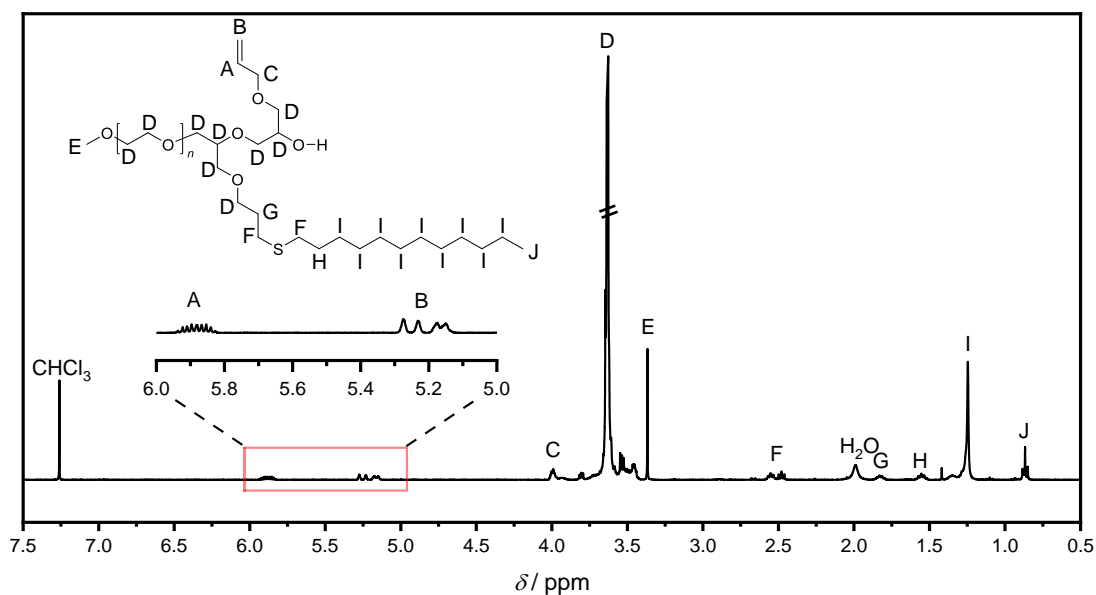


Figure 116: ^1H NMR spectrum of modified mPEG-1900 after the second CE with AGE. The new signals between 6.00 – 5.00 ppm confirm a successful CE. Solvent: CDCl_3 .

^1H NMR (400 MHz, CDCl_3) δ in ppm: 5.96 – 5.80 (m, 1H, A), 5.30 – 5.11 (m, 2H, B), 4.06 – 3.86 (m, 2H, C), 3.85 – 3.41 (m, 184H, D), 3.37 (s, 3H, E), 2.62 – 2.40 (m, 4H, F), 1.89 – 1.77 (m, 2H, G), 1.60 – 1.51 (m, 2H, H), 1.40 – 1.16 (m, 18H, I), 0.87 (t, 3H, J).

Impurities:

- 1.99 ppm: H_2O

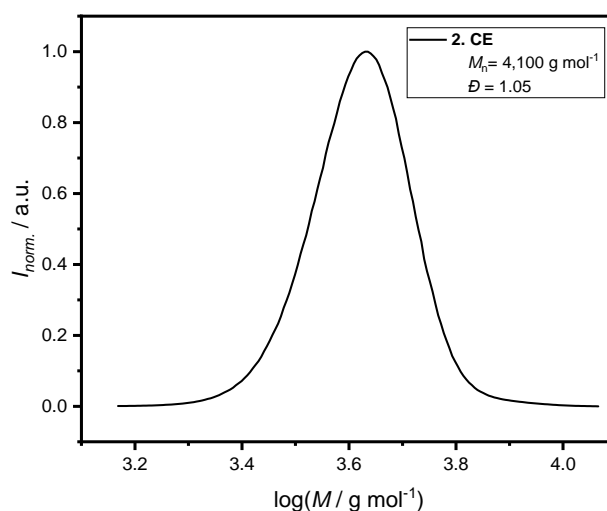


Figure 117: Size exclusion chromatogram after the second CE of mPEG-1900 with AGE.

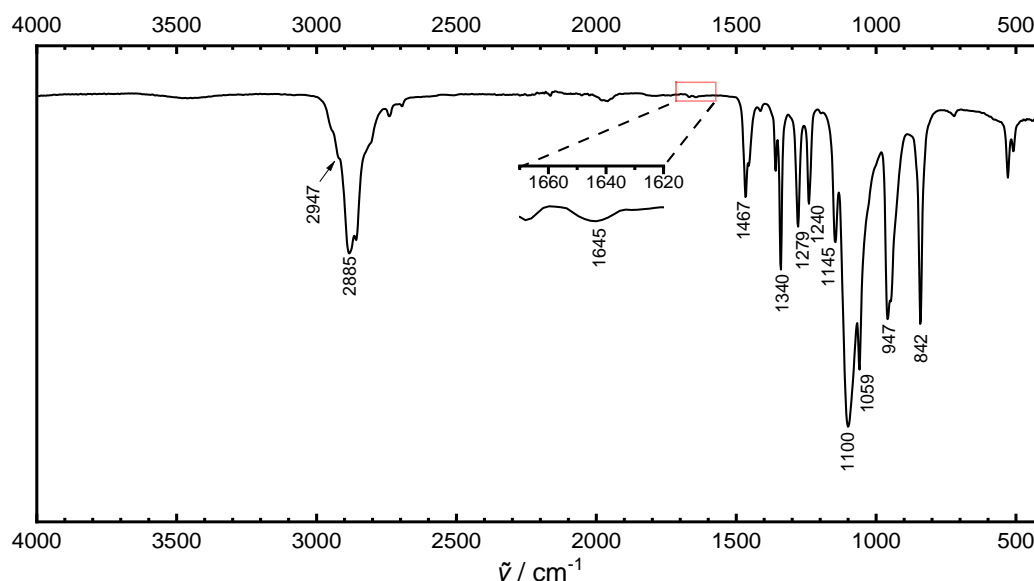


Figure 118: ATR FT-IR spectrum of twice chain extended mPEG-1900 with AGE. After the CE a new signal at $1,645\text{ cm}^{-1}$ appears, which could be assigned to the C=C double bond of the AGE.

IR Assignment (based on literature)^{179–181}

- C–O, C–C stretching, CH₂ rocking at 842 cm^{-1}
- CH₂ rocking, CH₂ twisting at 947 cm^{-1}
- C–O, C–C stretching, CH₂ rocking at $1,059\text{ cm}^{-1}$
- C–O, C–C stretching at $1,100\text{ cm}^{-1}$
- C–O stretching, CH₂ rocking at $1,145\text{ cm}^{-1}$
- CH₂ twisting at $1,240$ and $1,279\text{ cm}^{-1}$
- CH₂ wagging at $1,340\text{ cm}^{-1}$
- CH₂ scissoring at $1,467\text{ cm}^{-1}$
- C=C double bond's stretching vibration at $1,645\text{ cm}^{-1}$
- Symmetric and asymmetric stretching vibration bands of the methylene group C–H bonds at $2,885$ and $2,947\text{ cm}^{-1}$

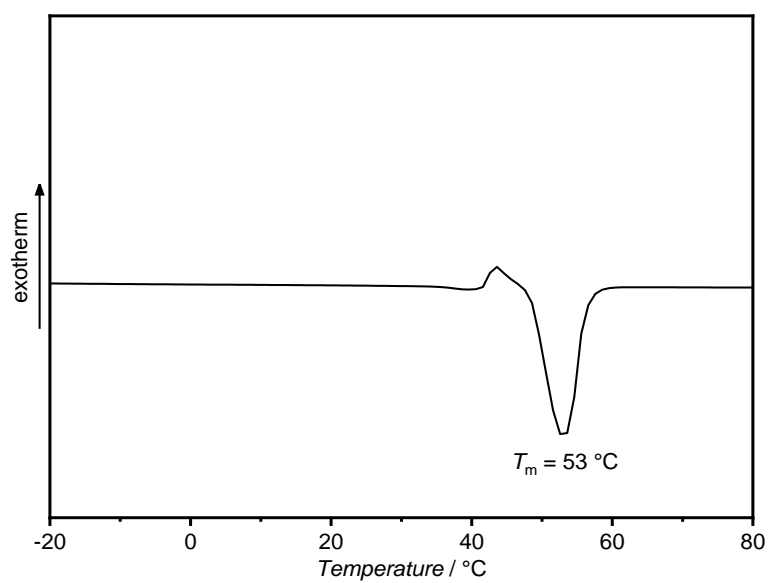
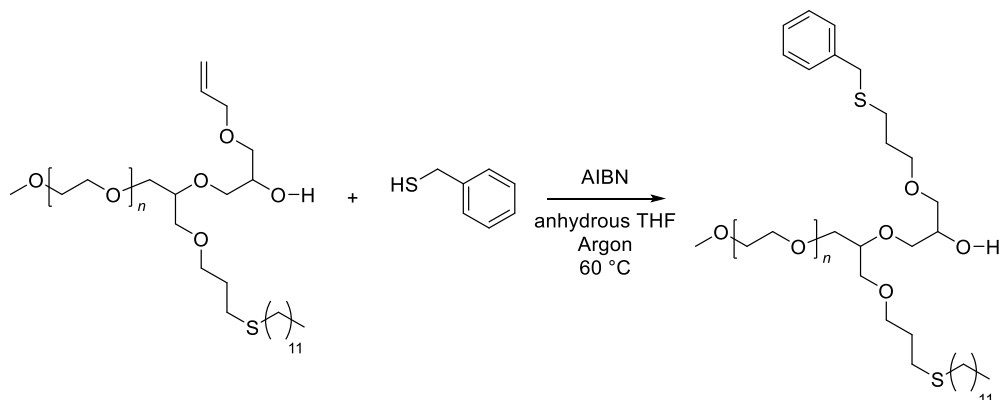


Figure 119: DSC thermogram (heating curve; 2. cycle) of twice chain extended mPEG-1900 with a visible T_m at 53 °C.

6.3.5.7. Post-Polymerization Modification of Twice Chain Extended mPEG-1900 via Thiol-ene Reaction using Benzyl Mercaptan



Twice chain extended mPEG-1900 (21.1 mg, 9.05 μmol , 1.00 eq.) was given into a round-bottom flask, followed by AIBN (743 μg , 4.53 μmol , 0.50 eq.) and anhydrous THF (250 μL). Afterwards, benzyl mercaptan (4.24 μL , 4.50 mg, 36.2 μmol , 4.00 eq.) was added and the atmosphere was changed to argon. The flask was placed into a preheated oil bath (60 °C) and stirred for 20 hours. The next day, the system was quenched by contact to air and cooling. The solvent was removed under reduced pressure and the residue dissolved in THF. After the precipitation in cold Et₂O (three times), the product was dried under reduced pressure at 40 °C overnight. A white solid was obtained.

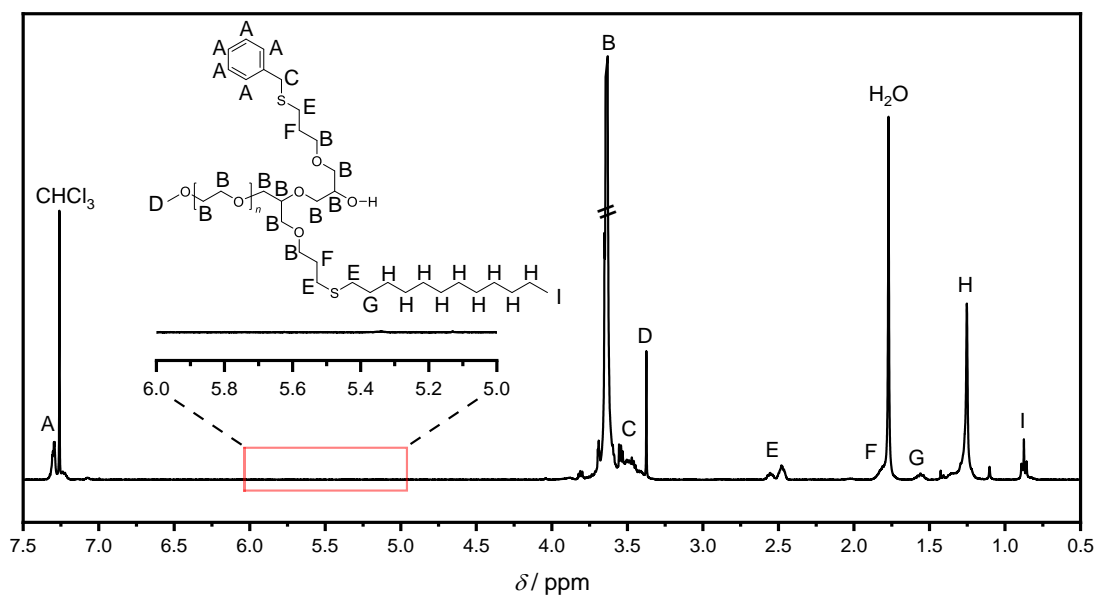


Figure 120: ^1H NMR spectrum of twice chain extended mPEG-1900 after the thiol-ene reaction with benzyl mercaptan. After the reaction the signals of the double bond between 6.00 – 5.00 ppm disappeared and the thiol signals (e.g., around 7.30 ppm) appeared, confirming a successful modification reaction. Solvent: CDCl_3 .

^1H NMR (400 MHz, CDCl_3) δ in ppm: 7.34 – 7.18 (m, 5H, A), 3.84 – 3.44 (m, 186H, B), 3.44 – 3.39 (m, 2H, C), 3.37 (s, 3H, D), 2.60 – 2.43 (m, 6H, E), 1.84 – 1.73 (m, 4H, F), 1.61 – 1.50 (m, 2H, G), 1.39 – 1.16 (m, 18H, H), 0.87 (t, 3H, I).

Impurities:

- 1.77 ppm: H_2O

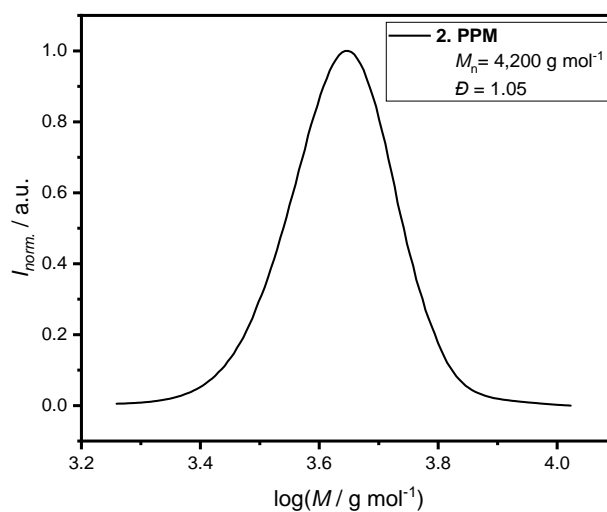
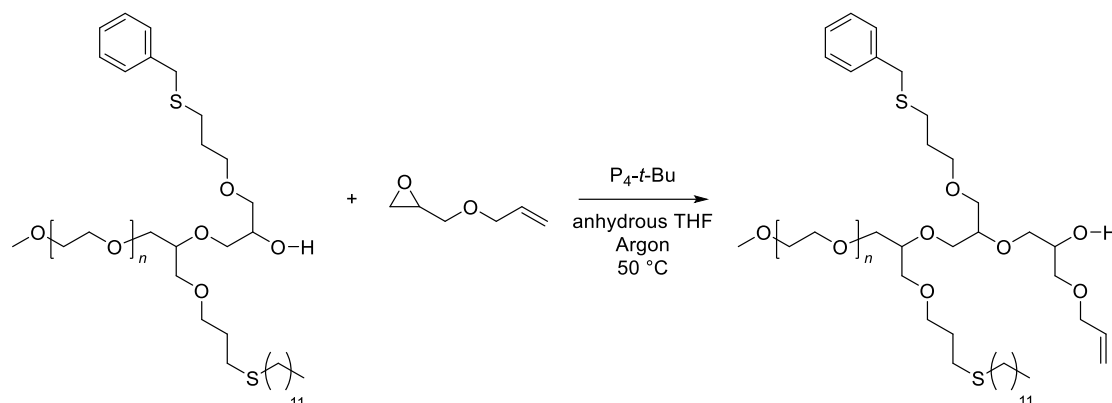


Figure 121: Size exclusion chromatogram of twice chain extended mPEG-1900 after the thiol-ene reaction with benzyl thiol.

6.3.5.8. Third Chain Extension Reaction of mPEG-1900 with AGE using P_4 -*t*-Bu (3. AROMA)



Twice modified mPEG-1900 (75.0 mg, 30.6 μ mol, 1.00 eq.) and a stirring bar were given into a round-bottom flask and the atmosphere was changed to argon. Afterwards, anhydrous THF (2.40 mL) and AGE (4.50 μ L, 4.36 mg, 38.2 μ mol, 1.25 eq.) were added to the flask, followed by a 0.8 M P_4 -*t*-Bu solution (38.2 μ L, 30.6 μ mol of pure P_4 -*t*-Bu, 1.00 eq.). The flask was placed in a preheated oil bath (50 °C). After 5.5 hours the reaction was stopped by the addition of acetic acid. The solvent was removed under reduced pressure and the residue was dissolved in THF. After precipitation in cold Et₂O (three times), the polymer was dried at 40 °C under reduced pressure overnight. A white solid was obtained (57.4 mg; 73 %).

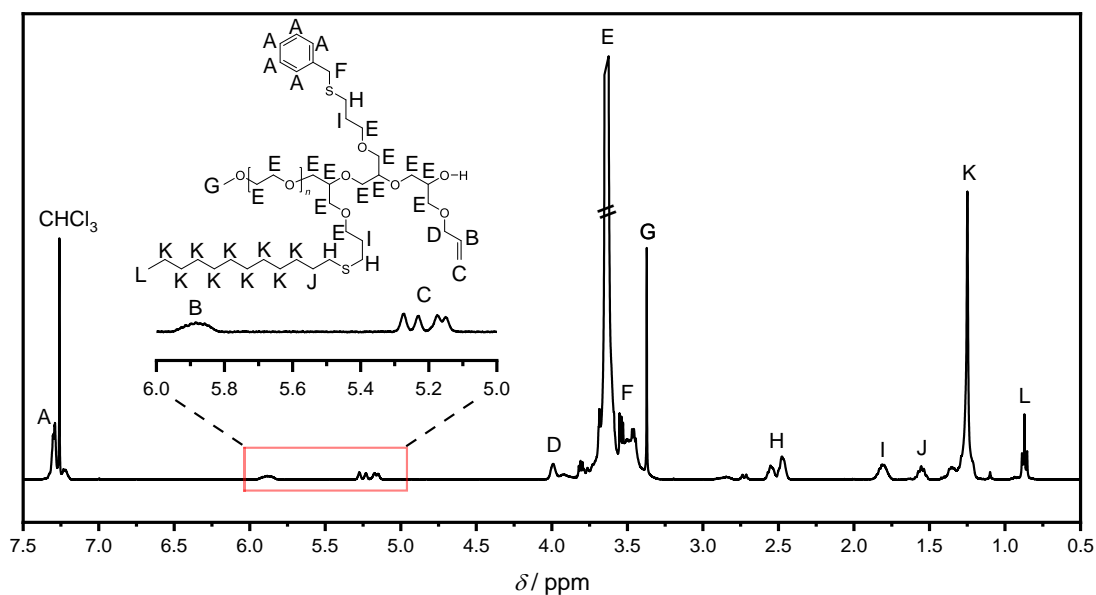


Figure 122: ^1H NMR spectrum of modified mPEG-1900 after the third CE with AGE. The new signals between 6.00 – 5.00 ppm confirm a successful CE. Solvent: CDCl_3 .

^1H NMR (400 MHz, CDCl_3) δ in ppm: 7.34 – 7.18 (m, 5H, A), 5.95 – 5.81 (m, 1H, B), 5.30 – 5.11 (m, 2H, C), 4.04 – 3.86 (m, 2H, D), 3.83 – 3.42 (m, 191H, E), 3.42 – 3.39 (m, 2H, F), 3.37 (s, 3H, G), 2.59 – 2.42 (m, 6H, H), 1.89 – 1.73 (m, 4H, I), 1.61 – 1.50 (m, 2H, J), 1.42 – 1.16 (m, 18H, K), 0.87 (t, 3H, L).

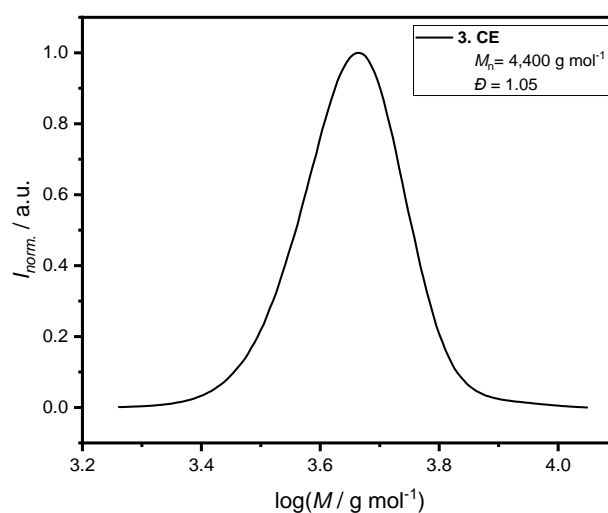
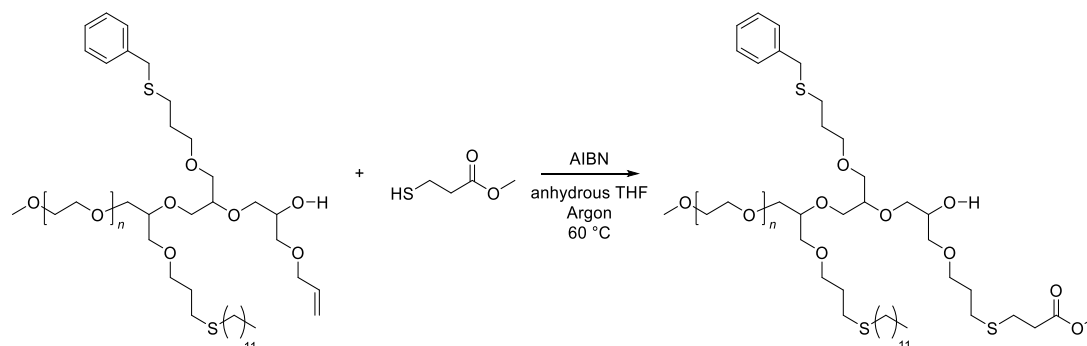


Figure 123: Size exclusion chromatogram after the third CE of mPEG-1900 with AGE.

6.3.5.9. Post-Polymerization Modification of Thrice Chain Extended mPEG-1900 via Thiol-ene Reaction using Methyl-3-mercaptopropionate



Thrice chain extended mPEG-1900 (57.4 mg, 22.4 μmol , 1.00 eq.) was given into a round-bottom flask, followed by AIBN (1.84 mg, 11.2 μmol , 0.500 eq.) and anhydrous THF (670 μL). Afterwards, methyl-3-mercaptopropionate (9.90 μL , 10.7 mg, 89.4 μmol , 4.00 eq.) was added and the atmosphere was changed to argon. The flask was placed into a preheated oil bath (60 °C) and stirred for 20 hours. The next day, the system was quenched by contact to air and cooling. The solvent was removed under reduced pressure and the residue dissolved in THF. After the precipitation in cold Et_2O (three times), the product was dried under reduced pressure at 40 °C overnight. A white solid was obtained (47.0 mg; 78%).

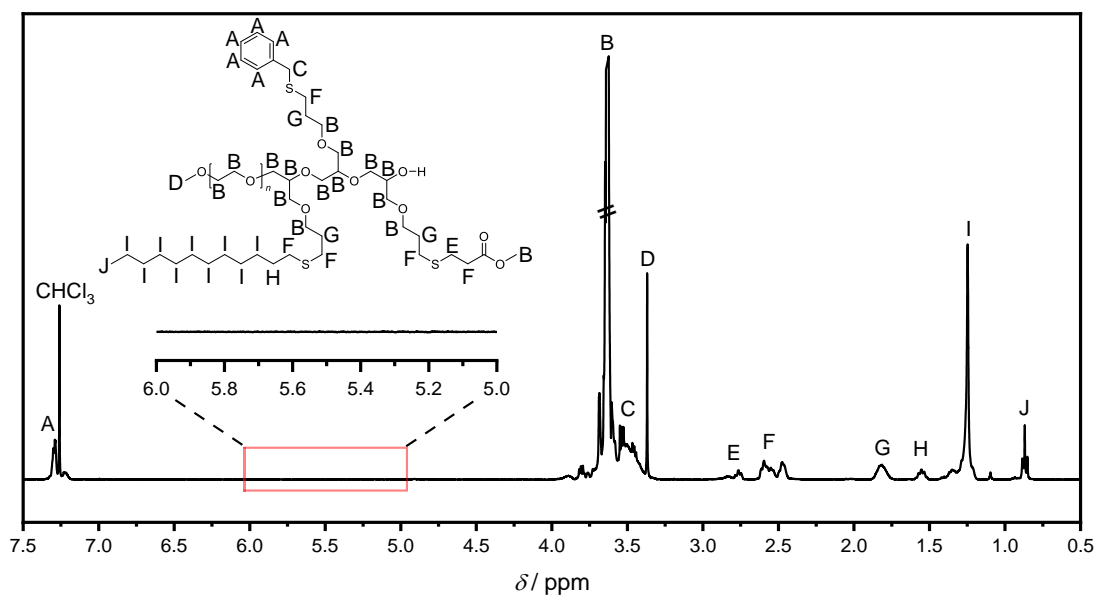


Figure 124: ^1H NMR spectrum of thrice chain extended mPEG-1900 after the thiol-ene reaction with methyl-3-mercaptopropionate. After the reaction the signals of the double bond between 6.00 – 5.00 ppm disappeared and the thiol signals (e.g., around 2.75 ppm) appeared, confirming a successful modification reaction. Solvent: CDCl_3 .

^1H NMR (400 MHz, CDCl_3) δ in ppm: 7.34 – 7.18 (m, 5H, A), 3.83 – 3.42 (m, 193H, B), 3.42 – 3.39 (m, 2H, C), 3.37 (s, 3H, D), 2.80 – 2.73 (m, 2H, E), 2.66 – 2.43 (m, 10H, F), 1.89 – 1.73 (m, 6H, G), 1.61 – 1.50 (m, 2H, H), 1.42 – 1.16 (m, 18H, I), 0.87 (t, 3H, J).

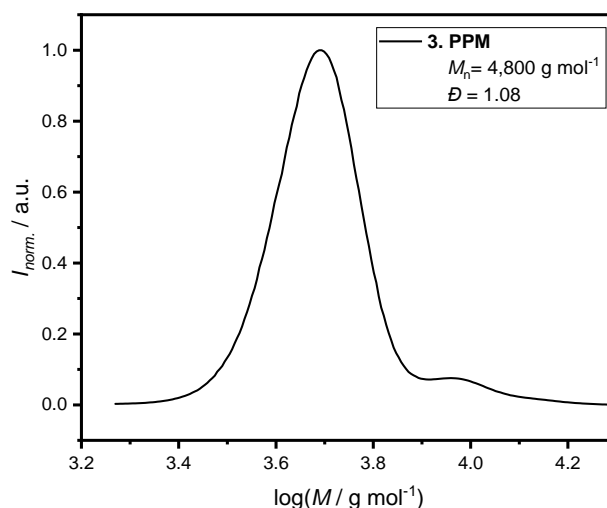


Figure 125: Size exclusion chromatogram of thrice chain extended mPEG-1900 after the thiol-ene reaction with methyl-3-mercaptopropionate.

7. Abbreviations

%	Percentage
°C	Degree Celsius
μm	Micrometer
Å	Angstrom
a.t.	Ambient temperature
a.u.	Arbitrary unit
ACL	α-Allyl-caprolactone
AGE	Allyl glycidyl ether
AIBN	2,2' Azobis(2 methylpropionitrile)
Alox	Aluminium oxide
approx.	Approximate/approximately
AROMA	Anionic ring-opening monomer addition
AROP	Anionic ring-opening polymerization
ATR FT-IR	Attenuated total reflection Fourier-transform infrared
ATRP	Atom transfer radical polymerization
<i>b</i>	Block
BHT	Butylated hydroxytoluene
BnOH	Benzyl alcohol
BPO	Benzoyl peroxide
CDCl ₃	Chloroform-d ₁
CDTPA	4-Cyano-4-[(dodecylsulfanylthiocarbonyl)sulfanyl]pentanoic acid
CE	Chain extension

CL	ϵ -Caprolactone
cm	Centimeter
CO ₂	Carbon dioxide
CROP	Cationic ring-opening polymerization
CTA	Chain transfer agent
Cu(I)Br	Copper(I) bromide
Cu(I)Cl	Copper(I) chloride
CuAAC	Copper(I)-catalyzed alkyne-azide cycloaddition
\bar{D}	Dispersity
DCM	Dichloromethane
DCM-d ₂	Dichloromethane-d ₂
dd	Doublet of doublets signal in NMR spectroscopy
DMAP	4-Dimethylaminopyridine
DMF	Dimethylformamide
DMPU	1,3-Dimethyl-1,3-diazinan-2-one
DNA	Deoxyribonucleic acid
dNbpy	4,4'-Dinonyl-2,2'-dipyridyl
DPP	Diphenyl phosphate
DSC	Differential scanning calorimetry
e.g.	Exempli gratia
EBiB	Ethyl 2-bromoisobutyrate
EO	Ethylene oxide
eq.	Equivalents
est.	Estimated

et al.	et alia
Et ₂ O	Diethyl ether
EtOH	Ethanol
g	Gram
H ₂ O	Water
HDPE	High-density polyethylene
HPLC	High performance liquid chromatography
i.a.	Inter alia
IUPAC	International Union of Pure and Applied Chemistry
IV	Inverse vulcanization
J	Coupling constant
K	Kelvin
k _{act.}	Activation rate
k _{deact.}	Deactivation rate
k _p	Propagation constant
L	Liter
LDA	Lithium diisopropylamide solution
LDPE	Low-density polyethylene
m	Multiplet signal in NMR spectroscopy
M	Molar
MBP	Methyl 2-bromopropionate
MEHQ	4-Methoxyphenol
MeOH	Methanol
mg	Milligram

MgSO ₄	Magnesium sulphate
MHz	Megahertz
min	Minute
mL	Milliliter
mm	Millimeter
MMA	Methyl methacrylate
mmol	Millimole
M_n	Number average molar mass
mol	Mole
M_p	Peak molar mass
mPEG	Methoxy polyethylene glycol
NaCl	Sodium chloride
n-BuLi	n-Butyllithium
NH ₄ Cl	Ammonium chloride
NMP	Nitroxide-mediated polymerization
NMR	Nuclear magnetic resonance
P ₄ - <i>t</i> -Bu	1-tert-Butyl-4,4,4-tris(dimethylamino)-2,2-bis[tris(dimethylamino)-phosphoranylidenamino]-2λ5,4λ5-catenadi(phosphazene)
Pa	Pascal
PACL	Poly(α-allyl-caprolactone)
PAGE	Poly(allyl glycidyl ether)
PCL	Poly(ε-caprolactone)
PE	Polyethylene
PE	Petroleum ether

PFP	Pentafluorophenol
PFPA	Pentafluorophenyl acrylate
PFPMA	Pentafluorophenyl methacrylate
PMDTA	N,N,N',N'',N''-Pentamethyldiethylenetriamine
PMMA	Poly(methyl methacrylate)
PPFPA	Poly(pentafluorophenyl acrylate)
PPFPMA	Poly(pentafluorophenyl methacrylate)
PPM	Post-polymerization modification
ppm	Parts per million
PRE	Persistent radical effect
PS	Polystyrene
RAFT	Reversible addition–fragmentation chain-transfer
RDRP	Reversible-deactivation radical polymerization
R _f	Retention factor
s	Singlet signal in NMR spectroscopy
S	Siemens
SEC	Size exclusion chromatography
t	Time
t	Triplet signal in NMR spectroscopy
T_{cc}	Cold crystallization temperature
TEA	Triethylamine
Temp.	Temperature
TEMPO	2,2,6,6-Tetramethylpiperidin-1-yl)oxyl
T_g	Glass transition temperature

THF	Tetrahydrofuran
T_m	Melting temperature
UHMWPE	Ultra-high-molecular-weight polyethylene
UV	Ultraviolet
vs.	Versus
wt%	Percentage by weight
$\tilde{\nu}$	Wavenumber
α	Alpha
β	Beta
δ	Chemical shift in NMR spectroscopy
μg	Microgram
μL	Microliter
μmol	Micromole
ν	Frequency
ω	Omega

8. List of Figures

- Figure 1:** Size exclusion chromatogram of PPFPA synthesized via RAFT polymerization. 29
- Figure 2:** Size exclusion chromatograms of PPFPA before (gray) and after (red) the partial PPM with 2,2,2- trifluoroethylamine. A decrease in M_n and increase in \bar{D} is visible, indicating the success of the modification..... 30
- Figure 3:** Size exclusion chromatograms of modified PPFPA before (gray) and after (red) the CE with PFPFA. No noticeable change was observed, suggesting an unsuccessful reaction. 31
- Figure 4:** ^{19}F NMR spectra of the transesterification of PPFPA with 2,2,2-trifluoroethanol at ambient temperature (bottom) and at 80 °C (top). The reaction done at ambient temperature still has unreacted PPFPA moieties present. Solvent: CDCl_3 34
- Figure 5:** Size exclusion chromatograms of PPFPA before (gray) and after (red) the transesterification with 2,2,2-trifluoroethanol. A slight decrease in M_n and \bar{D} is visible, indicating a change in the structure. 35
- Figure 6:** Size exclusion chromatograms of modified PPFPA before (gray) and after (red) the CE with PFPFA. Two peaks are visible after the reaction, a smaller one with a similar M_p as the precursor polymer and a larger one at approx. $47,900 \text{ g mol}^{-1}$. Additionally, an increase in \bar{D} to almost 2 could also be observed. 36
- Figure 7:** Size exclusion chromatogram of PPFPMMA synthesized via ATRP. A long tailing at the lower molar mass side is visible. 38
- Figure 8:** Size exclusion chromatogram of PPFPMMA before (gray) and after (red) the partial PPM with 2,2,2-trifluoroethylamine. A small increase in M_n is visible, as well as an improvement in the \bar{D} 39
- Figure 9:** Crude ^{19}F NMR spectrum of the PPM pf PPFPMMA with 2,2,3,3,3-pentafluoropropylamine after 48 hours. The still present PPFPMMA signals indicate an unsuccessful PPM. Solvent: CDCl_3 40
- Figure 10:** Size exclusion chromatograms of PCL (gray) and the first (red) and second (blue) CE with CL. After each reaction a shift to higher M_n is visible, indicating a successful extension of the chain. 42
- Figure 11:** Size exclusion chromatogram of PACL. Multiple sharp peaks are visible, indicating an oligomeric material. 43

Figure 12: ^1H NMR spectrum of PAGE. Solvent: CDCl_3 .	46
Figure 13: Size exclusion chromatogram of PAGE. A single peak with a small shoulder at its higher molar mass side is visible.	46
Figure 14: Comparison of the ^1H NMR spectra of PAGE before (bottom) and after (top) the PPM with 1-dodecanethiol. After the modification the disappearance of the $\text{H}_2\text{C}=\text{CH}-\text{R}$ signals of AGE (red) and the appearance of the thiol signals (green) could be observed, confirming a change in the structure.	47
Figure 15: Size exclusion chromatograms of PAGE before (gray) and after (red) the PPM with 1-dodecanethiol. After the modification a shift to higher molar masses is noticeable, indicating a change in the structure of the chain.	48
Figure 16: Crude ^1H NMR spectrum of the CE reaction of modified PAGE with AGE at ambient temperature. Solvent: CDCl_3 .	49
Figure 17: Size exclusion chromatograms of modified PAGE before (gray) and after (red) the CE attempts with AGE. No significant change is visible, indicating a failed attempt.	50
Figure 18: ^1H NMR spectrum of PAGE after the synthesis without an initiator. Solvent: CDCl_3 .	51
Figure 19: Size exclusion chromatogram of PAGE synthesized without additional initiator. A broad peak with a Đ of 1.31 is visible, indicating an uncontrolled polymerization.	51
Figure 20: Comparison of the ^1H NMR spectra of modified PAGE before (bottom) and after (top) the CE with AGE at $50\text{ }^\circ\text{C}$. After the reaction, the $\text{H}_2\text{C}=\text{CH}-\text{R}$ signals of the attached AGE units in the range of 6.00 – 5.00 ppm (green area) could be observed. Solvent: CDCl_3 .	52
Figure 21: Crude size exclusion chromatogram of the first CE of modified PAGE with AGE. Two peaks are visible, a smaller one at $M_p = 3,700\text{ g mol}^{-1}$ and a larger one at $M_p = 11,200\text{ g mol}^{-1}$.	53
Figure 22: Size exclusion chromatograms of modified PAGE before (gray) and after (red) the first CE with AGE. After the reaction, a noticeable shift of the peak to a higher molar mass could be observed, indicating a change of the chain structure.	54
Figure 23: ^1H NMR spectra of once chain extended modified PAGE before (bottom) and after (top) the second PPM via thiol-ene reaction using benzyl thiol. Solvent: CDCl_3 .	55

Figure 24: Size exclusion chromatograms of once chain extended modified PAGE before (gray) and after (red) the PPM via thiol-ene reaction with benzyl thiol.....	56
Figure 25: ^1H NMR spectra of twice modified PAGE before (bottom) and after (top) the second CE with AGE. After the reaction, the $\text{H}_2\text{C}=\text{CH-R}$ signals of the AGE in the range of 6.00 – 5.00 (green area) could be observed, indicating a successful CE. Solvent: CDCl_3	57
Figure 26: Size exclusion chromatograms of twice modified PAGE before (gray) and after (red) the second CE with AGE. After the reaction, a shift to higher molar mass was observed, indicating the success of the reaction.	58
Figure 27: Crude ^1H NMR spectra of twice chain extended modified PAGE before (bottom) and after (top) the third PPM via thiol-ene reaction using methyl-3-mercaptopropionate. After the reaction, the disappearance of the $\text{H}_2\text{C}=\text{CH-R}$ signal of the AGE (6.00 – 5.00 ppm; red area) as well as the appearance of the newly added thiol signals (e.g., 2.97 – 2.39 ppm; green area).	59
Figure 28: Size exclusion chromatograms of twice chain extended modified PAGE before (gray) and after (red) the third PPM via thiol-ene reaction using methyl-3-mercaptopropionate. After the reaction a small shift to higher molar mass as well as the formation of a shoulder could be observed.....	60
Figure 29: Collection of all size exclusion chromatograms for each CE and PPM reaction of PAGE. A clear shift in the molar mass from the beginning (PAGE; gray) to the last modification (3. PPM; yellow) can be observed.	61
Figure 30: Collection of all ^1H NMR spectra for each CE and PPM reaction of PAGE. With each reaction, the appearance and disappearance of the $\text{H}_2\text{C}=\text{CH-R}$ signal of the AGE units can be observed.	61
Figure 31: ^1H NMR spectra of twice chain extended modified PAGE before (bottom) and after (top) the PPM via thiol-ene reaction using pentaerythritol tetrakis(3-mercaptopropionate). After the reaction, the disappearance of the $\text{H}_2\text{C}=\text{CH-R}$ signals of the AGE (6.00 – 5.00 ppm; red area) and the appearance of the thiol signals (e.g., 4.17 ppm; green area) could be observed. Solvent: CDCl_3	63
Figure 32: Size exclusion chromatogram of crosslinked modified PAGE. Multiple peaks and shoulder are visible with an overall \bar{M} of 101 and molar masses up to 7,943,000 g mol^{-1}	64
Figure 33: ^1H NMR spectrum of PAGE using mPEG-1900 as initiator. Solvent: CDCl_3	68

- Figure 34:** Size exclusion chromatogram of PAGE using mPEG-1900 as initiator. A single symmetrical peak could be observed. 68
- Figure 35:** Kinetic study of the polymerization of AGE using untreated (black, **K1**) and pre-dried (blue, **K2**) mPEG-1900 as initiator. In case of the untreated initiator, a clear flattening of the curve with longer reaction time could be observed. 71
- Figure 36:** Kinetic study of the polymerization of AGE using pre-dried mPEG-1900 as initiator for a shorter time frame. At 4 minutes, an outlier due to late quenching is visible..... 73
- Figure 37:** Monomer conversion vs. time of the polymerization of AGE using pre-dried mPEG-1900 as initiator. With increasing reaction time, a flattening of the curve is noticeable. 75
- Figure 38:** I. Size exclusion chromatogram after the first CE of mPEG-1900 with AGE. II. ^1H NMR spectrum of the AGE chain extended mPEG-1900. The new signals between 6.00 – 5.00 ppm confirm a successful CE. Solvent: CDCl_3 . III. DSC thermogram (heating curve; 2. cycle) of AGE chain extended mPEG with a visible T_m at 54.2 °C. IV. ATR FT-IR spectrum of mPEG-1900 (black) and the first CE (blue). After the CE a new signal at $1,645\text{ cm}^{-1}$ appears, which could be assigned to the C=C double bond of the AGE. 76
- Figure 39:** I. Size exclusion chromatogram of chain extended mPEG-1900 before (blue) and after (violet) the first PPM via thiol-ene reaction using 1-dodecanethiol. After the modification, a shift to higher molar masses is visible in comparison to the previous polymer. II. ^1H NMR spectrum of chain extended mPEG-1900 after the thiol-ene reaction with 1-dodecanethiol. After the reaction the signals of the double bond between 6.00 – 5.00 ppm disappeared and the thiol signals (e.g., 0.87 ppm) appeared, confirming a successful modification reaction. Solvent: CDCl_3 . III. DSC thermogram (heating curve; 2. cycle) of 1-dodecanethiol modified chain extended mPEG-1900 with a visible T_m at 55.2 °C. IV. ATR FT-IR spectrum of once chain extended mPEG-1900 (blue) and the 1-dodecanethiol modified polymer (violet). After the modification the signal at $1,645\text{ cm}^{-1}$ disappeared, confirming a successful modification..... 79
- Figure 40:** I. Size exclusion chromatogram of modified mPEG-1900 before (violet) and after (red) the second CE with AGE. After the extension, a shift to higher molar masses is visible. II. ^1H NMR spectrum of the twice chain extended mPEG-1900. Again, the signals of the double bond between 6.00 – 5.00 ppm are visible, confirming a successful CE. III. DSC thermogram (heating curve; 2. cycle) of twice chain extended

mPEG-1900 with a visible T_m at 53 °C. IV. ATR FT-IR spectrum of once modified mPEG-1900 (violet) and twice chain extended mPEG-1900 (red). After the CE a new signal at 1,645 cm^{-1} appears, which could be assigned to the C=C double bond of the AGE..... 81

Figure 41: ^1H NMR spectrum of twice chain extended mPEG-1900 after the PPM via thiol-ene reaction using benzyl mercaptan. After the reaction, the disappearance of the $\text{H}_2\text{C}=\text{CH-R}$ signals of AGE (6.00 – 5.00 ppm) and appearance of the thiol signals could be observed. Solvent: CDCl_3 83

Figure 42: Size exclusion chromatogram of twice chain extended mPEG-1900 before (red) and after (green) the PPM via thiol-ene reaction using benzyl mercaptan. After the reaction, a minimal shift in the molar mass is noticeable. 83

Figure 43: ^1H NMR spectrum of twice modified mPEG-1900 after the third CE with AGE. After the reaction, the appearance of the $\text{H}_2\text{C}=\text{CH-R}$ signals of AGE between 6.00 – 5.00 ppm could be observed, confirming the addition of the monomer to the chain. Solvent: CDCl_3 85

Figure 44: Size exclusion chromatogram of twice modified mPEG-1900 before (green) and after (orange) the third CE with AGE. A slight shift in the molar mass and an improvement of the \bar{D} could be observed. 86

Figure 45: ^1H NMR spectrum of thrice chain extended mPEG-1900 after the PPM via thiol-ene reaction using methyl-3-mercaptopropionate. After the reaction, the disappearance of the $\text{H}_2\text{C}=\text{CH-R}$ signals of AGE between 6.00 – 5.00 ppm could be observed. Solvent: CDCl_3 87

Figure 46: Size exclusion chromatogram of thrice chain extended mPEG-1900 before (orange) and after (black) the PPM via thiol-ene reaction using methyl-3-mercaptopropionate. After the reaction, a shift to higher molar masses could be observed, indicating the success of the reaction. 88

Figure 47: ^1H NMR spectrum of PFPA. Solvent: CDCl_3 97

Figure 48: ^{19}F NMR spectrum of PFPA. Solvent: CDCl_3 97

Figure 49: ^1H NMR spectrum of PPFPA. Solvent: CDCl_3 99

Figure 50: ^{19}F NMR spectrum of the RAFT polymerization of PFPA after 30 minutes. Solvent: CDCl_3 100

Figure 51: ^{19}F NMR spectrum of PPFPA. Solvent: CDCl_3 101

Figure 52: Size exclusion chromatogram of PPFPA. 101

Figure 53: ^{19}F NMR spectrum of partially modified PPFPA. Solvent: CDCl_3 103

Figure 54: Size exclusion chromatogram of partially modified PPFPA.	103
Figure 55: ^{19}F NMR spectrum of the chain extended modified PPFPA. Solvent: CDCl_3	105
Figure 56: Size exclusion chromatogram of once chain extended modified PPFPA.	105
Figure 57: ^1H NMR spectrum of the base stability test of CDTPA with DMAP at ambient temperature after 48 hours. Solvent: CDCl_3	107
Figure 58: ^1H NMR spectrum of the base stability test of CDTPA with DMAP at 80 °C after 48 hours. Solvent: CDCl_3	108
Figure 59: ^{19}F NMR of the transesterification of PPFPA with 2,2,2-trifluoroethanol at ambient temperature. Solvent: CDCl_3	110
Figure 60: ^{19}F NMR spectrum of the transesterification of PPFPA with 2,2,2-trifluoroethanol at 80 °C. Solvent: CDCl_3	110
Figure 61: Size exclusion chromatogram of PPFPA after the transesterification with 2,2,2-trifluoroethanol at ambient temperature.	111
Figure 62: ^{19}F NMR spectrum of the first CE of 2,2,2-trifluoroethanol modified PPFPA. Solvent: CDCl_3	113
Figure 63: Size exclusion chromatogram of once chain extended 2,2,2-trifluoroethanol modified PPFPA.	113
Figure 64: ^1H NMR spectrum of PFPMA. Solvent: CDCl_3	115
Figure 65: ^{19}F NMR spectrum of PFPMA. Solvent: CDCl_3	115
Figure 66: ^1H NMR of PFPMA. Solvent: CDCl_3	117
Figure 67: ^{19}F NMR spectrum of PFPMA. Solvent: CDCl_3	117
Figure 68: Size exclusion chromatogram of PFPMA.	118
Figure 69: ^{19}F NMR spectrum of the PPM of PFPMA with 2,2,2-trifluoroethanol. No modification could be observed. Solvent: CDCl_3	120
Figure 70: Size exclusion chromatogram of the PPM of PFPMA with 2,2,2-trifluoroethanol.	120
Figure 71: Crude ^{19}F NMR of the PPM of PFPMA with 2,2,3,3,3-pentafluoropropylamine after 48 hours. The still present PFPMA signals indicate an unsuccessful PPM. Solvent: CDCl_3	122
Figure 72: ^1H NMR spectrum of PCL. Solvent: DCM-d_2	124
Figure 73: Size exclusion chromatogram of PCL.	124
Figure 74: ^1H NMR spectrum of once chain extended PCL. Solvent: DCM-d_2	126

Figure 75: Size exclusion chromatogram of once chain extended PCL.	126
Figure 76: ^1H NMR spectrum of twice chain extended PCL. Solvent: CDCl_3	128
Figure 77: Size exclusion chromatogram of twice chain extended PCL.	128
Figure 78: ^1H NMR spectrum of α -allyl-caprolactone. Solvent: CDCl_3	130
Figure 79: Crude ^1H NMR spectrum of PACL. Solvent: CDCl_3	132
Figure 80: Size exclusion chromatogram of PACL.	132
Figure 81: ^1H NMR spectrum of the first CE of PACL with ϵ -caprolactone. No CE could be observed, only the formation of PCL. Solvent CDCl_3	134
Figure 82: ^1H NMR spectrum of PAGE. Solvent: CDCl_3	136
Figure 83: Size exclusion chromatogram of PAGE.	136
Figure 84: ^1H NMR spectrum of 1-dodecanethiol modified PAGE. Solvent: CDCl_3	138
Figure 85: Size exclusion chromatogram of 1-dodecanethiol modified PAGE.	138
Figure 86: Crude ^1H NMR spectrum of the CE reaction of modified PAGE with AGE at ambient temperature. Solvent: CDCl_3	140
Figure 87: Size exclusion chromatogram of the first CE of modified PAGE with AGE at ambient temperature.	141
Figure 88: ^1H NMR spectrum of the CE reaction of modified PAGE with AGE at 50 °C. Solvent: CDCl_3	142
Figure 89: Size exclusion chromatogram of once chain extended modified PAGE at 50 °C.	143
Figure 90: ^1H NMR spectrum of the residue in MeOH after the first CE reaction of modified PAGE with AGE at 50 °C. The spectrum matches the one of PAGE. Solvent: CDCl_3	143
Figure 91: ^1H NMR spectrum of once chain extended PAGE after the thiol-ene reaction with benzyl mercaptan. Solvent: CDCl_3	145
Figure 92: Size exclusion chromatogram of once chain extended PAGE after the thiol-ene reaction with benzyl mercaptan.	145
Figure 93: ^1H NMR spectrum of twice chain extended PAGE with AGE. Solvent: CDCl_3	147
Figure 94: Size exclusion chromatogram of twice chain extended PAGE with AGE.	147
Figure 95: Crude ^1H NMR spectrum of twice chain extended PAGE after the thiol-ene reaction with methyl-3-mercaptopropionate. Solvent: CDCl_3	149

Figure 96: Crude size exclusion chromatogram of twice chain extended PAGE after the thiol-ene reaction with methyl-3-mercaptopropionate.	150
Figure 97: Crude ^1H NMR spectrum of twice chain extended PAGE after the thiol-ene reaction with pentaerythritol tetrakis(3-mercaptopropionate). Solvent: CDCl_3	152
Figure 98: Crude size exclusion chromatogram of twice chain extended PAGE after the thiol-ene reaction with pentaerythritol tetrakis(3-mercaptopropionate).	153
Figure 99: ^1H NMR spectrum of PAGE synthesized without additional initiator. Solvent: CDCl_3	155
Figure 100: Size exclusion chromatogram of PAGE synthesized without additional initiator.	155
Figure 101: ^1H NMR spectrum of the AROP of AGE using mPEG-1900 as initiator. Solvent: CDCl_3	157
Figure 102: Size exclusion chromatogram of the AROP of AGE using mPEG-1900 as initiator.	157
Figure 103: Kinetic study of the polymerization of AGE using untreated mPEG-1900 as initiator. A clear flattening of the curve with longer reaction time could be observed.	159
Figure 104: Kinetic study of the polymerization of AGE using pre-dried mPEG-1900 as initiator. An almost linear behavior with longer reaction time could be observed.	159
Figure 105: ^1H NMR spectrum of once chain extended mPEG-1900 with AGE based on the kinetic approach after 10 minutes and 46 seconds. The repeating unit of AGE is 2.01. Solvent: CDCl_3	161
Figure 106: ^1H NMR spectrum of once chain extended mPEG-1900 with AGE based on the kinetic approach after 10 minutes and 46 seconds. The repeating unit of AGE is 2.14. Solvent: CDCl_3	162
Figure 107: ^1H NMR spectrum of once chain extended mPEG-1900 with AGE based on the kinetic approach after 7 minutes and 25 seconds. The repeating unit of AGE is 1.28. Solvent: CDCl_3	163
Figure 108: ^1H NMR spectrum of mPEG-1900 after the first CE with AGE. The new signals between 6.00 – 5.00 ppm confirm a successful CE. Solvent: CDCl_3	165
Figure 109: Size exclusion chromatogram after the first CE of mPEG-1900 with AGE.	165

Figure 110: ATR FT-IR spectrum of once chain extended mPEG-1900 with AGE. After the CE a new signal at 1,645 cm ⁻¹ appears, which could be assigned to the C=C double bond of the AGE.	166
Figure 111: DSC thermogram (heating curve; 2. cycle) of AGE chain extended mPEG-1900 with a visible T _m at 54.2 °C.	167
Figure 112: ¹ H NMR spectrum of once chain extended mPEG-1900 after the thiol-ene reaction with 1-dodecanethiol. After the reaction, the signals of the double bond between 5.00 – 6.00 ppm disappeared and the thiol signals (e.g., around 0.8 ppm) appeared, confirming a successful modification reaction. Solvent: CDCl ₃	169
Figure 113: Size exclusion chromatogram of once chain extended mPEG-1900 after the thiol-ene reaction with 1-dodecanethiol.	169
Figure 114: ATR FT-IR spectrum of once chain extended mPEG-1900 after the thiol-ene reaction with 1-dodecanethiol. After the modification the signal at 1,645 cm ⁻¹ disappeared, which confirms a successful modification.	170
Figure 115: DSC thermogram (heating curve; 2. cycle) of once chain extended mPEG-1900 after the thiol-ene reaction with 1-dodecanethiol with a visible T _m at 55.2 °C.	171
Figure 116: ¹ H NMR spectrum of modified mPEG-1900 after the second CE with AGE. The new signals between 6.00 – 5.00 ppm confirm a successful CE. Solvent: CDCl ₃	173
Figure 117: Size exclusion chromatogram after the second CE of mPEG-1900 with AGE.	173
Figure 118: ATR FT-IR spectrum of twice chain extended mPEG-1900 with AGE. After the CE a new signal at 1,645 cm ⁻¹ appears, which could be assigned to the C=C double bond of the AGE.	174
Figure 119: DSC thermogram (heating curve; 2. cycle) of twice chain extended mPEG-1900 with a visible T _m at 53 °C.	175
Figure 120: ¹ H NMR spectrum of twice chain extended mPEG-1900 after the thiol-ene reaction with benzyl mercaptan. After the reaction the signals of the double bond between 6.00 – 5.00 ppm disappeared and the thiol signals (e.g., around 7.30 ppm) appeared, confirming a successful modification reaction. Solvent: CDCl ₃	177
Figure 121: Size exclusion chromatogram of twice chain extended mPEG-1900 after the thiol-ene reaction with benzyl thiol.	177

Figure 122: ^1H NMR spectrum of modified mPEG-1900 after the third CE with AGE. The new signals between 6.00 – 5.00 ppm confirm a successful CE. Solvent: CDCl_3	179
Figure 123: Size exclusion chromatogram after the third CE of mPEG-1900 with AGE.	179
Figure 124: ^1H NMR spectrum of thrice chain extended mPEG-1900 after the thiol-ene reaction with methyl-3-mercaptopropionate. After the reaction the signals of the double bond between 6.00 – 5.00 ppm disappeared and the thiol signals (e.g., around 2.75 ppm) appeared, confirming a successful modification reaction. Solvent: CDCl_3	181
Figure 125: Size exclusion chromatogram of thrice chain extended mPEG-1900 after the thiol-ene reaction with methyl-3-mercaptopropionate.	181

9. List of Schemes

Scheme 1: Reaction of an anionic initiator with a monomer, forming an active macromolecule.	4
Scheme 2: Mechanism of the anionic polymerization divided into (i) initiation, (ii) propagation, (iii) termination and (iv) transfer. Redrawn after reference. ⁴³	5
Scheme 3: (I) Initiation of styrene by single electron transfer using sodium naphthalene. Two possible resonance structures of the naphthalene radical anion are displayed. (II) Initiation of styrene by the nucleophilic addition using n-butyllithium. Redrawn after reference. ⁴³	6
Scheme 4: Transition state of the monomer addition of an epoxide promoted by P ₄ -t-Bu, depending on the substituents. Redrawn after reference. ⁵³	7
Scheme 5: Cationic initiation of a vinyl monomer, creating an active macromolecule in the end.....	8
Scheme 6: Cationic polymerization of styrene using the protonic acid initiator trifluoromethanesulfonic acid. ⁶⁹	8
Scheme 7: Cationic polymerization of styrene using the Lewis acid boron trifluoride with water as co-initiator. Redrawn after reference. ³⁵	9
Scheme 8: General mechanism of ATRP showing the equilibrium between the dormant (left) and active (right) state. While the system is in the active state the propagation of the chain occurs. Redrawn after reference. ⁸⁸	11
Scheme 9: Dithioester, trithiocarbonate and dithiocarbamate, three common classes of RAFT agents.	12
Scheme 10: Schematic depiction of the general RAFT mechanism split into the respective parts: (I) Initiation, (II) reversible chain transfer, (III) reinitiation, (IV) chain equilibrium, (V) termination. Redrawn after reference. ¹¹⁹	13
Scheme 11: General mechanism of NMP displaying two different approaches in which a) a conventional radical initiator or b) a monocomponent system is used. Redrawn after reference. ¹²⁶	14
Scheme 12: RAFT polymerization of PFPMA with subsequential PPM via aminolysis with monomethoxy triethyleneglycol amine to form a polymer with a pendant mPEG-group. Redrawn after reference. ¹²⁷	15
Scheme 13: General depiction of a thiol-ene reaction of a primary thiol with a double bond either by radical or the nucleophilic mechanism. Redrawn after reference. ¹³⁶	16

Scheme 14: Catalytic cycle of the thiol-ene reaction including the steps of thiyl radical formation by a radical source and the subsequent propagation. After a proton abstraction the desired product is formed. Redrawn after reference. ¹³⁹	16
Scheme 15: Exemplary depiction of the five main groups of copolymers (I) statistical, (II) gradient, (III) alternating, (IV) block and (V) graft copolymer.....	18
Scheme 16: Schematic depiction of the difference between sequence-defined and sequence-controlled polymers. While both are built from the same choices of monomer in the same order, only sequence-defined polymers have the same number of units per block and therefore an identical chain length. This is also noticeable in the \bar{D} because sequence-defined polymers have a $\bar{D} = 1$, while sequence-controlled polymers have a $\bar{D} > 1$	19
Scheme 17: Comparison of the structures of PEG/PEO and PAGE. The structure is almost identical except for the pendant C=C double bond.	20
Scheme 18: General concept of the sequence-controlled multiblock copolymer synthesis by combining CE and PPM reactions. After the polymerization of a functional monomer resulting in POLY-1A, a follow-up modification reaction with a reactant containing the group R_1 is conducted. The obtained modified polymer (POLY-1B) functions as a macroinitiator in a subsequent polymerization with the identical monomer, resulting in POLY-2A, followed by a second PPM with a reactant containing the group R_2 . This procedure can be continued x times, resulting in a sequence-controlled multiblock copolymer with x blocks.	23
Scheme 19: Comparison between the “traditional” and the approach presented in this thesis to synthesize a sequence-controlled triblock copolymer. The former uses three different monomers (A, B, C) to introduce properties into the polymer, while the latter uses a single monomer in combination with reactants. This allows to simplify the synthesis by bypassing laborious and time-consuming monomer syntheses.....	24
Scheme 20: RAFT polymerization of PFPA with subsequential PPM using a primary amine. Redrawn after reference. ¹⁶⁵	27
Scheme 21: Reaction equation of the RAFT polymerization of PFPA using CDTPA and AIBN in anhydrous dioxane under inert atmosphere at 80 °C.	28
Scheme 22: Reaction equation of the partial PPM of PPFA with 2,2,2-trifluoroethylamine in DMF at ambient temperature for 24 hours.....	29
Scheme 23: Reaction equation of the first CE of the modified PPFA with PFPA and AIBN in anhydrous dioxane under inert atmosphere at 70 °C.	31

Scheme 24: Reaction equation of the base compatibility test reactions of CDTPA with DMAP in anhydrous DMF under inert atmosphere at ambient temperature and 80 °C.	32
Scheme 25: Reaction equation of the transesterification PPFPA and 2,2,2-trifluoroethanol using DMAP in anhydrous DMF under inert atmosphere at ambient temperature or 80 °C.	33
Scheme 26: Reaction equation of the CE of modified PPFPA with PFPA and AIBN in anhydrous dioxane under inert atmosphere at 70 °C.	35
Scheme 27: Reaction equation of the ATRP of PFPMA and EBiB using dNbpy and Cu(I)Cl in anhydrous toluene under inert atmosphere at 70 °C.	37
Scheme 28: Reaction equation of the partial PPM of PFPMA with 2,2,2-trifluoroethylamine in DMF at ambient temperature.	38
Scheme 29: Reaction equation of the PPM of PFPMA with 2,2,3,3,3-pentafluoropropylamine in DMF at 50 °C for 48 hours.	39
Scheme 30: I. General reaction equation of the polymerization of CL using a primary alcohol and DPP. II. General reaction equation of the second and third CE of PCL with CL in presence of DPP.	41
Scheme 31: Reaction equation of the CROP of ACL with benzyl alcohol and DPP in anhydrous dioxane under inert atmosphere at 50 °C.	43
Scheme 32: Reaction equation of the first CE of PACL with CL using DPP in anhydrous dioxane under inert atmosphere at 50 °C.	44
Scheme 33: Reaction equation of the AROP of AGE with benzyl alcohol using P ₄ -t-Bu in anhydrous THF under inert atmosphere at ambient temperature.	45
Scheme 34: Reaction equation of the thiol-ene reaction of PAGE and 1-dodecanethiol with AIBN in anhydrous THF under inert atmosphere at 60 °C.	47
Scheme 35: Reaction equation of the first CE of modified PAGE with AGE using P ₄ -t-Bu in anhydrous THF under inert atmosphere at ambient temperature.	48
Scheme 36: Reaction equation of the AROP of AGE using no initiator but P ₄ -t-Bu in anhydrous THF under inert atmosphere at ambient temperature.	50
Scheme 37: Reaction equation of the thiol-ene reaction of once chain extended PAGE and benzyl mercaptan with AIBN in anhydrous THF under inert atmosphere at 60 °C.	54
Scheme 38: Reaction equation of the second CE of modified PAGE with AGE using P ₄ -t-Bu in anhydrous THF under inert atmosphere at 50 °C.	56

Scheme 39: Reaction equation of the thiol-ene reaction of twice chain extended PAGE methyl-3-mercaptopropionate with AIBN in anhydrous THF under inert atmosphere at 60 °C.	58
Scheme 40: Reaction equation of the thiol-ene reaction of twice chain extended PAGE using pentaerythritol tetrakis(3-mercaptopropionate) with AIBN in anhydrous THF under inert atmosphere at 60 °C.....	62
Scheme 41: Reaction equation of the AROP of AGE with mPEG-1900 using P ₄ -t-Bu in anhydrous THF under inert atmosphere at ambient temperature.	67
Scheme 42: General reaction equation of the first CE of mPEG-1900 with AGE via the kinetic approach, using P ₄ -t-Bu in anhydrous THF under inert atmosphere at ambient temperature.	72
Scheme 43: Reaction equation of the first CE of mPEG-1900 with AGE via the small excess approach, using P ₄ -t-Bu in anhydrous THF under inert atmosphere at ambient temperature.	75
Scheme 44: Reaction equation of the first PPM of the AROMA-polymer using 1-dodecanethiol and AIBN in anhydrous THF under inter atmosphere at 60 °C.....	77
Scheme 45: Reaction equation of the second CE of mPEG-1900 with AGE via the small excess approach, using P ₄ -t-Bu in anhydrous THF under inert atmosphere at 50 °C.	80
Scheme 46: Reaction equation of the second PPM of the AROMA-polymer using benzyl mercaptan and AIBN in anhydrous THF under inter atmosphere at 60 °C....	82
Scheme 47: Reaction equation of the third CE of mPEG-1900 with AGE via the small excess approach, using P ₄ -t-Bu in anhydrous THF under inert atmosphere at 50 °C.	84
Scheme 48: Reaction equation of the third PPM of the AROMA-polymer using methyl-3-mercaptopropionate and AIBN in anhydrous THF under inert atmosphere at 60 °C.	86
Scheme 49: Possible applications for the newly established system: I. Synthesis of sequence-controlled multiarm (star) copolymers; II: High sulfur containing polymer networks; III. Sequence-controlled hydrogels; IV: Sequence-controlled ABCBA pentablock copolymers.....	92

10. List of Tables

Table 1: Overview of the polymerization of AGE with each CE and PPM, including equivalents of monomer, equivalents of thiol, M_n and \bar{D}	60
Table 2: Reaction time, monomer conversion and $\ln([M]_0/[M])$ of the kinetic study (K1) of the polymerization of AGE using untreated mPEG-1900 as initiator.	70
Table 3: Reaction time, monomer conversion and $\ln([M]_0/[M])$ of the kinetic study (K2) of the polymerization of AGE using pre-dried mPEG-1900 as initiator.	71
Table 4: Reaction time, monomer conversion and $\ln([M]_0/[M])$ of the kinetic study (K3) of the polymerization of AGE using pre-dried mPEG-1900 as initiator.	73
Table 5: Overview of each kinetic study with their respective k_p , estimated addition time and the resulted average repeating unit.....	74
Table 6: Overview of each CE and PPM including equivalents, reaction time, temperature, M_n , \bar{D} and the average repeating unit.	88

11. Acknowledgments

An dieser Stelle möchte ich mich bei allen bedanken, die mich während meiner Promotion begleitet haben und ohne die die Erstellung dieser Arbeit nicht möglich gewesen wäre.

Zunächst einmal möchte ich mich bei meinem Doktorvater PROFESSOR DR. PATRICK THÉATO bedanken, nicht nur für die Möglichkeit in seinem Arbeitskreis diese Arbeit anfertigen zu dürfen, sondern viel mehr für die stets angenehme und freundliche Zusammenarbeit. Danke für die gesunde Balance zwischen wissenschaftlichem Freiraum und kompetenter Unterstützung, bei der ich egal bei welchen Fragen, ob wissenschaftlicher oder organisatorischer Natur, stets auf deinen Rat und deine Hilfe bauen konnte.

Ferner möchte ich mich auch bei DR. DOMINIK VOLL und DR. CHRISTIAN SCHMITT für das stets gute Verhältnis, den wissenschaftlichen Austausch und die Hilfe bedanken.

Ein besonderes Dankeschön gilt KATHARINA KUPPINGER, die mit ihrer freundlichen und hilfsbereiten Art immer zur Stelle war, egal welches Problem auftrat, Sie hat sich immer darum gekümmert.

Dank auch an MARTINA RITTER und BÄRBEL SEUFERT-DAUSMANN für die organisatorische und verwaltungstechnische Unterstützung über all die Zeit.

Des Weiteren bedanke ich mich bei DR. ANDREAS BUTZELAAR und DR. STEFAN FRECH, die mich bereits anlässlich meiner Vertieferarbeit als Erstes auf freundlich in im Arbeitskreis willkommen hießen. Ihr habt mir viele Dinge im Labor beigebracht und standet mir mit Rat und Tat zur Seite. Auch außerhalb des Labors wart ihr immer für einen Spaß zu haben.

Selbstverständlich danke ich auch allen aktiven Mitgliedern und Ehemaligen des Labors 322, darunter LARS WESTENDARP, JAKOB BECKER, BENEDIKT SCHWALM und MAX MIKUROV, aber vor allem DR. SERGEJ BARABAN und NICO ZUBER. Nicht nur wart ihr beiden die besten Laborkollegen, die ich mir hätte wünschen können, sondern ihr

wurdet auch zu sehr guten Freunden für mich. Unsere gemeinsame Zeit, egal ob im Labor, im „Spezizimmer“ oder außerhalb der Uni, habe ich sehr genossen. Dank euch konnte man sich jeden Tag freuen, zur Arbeit zu kommen.

In diesem Zusammenhang möchte ich mich auch bei DANIEL DÖPPING und ALEXANDER GRIMM bedanken, die mir in wissenschaftlichen Diskussionen oft weiterhalfen und ohne die der donnerstägliche Feierabend nicht der gewesen wäre, der er war.

Natürlich möchte ich mich auch bei allen anderen Mitgliedern und Ehemaligen des Arbeitskreises bedanken, die mich auf diesem Weg begleitet haben, unter anderem DR. YOSUKE AKAE, CORNELIUS HUB, DR. MORITZ KÖHLER, DR. VICTORIA LE, BJÖRN SCHMIDT und KLARA URBSCHAT.

Meinen langjährigen Freunden aus dem gemeinsamen Studium, insbesondere DR. STEFAN HERZOG und DR. FABIAN WEICK, möchte ich von Herzen danken. Von den 8-Uhr-Vorlesungen an einem Montag, über die geteilten Abzüge in den Praktika bis hin zur gemeinsamen Abschlussarbeit ihr wart immer an meiner Seite und seid mit mir durch alle Höhen und Tiefen des Studiums gegangen. Auch wenn sich jetzt unsere Wege getrennt haben, wird diese Freundschaft, welche vor knapp 10 Jahren begonnen hat, weiter bestehen.

Dank gilt den Mitgliedern des Arbeitskreis Wilhelm, darunter ANIKA GOECKE, TAMARA MEYER, SARAH PALLOKS und MAX SCHUßMANN, für die gemeinsame Zeit in der Mensa, dem Kaffee danach und den lustigen Gesprächen am Feierabend.

LISA HIRSCH, SVEN KLEHENZ und RITA MICHENFELDER möchte ich für die großartigen Gespräche und Unternehmung abseits der Arbeit danken. Auch wenn wir uns erst recht spät in der Promotion kennengelernt haben, habe ich jede Sekunde davon genossen.

Zu guter Letzt aber nicht weniger wichtig, danke ich meiner Familie und meinen Freunden, welche über die Jahre hinweg immer an meiner Seite waren und die mich unterschützt haben.

12. Literature

- (1) Njuguna, J.; Pielichowski, K. Polymer Nanocomposites for Aerospace Applications: Properties. *Adv Eng Mater* **2003**, *5* (11), 769–778. <https://doi.org/10.1002/adem.200310101>.
- (2) *Polymer Composites in the Aerospace Industry*; Elsevier, 2020. <https://doi.org/10.1016/C2017-0-03502-4>.
- (3) Xu, X.; He, L.; Zhu, B.; Li, J.; Li, J. Advances in Polymeric Materials for Dental Applications. *Polym Chem* **2017**, *8* (5), 807–823. <https://doi.org/10.1039/C6PY01957A>.
- (4) Rokaya, D.; Srimaneepong, V.; Sapkota, J.; Qin, J.; Siraleartmukul, K.; Siriwongrungson, V. Polymeric Materials and Films in Dentistry: An Overview. *J Adv Res* **2018**, *14*, 25–34. <https://doi.org/10.1016/j.jare.2018.05.001>.
- (5) Selim, M. S.; El-Safty, S. A.; Shenashen, M. A.; Elmarakbi, A. Advances in Polymer/Inorganic Nanocomposite Fabrics for Lightweight and High-Strength Armor and Ballistic-Proof Materials. *Chemical Engineering Journal* **2024**, 152422. <https://doi.org/10.1016/j.cej.2024.152422>.
- (6) Selke, S. E. M. Packaging: Polymers in Flexible Packaging. In *Reference Module in Materials Science and Materials Engineering*; Elsevier, 2019. <https://doi.org/10.1016/B978-0-12-803581-8.02168-8>.
- (7) Kurtz, S. M. *UHMWPE Biomaterials Handbook: Ultra High Molecular Weight Polyethylene in Total Joint Replacement and Medical Devices*, 2nd ed.; Academic Press, 2009.
- (8) SHEN, F.-W. Ultrahigh-Molecular-Weight Polyethylene (UHMWPE) in Joint Replacement. In *Biomedical Polymers*; Elsevier, 2007; pp 141–173. <https://doi.org/10.1533/9781845693640.141>.
- (9) Bistolfi, A.; Giustra, F.; Bosco, F.; Sabatini, L.; Aprato, A.; Bracco, P.; Bellare, A. Ultra-High Molecular Weight Polyethylene (UHMWPE) for Hip and Knee Arthroplasty: The Present and the Future. *J Orthop* **2021**, *25*, 98–106. <https://doi.org/10.1016/j.jor.2021.04.004>.
- (10) Nawaz Khan, A.; Gupta, M.; Mahajan, P.; Das, A.; Alagirusamy, R. UHMWPE Textiles and Composites. *Textile Progress* **2021**, *53* (4), 183–335. <https://doi.org/10.1080/00405167.2022.2087400>.

- (11) SZWARC, M. 'Living' Polymers. *Nature* **1956**, 178 (4543), 1168–1169. <https://doi.org/10.1038/1781168a0>.
- (12) Morsbach, J.; Müller, A. H. E.; Berger-Nicoletti, E.; Frey, H. Living Polymer Chains with Predictable Molecular Weight and Dispersity via Carbanionic Polymerization in Continuous Flow: Mixing Rate as a Key Parameter. *Macromolecules* **2016**, 49 (14), 5043–5050. <https://doi.org/10.1021/acs.macromol.6b00975>.
- (13) Jenkins, A. D.; Jones, R. G.; Moad, G. Terminology for Reversible-Deactivation Radical Polymerization Previously Called "Controlled" Radical or "Living" Radical Polymerization (IUPAC Recommendations 2010). *Pure and Applied Chemistry* **2009**, 82 (2), 483–491. <https://doi.org/10.1351/PAC-REP-08-04-03>.
- (14) Kato, M.; Kamigaito, M.; Sawamoto, M.; Higashimura, T. Polymerization of Methyl Methacrylate with the Carbon Tetrachloride/Dichlorotris-(Triphenylphosphine)Ruthenium(II)/Methylaluminum Bis(2,6-Di-Tert-Butylphenoxide) Initiating System: Possibility of Living Radical Polymerization. *Macromolecules* **1995**, 28 (5), 1721–1723. <https://doi.org/10.1021/ma00109a056>.
- (15) Wang, J.-S.; Matyjaszewski, K. Controlled/"living" Radical Polymerization. Atom Transfer Radical Polymerization in the Presence of Transition-Metal Complexes. *J Am Chem Soc* **1995**, 117 (20), 5614–5615. <https://doi.org/10.1021/ja00125a035>.
- (16) Solomon, D. H.; Waverley, G. *11 Patent Number: 4*; Vol. 581.
- (17) Chiefari, J.; Chong, Y. K. (Bill); Ercole, F.; Krstina, J.; Jeffery, J.; Le, T. P. T.; Mayadunne, R. T. A.; Meijs, G. F.; Moad, C. L.; Moad, G.; Rizzardo, E.; Thang, S. H. Living Free-Radical Polymerization by Reversible Addition–Fragmentation Chain Transfer: The RAFT Process. *Macromolecules* **1998**, 31 (16), 5559–5562. <https://doi.org/10.1021/ma9804951>.
- (18) Martin, L.; Gody, G.; Perrier, S. Preparation of Complex Multiblock Copolymers via Aqueous RAFT Polymerization at Room Temperature. *Polym Chem* **2015**, 6 (27), 4875–4886. <https://doi.org/10.1039/C5PY00478K>.
- (19) Wieczorek, S.; Krause, E.; Hackbarth, S.; Röder, B.; Hirsch, A. K. H.; Börner, H. G. Exploiting Specific Interactions toward Next-Generation Polymeric Drug Transporters. *J Am Chem Soc* **2013**, 135 (5), 1711–1714. <https://doi.org/10.1021/ja311895z>.

-
- (20) Celasun, S.; Remmler, D.; Schwaar, T.; Weller, M. G.; Du Prez, F.; Börner, H. G. Digging into the Sequential Space of Thiolactone Precision Polymers: A Combinatorial Strategy to Identify Functional Domains. *Angewandte Chemie International Edition* **2019**, *58* (7), 1960–1964. <https://doi.org/10.1002/anie.201810393>.
- (21) Hamuro, Y.; Schneider, J. P.; DeGrado, W. F. De Novo Design of Antibacterial β -Peptides. *J Am Chem Soc* **1999**, *121* (51), 12200–12201. <https://doi.org/10.1021/ja992728p>.
- (22) Porter, E. A.; Wang, X.; Lee, H.-S.; Weisblum, B.; Gellman, S. H. Non-Haemolytic β -Amino-Acid Oligomers. *Nature* **2000**, *404* (6778), 565–565. <https://doi.org/10.1038/35007145>.
- (23) Trinh, T. T.; Oswald, L.; Chan-Seng, D.; Lutz, J. Synthesis of Molecularly Encoded Oligomers Using a Chemoselective “AB + CD” Iterative Approach. *Macromol Rapid Commun* **2014**, *35* (2), 141–145. <https://doi.org/10.1002/marc.201300774>.
- (24) Holloway, J. O.; Wetzel, K. S.; Martens, S.; Du Prez, F. E.; Meier, M. A. R. Direct Comparison of Solution and Solid Phase Synthesis of Sequence-Defined Macromolecules. *Polym Chem* **2019**, *10* (28), 3859–3867. <https://doi.org/10.1039/C9PY00558G>.
- (25) Hartmann, L.; Krause, E.; Antonietti, M.; Börner, H. G. Solid-Phase Supported Polymer Synthesis of Sequence-Defined, Multifunctional Poly(Amidoamines). *Biomacromolecules* **2006**, *7* (4), 1239–1244. <https://doi.org/10.1021/bm050884k>.
- (26) Lutz, J.-F.; Ouchi, M.; Liu, D. R.; Sawamoto, M. Sequence-Controlled Polymers. *Science (1979)* **2013**, *341* (6146). <https://doi.org/10.1126/science.1238149>.
- (27) Lutz, J.-F. The Future of Sequence-Defined Polymers. *Eur Polym J* **2023**, *199*, 112465. <https://doi.org/10.1016/j.eurpolymj.2023.112465>.
- (28) Nanjan, P.; Porel, M. Sequence-Defined Non-Natural Polymers: Synthesis and Applications. *Polym Chem* **2019**, *10* (40), 5406–5424. <https://doi.org/10.1039/C9PY00886A>.
- (29) Houshyar, S.; Keddie, D. J.; Moad, G.; Mulder, R. J.; Saubern, S.; Tsanaktsidis, J. The Scope for Synthesis of Macro-RAFT Agents by Sequential Insertion of Single Monomer Units. *Polym Chem* **2012**, *3* (7), 1879. <https://doi.org/10.1039/c2py00529h>.
-

- (30) Tong, X.; Guo, B.; Huang, Y. Toward the Synthesis of Sequence-Controlled Vinyl Copolymers. *Chem. Commun.* **2011**, 47 (5), 1455–1457. <https://doi.org/10.1039/C0CC04807K>.
- (31) *Anionic Polymerization*; Hadjichristidis, N., Hirao, A., Eds.; Springer Japan: Tokyo, 2015. <https://doi.org/10.1007/978-4-431-54186-8>.
- (32) *Functional Polymers by Post-Polymerization Modification*; Theato, P., Klok, H., Eds.; Wiley, 2012. <https://doi.org/10.1002/9783527655427>.
- (33) Singha, N. K.; Gibson, M. I.; Koiry, B. P.; Danial, M.; Klok, H.-A. Side-Chain Peptide-Synthetic Polymer Conjugates via Tandem “Ester-Amide/Thiol–Ene” Post-Polymerization Modification of Poly(Pentafluorophenyl Methacrylate) Obtained Using ATRP. *Biomacromolecules* **2011**, 12 (8), 2908–2913. <https://doi.org/10.1021/bm200469a>.
- (34) Butzelaar, A. J.; Schneider, S.; Molle, E.; Theato, P. Synthesis and Post-Polymerization Modification of Defined Functional Poly(Vinyl Ether)s. *Macromol Rapid Commun* **2021**, 42 (13). <https://doi.org/10.1002/marc.202100133>.
- (35) Odian, G. *Principles of Polymerization*; Wiley, 2004. <https://doi.org/10.1002/047147875X>.
- (36) Stretch, C.; Allen, G. Anionic Polymerization of Styrene. *Polymer (Guildf)* **1961**, 2, 151–160. [https://doi.org/10.1016/0032-3861\(61\)90019-2](https://doi.org/10.1016/0032-3861(61)90019-2).
- (37) Geacintov, C.; Smid, J.; Szwarc, M. **Kinetics of Anionic Polymerization of Styrene in Tetrahydrofuran**. *J Am Chem Soc* **1962**, 84 (13), 2508–2514. <https://doi.org/10.1021/ja00872a012>.
- (38) Patterson, D. B.; Halasa, A. F. Anionic Polymerization of 1,3-Butadiene to Highly Crystalline High Trans-1,4-Poly(Butadiene) with Potassium Catalysts Generated from an Alkyl lithium and Potassium Tert-Amyloxide. *Macromolecules* **1991**, 24 (16), 4489–4494. <https://doi.org/10.1021/ma00016a002>.
- (39) Schulze, S.; Cortese, B.; Rupp, M.; de Croon, M. H. J. M.; Hessel, V.; Couet, J.; Lang, J.; Klemm, E. Investigations on the Anionic Polymerization of Butadiene in Capillaries by Kinetic Measurements and Reactor Simulation. *Green Processing and Synthesis* **2013**, 2 (5). <https://doi.org/10.1515/gps-2013-0059>.
- (40) Xiaolin Shi; Jingyang Jiang. Anionic Polymerization of Acrylonitrile Using a Flow Microreactor System. *Polymer Science, Series B* **2019**, 61 (5), 511–518. <https://doi.org/10.1134/S1560090419050166>.

-
- (41) Estrin, Y. I.; Tarasov, A. E.; Grishchuk, A. A.; Chernyak, A. V.; Badamshina, E. R. Initiation of Anionic Polymerization of Acrylonitrile with Tertiary Amines and Ethylene or Propylene Oxide: Some Mechanistic Aspects. *RSC Adv* **2016**, *6* (108), 106064–106073. <https://doi.org/10.1039/C6RA21181J>.
- (42) Cundall, R. B.; Eley, D. D.; Worrall, J. The Anionic Polymerization of Acrylonitrile. *Journal of Polymer Science* **1962**, *58* (166), 869–880. <https://doi.org/10.1002/pol.1962.1205816655>.
- (43) Ishizone, T.; Goseki, R. Anionic Addition Polymerization (Fundamental). In *Encyclopedia of Polymeric Nanomaterials*; Springer Berlin Heidelberg: Berlin, Heidelberg, 2015; pp 23–33. https://doi.org/10.1007/978-3-642-29648-2_171.
- (44) Herzberger, J.; Niederer, K.; Pohlit, H.; Seiwert, J.; Worm, M.; Wurm, F. R.; Frey, H. Polymerization of Ethylene Oxide, Propylene Oxide, and Other Alkylene Oxides: Synthesis, Novel Polymer Architectures, and Bioconjugation. *Chem Rev* **2016**, *116* (4), 2170–2243. <https://doi.org/10.1021/acs.chemrev.5b00441>.
- (45) Bawn, C. E. H.; Ledwith, A.; McFarlane, N. Anionic Polymerization of Ethylene Oxide in Dimethyl Sulphoxide. *Polymer (Guildf)* **1969**, *10*, 653–659. [https://doi.org/10.1016/0032-3861\(69\)90085-8](https://doi.org/10.1016/0032-3861(69)90085-8).
- (46) Grobelny, Z.; Golba, S.; Jurek-Suliga, J. Mechanism of ϵ -Caprolactone Polymerization in the Presence of Alkali Metal Salts: Investigation of Initiation Course and Determination of Polymers Structure by MALDI-TOF Mass Spectrometry. *Polymer Bulletin* **2019**, *76* (7), 3501–3515. <https://doi.org/10.1007/s00289-018-2554-0>.
- (47) Hsieh, H.; Quirk, R. P. *Anionic Polymerization*; CRC Press, 1996. <https://doi.org/10.1201/9780585139401>.
- (48) Lechner, Gehrke, Nordmeier - *Makromolekulare Chemie*; Seiffert, S., Kummerlöwe, C., Vennemann, N., Eds.; Springer Berlin Heidelberg: Berlin, Heidelberg, 2020. <https://doi.org/10.1007/978-3-662-61109-8>.
- (49) Braun, D. Origins and Development of Initiation of Free Radical Polymerization Processes. *Int J Polym Sci* **2009**, *2009*, 1–10. <https://doi.org/10.1155/2009/893234>.
- (50) Kwon, W.; Rho, Y.; Kamoshida, K.; Kwon, K. H.; Jeong, Y. C.; Kim, J.; Misaka, H.; Shin, T. J.; Kim, J.; Kim, K. W.; Jin, K. S.; Chang, T.; Kim, H.; Satoh, T.; Kakuchi, T.; Ree, M. Well-Defined Functional Linear Aliphatic Diblock Copolyethers: A Versatile Linear Aliphatic Polyether Platform for Selective
-

- Functionalizations and Various Nanostructures. *Adv Funct Mater* **2012**, 22 (24), 5194–5208. <https://doi.org/10.1002/adfm.201201101>.
- (51) Schwesinger, R.; Schlemper, H.; Hasenfratz, C.; Willaredt, J.; Dambacher, T.; Breuer, T.; Ottaway, C.; Fletschinger, M.; Boele, J.; Fritz, H.; Putzas, D.; Rotter, H. W.; Bordwell, F. G.; Satish, A. V.; Ji, G.; Peters, E.; Peters, K.; von Schnering, H. G.; Walz, L. Extremely Strong, Uncharged Auxiliary Bases; Monomeric and Polymer-Supported Polyaminophosphazenes (P_2-P_5). *Liebigs Annalen* **1996**, 1996 (7), 1055–1081. <https://doi.org/10.1002/jlac.199619960705>.
- (52) Esswein, B.; Möller, M. Polymerization of Ethylene Oxide with Alkylolithium Compounds and the Phosphazene Base “ $t\text{Bu}P_4$.” *Angewandte Chemie International Edition in English* **1996**, 35 (6), 623–625. <https://doi.org/10.1002/anie.199606231>.
- (53) Puchelle, V.; Du, H.; Illy, N.; Guégan, P. Polymerization of Epoxide Monomers Promoted by: $t\text{Bu}P_4$ phosphazene Base: A Comparative Study of Kinetic Behavior. *Polym Chem* **2020**, 11 (21), 3585–3592. <https://doi.org/10.1039/d0py00437e>.
- (54) Clark, J.; Macquarrie, D.; Sage, V.; Shorrock, K.; Wilson, K. Polymerisations in Mesoporous Environments; 2002; pp 631–633. [https://doi.org/10.1016/S0167-2991\(02\)80599-7](https://doi.org/10.1016/S0167-2991(02)80599-7).
- (55) Karthikeyan, S.; Gupta, V. K. Highly Reactive Polyisobutylene through Cationic Polymerization of Isobutylene. *Journal of Polymer Research* **2023**, 30 (9), 337. <https://doi.org/10.1007/s10965-023-03706-6>.
- (56) Shiman, D. I.; Vasilenko, I. V.; Kostjuk, S. V. Cationic Polymerization of Isobutylene by $AlCl_3$ /Ether Complexes in Non-Polar Solvents: Effect of Ether Structure on the Selectivity of β -H Elimination. *Polymer (Guildf)* **2013**, 54 (9), 2235–2242. <https://doi.org/10.1016/j.polymer.2013.02.039>.
- (57) Hulnik, M.; Trofimuk, D.; Nikishau, P. A.; Kiliclar, H. C.; Kiskan, B.; Kostjuk, S. V. Visible-Light-Induced Cationic Polymerization of Isobutylene: A Route toward the Synthesis of End-Functional Polyisobutylene. *ACS Macro Lett* **2023**, 12 (8), 1125–1131. <https://doi.org/10.1021/acsmacrolett.3c00384>.
- (58) Kottisch, V.; O’Leary, J.; Michaudel, Q.; Stache, E. E.; Lambert, T. H.; Fors, B. P. Controlled Cationic Polymerization: Single-Component Initiation under Ambient Conditions. *J Am Chem Soc* **2019**, 141 (27), 10605–10609. <https://doi.org/10.1021/jacs.9b04961>.

- (59) You, S.; Wei, X.; Liu, R.; Zhao, C.; Zhao, M.; Shi, Q.; Gong, G.; Wu, Y. Suspension and Emulsion Aqueous Cationic Homopolymerization and Copolymerization of Cyclohexyl Vinyl Ether by B(C₆F₅)₃ Initiating System. *Polymer (Guildf)* **2022**, *256*, 125183. <https://doi.org/10.1016/j.polymer.2022.125183>.
- (60) Cramail, H.; Deffieux, A. Living Cationic Polymerization of Cyclohexyl Vinyl Ether. *Macromol Chem Phys* **1994**, *195* (1), 217–227. <https://doi.org/10.1002/macp.1994.021950120>.
- (61) Verebéli, K.; Iván, B. Cationic Polymerization of Styrene by the TiCl₄/N,N,N',N'-Tetramethylethylenediamine(TMEDA) Catalyst System in Benzotrifluoride, an Environmentally Benign Solvent, at Room Temperature. *Polymer (Guildf)* **2012**, *53* (16), 3426–3431. <https://doi.org/10.1016/j.polymer.2012.05.055>.
- (62) Banerjee, S.; Paira, T. K.; Kotal, A.; Mandal, T. K. Room Temperature Living Cationic Polymerization of Styrene with HX-Styrenic Monomer Adduct/FeCl₃ Systems in the Presence of Tetrabutylammonium Halide and Tetraalkylphosphonium Bromide Salts. *Polymer (Guildf)* **2010**, *51* (6), 1258–1269. <https://doi.org/10.1016/j.polymer.2010.01.051>.
- (63) Aoshima, S.; Segawa, Y.; Okada, Y. Cationic Polymerization of Styrene in the Presence of Added Base: Living Nature of the Propagating Species and Synthesis of Poly(Vinyl Alcohol)-Graft-Polystyrene. *J Polym Sci A Polym Chem* **2001**, *39* (5), 751–755. [https://doi.org/10.1002/1099-0518\(20010301\)39:5<751::AID-POLA1048>3.0.CO;2-H](https://doi.org/10.1002/1099-0518(20010301)39:5<751::AID-POLA1048>3.0.CO;2-H).
- (64) Masuda, T.; Sawamoto, M.; Higashimura, T. Cationic Polymerization of Styrenes by Protonic Acids and Their Derivatives, 1. Rates and Molecular Weight Distributions of Polystyrenes Formed by Some Sulfonic Superacids. *Die Makromolekulare Chemie* **1976**, *177* (10), 2981–2993. <https://doi.org/10.1002/macp.1976.021771014>.
- (65) Sawamoto, M.; Masuda, T.; Higashimura, T.; Kobayashi, S.; Saegusa, T. Cationic Polymerization of Styrenes by Protonic Acids and Their Derivatives, 3. Propagating Species in the Polymerization of Styrene by Trifluoroacetic Acid. *Die Makromolekulare Chemie* **1977**, *178* (2), 389–399. <https://doi.org/10.1002/macp.1977.021780211>.
- (66) Saitoh, R.; Kanazawa, A.; Kanaoka, S.; Aoshima, S. Cationic Polymerization of P-Methylstyrene Using Various Metal Chlorides: Design Rationale of Initiating

- Systems for Controlled Polymerization of Styrenes. *Polym J* **2016**, 48 (9), 933–940. <https://doi.org/10.1038/pj.2016.43>.
- (67) Rashkov, I.; Gitsov, I.; Panayotov, I. Cationic Polymerization Initiated by Intercalation Compounds of Lewis Acids. *Polymer Bulletin* **1983**, 10 (11–12), 487–490. <https://doi.org/10.1007/BF00285365>.
- (68) Kanazawa, A.; Kanaoka, S.; Aoshima, S. Cationic Polymerization of Isobutyl Vinyl Ether Using Alcohols Both as Cationogen and Catalyst-modifying Reagent: Effect of Lewis Acids and Alcohols on Living Nature. *J Polym Sci A Polym Chem* **2010**, 48 (11), 2509–2516. <https://doi.org/10.1002/pola.24009>.
- (69) Kunitake, T.; Takarabe, K. Cationic Polymerization of Styrene by CF₃SO₃H. An Investigation by Stopped-Flow/Rapid-Scan Spectrophotometry and Rapid Quenching. *Polym J* **1978**, 10 (1), 105–110. <https://doi.org/10.1295/polymj.10.105>.
- (70) Evans, A. G.; Meadows, G. W. Polymerization of Isobutene Catalyzed by Boron Trifluoride. *Journal of Polymer Science* **1949**, 4 (3), 359–376. <https://doi.org/10.1002/pol.1949.120040311>.
- (71) Rozentsvet, V. A.; Ulyanova, D. M.; Sablina, N. A.; Kostjuk, S. V.; Sidorenko, N. V.; Tolstoy, P. M. Diethylaluminum Chloride-Co-Initiated Cationic Polymerization of Isoprene: Dramatic Effect of the Nature of Alkyl Halide on the Properties of Synthesized Polymers. *Journal of Macromolecular Science, Part A* **2023**, 60 (10), 705–716. <https://doi.org/10.1080/10601325.2023.2257739>.
- (72) Sawamoto, M.; Ouchi, M. Cationic Addition Polymerization (Fundamental). In *Encyclopedia of Polymeric Nanomaterials*; Springer Berlin Heidelberg: Berlin, Heidelberg, 2015; pp 320–324. https://doi.org/10.1007/978-3-642-29648-2_175.
- (73) Kricheldorf, H. R.; Jonté, J. M.; Dunsing, R. Polylactones, 7. The Mechanism of Cationic Polymerization of B-propiolactone and E-caprolactone. *Die Makromolekulare Chemie* **1986**, 187 (4), 771–785. <https://doi.org/10.1002/macp.1986.021870408>.
- (74) Kricheldorf, H. R.; Kreiser-Saunders, I. Polylactones, 19. Anionic Polymerization of ϵ -lactide in Solution. *Die Makromolekulare Chemie* **1990**, 191 (5), 1057–1066. <https://doi.org/10.1002/macp.1990.021910508>.
- (75) Hofman, A.; Słomkowski, S.; Penczek, S. Structure of Active Centers and Mechanism of the Anionic Polymerization of Lactones. *Die Makromolekulare Chemie* **1984**, 185 (1), 91–101. <https://doi.org/10.1002/macp.1984.021850110>.

-
- (76) ROTHE, M.; BERTALAN, G. Mechanism of the Cationic Polymerization of Lactams; 1977; pp 129–144. <https://doi.org/10.1021/bk-1977-0059.ch009>.
- (77) Winnacker, M.; Neumeier, M.; Zhang, X.; Papadakis, C. M.; Rieger, B. Sustainable Chiral Polyamides with High Melting Temperature via Enhanced Anionic Polymerization of a Menthone-Derived Lactam. *Macromol Rapid Commun* **2016**, 37 (10), 851–857. <https://doi.org/10.1002/marc.201600056>.
- (78) Dane, E. L.; Grinstaff, M. W. Poly-Amido-Saccharides: Synthesis via Anionic Polymerization of a β -Lactam Sugar Monomer. *J Am Chem Soc* **2012**, 134 (39), 16255–16264. <https://doi.org/10.1021/ja305900r>.
- (79) Hashimoto, K. Ring-Opening Polymerization of Lactams. Living Anionic Polymerization and Its Applications. *Prog Polym Sci* **2000**, 25 (10), 1411–1462. [https://doi.org/10.1016/S0079-6700\(00\)00018-6](https://doi.org/10.1016/S0079-6700(00)00018-6).
- (80) Hrkach, J. S.; Matyjaszewski, K. Cationic Polymerization of Tetrahydrofuran Initiated by Trimethylsilyl Trifluoromethanesulfonate. *Macromolecules* **1990**, 23 (18), 4042–4046. <https://doi.org/10.1021/ma00220a003>.
- (81) Shipp, D. A. Reversible-Deactivation Radical Polymerizations. *Polymer Reviews* **2011**, 51 (2), 99–103. <https://doi.org/10.1080/15583724.2011.566406>.
- (82) Perrier, S. *50th Anniversary Perspective*: RAFT Polymerization—A User Guide. *Macromolecules* **2017**, 50 (19), 7433–7447. <https://doi.org/10.1021/acs.macromol.7b00767>.
- (83) Truong, N. P.; Jones, G. R.; Bradford, K. G. E.; Konkolewicz, D.; Anastasaki, A. A Comparison of RAFT and ATRP Methods for Controlled Radical Polymerization. *Nat Rev Chem* **2021**, 5 (12), 859–869. <https://doi.org/10.1038/s41570-021-00328-8>.
- (84) Chen, J.; Chu, J.; Zhang, K. Atom Transfer Radical Polymerizations of Methyl Methacrylate Catalyzed by EBiB/SnCl₂·2H₂O(FeCl₂·4H₂O)/FeCl₃·6H₂O/MA5-DETA Systems. *Polymer (Guildf)* **2004**, 45 (1), 151–155. <https://doi.org/10.1016/j.polymer.2003.10.050>.
- (85) Wang, Y.; Kwak, Y.; Matyjaszewski, K. Enhanced Activity of ATRP Fe Catalysts with Phosphines Containing Electron Donating Groups. *Macromolecules* **2012**, 45 (15), 5911–5915. <https://doi.org/10.1021/ma3010795>.
- (86) Britten, C. N.; Lason, K.; Walters, K. B. Facile Synthesis of Tertiary Amine Pendant Polymers by Cu⁰-Mediated ATRP under Aqueous Conditions.
-

- Macromolecules* **2021**, *54* (22), 10360–10369. <https://doi.org/10.1021/acs.macromol.1c01234>.
- (87) Tang, H.; Shen, Y.; Li, B.; Radosz, M. Tertiary Amine — Enhanced Activity of ATRP Catalysts CuBr/TPMA and CuBr/Me₆TREN. *Macromol Rapid Commun* **2008**, *29* (22), 1834–1838. <https://doi.org/10.1002/marc.200800378>.
- (88) Matyjaszewski, K.; Xia, J. Atom Transfer Radical Polymerization. *Chem Rev* **2001**, *101* (9), 2921–2990. <https://doi.org/10.1021/cr940534g>.
- (89) Whitfield, R.; Parkatzidis, K.; Bradford, K. G. E.; Truong, N. P.; Konkolewicz, D.; Anastasaki, A. Low Ppm CuBr-Triggered Atom Transfer Radical Polymerization under Mild Conditions. *Macromolecules* **2021**, *54* (7), 3075–3083. <https://doi.org/10.1021/acs.macromol.0c02519>.
- (90) Averick, S.; Simakova, A.; Park, S.; Konkolewicz, D.; Magenau, A. J. D.; Mehl, R. A.; Matyjaszewski, K. ATRP under Biologically Relevant Conditions: Grafting from a Protein. *ACS Macro Lett* **2012**, *1* (1), 6–10. <https://doi.org/10.1021/mz200020c>.
- (91) Matyjaszewski, K.; Wang, J.-L.; Grimaud, T.; Shipp, D. A. Controlled/"Living" Atom Transfer Radical Polymerization of Methyl Methacrylate Using Various Initiation Systems. *Macromolecules* **1998**, *31* (5), 1527–1534. <https://doi.org/10.1021/ma971298p>.
- (92) Li, X.; Zhu, X.; Cheng, Z.; Xu, W.; Chen, G. Atom-transfer Radical Polymerization of Methyl Methacrylate with α ,A'-dichloroxylene/CuCl/ N,N,N',N'',N''' - pentamethyldiethylenetriamine Initiation System under Microwave Irradiation. *J Appl Polym Sci* **2004**, *92* (4), 2189–2195. <https://doi.org/10.1002/app.20233>.
- (93) Gurr, P. A.; Mills, M. F.; Qiao, G. G.; Solomon, D. H. Initiator Efficiency in ATRP: The Tosyl Chloride/CuBr/PMDETA System. *Polymer (Guildf)* **2005**, *46* (7), 2097–2104. <https://doi.org/10.1016/j.polymer.2005.01.015>.
- (94) Xue, Z.; He, D.; Xie, X. Iron-Catalyzed Atom Transfer Radical Polymerization. *Polym Chem* **2015**, *6* (10), 1660–1687. <https://doi.org/10.1039/C4PY01457J>.
- (95) Zhu, G.; Zhang, L.; Zhang, Z.; Zhu, J.; Tu, Y.; Cheng, Z.; Zhu, X. Iron-Mediated ICAR ATRP of Methyl Methacrylate. *Macromolecules* **2011**, *44* (9), 3233–3239. <https://doi.org/10.1021/ma102958y>.
- (96) Kim, S.; Kim, C.; Chung, H. N-Heterocyclic Carbene Containing Homogeneous Ru Catalyst for Aqueous Atom Transfer Radical Polymerization of Water-Soluble

- Vinyl Monomers. *Polymer (Guildf)* **2022**, 241, 124537. <https://doi.org/10.1016/j.polymer.2022.124537>.
- (97) Afonso, M. B. A.; Cruz, T. R.; Silva, Y. F.; Pereira, J. C. A.; Machado, A. E. H.; Goi, B. E.; Lima-Neto, B. S.; Carvalho-Jr, V. P. Ruthenium(II) Complexes of Schiff Base Derived from Cycloalkylamines as Pre-Catalysts for ROMP of Norbornene and ATRP of Methyl Methacrylate. *J Organomet Chem* **2017**, 851, 225–234. <https://doi.org/10.1016/j.jorganchem.2017.09.043>.
- (98) Braunecker, W. A.; Itami, Y.; Matyjaszewski, K. Osmium-Mediated Radical Polymerization. *Macromolecules* **2005**, 38 (23), 9402–9404. <https://doi.org/10.1021/ma051877r>.
- (99) Szczepaniak, G.; Fu, L.; Jafari, H.; Kapil, K.; Matyjaszewski, K. Making ATRP More Practical: Oxygen Tolerance. *Acc Chem Res* **2021**, 54 (7), 1779–1790. <https://doi.org/10.1021/acs.accounts.1c00032>.
- (100) Buss, B. L.; Beck, L. R.; Miyake, G. M. Synthesis of Star Polymers Using Organocatalyzed Atom Transfer Radical Polymerization through a Core-First Approach. *Polym Chem* **2018**, 9 (13), 1658–1665. <https://doi.org/10.1039/C7PY01833A>.
- (101) Gao, H.; Matyjaszewski, K. Structural Control in ATRP Synthesis of Star Polymers Using the Arm-First Method. *Macromolecules* **2006**, 39 (9), 3154–3160. <https://doi.org/10.1021/ma060223v>.
- (102) Gao, H.; Matyjaszewski, K. Synthesis of Star Polymers by a Combination of ATRP and the “Click” Coupling Method. *Macromolecules* **2006**, 39 (15), 4960–4965. <https://doi.org/10.1021/ma060926c>.
- (103) un Nisa, Q.; Theobald, W.; Hepburn, K. S.; Riddlestone, I.; Bingham, N. M.; Kopeć, M.; Roth, P. J. Degradable Linear and Bottlebrush Thioester-Functional Copolymers through Atom-Transfer Radical Ring-Opening Copolymerization of a Thionolactone. *Macromolecules* **2022**, 55 (17), 7392–7400. <https://doi.org/10.1021/acs.macromol.2c01317>.
- (104) Mukumoto, K.; Li, Y.; Nese, A.; Sheiko, S. S.; Matyjaszewski, K. Synthesis and Characterization of Molecular Bottlebrushes Prepared by Iron-Based ATRP. *Macromolecules* **2012**, 45 (23), 9243–9249. <https://doi.org/10.1021/ma3020867>.
- (105) Xu, J.; Qiu, M.; Ma, B.; He, C. “Near Perfect” Amphiphilic Conetwork Based on End-Group Cross-Linking of Polydimethylsiloxane Triblock Copolymer via Atom

- Transfer Radical Polymerization. *ACS Appl Mater Interfaces* **2014**, 6 (17), 15283–15290. <https://doi.org/10.1021/am5037252>.
- (106) Sha, J.; Lippmann, E. S.; McNulty, J.; Ma, Y.; Ashton, R. S. Sequential Nucleophilic Substitutions Permit Orthogonal Click Functionalization of Multicomponent PEG Brushes. *Biomacromolecules* **2013**, 14 (9), 3294–3303. <https://doi.org/10.1021/bm400900r>.
- (107) Tsarevsky, N. V.; Sumerlin, B. S.; Matyjaszewski, K. Step-Growth “Click” Coupling of Telechelic Polymers Prepared by Atom Transfer Radical Polymerization. *Macromolecules* **2005**, 38 (9), 3558–3561. <https://doi.org/10.1021/ma050370d>.
- (108) Yurteri, S.; Cianga, I.; Yagci, Y. Synthesis and Characterization of α , ω - Telechelic Polymers by Atom Transfer Radical Polymerization and Coupling Processes. *Macromol Chem Phys* **2003**, 204 (14), 1771–1783. <https://doi.org/10.1002/macp.200300030>.
- (109) Moad, G. Dithioesters in <sc>RAFT</Sc> Polymerization. In *RAFT Polymerization*; Wiley, 2021; pp 223–358. <https://doi.org/10.1002/9783527821358.ch8>.
- (110) Favier, A.; Charreyre, M.-T.; Chaumont, P.; Pichot, C. Study of the RAFT Polymerization of a Water-Soluble Bisubstituted Acrylamide Derivative. 1. Influence of the Dithioester Structure. *Macromolecules* **2002**, 35 (22), 8271–8280. <https://doi.org/10.1021/ma020550c>.
- (111) Benaglia, M.; Rizzardo, E.; Alberti, A.; Guerra, M. Searching for More Effective Agents and Conditions for the RAFT Polymerization of MMA: Influence of Dithioester Substituents, Solvent, and Temperature. *Macromolecules* **2005**, 38 (8), 3129–3140. <https://doi.org/10.1021/ma0480650>.
- (112) Gapin, A.; Wurm, F. R. Trithiocarbonate-Mediated RAFT Polymerization Enables the Synthesis of Homotelechelic *N*-Vinylpyrrolidone Oligomers with Surfactant Properties. *ACS Appl Polym Mater* **2022**, 4 (10), 6863–6870. <https://doi.org/10.1021/acsapm.2c00796>.
- (113) Chen, S.; Binder, W. H. Controlled Copolymerization of *N*-Butyl Acrylate with Semifluorinated Acrylates by RAFT Polymerization. *Polym Chem* **2015**, 6 (3), 448–458. <https://doi.org/10.1039/C4PY01084A>.
- (114) Mayadunne, R. T. A.; Rizzardo, E.; Chiefari, J.; Krstina, J.; Moad, G.; Postma, A.; Thang, S. H. Living Polymers by the Use of Trithiocarbonates as Reversible

- Addition–Fragmentation Chain Transfer (RAFT) Agents: ABA Triblock Copolymers by Radical Polymerization in Two Steps. *Macromolecules* **2000**, *33* (2), 243–245. <https://doi.org/10.1021/ma991451a>.
- (115) Gardiner, J.; Martinez-Botella, I.; Tsanaktsidis, J.; Moad, G. Dithiocarbamate RAFT Agents with Broad Applicability – the 3,5-Dimethyl-1H-Pyrazole-1-Carbodithioates. *Polym Chem* **2016**, *7* (2), 481–492. <https://doi.org/10.1039/C5PY01382H>.
- (116) Moad, G. A Critical Survey of Dithiocarbamate Reversible Addition-Fragmentation Chain Transfer (RAFT) Agents in Radical Polymerization. *J Polym Sci A Polym Chem* **2019**, *57* (3), 216–227. <https://doi.org/10.1002/pola.29199>.
- (117) Keddie, D. J.; Moad, G.; Rizzardo, E.; Thang, S. H. RAFT Agent Design and Synthesis. *Macromolecules* **2012**, *45* (13), 5321–5342. <https://doi.org/10.1021/ma300410v>.
- (118) Werner, M.; Oliveira, J. C. A.; Meiser, W.; Buback, M.; Mata, R. A. Critical Assessment of RAFT Equilibrium Constants: Theory Meets Experiment. *Macromol Theory Simul* **2020**, *29* (5). <https://doi.org/10.1002/mats.202000022>.
- (119) Moad, G.; Rizzardo, E.; Thang, S. H. Living Radical Polymerization by the RAFT Process. *Aust J Chem* **2005**, *58* (6), 379. <https://doi.org/10.1071/CH05072>.
- (120) Gody, G.; Maschmeyer, T.; Zetterlund, P. B.; Perrier, S. Rapid and Quantitative One-Pot Synthesis of Sequence-Controlled Polymers by Radical Polymerization. *Nat Commun* **2013**, *4* (1), 2505. <https://doi.org/10.1038/ncomms3505>.
- (121) Fischer, H. The Persistent Radical Effect: A Principle for Selective Radical Reactions and Living Radical Polymerizations. *Chem Rev* **2001**, *101* (12), 3581–3610. <https://doi.org/10.1021/cr990124y>.
- (122) Georges, M. K.; Veregin, R. P. N.; Kazmaier, P. M.; Hamer, G. K. Narrow Molecular Weight Resins by a Free-Radical Polymerization Process. *Macromolecules* **1993**, *26* (11), 2987–2988. <https://doi.org/10.1021/ma00063a054>.
- (123) Hawker, C. J. Molecular Weight Control by a “Living” Free-Radical Polymerization Process. *J Am Chem Soc* **1994**, *116* (24), 11185–11186. <https://doi.org/10.1021/ja00103a055>.

- (124) Miura, Y.; Hirota, K.; Moto, H.; Yamada, B. High-Yield Synthesis of Functionalized Alkoxyamine Initiators and Approach to Well-Controlled Block Copolymers Using Them. *Macromolecules* **1999**, *32* (25), 8356–8362. <https://doi.org/10.1021/ma9907542>.
- (125) Li, I. Q.; Knauss, D. M.; Priddy, D. B.; Howell, B. A. Synthesis and Reactivity of Functionalized Alkoxyamine Initiators for Nitroxide-mediated Radical Polymerization of Styrene. *Polym Int* **2003**, *52* (5), 805–812. <https://doi.org/10.1002/pi.1168>.
- (126) Nicolas, J.; Guillaneuf, Y. Living Radical Polymerization: Nitroxide-Mediated Polymerization. In *Encyclopedia of Polymeric Nanomaterials*; Springer Berlin Heidelberg: Berlin, Heidelberg, 2014; pp 1–16. https://doi.org/10.1007/978-3-642-36199-9_191-1.
- (127) Gibson, M. I.; Fröhlich, E.; Klok, H. Postpolymerization Modification of Poly(Pentafluorophenyl Methacrylate): Synthesis of a Diverse Water-soluble Polymer Library. *J Polym Sci A Polym Chem* **2009**, *47* (17), 4332–4345. <https://doi.org/10.1002/pola.23486>.
- (128) Kolb, H. C.; Finn, M. G.; Sharpless, K. B. Click Chemistry: Diverse Chemical Function from a Few Good Reactions. *Angewandte Chemie International Edition* **2001**, *40* (11), 2004–2021. [https://doi.org/10.1002/1521-3773\(20010601\)40:11<2004::AID-ANIE2004>3.0.CO;2-5](https://doi.org/10.1002/1521-3773(20010601)40:11<2004::AID-ANIE2004>3.0.CO;2-5).
- (129) Liang, L.; Astruc, D. The Copper(I)-Catalyzed Alkyne-Azide Cycloaddition (CuAAC) “Click” Reaction and Its Applications. An Overview. *Coord Chem Rev* **2011**, *255* (23–24), 2933–2945. <https://doi.org/10.1016/j.ccr.2011.06.028>.
- (130) Döhler, D.; Michael, P.; Binder, W. H. CuAAC-Based Click Chemistry in Self-Healing Polymers. *Acc Chem Res* **2017**, *50* (10), 2610–2620. <https://doi.org/10.1021/acs.accounts.7b00371>.
- (131) Meldal, M. Polymer “Clicking” by CuAAC Reactions. *Macromol Rapid Commun* **2008**, *29* (12–13), 1016–1051. <https://doi.org/10.1002/marc.200800159>.
- (132) Kaczmarek, M.; Przybylska, A.; Szymańska, A.; Dutkiewicz, A.; Maciejewski, H. Thiol-Ene Click Reaction as an Effective Tool for the Synthesis of PEG-Functionalized Alkoxysilanes-Precursors of Anti-Fog Coatings. *Sci Rep* **2023**, *13* (1), 21025. <https://doi.org/10.1038/s41598-023-48192-4>.

- (133) Shibata, M.; Sugane, K.; Yanagisawa, Y. Biobased Polymer Networks by the Thiol-Ene Photopolymerization of Allylated p-Coumaric and Caffeic Acids. *Polym J* **2019**, *51* (5), 461–470. <https://doi.org/10.1038/s41428-018-0165-0>.
- (134) Lowe, A. B. Thiol–Ene “Click” Reactions and Recent Applications in Polymer and Materials Synthesis: A First Update. *Polym. Chem.* **2014**, *5* (17), 4820–4870. <https://doi.org/10.1039/C4PY00339J>.
- (135) Posner, T. Beiträge Zur Kenntniss Der Ungesättigten Verbindungen. II. Ueber Die Addition von Mercaptanen an Ungesättigte Kohlenwasserstoffe. *Berichte der deutschen chemischen Gesellschaft* **1905**, *38* (1), 646–657. <https://doi.org/10.1002/cber.190503801106>.
- (136) Lowe, A. B. Thiol-Ene “Click” Reactions and Recent Applications in Polymer and Materials Synthesis. *Polym. Chem.* **2010**, *1* (1), 17–36. <https://doi.org/10.1039/B9PY00216B>.
- (137) Hoyle, C. E.; Bowman, C. N. Thiol–Ene Click Chemistry. *Angewandte Chemie International Edition* **2010**, *49* (9), 1540–1573. <https://doi.org/10.1002/anie.200903924>.
- (138) Griesbaum, K. Problems and Possibilities of the Free-Radical Addition of Thiols to Unsaturated Compounds. *Angewandte Chemie International Edition in English* **1970**, *9* (4), 273–287. <https://doi.org/10.1002/anie.197002731>.
- (139) Sinha, A. K.; Equbal, D. Thiol–Ene Reaction: Synthetic Aspects and Mechanistic Studies of an Anti-Markovnikov-Selective Hydrothiolation of Olefins. *Asian J Org Chem* **2019**, *8* (1), 32–47. <https://doi.org/10.1002/ajoc.201800639>.
- (140) Semenov, A. N.; Nyrkova, I. A. Statistical Description of Chain Molecules. In *Polymer Science: A Comprehensive Reference*; Elsevier, 2012; pp 3–29. <https://doi.org/10.1016/B978-0-444-53349-4.00002-9>.
- (141) Jenkins, A. D.; Loening, K. L. Nomenclature. In *Comprehensive Polymer Science and Supplements*; Elsevier, 1989; pp 13–54. <https://doi.org/10.1016/B978-0-08-096701-1.00002-1>.
- (142) Bhanu, V. A.; Rangarajan, P.; Wiles, K.; Bortner, M.; Sankarpandian, M.; Godshall, D.; Glass, T. E.; Banthia, A. K.; Yang, J.; Wilkes, G. Synthesis and Characterization of Acrylonitrile Methyl Acrylate Statistical Copolymers as Melt Processable Carbon Fiber Precursors. *Polymer (Guildf)* **2002**, *43* (18), 4841–4850. [https://doi.org/10.1016/S0032-3861\(02\)00330-0](https://doi.org/10.1016/S0032-3861(02)00330-0).

- (143) Jouenne, S.; González-León, J. A.; Ruzette, A.-V.; Lodefier, P.; Tencé-Girault, S.; Leibler, L. Styrene/Butadiene Gradient Block Copolymers: Molecular and Mesoscopic Structures. *Macromolecules* **2007**, *40* (7), 2432–2442. <https://doi.org/10.1021/ma062723u>.
- (144) Hill, D. J. T.; O'Donnell, J. H.; O'Sullivan, P. W. Analysis of the Mechanism of Copolymerization of Styrene and Maleic Anhydride. *Macromolecules* **1985**, *18* (1), 9–17. <https://doi.org/10.1021/ma00143a002>.
- (145) Galindo, C.; Beaudoin, E.; Gigmes, D.; Bertin, D. Polybutadiene-Graft-Polystyrene Copolymer: Grafting Quantification by Liquid Chromatography at Critical Conditions Using Single UV Detection. *J Chromatogr A* **2009**, *1216* (47), 8386–8390. <https://doi.org/10.1016/j.chroma.2009.09.065>.
- (146) Matyjaszewski, K.; Tsarevsky, N. V. Nanostructured Functional Materials Prepared by Atom Transfer Radical Polymerization. *Nat Chem* **2009**, *1* (4), 276–288. <https://doi.org/10.1038/nchem.257>.
- (147) De Neve, J.; Haven, J. J.; Maes, L.; Junkers, T. Sequence-Definition from Controlled Polymerization: The next Generation of Materials. *Polym Chem* **2018**, *9* (38), 4692–4705. <https://doi.org/10.1039/C8PY01190G>.
- (148) Mallela, Y. L. N. K.; Kim, S.; Seo, G.; Kim, J. W.; Kumar, S.; Lee, J.; Lee, J.-S. Crosslinked Poly(Allyl Glycidyl Ether) with Pendant Nitrile Groups as Solid Polymer Electrolytes for Li–S Batteries. *Electrochim Acta* **2020**, *362*, 137141. <https://doi.org/10.1016/j.electacta.2020.137141>.
- (149) Bentley, C. L.; Song, T.; Pedretti, B. J.; Lubben, M. J.; Lynd, N. A.; Brennecke, J. F. Effects of Poly(Glycidyl Ether) Structure and Ether Oxygen Placement on CO₂ Solubility. *J Chem Eng Data* **2021**, *66* (7), 2832–2843. <https://doi.org/10.1021/acs.jced.1c00219>.
- (150) Dimitriou, M. D.; Zhou, Z.; Yoo, H.-S.; Killops, K. L.; Finlay, J. A.; Cone, G.; Sundaram, H. S.; Lynd, N. A.; Barteau, K. P.; Campos, L. M.; Fischer, D. A.; Callow, M. E.; Callow, J. A.; Ober, C. K.; Hawker, C. J.; Kramer, E. J. A General Approach to Controlling the Surface Composition of Poly(Ethylene Oxide)-Based Block Copolymers for Antifouling Coatings. *Langmuir* **2011**, *27* (22), 13762–13772. <https://doi.org/10.1021/la202509m>.
- (151) Feng, J.; Nie, C.; Xie, E.; Thongrom, B.; Reiter-Scherer, V.; Block, S.; Herrmann, A.; Quaas, E.; Sieben, C.; Haag, R. Sulfated Polyglycerol-Modified Hydrogels

- for Binding HSV-1 and RSV. *ACS Appl Mater Interfaces* **2023**, *15* (44), 51894–51904. <https://doi.org/10.1021/acsami.3c09553>.
- (152) Karakyriazis, K.; Lührs, V.; Stößlein, S.; Grunwald, I.; Hartwig, A. Synthesis and Characterization of a Schiff Base Crosslinked Hydrogel Based on Hyperbranched Polyglycerol. *Mater Adv* **2023**, *4* (7), 1648–1655. <https://doi.org/10.1039/D2MA01050J>.
- (153) Lee, B. F.; Kade, M. J.; Chute, J. A.; Gupta, N.; Campos, L. M.; Fredrickson, G. H.; Kramer, E. J.; Lynd, N. A.; Hawker, C. J. Poly(Allyl Glycidyl Ether)-A Versatile and Functional Polyether Platform. *J Polym Sci A Polym Chem* **2011**, *49* (20), 4498–4504. <https://doi.org/10.1002/pola.24891>.
- (154) Antoine, S.; Geng, Z.; Zofchak, E. S.; Chwatko, M.; Fredrickson, G. H.; Ganesan, V.; Hawker, C. J.; Lynd, N. A.; Segalman, R. A. Non-Intuitive Trends in Flory–Huggins Interaction Parameters in Polyether-Based Polymers. *Macromolecules* **2021**, *54* (14), 6670–6677. <https://doi.org/10.1021/acs.macromol.1c00134>.
- (155) Bentley, C. L.; Chwatko, M.; Wheatle, B. K.; Burkey, A. A.; Helenic, A.; Morales-Collazo, O.; Ganesan, V.; Lynd, N. A.; Brennecke, J. F. Modes of Interaction in Binary Blends of Hydrophobic Polyethers and Imidazolium Bis(Trifluoromethylsulfonyl)Imide Ionic Liquids. *Macromolecules* **2020**, *53* (15), 6519–6528. <https://doi.org/10.1021/acs.macromol.0c01155>.
- (156) Puchelle, V.; Latreyte, Y.; Girardot, M.; Garnotel, L.; Levesque, L.; Coutelier, O.; Destarac, M.; Guégan, P.; Illy, N. Functional Poly(Ester-Alt-Sulfide)s Synthesized by Organo-Catalyzed Anionic Ring-Opening Alternating Copolymerization of Oxiranes and γ -Thiobutyrolactones. *Macromolecules* **2020**, *53* (13), 5188–5198. <https://doi.org/10.1021/acs.macromol.0c00261>.
- (157) Gao, T.; Xia, X.; Tajima, K.; Yamamoto, T.; Isono, T.; Satoh, T. Polyether/Polythioether Synthesis via Ring-Opening Polymerization of Epoxides and Episulfides Catalyzed by Alkali Metal Carboxylates. *Macromolecules* **2022**, *55* (21), 9373–9383. <https://doi.org/10.1021/acs.macromol.2c00656>.
- (158) Neitzel, A. E.; Fang, Y. N.; Yu, B.; Romyantsev, A. M.; de Pablo, J. J.; Tirrell, M. V. Polyelectrolyte Complex Coacervation across a Broad Range of Charge Densities. *Macromolecules* **2021**, *54* (14), 6878–6890. <https://doi.org/10.1021/acs.macromol.1c00703>.
- (159) Viviani, M.; Meereboer, N. L.; Saraswati, N. L. P. A.; Loos, K.; Portale, G. Lithium and Magnesium Polymeric Electrolytes Prepared Using Poly(Glycidyl Ether)-

- Based Polymers with Short Grafted Chains. *Polym Chem* **2020**, 11 (12), 2070–2079. <https://doi.org/10.1039/C9PY01735F>.
- (160) Barteau, K. P.; Wolffs, M.; Lynd, N. A.; Fredrickson, G. H.; Kramer, E. J.; Hawker, C. J. Allyl Glycidyl Ether-Based Polymer Electrolytes for Room Temperature Lithium Batteries. *Macromolecules* **2013**, 46 (22), 8988–8994. <https://doi.org/10.1021/ma401267w>.
- (161) Heinen, S.; Rackow, S.; Cuellar-Camacho, J. L.; Donskyi, I. S.; Unger, W. E. S.; Weinhart, M. Transfer of Functional Thermoresponsive Poly(Glycidyl Ether) Coatings for Cell Sheet Fabrication from Gold to Glass Surfaces. *J Mater Chem B* **2018**, 6 (10), 1489–1500. <https://doi.org/10.1039/C7TB03263C>.
- (162) Jain, S.; Neumann, K.; Zhang, Y.; Geng, J.; Bradley, M. Tetrazine-Mediated Postpolymerization Modification. *Macromolecules* **2016**, 49 (15), 5438–5443. <https://doi.org/10.1021/acs.macromol.6b00867>.
- (163) Park, S.; Chung, M.; Lamprou, A.; Seidel, K.; Song, S.; Schade, C.; Lim, J.; Char, K. High Strength, Epoxy Cross-Linked High Sulfur Content Polymers from One-Step Reactive Compatibilization Inverse Vulcanization. *Chem Sci* **2022**, 13 (2), 566–572. <https://doi.org/10.1039/D1SC05896G>.
- (164) Burkey, A. A.; Ghousifam, N.; Hillsley, A. V.; Brotherton, Z. W.; Rezaeeyazdi, M.; Hatridge, T. A.; Harris, D. T.; Sprague, W. W.; Sandoval, B. E.; Rosales, A. M.; Rylander, M. N.; Lynd, N. A. Synthesis of Poly(Allyl Glycidyl Ether)-Derived Polyampholytes and Their Application to the Cryopreservation of Living Cells. *Biomacromolecules* **2023**, 24 (3), 1475–1482. <https://doi.org/10.1021/acs.biomac.2c01488>.
- (165) Son, H.; Jang, Y.; Koo, J.; Lee, J.-S.; Theato, P.; Char, K. Penetration and Exchange Kinetics of Primary Alkyl Amines Applied to Reactive Poly(Pentafluorophenyl Acrylate) Thin Films. *Polym J* **2016**, 48 (4), 487–495. <https://doi.org/10.1038/pj.2016.6>.
- (166) Lin, J.; Ma, H.; Wang, Z.; Zhou, S.; Yan, B.; Shi, F.; Yan, Q.; Wang, J.; Fan, H.; Xiang, J. 808 Nm Near-Infrared Light-Triggered Payload Release from Green Light-Responsive Donor–Acceptor Stenhouse Adducts Polymer-Coated Upconversion Nanoparticles. *Macromol Rapid Commun* **2021**, 42 (19). <https://doi.org/10.1002/marc.202100318>.
- (167) Lee, Y.; Pyun, J.; Lim, J.; Char, K. Modular Synthesis of Functional Polymer Nanoparticles from a Versatile Platform Based on

- Poly(Pentafluorophenylmethacrylate). *J Polym Sci A Polym Chem* **2016**, *54* (13), 1895–1901. <https://doi.org/10.1002/pola.28071>.
- (168) Lee, Y.; Hanif, S.; Theato, P.; Zentel, R.; Lim, J.; Char, K. Facile Synthesis of Fluorescent Polymer Nanoparticles by Covalent Modification–Nanoprecipitation of Amine-Reactive Ester Polymers. *Macromol Rapid Commun* **2015**, *36* (11), 1089–1095. <https://doi.org/10.1002/marc.201500003>.
- (169) Jafari, A.; Rajabian, N.; Zhang, G.; Alaa Mohamed, M.; Lei, P.; Andreadis, S. T.; Pfeifer, B. A.; Cheng, C. PEGylated Amine-Functionalized Poly(ϵ -Caprolactone) for the Delivery of Plasmid DNA. *Materials* **2020**, *13* (4), 898. <https://doi.org/10.3390/ma13040898>.
- (170) Desmet, G. B.; D'hooge, D. R.; Sabbe, M. K.; Reyniers, M.-F.; Marin, G. B. Computational Investigation of the Aminolysis of RAFT Macromolecules. *J Org Chem* **2016**, *81* (23), 11626–11634. <https://doi.org/10.1021/acs.joc.6b01844>.
- (171) Roth, P. J.; Haase, M.; Basché, T.; Theato, P.; Zentel, R. Synthesis of Heterotelechelic α,ω Dye-Functionalized Polymer by the RAFT Process and Energy Transfer between the End Groups. *Macromolecules* **2010**, *43* (2), 895–902. <https://doi.org/10.1021/ma902391b>.
- (172) Molle, E. Functional Polymers by Post-Polymerization Modification and Electrochemistry, Karlsruher Institut für Technologie, Karlsruhe, 2021.
- (173) Das, A.; Theato, P. Multifaceted Synthetic Route to Functional Polyacrylates by Transesterification of Poly(Pentafluorophenyl Acrylates). *Macromolecules* **2015**, *48* (24), 8695–8707. <https://doi.org/10.1021/acs.macromol.5b02293>.
- (174) Makiguchi, K.; Satoh, T.; Kakuchi, T. Diphenyl Phosphate as an Efficient Cationic Organocatalyst for Controlled/Living Ring-Opening Polymerization of δ -Valerolactone and ϵ -Caprolactone. *Macromolecules* **2011**, *44* (7), 1999–2005. <https://doi.org/10.1021/ma200043x>.
- (175) Kerman, I.; Toppare, L.; Yilmaz, F.; Yagci, Y. Thiophene Ended ϵ -Caprolactone Conducting Copolymers and Their Electrochromic Properties. *Journal of Macromolecular Science, Part A* **2005**, *42* (4), 509–520. <https://doi.org/10.1081/MA-200054363>.
- (176) Wang, J.; Shi, Y.; Mao, B.; Zhang, B.; Yang, J.; Hu, Z.; Liao, W. Biomaterials for Inflammatory Bowel Disease: Treatment, Diagnosis and Organoids. *Appl Mater Today* **2024**, *36*, 102078. <https://doi.org/10.1016/j.apmt.2024.102078>.

- (177) Schneider, S.; Schwalm, B. L.; Theato, P. AROMA: Anionic Ring-Opening Monomer Addition of Allyl Glycidyl Ether to Methoxy Poly(Ethylene Glycol) for the Synthesis of Sequence-Controlled Polymers. *Programmable Materials* **2023**, *1*, e8. <https://doi.org/10.1017/pma.2023.7>.
- (178) Baskaran, D.; Müller, A. H. E. Anionic Vinyl Polymerization. In *Controlled and Living Polymerizations*; Wiley, 2009; pp 1–56. <https://doi.org/10.1002/9783527629091.ch1>.
- (179) Gorin, Yu. A.; Skripova, L. S.; Charskaya, K. N.; Menligaziev, E. Zh. A Spectroscopic Study of the Interaction of Some Cyclic Oxides with Triisobutylaluminum. *J Appl Spectrosc* **1971**, *15* (1), 889–892. <https://doi.org/10.1007/BF00611366>.
- (180) Vrandečić, N. S.; Erceg, M.; Jakić, M.; Klarić, I. Kinetic Analysis of Thermal Degradation of Poly(Ethylene Glycol) and Poly(Ethylene Oxide)s of Different Molecular Weight. *Thermochim Acta* **2010**, *498* (1–2), 71–80. <https://doi.org/10.1016/j.tca.2009.10.005>.
- (181) Carrillo-Castillo, T. D.; Castro-Carmona, J. S.; Luna-Velasco, A.; Zaragoza-Contreras, E. A. PH-Responsive Polymer Micelles for Methotrexate Delivery at Tumor Microenvironments. *e-Polymers* **2020**, *20* (1), 624–635. <https://doi.org/10.1515/epoly-2020-0064>.

13. Publications & Conference Contributions

Publications resulting from this Thesis

- Schneider, S.; Schwalm, B. L.; Theato, P. AROMA: Anionic Ring-Opening Monomer Addition of Allyl Glycidyl Ether to Methoxy Poly(Ethylene Glycol) for the Synthesis of Sequence-Controlled Polymers. *Programmable Materials* **2023**, 1, e8. <https://doi.org/10.1017/pma.2023.7>.

Other Publications

- Butzelaar, A. J.; Schneider, S.; Molle, E.; Theato, P. Synthesis and Post-Polymerization Modification of Defined Functional Poly(Vinyl Ether)s. *Macromol Rapid Commun* **2021**, 42 (13). <https://doi.org/10.1002/marc.202100133>.

Conference Contributions

- Schneider, S.; Theato, P. "Sequence-Controlled Multiblock Copolymers by Combination of Chain Extension and Post-Polymerization Modification" Poster presented at the "International Conference on Programmable Materials - ProgMatCon 2022" from 12. – 14.07.2022 in Berlin.
- Schneider, S.; Theato, P. "Sequence-Controlled Multiblock Copolymers by Combination of Chain Extension and Post-Polymerization Modification" Poster presented at the "Macromolecular Colloquium Freiburg – MAKRO 2023" from 16. – 17.02.2023 in Freiburg.